E-ISSN: 2148-6247

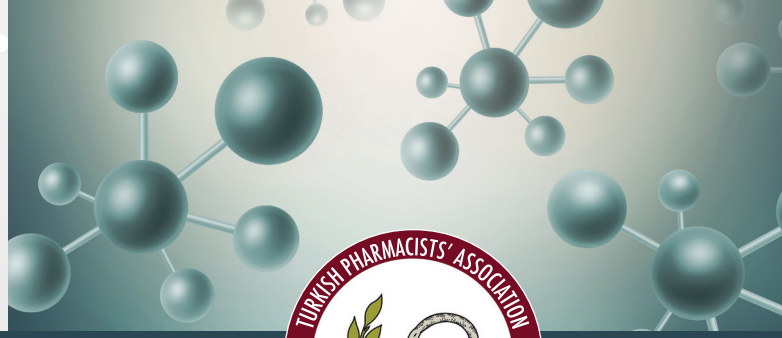

Turkish Journal of PHARMACEUTICAL SCIENCES

An Official Journal of the Turkish Pharmacists' Association, Academy of Pharmacy

Volume: 19 Issue: 1 February 2022

www.turkjps.org

PubMed Central PubMed Scopus TR DİZİN

galenos Publishing House

Turkish Journal of
PHARMACEUTICAL SCIENCES

Turkish Journal of
PHARMACEUTICAL SCIENCES

AIMS AND SCOPE

The Turkish Journal of Pharmaceutical Sciences is the only scientific periodical publication of the Turkish Pharmacists' Association and has been published since April 2004.
Turkish Journal of Pharmaceutical Sciences journal is regularly published 6 times in a year (February, April, June, August, October, December). The issuing body of the journal is Galenos Yayinevi/Publishing House level. The aim of Turkish Journal of Pharmaceutical Sciences is to publish original research papers of the highest scientific and clinical value at an international level.
The target audience includes specialists and professionals in all fields of pharmaceutical sciences.
The editorial policies are based on the "Recommendations for the Conduct, Reporting, Editing, and Publication of Scholarly Work in Medical Journals (ICMJE Recommendations)" by the International Committee of Medical Journal Editors (201, archived at http://www.icmje.org/) rules.

Editorial Independence

Turkish Journal of Pharmaceutical Sciences is an independent journal with independent editors and principles and has no commerical relationship with the commercial product, drug or pharmaceutical company regarding decisions and review processes upon articles.

ABSTRACTED/INDEXED IN

PubMed
PubMed Central
Web of Science-Emerging Sources Citation Index (ESCI)
SCOPUS SJR
TÜBİTAK/ULAKBİM TR Dizin
ProQuest
Chemical Abstracts Service (CAS)
EBSCO
EMBASE
GALE
Index Copernicus
Analytical Abstracts
International Pharmaceutical Abstracts (IPA)
Medicinal & Aromatic Plants Abstracts (MAPA)
British Library
CSIR INDIA
GOALI
Hinari
OARE
ARDI
AGORA
Türkiye Atıf Dizini
Türk Medline
UDL-EDGE
J- Gate
Idealonline
CABI

OPEN ACCESS POLICY

This journal provides immediate open access to its content on the principle that making research freely available to the public supports a greater global exchange of knowledge.
Open Access Policy is based on the rules of the Budapest Open Access Initiative (BOAI) http://www.budapestopenaccessinitiative.org/. By "open access" to peer-reviewed research literature, we mean its free availability on the public internet, permitting any users to read, download, copy, distribute, print, search, or link to the full texts of these articles, crawl them for indexing, pass them as data to software, or use them for any other lawful purpose, without financial, legal, or technical barriers other than those inseparable from gaining access to the internet itself. The only constraint on reproduction and distribution, and the only role for copyright in this domain, should be to give authors control over the integrity of their work and the right to be properly acknowledged and cited.

CORRESPONDENCE ADDRESS

All correspondence should be directed to the Turkish Journal of Pharmaceutical Sciences Editorial Board

Post Address: Turkish Pharmacists' Association, Mustafa Kemal Mah 2147.Sok No:3 06510 Çankaya/Ankara, TURKEY
Phone: +90 (312) 409 81 00
Fax: +90 (312) 409 81 09
Web Page: http://turkjps.org
E-mail: turkjps@gmail.com

PERMISSIONS

Requests for permission to reproduce published material should be sent to the publisher.
Publisher: Erkan Mor
Adress: Molla Gürani Mah. Kaçamak Sok. 21/1 Fındıkzade, Fatih, Istanbul, Turkey
Telephone: +90 212 621 99 25
Fax: +90 212 621 99 27
Web page: http://www.galenos.com.tr/en
E-mail: info@galenos.com.tr

ISSUING BODY CORRESPONDING ADDRESS

Issuing Body : Galenos Yayınevi
Address: Molla Gürani Mah. Kaçamak Sk. No: 21/, 34093 İstanbul, Turkey
Phone: +90 212 621 99 25 Fax: +90 212 621 99 27
E-mail: info@galenos.com.tr

MATERIAL DISCLAIMER

The author(s) is (are) responsible for the articles published in the JOURNAL.
The editors, editorial board and publisher do not accept any responsibility for the articles.

Publisher Contact
Address: Molla Gürani Mah. Kaçamak Sk. No: 21/1
34093 İstanbul, Turkey
Phone: +90 (212) 621 99 25 **Fax:** +90 (212) 621 99 27
E-mail: info@galenos.com.tr/yayin@galenos.com.tr
Web: www.galenos.com.tr | Publisher Certificate Number: 14521

Publication Date: February 2022
E-ISSN: 2148-6247
International scientific journal published bimonthly.

Turkish Journal of
PHARMACEUTICAL SCIENCES

INSTRUCTIONS TO AUTHORS

Turkish Journal of Pharmaceutical Sciences journal is published 6 times (February, April, June, August, October, December) per year and publishes the following articles:

- Research articles
- Reviews (only upon the request or consent of the Editorial Board)
- Preliminary results/Short communications/Technical notes/Letters to the Editor in every field of pharmaceutical sciences.

The publication language of the journal is English.

The Turkish Journal of Pharmaceutical Sciences does not charge any article submission or processing charges.

A manuscript will be considered only with the understanding that it is an original contribution that has not been published elsewhere.

The Journal should be abbreviated as "Turk J Pharm Sci" when referenced.

The scientific and ethical liability of the manuscripts belongs to the authors and the copyright of the manuscripts belongs to the Journal. Authors are responsible for the contents of the manuscript and accuracy of the references. All manuscripts submitted for publication must be accompanied by the Copyright Transfer Form [copyright transfer]. Once this form, signed by all the authors, has been submitted, it is understood that neither the manuscript nor the data it contains have been submitted elsewhere or previously published and authors declare the statement of scientific contributions and responsibilities of all authors.

Experimental, clinical and drug studies requiring approval by an ethics committee must be submitted to the JOURNAL with an ethics committee approval report including approval number confirming that the study was conducted in accordance with international agreements and the Declaration of Helsinki (revised 2013) (http://www.wma.net/en/30publications/10policies/b3/). The approval of the ethics committee and the fact that informed consent was given by the patients should be indicated in the Materials and Methods section. In experimental animal studies, the authors should indicate that the procedures followed were in accordance with animal rights as per the Guide for the Care and Use of Laboratory Animals (http://oacu.od.nih.gov/regs/guide/guide.pdf) and they should obtain animal ethics committee approval.

Authors must provide disclosure/acknowledgment of financial or material support, if any was received, for the current study.

If the article includes any direct or indirect commercial links or if any institution provided material support to the study, authors must state in the cover letter that they have no relationship with the commercial product, drug, pharmaceutical company, etc. concerned; or specify the type of relationship (consultant, other agreements), if any.

Authors must provide a statement on the absence of conflicts of interest among the authors and provide authorship contributions.

All manuscripts submitted to the journal are screened for plagiarism using the 'iThenticate' software. Results indicating plagiarism may result in manuscripts being returned or rejected.

The Review Process

This is an independent international journal based on double-blind peer-review principles. The manuscript is assigned to the Editor-in-Chief, who reviews the manuscript and makes an initial decision based on manuscript quality and editorial priorities. Manuscripts that pass initial evaluation are sent for external peer review, and the Editor-in-Chief assigns an Associate Editor. The Associate Editor sends the manuscript to at least two reviewers (internal and/or external reviewers). The Associate Editor recommends a decision based on the reviewers' recommendations and returns the manuscript to the Editor-in-Chief. The Editor-in-Chief makes a final decision based on editorial priorities, manuscript quality, and reviewer recommendations. If there are any conflicting recommendations from reviewers, the Editor-in-Chief can assign a new reviewer.

The scientific board guiding the selection of the papers to be published in the Journal consists of elected experts of the Journal and if necessary, selected from national and international authorities. The Editor-in-Chief, Associate Editors may make minor corrections to accepted manuscripts that do not change the main text of the paper.

In case of any suspicion or claim regarding scientific shortcomings or ethical infringement, the Journal reserves the right to submit the manuscript to the supporting institutions or other authorities for investigation. The Journal accepts the responsibility of initiating action but does not undertake any responsibility for an actual investigation or any power of decision.

The Editorial Policies and General Guidelines for manuscript preparation specified below are based on "Recommendations for the Conduct, Reporting, Editing, and Publication of Scholarly Work in Medical Journals (ICMJE Recommendations)" by the International Committee of Medical Journal Editors (201, archived at http://www.icmje.org/).

Preparation of research articles, systematic reviews and meta-analyses must comply with study design guidelines:

CONSORT statement for randomized controlled trials (Moher D, Schultz KF, Altman D, for the CONSORT Group. The CONSORT statement revised recommendations for improving the quality of reports of parallel group randomized trials. JAMA 2001; 285: 1987-91) (http://www.consort-statement.org/);

PRISMA statement of preferred reporting items for systematic reviews and meta-analyses (Moher D, Liberati A, Tetzlaff J, Altman DG, The PRISMA Group. Preferred Reporting Items for Systematic Reviews and Meta-Analyses: The PRISMA Statement. PLoS Med 2009; 6(7): e1000097.) (http://www.prisma-statement.org/);

STARD checklist for the reporting of studies of diagnostic accuracy (Bossuyt PM, Reitsma JB, Bruns DE, Gatsonis CA, Glasziou PP, Irwig LM, et al., for the STARD Group. Towards complete and accurate reporting of studies of diagnostic accuracy: the STARD initiative. Ann Intern Med 2003;138:40-4.) (http://www.stard-statement.org/);

STROBE statement, a checklist of items that should be included in reports of observational studies (http://www.strobe-statement.org/);

MOOSE guidelines for meta-analysis and systemic reviews of observational studies (Stroup DF, Berlin JA, Morton SC, et al. Meta-analysis of observational studies in epidemiology: a proposal for reporting Meta-analysis of observational Studies in Epidemiology (MOOSE) group. JAMA 2000; 283: 2008-12).

Turkish Journal of
PHARMACEUTICAL SCIENCES

INSTRUCTIONS TO AUTHORS

GENERAL GUIDELINES

Manuscripts can only be submitted electronically through the Journal Agent website (http://journalagent.com/tjps/) after creating an account. This system allows online submission and review.

Format: Manuscripts should be prepared using Microsoft Word, size A4 with 2.5 cm margins on all sides, 12 pt Arial font and 1.5 line spacing.

Abbreviations: Abbreviations should be defined at first mention and used consistently thereafter. Internationally accepted abbreviations should be used; refer to scientific writing guides as necessary.

Cover letter: The cover letter should include statements about manuscript type, single-Journal submission affirmation, conflict of interest statement, sources of outside funding, equipment (if applicable), for original research articles.

ETHICS COMMITTEE APPROVAL

The editorial board and our reviewers systematically ask for ethics committee approval from every research manuscript submitted to the Turkish Journal of Pharmaceutical Sciences. If a submitted manuscript does not have ethical approval, which is necessary for every human or animal experiment as stated in international ethical guidelines, it must be rejected on the first evaluation.

Research involving animals should be conducted with the same rigor as research in humans; the Turkish Journal of Pharmaceutical Sciences asks original approval document to show implements the 3Rs principles. If a study does not have ethics committee approval or authors claim that their study does not need approval, the study is consulted to and evaluated by the editorial board for approval.

SIMILARITY

The Turkish Journal of Pharmaceutical Sciences is routinely looking for similarity index score from every manuscript submitted before evaluation by the editorial board and reviewers. The journal uses iThenticate plagiarism checker software to verify the originality of written work. There is no acceptable similarity index; but, exceptions are made for similarities less than 15 %.

REFERENCES

Authors are solely responsible for the accuracy of all references.

In-text citations: References should be indicated as a superscript immediately after the period/full stop of the relevant sentence. If the author(s) of a reference is/are indicated at the beginning of the sentence, this reference should be written as a superscript immediately after the author's name. If relevant research has been conducted in Turkey or by Turkish investigators, these studies should be given priority while citing the literature.

Presentations presented in congresses, unpublished manuscripts, theses, Internet addresses, and personal interviews or experiences should not be indicated as references. If such references are used, they should be indicated in parentheses at the end of the relevant sentence in the text, without reference number and written in full, in order to clarify their nature.

References section: References should be numbered consecutively in the order in which they are first mentioned in the text. All authors should be listed regardless of number. The titles of Journals should be abbreviated according to the style used in the Index Medicus.

Reference Format

Journal: Last name(s) of the author(s) and initials, article title, publication title and its original abbreviation, publication date, volume, the inclusive page numbers. Example: Collin JR, Rathbun JE. Involutional entropion: a review with evaluation of a procedure. Arch Ophthalmol. 1978;96:1058-1064.

Book: Last name(s) of the author(s) and initials, book title, edition, place of publication, date of publication and inclusive page numbers of the extract cited.

Example: Herbert L. The Infectious Diseases (1st ed). Philadelphia; Mosby Harcourt; 1999:11;1-8.

Book Chapter: Last name(s) of the author(s) and initials, chapter title, book editors, book title, edition, place of publication, date of publication and inclusive page numbers of the cited piece.

Example: O'Brien TP, Green WR. Periocular Infections. In: Feigin RD, Cherry JD, eds. Textbook of Pediatric Infectious Diseases (4th ed). Philadelphia; W.B. Saunders Company;1998:1273-1278.

Books in which the editor and author are the same person: Last name(s) of the author(s) and initials, chapter title, book editors, book title, edition, place of publication, date of publication and inclusive page numbers of the cited piece. Example: Solcia E, Capella C, Kloppel G. Tumors of the exocrine pancreas. In: Solcia E, Capella C, Kloppel G, eds. Tumors of the Pancreas. 2nd ed. Washington: Armed Forces Institute of Pathology; 1997:145-210.

TABLES, GRAPHICS, FIGURES, AND IMAGES

All visual materials together with their legends should be located on separate pages that follow the main text.

Images: Images (pictures) should be numbered and include a brief title. Permission to reproduce pictures that were published elsewhere must be included. All pictures should be of the highest quality possible, in

JPEG format, and at a minimum resolution of 300 dpi.

Tables, Graphics, Figures: All tables, graphics or figures should be enumerated according to their sequence within the text and a brief descriptive caption should be written. Any abbreviations used should be defined in the accompanying legend. Tables in particular should be explanatory and facilitate readers' understanding of the manuscript, and should not repeat data presented in the main text.

MANUSCRIPT TYPES

Original Articles

Clinical research should comprise clinical observation, new techniques or laboratories studies. Original research articles should include title, structured abstract, key words relevant to the content of the article, introduction, materials and methods, results, discussion, study limitations, conclusion references, tables/figures/images and

Turkish Journal of
PHARMACEUTICAL SCIENCES

INSTRUCTIONS TO AUTHORS

acknowledgement sections. Title, abstract and key words should be written in both Turkish and English. The manuscript should be formatted in accordance with the above-mentioned guidelines and should not exceed 16 A4 pages.

Title Page: This page should include the title of the manuscript, short title, name(s) of the authors and author information. The following descriptions should be stated in the given order:

1. Title of the manuscript (Turkish and English), as concise and explanatory as possible, including no abbreviations, up to 135 characters

2. Short title (Turkish and English), up to 60 characters

3. Name(s) and surname(s) of the author(s) (without abbreviations and academic titles) and affiliations

4. Name, address, e-mail, phone and fax number of the corresponding author

5. The place and date of scientific meeting in which the manuscript was presented and its abstract published in the abstract book, if applicable

Abstract: A summary of the manuscript should be written in both Turkish and English. References should not be cited in the abstract. Use of abbreviations should be avoided as much as possible; if any abbreviations are used, they must be taken into consideration independently of the abbreviations used in the text. For original articles, the structured abstract should include the following sub-headings:

Objectives: The aim of the study should be clearly stated.

Materials and Methods: The study and standard criteria used should be defined; it should also be indicated whether the study is randomized or not, whether it is retrospective or prospective, and the statistical methods applied should be indicated, if applicable.

Results: The detailed results of the study should be given and the statistical significance level should be indicated.

Conclusion: Should summarize the results of the study, the clinical applicability of the results should be defined, and the favorable and unfavorable aspects should be declared.

Keywords: A list of minimum , but no more than 5 key words must follow the abstract. Key words in English should be consistent with "Medical Subject Headings (MESH)" (www.nlm.nih.gov/mesh/MBrowser.html). Turkish key words should be direct translations of the terms in MESH.

Original research articles should have the following sections:

Introduction: Should consist of a brief explanation of the topic and indicate the objective of the study, supported by information from the literature.

Materials and Methods: The study plan should be clearly described, indicating whether the study is randomized or not, whether it is retrospective or prospective, the number of trials, the characteristics, and the statistical methods used.

Results: The results of the study should be stated, with tables/figures given in numerical order; the results should be evaluated according to the statistical analysis methods applied. See General Guidelines for details about the preparation of visual material.

Discussion: The study results should be discussed in terms of their favorable and unfavorable aspects and they should be compared with the literature. The conclusion of the study should be highlighted.

Study Limitations: Limitations of the study should be discussed. In addition, an evaluation of the implications of the obtained findings/results for future research should be outlined.

Conclusion: The conclusion of the study should be highlighted.

Acknowledgements: Any technical or financial support or editorial contributions (statistical analysis, English/Turkish evaluation) towards the study should appear at the end of the article.

References: Authors are responsible for the accuracy of the references. See General Guidelines for details about the usage and formatting required.

Review Articles

Review articles can address any aspect of clinical or laboratory pharmaceuticals. Review articles must provide critical analyses of contemporary evidence and provide directions of or future research. Most review articles are commissioned, but other review submissions are also welcome. Before sending a review, discussion with the editor is recommended.

Reviews articles analyze topics in depth, independently and objectively. The first chapter should include the title in Turkish and English, an unstructured summary and key words. Source of all citations should be indicated. The entire text should not exceed 25 pages (A, formatted as specified above).

Turkish Journal of
PHARMACEUTICAL SCIENCES

CONTENTS

Original Articles

Turkish Journal of
PHARMACEUTICAL SCIENCES

CONTENTS

Turkish Journal of
PHARMACEUTICAL SCIENCES

EDITORIAL

Dear Colleagues,

Turkish Journal of Pharmaceutical Sciences (TJPS) serves as an important scientific platform to all research areas of pharmaceutical sciences. In the upcoming term, I myself, being the new Editor-in-Chief, and Editorial Team along with our renewed Editorial Board members, we have decided to keep going with new cover of the journal from the current volume on. Our aim is to improve scientific quality of the papers published in the journal, which is being rapidly reputed, as well as the raise its quartile status and enable the journal to be listed in SCI. For this purpose, citations to the journal are highly critical and we would like you to cite more articles published in TJPS. This journal is for all of us and we should support our journal in every way with support from scientific community.

Within this year, we are planning to publish two special issues focused on specific topics and also invite worldwide reputed scientists to submit article to increase recognition of the journal. In this endeavor, we are also open to your offers. New activities planned for TJPS with our new Editorial Board and Academy of Pharmacy will be shared with you in turn. One of them was to present you the new cover as I have just mentioned and the second one is to remove the titles and abstracts in Turkish. Starting today, TJPS will be published completely in English. The third one is that TJPS will be an online journal starting from 2022 with environmentally-friendly policy and, therefore, no hardcopy will be provided anymore.

As you may know, we keep receiving many article submissions, which have already piled up in our hand. However, due to this pile up, please be aware that many of the newly accepted papers will be forwarded to next year after the consent of researchers. Before you submit your paper to TJPS, please make sure it to be strictly in accordance with the journal guidelines. In order to guide the authors, the statistics tab of our journal website, acceptance, rejection, and assessment durations of the candidate articles are transparently shared with the authors. No articles without the ethical permission and proper statistical analysis (if needed) will be possible to publish in our journal with direct rejection.

Finally, we are grateful to Turkish Pharmacists Association for their precious support to TJPS. As the new Editorial Team, we would like to thank to previous Editors, Associate Editors, and Editorial Board members of the journal, who brought the journal to its current position by making invaluable efforts. We are aware of our responsibility and work hard to take TJPS at higher levels. Many thanks from us also go to the authors and reviewers who have contributed and supported the journal up to date.

Please enjoy volume 19 (1), February issue of TJPS and follow website of the journal for upcoming news.

With my kind regards,

Prof. İlkay Erdoğan Orhan, Ph.D.
Editor-in-Chief

Turk J Pharm Sci 2022;19(1):1-8
DOI: 10.4274/tjps.galenos.2021.30806

ORIGINAL ARTICLE

The Ameliorate Effects of Nerolidol on Thioacetamide-induced Oxidative Damage in Heart and Kidney Tissue

Kalp ve Böbrek Dokusunda Tiyoasetamid Kaynaklı Oksidatif Hasarın Üzerine Nerolidolün Koruyucu Etkileri

Neşe Başak TÜRKMEN[1]*, Hande YÜCE[1], Aslı TAŞLIDERE[2], Yasemin ŞAHİN[3], Osman ÇİFTÇİ[3]

[1]İnönü University Faculty of Pharmacy, Department of Pharmaceutical Toxicology, Malatya, Turkey
[2]İnönü University Faculty of Medicine, Department of Histology and Embryology, Malatya, Turkey
[3]Pamukkale University Faculty of Medicine, Department of Medicinal Pharmacology, Denizli, Turkey

ABSTRACT

Objectives: Thioacetamide (TAA) is an organosulfur, white crystalline compound having liver injury. However, it shows toxic effects on many organs. The reverts the oxidative stress created by TAA on the heart and kidney, and decreased lipid peroxide peroxidation back with antioxidant-properties nerolidol (NRL). This study hypothesized that NRL treatment a potential ameliorate nephrotoxicity and cardiotoxicity caused by TAA.

Materials and Methods: Thirty-two Wistar Albino male rats (3-4 months old and 280-300 g in weight) were divided into four groups. (a) Control, (b) TAA was administered 200 mg/kg *i.p.* twice a weekly (c) NRL was orally administered at the dose of 100 mg/kg *per* every other day by gavages. (d) TAA and NRL-treated groups were assigned 200 mg/kg TAA and 100 mg/kg NRL for three weeks.

Results: As a result of these dose administration thiobarbituric acid reactive substances (TBARS) levels, superoxide dismutase (SOD), catalase (CAT), glutathione (GSH), and glutathione peroxidase (GPx) levels were detected. The results were shown that TAA leads to a significant rise in TBARS level and a significant decrease in GPx, CAT, SOD, and GSH levels in the heart and kidney tissue according to the control group. The finding of this study the NRL treatment reduced TBARS levels and increased antioxidant level. Administration of NRL prevents the biochemical and histopathological alterations induced by TAA.

Conclusion: The findings of this study show that the antioxidant activity of NRL can protect against biochemical and histological damage caused by TAA in heart and kidney tissue.

Key words: Nerolidol, thioacetamide, lipid peroxidation, nephrotoxicity, cardiotoxicity

ÖZ

Amaç: Tiyoasetamid (TAA), karaciğere zarar veren beyaz kristalli bir organosülfür bileşiğidir. Ancak birçok organ üzerine toksik etkiler gösterir. Antioksidan özelikleri ile bilinen nerolidol (NRL) tiyoasetamitin kalp ve böbrek dokularında neden olduğu oksidatif stresi önler ve lipit peroksidasyonunu azaltır. Bu çalışmanın amacı, NRL'nin TAA kaynaklı nefrotoksisite ve kardiyotoksisitesinin ratların üzerindeki koruyucu etkisi araştırmaktır.

Gereç ve Yöntemler: Otuz iki adet Wistar Albino erkek sıçan (3-4 aylık ve ağırlıkları 280-300 gr) dört gruba ayrıldı. (a) Kontrol grubu, (b) TAA grubu haftada iki kez 200 mg/kg *i.p.* olarak uygulanmıştır, (c) NRL grubu, gavaj yoluyla her gün 100 mg/kg dozunda oral yoldan uygulanmıştır. (d) TAA ve NRL grubu, üç hafta süreyle 200 mg/kg TAA ve 100 mg/kg NRL uygulanmıştır.

Bulgular: Bu dozların uygulaması sonucunda tiyobarbitürik asit reaktif maddelerin (TBARS) seviyeleri, süperoksit dismutaz (SOD), katalaz (CAT), glutatyon (GSH) ve glutatyon peroksidaz (GPx) seviyeleri tespit edilmiştir. Sonuçlar, TAA'nın kontrol grubuna kıyasla TBARS seviyesinde önemli bir artışa ve kalp ve böbrek dokularında GPx, CAT, SOD ve GSH seviyelerinde önemli bir düşüşe neden olduğu gösterilmiştir. Bu çalışmanın sonucunda, NRL uygulamasının TBARS düzeylerini önemli ölçüde azalttığı ve antioksidan enzimleri artırdığı bulunmuştur.

Sonuç: Bu çalışmanın sonuçları, NRL'nin antioksidan aktivitesinin, TAA'nın kalp ve böbrek dokusunda neden olduğu biyokimyasal ve histolojik hasara karşı koruyabildiğini göstermektedir.

Anahtar kelimeler: Nerolidol, tiyoasetamid, lipid peroksidasyonu, nefrotoksisite, kardiyotoksisite

***Correspondence:** nese.basak@inonu.edu.tr, **Phone:** +90 534 222 95 72, **ORCID-ID:** orcid.org/0000-0001-5566-8321

Received: 19.11.2020, **Accepted:** 03.04.2021

INTRODUCTION

Nowadays, it has increased serious organ damage as a result of acute and chronic exposure to toxic chemicals.[1] Thioacetamide (TAA); is a chemical used in industrial areas such as leather, textile, and paper and in laboratories as an organic solvent.[2] TAA has significant toxic effects on organs such as the liver, kidney, spleen, lung, intestine, stomach, and brain, causing structural and functional modification.[3] TAA is metabolized *in vivo* to free radical derivatives, TAA sulfoxide and TAA-S, S-dioxide, resulting in increased lipid peroxidation, resulting in reactive oxygen species (ROS) formation and thus multi-organ damage.[1,4]

Increased free radical development or reduced free radical scavenging is responsible for oxidative stress. Oxidative stress is a major imbalance between free radical development and defense mechanisms against antioxidants.[5,6] Pro-oxidant agents are primarily constituted by ROS and nitrogenous species.[7,8]

The generation of a large amount of ROS due to TAA can inhibit the antioxidant defense mechanism.[4] TAA can damage cellular ingredients such as lipids, proteins, and DNA; TAA can impair cellular structure and function. Intracellular antioxidant system compounds [like glutathione (GSH) and other thiols] can be insufficient to proper this damage. The damage of TAA on the heart was evaluated based on the oxidative stress both biochemical and histological. The heart damage is characterized by ROS occurrence, lipid peroxidation, and adverse impacts on the antioxidant-oxidant system.[9] Some studies have shown that oxidative stress plays an important role in TAA-induced toxicity. However, it has been suggested that various antioxidant treatments show beneficial effects by reducing oxidative stress.[10,11]

Recently, in addition to modern treatment methods, plant-based treatments have become more important.[12] The progression of technology and the serious side effects of pharmaceutical agents used in medical treatment have increased the interest in medicinal plants and enabled the investigation of bioactive compounds found in these plants.

Natural components are a present source of antioxidants and many researchers based on discovering new antioxidant compounds from plants. An increasing number of studies have shown that essential oils obtained from medicinal plants exhibit various biological properties.[13] Antioxidants found in plants are being investigated to treat many disorders such as cardiovascular diseases, cancer, and neurological condition.[13,14] Nerolidol (NRL) is found in different plant species, *Ferula fukanensis*, *Baccharis dracunculifolia*, *Amaranthus retroflexus* and *Canarium schweinfurthi*.[15-17] NRL, also known as '3,7,11-trimethyl-1,6,10-dodecatrien-3-ol' is aliphatic xylene alcohol derived from many plants with antioxidant properties.[18] The antioxidant, radical scavenging, and anti-inflammatory effects of NRL have been demonstrated in several studies. Nogueira Neto et al.[19] found that essential oils from *Ferula fukanensis* containing NRL induced a decrease in nitric oxide production and restricts gene expression NO-induced. In this context, NRL can be suggested utilization as an antioxidant agent.[19,20] Although there is currently limited information about the bioactivity of essential oils, it easily crosses the cell membrane and can interact with intracellular proteins. Therefore, many studies have implicated the free radical scavenging properties of essential oils. Studies have shown the antioxidant, radical scavenging, and antiinflammatory effects of NRL.[21] Additionally, Javed et al.[22] found that administration of NRL (50 mg/kg, *i.p.*) to rats reversed inflammation and oxidative stress by increasing levels of the antioxidant enzymes superoxide dismutase (SOD), catalase (CAT), GSH and decreasing lipid peroxidation and thiobarbituric acid reactive substances (TBARS) levels. In this context, Nogueira Neto et al.[19] found that treatment with NRL (75 mg/kg, *i.p.*) decreased oxidative stress in the mouse, resulting in increased SOD and CAT activity. Previous studies have suggested that therapeutic potential of NRL to treat and prevent diseases associated with oxidative stress. According to the literature, no previous study investigated the efficacy of NRL on cardiac ameliorates.[23,24]

Therefore, this study investigated the protection of NRL, which is thought to have high antioxidant potential against the cardiotoxic and nephrotoxic effects of TAA. For this purpose, histopathological and biochemical effects of TAA on the heart and kidney were examined and the protective effect of NRL on these parameters was investigated.

MATERIALS AND METHODS

Animals and treatment

This study was approved by the Ethics Committee on Animal Research of Pamukkale University (protocol number: 2020/20) and conducted in accordance with the Guidelines for Animal Research from the National Institutes of Health. Pamukkale University Laboratory Animals Reserch Center (Denizli, Turkey) provided the male Wistar Albino rats (weighing 280-300 g). Animals were housed in sterilized polypropylene cages, and fed *ad libitum* with standard commercial food pellets and water.

Animals were randomly divided into 4 groups with eight animals in each group:

1) In the control group, the rats were administered with corn oil alone as vehicle.

2) In the TAA group, the rats were administered with TAA 200 mg/kg, intraperitoneal (*i.p.*) twice *per* week for three weeks,

3) In the NRL group, the rats were administered with NRL 100 mg/kg by gavage every other day,

4) In the TAA + NRL group, the rats were administered 200 mg/kg TAA *i.p.* twice a week and NRL 100 mg/kg for 21 consecutive days.

After three weeks of treatment, all rats were euthanized under anesthesia. Heart and kidney tissue samples were collected for biochemical analyses and histological examination.

Biochemical assay

Tissues were homogenized for biochemical parameters examination. TBARS-level tissue homogenates were determined using a spectrophotometric process that is focused

on the reaction between thiobarbituric acid and[25,26] GSH levels of tissues were determined at 412 nm according to the Sedlak and Lindsay[27] method. The results were expressed as nmol/mL. SOD activity was determined by the method of Sun et al.[28] using spectrophotometrically. SOD enzyme activity was determined in the inhibition of nitro blue tetrazolium depend on xanthine/xanthine oxidase enzyme activity O^{-2}. The tissues were measured at 560 nm in spectrophotometer.[28] We determined CAT levels of tissues according to the Aebi[29] method. Glutathione peroxides (GPx) level was determined as spectrophotometrically using method of Paglia and Valentine.[30] The tissue protein content was calculated by the method of Lowry et al.[31]

Histopathological assay

For light microscopic evaluation, liver and brain samples were fixed in 10% formalin. The tissue samples were processed by routine tissue techniques and were embedded in paraffin. Paraffin-embedded specimens were cut into 5 mm thick sections, mounted on slides, and stained with hematoxylin-eosin. We examined stained sections under a LeicaDFC280 light microscope by Leica Q Win and Image Analysis System.

We examined heart sections for hemorrhage, necrosis, vascular congestion, vacuolization, mononuclear cell infiltration, oedema and eosinophilic stained and pyknotic nuclei cells.

We examined kidney sections for inflammatory cell infiltration, hemorrhage, glomerular degeneration, vascular congestion, hemorrhage between the tubules, vacuolization of tubular epithelial cells and oedema between the tubules, epithelial atrophy, and cell desquamation in the tubules and casts in tubular lumen. Histopathologic damage score was calculated using these findings. Histopathologic damage score was calculated according to the degree of damage severity to 0 (none), 1 (mild), 2 (moderate), 3 (severe).

Statistical analysis

ANOVA (*post-hoc* Tukey test) was performed for comparing biochemical, histopathological, and immunohistochemical scores between the groups. Statistical calculations were carried out using the SPSS 18.0 program package (SPSS Inc., Chicago, IL, USA). Variables were presented as mean ± standard deviations and $p<0.05$ was the gauge to indicate statistical significance.

Histopathological data analysis was used SPSS 13.0 (SPSS Inc., Chicago, Ill., USA) and MedCalc 11.0 (Belgium) statistical programs. The data are expressed as the arithmetic mean ± standard error. Kruskal-Wallis and Connover tests were used. Exact p values were given where available, and $p<0.001$ was considered statistically significant.

RESULTS

Biochemical results

The antioxidant (SOD, CAT, GPx and GSH) and oxidant (TBARS) levels of the heart tissues are presented in Table 1. In TAA group, the results showed *t*hat the SOD, GPx, CAT, GPx and GSH levels were significantly ($p<0.001$) diminished, whereas the TBARS levels were significantly ($p<0.001$) increased compared with the control group. It was shown that TAA significantly increased the lipid peroxidation in heart tissue. Also, it was determined that there were not any significant changes between the control and NRL groups in terms of SOD, CAT and GSH levels. In TAA + NRL group, the values of TBARS and SOD were similar to control and reversed the effect of TAA on these values. However, the GSH, CAT, GPx levels were changed, but it was not in a statistically significant range. Besides, the TAA + NRL group showed SOD, GPx, CAT and GSH an increase in activities compared with the TAA group. Generally, the results showed that NRL significantly reduced lipid peroxidation in heart tissue.

The antioxidant (SOD, CAT, GPx and GSH) and oxidant (TBARS) levels of the kidney tissues are presented in Table 2. In TAA group, the results showed that the SOD, GPx, CAT, GPx and GSH levels were significantly ($p<0.001$) diminished, whereas the TBARS levels were significantly ($p<0.001$) increased compared with the control group. It was shown that TAA significantly increased the lipid peroxidation in kidney tissue. Also, it was showed that there were not any significant changes between the control and NRL groups in terms of SOD and CAT levels. In TAA + NRL group, the values of GSH, CAT and GPx were similar to control. Besides, the TAA+ NRL group showed SOD, GPx, CAT and GSH an increase in activities compared with the TAA group. Generally, the results showed that NRL significantly reduced lipid peroxidation in kidney tissue.

Histopathological results

In control (Figure 1A, Figure 2A) and NRL (Figure 1B, Figure 2B) groups, heart and kidney tissue were observed in normal histological appearance. In control and NRL groups heart tissue showed a normal myofibrillar structure with striations, branched appearances, and continuity with adjacent myofibrils. In control and NRL groups kidney tissue showed a normal

Table 1. The effect of nerolidol on oxidative stress markers of heart tissues in rats. Values are presented as means ± SD

	TBARS (nmol/g tissue)	Reduced GSH (nmol/mL tissue)	CAT (k U/mg protein)	SOD (U/mg protein)	GPx (U/mg protein)
Control	11.49±3.43^{y}	41.82±6.51$^{y, z}$	0.302±0.10$^{y, z}$	86.68±7.71^{z}	0.55±0.09$^{y, z}$
TAA	17.42±1.64$^{x, z}$	17.64±0.93$^{x, z}$	0.004±0.0002^{x}	66.98±9.32^{z}	0.12±0.02^{x}
NRL	3.79±0.46$^{x, y, z}$	49.38±6.78$^{x, y, z}$	0.013±0.0002^{x}	87.45±2.11	0.39±0.01$^{x, z}$
TAA + NRL	8.44±0.28^{y}	27.58±1.04$^{x, y, z}$	0.009±0.003^{x}	78.96±13.18$^{x, y}$	0.18±0.06^{x}

x, y, z <0.001. x: Compared with control group, y: Compared with TAA group, z: Compared with TAA + NRL group, TBARS: Thiobarbituric acid reactive substances, GSH: Glutathione, CAT: Catalase, SOD: Superoxide dismutase, GPx: Glutathione peroxidase, SD: Standard deviation, TAA: Thioacetamide, NRL: Nerolidol

Table 2. The effect of nerolidol on oxidative stress markers of kidney tissues in rats. Values are presented as means ± SD

	TBARS (nmol/g tissue)	Reduced GSH (nmol/ml tissue)	CAT (k U/mg protein)	SOD (U/mg protein)	GPx (U/mg protein)
Control	4.07±0.89$^{y, z}$	52.75±2.93^{z}	0.013±0.002	113.13±9.12^{z}	0.12±0.03^{y}
TAA	9.45±0.76^{x}	40.78±4.18$^{z, y, z}$	0.007±0.001$^{x, y, z}$	42.79±16.16$^{x, y}$	0.06±0.04$^{x, y, z}$
NRL	2.96±0.14$^{x, y, z}$	63.05±7.98$^{x, y}$	0.016±0.002^{z}	112.74±29.37^{z}	0.49±0.02$^{x, z}$
TAA + NRL	8.49±0.36^{x}	59.48±3.79^{z}	0.013±0.008^{y}	68.53±11.54$^{x, y}$	0.15±0.03^{y}

x, y, z <0.001. x: Compared with control group, y: Compared with TAA group, z: Compared with TAA + NRL group, TBARS: Thiobarbituric acid reactive substances, GSH: Glutathione, CAT: Catalase, SOD: Superoxide dismutase, GPx: Glutathione peroxidase, SD: Standard deviation, TAA: Thioacetamide, NRL: Nerolidol

tubular and glomerular structure. Cardiac muscle cells were also normal; their large purple nucleus was located in the center of their pink colored cytoplasm.

In heart tissue of the TAA group, we detected hemorrhage (Figure 3A-C, F), necrosis (Figure 3B), eosinophilic stained and pyknotic nuclei cells (Figure 3C), oedema and vacuolization (Figure 3D), vascular congestion (Figure 3E), mononuclear cell infiltration (Figure 3F).

In kidney tissue of the TAA group, we detected inflammatory cell infiltration (Figure 4A, B, D), hemorrhage (Figure 4A, D, E), glomerular degeneration (Figure 4B-D), vascular congestion (Figure 4D), vacuolization of tubular epithelial cells and oedema between the tubules (Figure 4E), epithelial atrophy and cell desquamation in the tubules and casts in tubular lumen (Figure 4F).

Histological changes were more severe in the TAA group than in the group of treatment. However, histopathological damage decreased in the TAA + NRL (Figure 5, 6) group. NRL administration reduced TAA induced in comparison to compare to that of TAA treated groups for heart and kidney tissues. In addition, microscopic damage score results of all four groups in are demonstrated in Table 3. Accordingly, NRL significantly decreased the histopathological damage score caused by TAA.

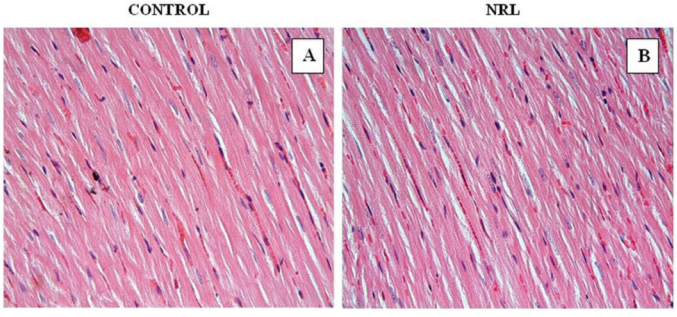

Figure 1. In control (A) and NRL (B) groups; heart tissue showed normal histological appearance. A, B: H-E; X40

NRL: Nerolidol, H-E: Hematoxylin-eosin

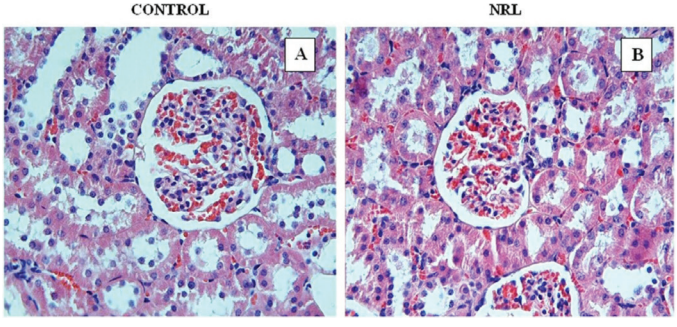

Figure 2. In control (A) and NRL (B) groups; kidney tissue showed normal histological appearance. A, B: H-E; X40

NRL: Nerolidol, H-E: Hematoxylin-eosin

DISCUSSION

The reason for the toxic effect of TAA, which is used as a metal sulfide source, on tissues such as the heart, liver, kidney, and

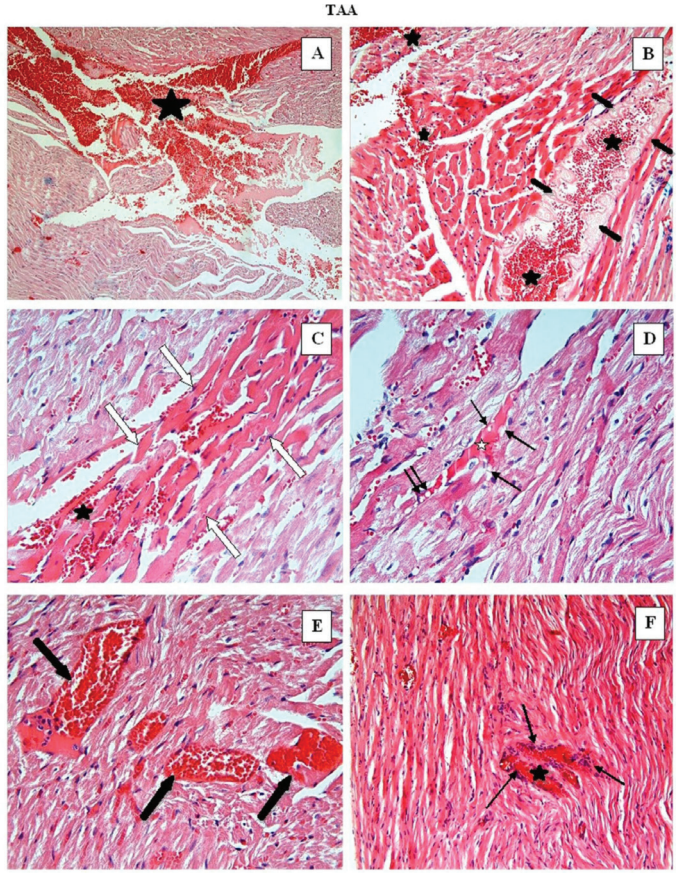

Figure 3. In TAA group: Hemorrhage (black asterisk) (A-C, F), necrosis (thick black arrows) (B), eosinophilic stained and pyknotic nuclei cells (white arrows) (C, F), oedema (white asterisk) and vacuolisation (thin black arrows) (D), vascular congestion (E), mononuclear cell infiltration (thin black arrows) were observed in heart tissue. A: H-E; X10 B, F: H-E; X20, C-E: H-E; X40

TAA: Thioacetamide, H-E: Hematoxylin-eosin

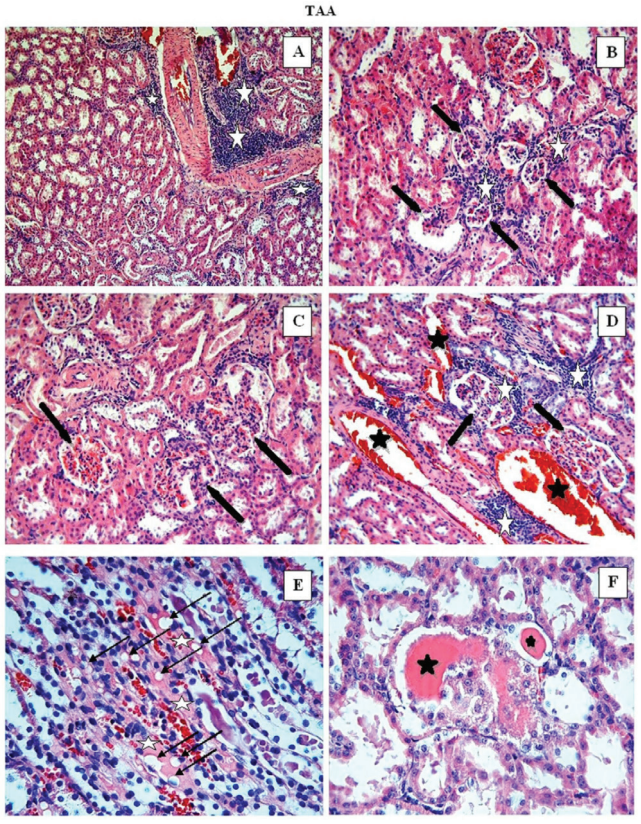

Figure 4. In TAA group; inflammatory cell infiltration (white asterisk) (A, B, D), hemorrhage (A, D, E), glomerular degeneration (black arrows) (B-D), vascular congestion (D), vacuolization of tubular epithelial cells (black arrows) and oedema between the tubules (white asterisk) (E), epithelial atrophy and cell desquamation in the tubules and casts in tubular lumen (F) were observed in kidney. A-C: H-E; X20, D-F: H-E; X40

TAA: Thioacetamide, H-E: Hematoxylin-eosin

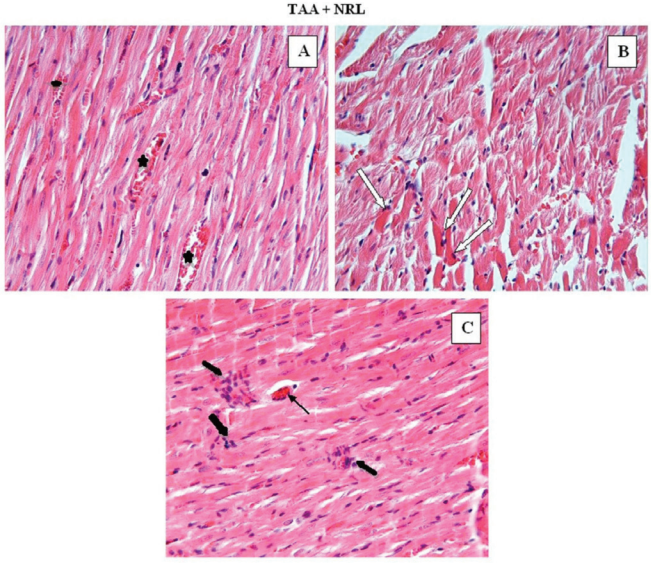

Figure 5. In the TAA + NRL group: Heart tissue findings were decreased compared with the TAA group. Little hemorrhage (black asterisk) (A), a few eosinophilic stained and pyknotic nuclei cells (white arrows) (B), little mononuclear cell infiltration (thick black arrows) and vascular congestion (thin black arrow) (C) were observed in heart tissue. A-C: H-E; X40

TAA: Thioacetamide, NRL: Nerolidol, H-E: Hematoxylin-eosin

brain is the induction of oxidative stress. TAA-related toxicity is characterized by increased TBARS levels and increased ROS production. In our study, NRL treatment against TAA-induced heart and kidney toxicity was investigated in terms of antioxidant parameters and histopathological changes. TAA significantly increased TBARS levels in heart and kidney tissue and decreased antioxidant enzymes. Therefore, NRL treatment potentially reduced the side effects of TAA and has been shown to be beneficial against these changes.

Chemicals taken into the organism through environmental and industrial can cause oxidative stress.[19] Compounds of natural origin can help reverse these effects. Natural antioxidant agents are thought to help prevent imbalances in the antioxidant system that develops because of exposure to toxic substances.

Bioflavonoids are naturally obtained and have antioxidant, anti-inflammatory, and antiapoptotic properties. Notably, they

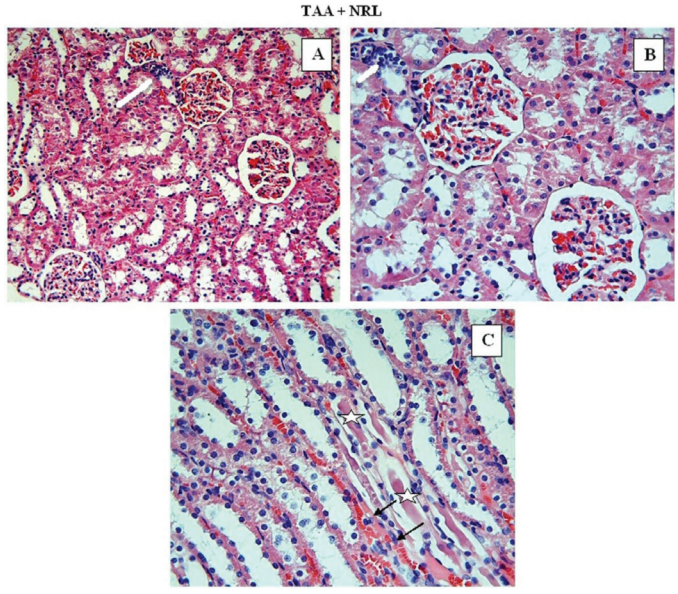

Figure 6. In the TAA + NRL group; kidney tissue findings decreased compared to the TAA group. We observed little inflammatory cell infiltration (white arrows) (A, B), casts in tubular lumen (white asterisk) (B) and a few vacuolization of tubular epithelial cells (B). A, B: H-E; X20, C: H-E; X40

TAA: Thioacetamide, NRL: Nerolidol, H-E: Hematoxylin-eosin

Table 3. Comparison of the effect of NRL on histopathological damage caused by TAA in heart and kidney tissues (arithmetic mean ± SE)

GROUPS	Histopathologic score of heart	Histopathologic score of kidney
Control	0.62±0.10	0.83±0.08
TAA	2.40±0.09[a]	2.10±0.14[a]
TAA + NRL	1.30±0.07[b]	1.45±0.07[b]
NRL	0.87±0.10	0.95±0.13

a: There is difference ($p \leq 0.0001$) between TAA and the other groups. b: There is difference ($p \leq 0.0001$) between the TAA + NRL group and the other groups. The mean differences the values bearing different superscript letters within the same column are statistically significant ($p \leq 0,0001$). TAA: Thioacetamide, NRL: Nerolidol, SE: Standard error

prevent multiple organ damage caused by oxidative stress and ROS. NRL shows antioxidant activity by eliminating free radicals and ROS.[32,33] NRL can prevent lipid peroxidation by lowering TBARS levels. It also prevents the generation of hydroxyl radicals and reduces nitric oxide production. Thus, NRL has radical scavenging activity and is a good antioxidant against oxidative stress.[19] In previous studies have shown that NRL exhibits strong antioxidant activity at the administration of 25, 50, and 75 mg/kg, causes a considerable reduction in nitric oxide levels and significantly increases SOD and CAT levels.[34] In this context, it protects cells from impairment due to oxidative damage by enhanced the generation of antioxidant enzymes.

Changes in oxidative stress parameters

The current different studies demonstrate that the most serious toxic effect of TAA was observed in the liver. TAA can act as an electrophilic agent and S-oxide groups formed by its metabolism attack biomolecules.[34] Active metabolites due to TAA metabolism bind to cell lipids and proteins by oxidative stress, total antioxidant levels, and binding them to cell lipids and proteins. Increased MDA levels indicate this toxicity. In previous studies, it was determined that increased TBARS in environmental chemical agents rats result from enhanced membrane lipid peroxidation by free radicals and the failure of antioxidant defense mechanisms that prevent formation of excessive free radicals.[35,36] In the same way, we found that TAA induced oxidative damage, increased TBARS levels, and decreased GSH levels and activities of antioxidant enzymes, including SOD and CAT, in the heart and kidney.

In this study, TAA induced nephrotoxicity by way of enhanced lipid peroxidation, decreased antioxidant enzyme system, and enhanced histopathological damage. Kidneys are highly vulnerable to damage from free radicals and oxidative stress from unsaturated fatty acids.[37] Free radicals from TAA lead to severe kidney damage. Inflammation, oxidative damage, and apoptosis mechanisms are the most important factors causing renal function impairment.[38] TAA exposure adversely affects the defense system, which prevents the accumulation of ROS. In another study on cardiac toxicity from 2,3,7,8-tetrachlorodibenzo-p-dioxin (TCDD), cardiac tissue had increased levels of TBARS. The parameters of the antioxidant enzyme activities decrease in the heart tissue due to xenobiotic exposure.[39] Another study demonstrated that administration of environmental chemical agents to rats leaded to oxidative stress and was associated with significantly lower antioxidant activities of GSH, CAT and SOD.[40] Thus, this literature confirms our results. In this study, TAA toxicity decreased the activity of GSH, SOD, CAT, and GPx in the kidney and heart tissue. No studies on heart damage caused by TAA exposure have been seen in the literature studies and we think that our study will be the first in this area.

The study demonstrated that TAA induced oxidative stress, which was approved by the decreases of serum SOD and GSH levels.[8] These results obviously showed that TAA induced oxidative stress in experimental rats.[41,42] Oxidative stress plays a primary role in the pathogenesis of multiorgan toxicity. ROS are one of the main causes leading to the progression of pathophysiological changes of the organ injury.

ROS formation occurs in an equilibrium created. However, when external or internal xenobiotics, oxidative stress forms disrupted balance in the heart tissue.[43] *In vivo* animal studies show that the resulting ROS lead to heart tissue damage.[44,45] Celik et al.[46] were shown that testicular damage induced by TAA is reversed with the antioxidant capacity of NRL. Our study provides a novel perspective on the ameliorating effect of NRL of TAA-induced toxicity in rats.

Histopathological changes

In different studies, histopathological effects from TAA indicate that the kidney cortex is more affected than the medulla. In the images of the light microscope, significant histopathological changes were observed as a result of glomerular blockage, focal mesangial cell proliferation, increased accumulation of collagen in the renal medulla and fibrin.[46] Thus, renal cell damage can occur as a decrease in tubules and glomerular filtration rate.[47]

Histopathologically, the toxic effects of TAA on the organs of experimental animals were investigated by several studies. These studies showed that the light microscopic examinations of renal and liver tissue revealed severe histopathological changes.[48,49] In the study by Ciftci et al.[49] TAA's tissue toxicity was examined and as part of our study, toxic effects on the kidney and heart tissue were observed. Other studies have shown that nephrons of kidneys are negatively affected by nephrotoxic, xenobiotic, and heavy metal exposure.[50] One of these adverse effects, a decrease in the functional mass of the kidneys can be shown, leading to a faster cell deaths. In this context, kidney tissue is very vulnerable to such situations. *In vivo* studies are suggested that exposure to nephrotoxicants has caused considerable cellular damage.[51] In the study of Barker and Smuckler[51] were determined renal tubular damage of kidneys TAA-induced as morphologically. The tubular damage is reversed with the *Vitex negundo* extract used in the study. According to the results of the study, it has been shown that basil leaf extract will be useful as a natural product in the treatment of TAA-induced nephrotoxicity.[42] The histopathological results of our study were found to be compatible with the literature.

In our previous studies, it was determined that TCDD exposure caused histopathological changes in heart tissue including severe necrosis and bleeding.[38] In our study, TAA causes histopathological changes in the heart tissue, such as necrosis and bleeding compared with the control group. In another study, TAA was shown to cause histopathological damage to the reproductive system.[46] We detected histopathological changes decreased significantly with NRL treatment. In this study results are the first to determine that NRL therapy reverts the histopathological damage of TAA on the heart tissue. In our study, it has been shown that NRL treatment can make a significant contribution to the literature as it reduces oxidative damage to the heart tissue and prevents histopathological damage.

CONCLUSION

This study shows that NRL can inhibit TAA-induced oxidative damage of the heart and kidneys. As a result, the administration of TAA led to a significant increase in TBARS levels and a significant decrease in antioxidant system (SOD, CAT, GPx and GSH) activities, causing histological damage to the heart and kidney tissue. Therefore, we found that the antioxidant activity of NRL reduces oxidative stress and histopathology in kidney and heart caused by TAA.

Conflict of interest: No conflict of interest was declared by the authors. The authors are solely responsible for the content and writing of this paper.

REFERENCES

1. Allen JH. The wicked problem of chemicals policy: opportunities for innovation. J Environ Stud Sci. 2012;3:101-108.
2. Caballero ME, Berlanga J, Ramirez D, Lopez-Saura P, Gozalez R, Floyd DN, Marchbank T, Playford RJ. Epidermal growth factor reduces multiorgan failure induced by thioacetamide. Gut. 2001;48:34-40.
3. Pallottini V, Martini C, Bassi AM, Romano P, Nanni G, Trentalance A. Rat HMGCoA reductase activation in thioacetamide-induced liver injury is related to an increased reactive oxygen species content. J Hepatol. 2006;44:368-374.
4. Fabregat I. Dysregulation of apoptosis in hepatocellular carcinoma cells. World J Gastroenterol. 2009;15:513-520.
5. Serafini M, Del Rio D. Understanding the association between dietary antioxidants, redox status and disease: is the total antioxidant capacity the right tool? Redox Rep. 2004;9:145-152.
6. Pisoschi AM, Pop A. The role of antioxidants in the chemistry of oxidative stress: a review. Eur J Med Chem. 2015;97:55-74.
7. Halliwell B, Gutteridge JM. Free radicals in biology and medicine. Oxford University Press, USA. 2015.
8. Winyard PG, Moody CJ, Jacob C. Oxidative activation of antioxidant defence. Trends Biochem Sci. 2005;30:453-461.
9. Lotková H, Cervinková Z, Kucera O, Rousar T, Kriváková P. S-adenosylmethionine exerts a protective effect against thioacetamide-induced injury in primary cultures of rat hepatocytes. Altern Lab Anim. 2007;35:363-371.
10. Osman A, El-Hadary A, Korish AA, AlNafea HM, Alhakbany MA, Awad AA, Abdel-Hamid M. Angiotensin-I converting enzyme inhibition and antioxidant activity of papain-hydrolyzed camel whey protein and its hepato-renal protective effects in thioacetamide-induced toxicity. Foods. 2021;10:468.
11. Saad HM, Oda SS, Sedeek EK. Protective effect of Lactéol® forte against thioacetamide-induced hepatic injury in male albino rats. Alex J Vet Sci. 2020;67:92-98.
12. Bakkali F, Averbeck S, Averbeck D, Idaomar M. Biological effects of essential oils--a review. Food Chem Toxicol. 2008;46:446-475.
13. Asaikumar L, Vennila L, Akila P, Sivasangari S, Kanimozhi K, Premalatha V, Sindhu G. Preventive effect of nerolidol on isoproterenol induced myocardial damage in Wistar rats: evidences from biochemical and histopathological studies. Drug Dev Res. 2019;80:814-823.
14. Abdelbaset MS, Abdel-Aziz M, Abuo-Rahma GEA, Abdelrahman MH, Ramadan M, Youssif BGM. Novel quinoline derivatives carrying nitrones/oximes nitric oxide donors: design, synthesis, antiproliferative and caspase-3 activation activities. Arch Pharm (Weinheim). 2019;352:e1800270.
15. Pinheiro BG, Silva ASB, Souza GEP, Figueiredo JG, Cunha FQ, Lahlou S, da Silva JKR, Maia LGS, Sousa PJC. Chemical composition, antinociceptive and anti-inflammatory effects in rodents of the essential oil of Peperomia serpens (Sw.) Loud. J Ethnopharmacol. 2011;138:479-486.
16. Parreira NA, Magalhães LG, Morais DR, Caixeta SC, de Sousa JP, Bastos JK, Cunha WR, Silva ML, Nanayakkara NP, Rodrigues V, da Silva Filho AA. Antiprotozoal, schistosomicidal, and antimicrobial activities of the essential oil from the leaves of *Baccharis dracunculifolia*. Chem Biodivers. 2010;7:993-1001.
17. Klopell FC, Lemos M, Sousa JP, Comunello E, Maistro EL, Bastos JK, de Andrade SF. Nerolidol, an antiulcer constituent from the essential oil of *Baccharis dracunculifolia* DC (Asteraceae). Z Naturforsch C J Biosci. 2007;62:537-542.
18. Chan WK, Tan LT, Chan KG, Lee LH, Goh BH. Nerolidol: A sesquiterpene alcohol with multi-faceted pharmacological and biological activities. Molecules. 2016;21:529.
19. Nogueira Neto JD, de Almeida AA, da Silva Oliveira J, Dos Santos PS, de Sousa DP, de Freitas RM. Antioxidant effects of nerolidol in mice hippocampus after open field test. Neurochem Res. 2013;38:1861-1870.
20. Bagamboula CF, Uyttendaele M, Debevere J. Inhibitory effect of thyme and basil essential oils, carvacrol, thymol, estragol, linalool and p-cymene towards *Shigella sonnei* and *S. flexneri*. Food Microbiol. 2004;21:33-42.
21. Péres VF, Moura DJ, Sperotto AR, Damasceno FC, Caramão EB, Zini CA, Saffi J. Chemical composition and cytotoxic, mutagenic and genotoxic activities of the essential oil from *Piper gaudichaudianum* Kunth leaves. Food Chem Toxicol. 2009;47:2389-2395.
22. Javed H, Azimullah S, Khair SBA, Ojha S, Haque ME. Neuroprotective effect of nerolidol against neuroinflammation and oxidative stress induced by rotenone. BMC Neurosci. 2016;17:1-12.
23. Motai T, Kitanaka S. Sesquiterpenoids from *Ferula fukanensis* and their inhibitory effects on nitric oxide production. Journal of Natural Medicines. 2006;60:54-57.
24. Lapczynski A, Bhatia SP, Letizia CS, Api AM. Fragrance material review on nerolidol (isomer unspecified). Food Chem Toxicol. 2008;(Suppl 11):S247-S250.
25. Yagi K. Simple assay for the level of total lipid peroxides in serum or plasma. Methods Mol Biol. 1988;108:101-106.
26. Montjean D, Ménézo Y, Benkhalifa M, Cohen M, Belloc S, Cohen-Bacrie P, de Mouzon J. Malonaldehyde formation and DNA fragmentation: two independent sperm decays linked to reactive oxygen species. Zygote. 2010;18:265-268.
27. Sedlak J, Lindsay RH. Estimation of total, protein-bound, and nonprotein sulfhydryl groups in tissue with Ellman's reagent. Anal Biochem. 1968;25:192-205.
28. Sun Y, Oberley LW, Li Y. A simple method for clinical assay of superoxide dismutase. Clin Chem. 1988;34:497-500.

29. Aebi H. Catalase In: Methods of Enzymatic Analysis. Bergmeyer HU (ed). 1974;673-677.
30. Paglia DE, Valentine WN. Studies on the quantitative and qualitative characterization of erythrocyte glutathione peroxidase. J Lab Clin Med. 1967;70:158-169.
31. Lowry OH, Rosebrough NJ, Farr AL, Randall RI. Protein measurement with Folin phenol reagent. J Biol Chem. 1951;193:265-275.
32. Vinholes J, Gonçalves P, Martel F, Coimbra MA, Rocha SM. Assessment of the antioxidant and antiproliferative effects of sesquiterpenic compounds in *in vitro* Caco-2 cell models. Food Chem. 2014;156:204-211.
33. Wang CY, Wang SY, Chen C. Increasing antioxidant activity and reducing decay of blueberries by essential oils. J Agric Food Chem. 2008;56:3587-3592.
34. Koen YM, Sarma D, Hajovsky H, Galeva NA, Williams TD, Staudinger JL, Hanzlik RP. Protein targets of thioacetamide metabolites in rat hepatocytes. Chem Res Toxicol. 2013;26:564-574.
35. Liu J, Tan H, Sun Y, Zhou S, Cao J, Wang F. The preventive effects of heparin-superoxide dismutase on carbon tetrachloride-induced acute liver failure and hepatic fibrosis in mice. Mol Cell Biochem. 2009;327:219-228.
36. Kim HY, Kim JK, Choi JH, Jung JY, Oh WY, Kim DC, Lee HS, Kim YS, Kang SS, Lee SH, Lee SM. Hepatoprotective effect of pinoresinol on carbon tetrachloride-induced hepatic damage in mice. J Pharmacol Sci. 2010;112:105-112.
37. Ozbek E. Induction of oxidative stress in kidney. Int J Nephrol. 2012;1-9.
38. Silva FG. Chemical-induced nephropathy: a review of the renal tubulointerstitial lesions in humans. Toxicol Pathol. 2004(Suppl 2):71-84.
39. Ciftci O, Disli OM, Timurkaan N. Protective effects of protocatechuic acid on TCDD-induced oxidative and histopathological damage in the heart tissue of rats. Toxicol Ind Health. 2013;29:806-811.
40. Çetin A, Çiftçi O, Otlu A. Protective effect of hesperidin on oxidative and histological liver damage following carbon tetrachloride administration in Wistar rats. Arch Med Sci. 2016;12:486-493.
41. El-Desouky MA, Mahmoud MH, Riad BY, Taha YM. Nephroprotective effect of green tea, rosmarinic acid and rosemary on *N*-diethylnitrosamine initiated and ferric nitrilotriacetate promoted acute renal toxicity in Wistar rats. Interdiscip Toxicol. 2019;12:98-110.
42. Alomar MY. Physiological and histopathological study on the influence of *Ocimum basilicum* leaves extract on thioacetamide-induced nephrotoxicity in male rats. Saudi J Biol Sci. 2020;27:1843-1849.
43. Braunwald E. Coronary blood flow and myocardial ischemia. Heart disease: a textbook of cardiovascular medicine. W.B. Saunders Company. Philadelphia, Pennsylvania, USA. 2001;1161-1183.
44. Sabri A, Hughie HH, Lucchesi PA. Regulation of hypertrophic and apoptotic signaling pathways by reactive oxygen species in cardiac myocytes. Antioxid Redox Signal. 2003;5:731-740.
45. Sawyer DB, Siwik DA, Xiao L, Pimentel DR, Singh K, Colucci WS. Role of oxidative stress in myocardial hypertrophy and failure. J Mol Cell Cardiol. 2002;34:379-388.
46. Celik H, Camtosun A, Ciftci O, Cetin A, Aydın M, Gürbüz S. Beneficial effects of nerolidol on thioacetamide-induced damage of the reproductive system in male rats. Biomed Res. 2016;725-730.
47. Mahmoud NH. Protective effect of *Panax ginseng* against thioacetamide cytotoxicity in liver and kidney of albino rat. J Egypt Soc Toxicol. 2006;34:43-54.
48. Kadir FA, Kassim NM, Abdulla MA, Yehye WA. Effect of oral administration of ethanolic extract of *Vitex negundo* on thioacetamide-induced nephrotoxicity in rats. BMC Complement Altern Med. 2013;13:294.
49. Ciftci O, Ozdemir I, Vardi N, Beytur A, Oguz F. Ameliorating effects of quercetin and chrysin on 2,3,7,8-tetrachlorodibenzo- p-dioxin-induced nephrotoxicity in rats. Toxicol Ind Health. 2012;28:947-954.
50. Ramos-Frendo B, Pérez-Garcia R, López-Novoa JM, Hernando-Avendaño L. Increased severity of the acute renal failure induced by HgCl2 on rats with reduced renal mass. Biomedicine. 1979;31:167-170.
51. Barker EA, Smuckler EA. Nonhepatic thioacetamide injury. II. The morphologic features of proximal renal tubular injury. Am J Pathol. 1974;74:575-590.

Turk J Pharm Sci 2022;19(1):9-18
DOI: 10.4274/tjps.galenos.2021.93195

ORIGINAL ARTICLE

Response Surface Methodology in Spectrophotometric Estimation of Saxagliptin, Derivatization with MBTH and Ninhydrin

Saksagliptinin Spektrofotometrik Tahmininde Tepki Yüzey Metodolojisi, MBTH ve Ninhidrin ile Türevlendirme

Sunitha GURRALA[1], Shiva RAJ[2]*, Subrahmanyam CVS[3], Durga Panikumar ANUMOLU[3], Swathi NARAPARAJU[3], Harika NIZAMPET[3]

[1]Osmania University, University College of Technology, Department of Pharmacy, Hyderabad, India
[2]Osmania University, University College of Science, Department of Chemistry, Hyderabad, India
[3]Osmania University, Gokaraju Rangaraju College of Pharmacy, Hyderabad, India

ABSTRACT

Objectives: Design of experiments assisted spectrophotometric methods have been established for the quantification of saxagliptin in pharmaceutical formulation *via* charge transfer complexation and Schiff's base formation.

Materials and Methods: Box-Behnken design was exploited in method-1, involved the measurement of absorbance of green/blue-colored complex (at 600 nm), formed by the reaction of saxagliptin with 3-methyl-2-benzothiazolinone hydrazone in the presence of ferric chloride. The central composite design was employed in method-2, involved the determination of absorbance of Ruhemann's purple (at 585 nm), formed by the reaction of the primary amine group of saxagliptin with ninhydrin reagent in presence of sodium hydroxide. Optimization of reaction variables namely, reagent concentration (A), oxidizing agent/alkalinity (B) and reaction/heat time (C) was performed through response surface methodology for the response (Y) *i.e.* absorbance of colored compound. The reliability of both methods was investigated through validation as *per* International Council for Harmonisation guidelines.

Results: Saxagliptin executed linearity in the concentration range of 0.01-0.25 µg/mL and 1-10 µg/mL by method-1 and 2. A high value of molar absorptivity, low values of Sandell's sensitivity and limit of detection/limit of quantification divulges the good sensitivity methods. The % assay of saxagliptin in the marketed formulation was found to be 100.27 and 99.86 by method-1 and method-2, respectively.

Conclusion: The proposed eco-friendly and economical methods can be routinely employed in quality control for the analysis of saxagliptin in the pharmaceutical dosage forms.

Key words: Saxagliptin, MBTH, ninhydrin, BBD, CCD

ÖZ

Amaç: Farmasötik formülasyonlarda saksagliptin miktarının yük transfer kompleksasyonu ve Schiff bazı oluşumu yolları ile belirlenmesi için spektrofotometrik yöntem destekli deney tasarımı oluşturulmuştur.

Gereç ve Yöntemler: Yöntem-1'de, demir klorür varlığında, saksagliptin ile 3-metil-2-benzotiazolinon hidrazonun reaksiyonuyla oluşturulan yeşil/mavi renkli kompleksin (600 nm'de) absorbansının ölçülmesini kapsayan Box-Behnken tasarımı kullanılmıştır. Yöntem-2'de, sodyum hidroksit varlığında, saksagliptinin primer amin grubunun ninhidrin reaktifi ile reaksiyonuyla oluşturulan Ruhemann morunun (585 nm'de) absorbansının belirlenmesini kapsayan merkezi kompozit tasarımı kullanılmıştır. Reaktif konsantrasyonu (A), oksitleyici ajan/alkalinite (B) ve reaksiyon/ısı süresi (C) belirlenen reaksiyon değişkenleridir ve optimizasyon, renkli bileşiğin absorbansı gibi cevaplar (Y) için, tepki yüzeyi metodolojisi yoluyla gerçekleştirilmiştir. Her iki yöntemin güvenilirliği, Uluslararası Harmonizasyon Konseyi yönergelerine göre validasyon yoluyla gerçekleştirilmiştir.

Bulgular: Saksagliptinin doğrusallık aralığı metot-1 ve 2 için sırasıyla 0,01-0,25 µg/mL ve 1-10 µg/mL konsantrasyon aralığında uygulanmıştır. Yüksek değerli molar absorptivite, düşük değerli Sandell duyarlılığı ve tayin limiti/teşhis limiti değerleri yöntemlerin duyarlılığını ortaya koymaktadır. Pazarlanan formülasyondaki saksagliptin % miktarı, yöntem-1 ve yöntem-2'ye göre sırasıyla 100,27 ve 99,86 olarak bulunmuştur.

*Correspondence: srajkavadi@gmail.com, Phone: +917337355879, ORCID-ID: orcid.org/0000-0002-2870-5112
Received: 23.10.2020, Accepted: 03.04.2021

Sonuç: Ortaya konulan/önerilen çevre dostu ve ekonomik yöntemler, saksagliptinin farmasötik dozaj formlarındaki analizlerinde rutin olarak uygulanabilir.

Anahtar kelimeler: Saksagliptin, MBTH, ninhidrin, BBD, CCD

INTRODUCTION

Saxagliptin (Onglyza) is an oral antihyperglycemic drug belonging to the dipeptidyl peptidase-4 inhibitor class.[1] Saxagliptin is indicated for patients with type 2 diabetes to improve glycemic control, used alone or along with metformin and/or insulin when these drugs do not provide adequate glycemic control. The recommended dose of saxagliptin is 2.5 mg/5 mg once daily.[2,3] Few methods were reported in the literature on the analysis of saxagliptin using ultraviolet (UV)-spectrophotometric,[4-11] spectrofluorometric, high-performance thin-layer chromatography[12] and high-performance liquid chromatography[13,14] techniques. Colorimetric methods are relatively simple, faster (in terms of sample preparation), inexpensive than chromatographic techniques, and more sensitive, specific over UV-spectrophotometry due to selective chemical reaction of analyte with the reagent to yield a colored derivative.[15-19] The literature review revealed, two colorimetric reports[20,21] for estimation of saxagliptin using chromogenic reagents [(2,3-dichloro-5,6-dicyano-1,4-benzoquinone); (7,7,8,8-tetracyanoquinodimethane); (1,2-naphthoquinone-4-sulfonic acid); (4-chloro-7-nitrobenzofurazan)]. There was no method developed using proposed chromogenic agents such as 3-methyl-2-benzothiazolinone hydrazone (MBTH), ninhydrin, which can produce more sensitive and specific methods for the analysis of saxagliptin.

The literature methods used conventional strategy in experimentation *i.e.*, varying one factor at a time, which may deliver ambiguous and inept optimization in analytical method development, so it must be avoided. This conventional strategy necessitating the use of systematic and statistical approach for optimization of method variables to attain consistent results,[22,23] which can be achieved through analytical quality by design (AQbD) strategy. The AQbD in method development facilitates the simultaneous evaluation of significant variables though design of experiments and response surface analysis for accomplishing enhanced method performance.[24,25]

The contemplated research exploited AQbD approach in the development of visible-spectrophotometric method for the estimation of the saxagliptin through chemical derivatization technique.

MATERIALS AND METHODS

Instrumentation and chemicals

The double beam 1800 UV-visible spectrophotometer (Shimadzu, Japan), analytical balance (Shimadzu AUX 220, Japan) and ultrasonic cleaner (Sonica) were used for the study. Ethanol was purchased from Qualigens, Mumbai. Ferric chloride, sodium hydroxide, MBTH and ninhydrin were purchased from SD Fine-Chem Ltd., Mumbai. Double distilled water was used throughout the study. Saxagliptin standard gift sample was provided by Hetero Laboratories Pvt Ltd., Hyderabad, India. Marketed dosage form (Onglyza®, AstraZeneca) of saxagliptin was procured from the local pharmacy.

Experimental design, data analysis and response surface plots were developed employing Design-Expert trial version 11.0.5.0 software (Stat-Ease Inc. Minneapolis).

Preparation of solutions

The standard stock solution (100 µg/mL) of saxagliptin was prepared by solubilizing accurately weighed 10-mg saxagliptin in 10-mL ethanol and diluted to 100 mL with distilled water. Working standard solution-1 was prepared by diluting 1 mL standard stock solution to 10 mL with distilled water to get 10 µg/mL of saxagliptin. Working standard solution-2 was prepared by diluting 0.1 mL working standard solution-1 to 10 mL with distilled water to get 0.1 µg/mL of saxagliptin.

Solutions of MBTH reagent (1.1% w/v), ferric chloride (3.5% w/v), ninhydrin (1% w/v) and sodium hydroxide (0.4 M) were prepared in distilled water.

Experimental design and optimization

Method-1: Box-Behnken design (BBD) with response surface methodology (RSM) was employed to optimize reaction (saxagliptin-MBTH) conditions for colorimetric method development. The effect of three method variables (at high, low levels), such as the concentration of MBTH (A1): 0.8, 1.2% w/v; concentration of ferric chloride (B1): 1, 5% w/v; reaction time (C1): 10-30 min; on the response (Y1) *i.e.*, absorbance of bluish-green coloured complex was studied at 600 nm in spectrophotometer. Randomized order in experimentation was followed to abate the bias effects of uncontrolled variables for 17 experimental runs under BBD using working standard solution-2 (0.1 µg/mL).

Method-2: Central composite design (CCD) with RSM was exploited to optimize experimental conditions for colorimetric estimation of saxagliptin, upon derivatization with ninhydrin reagent. Working standard solution-1 (10 µg/mL) was used for experimentation. This method optimization was premeditated with 15 experimental runs under CCD (4 factorial points, 5 center points and 6 axial points) to study the influence and interaction of three method parameters (at high, low levels) namely, concentration of ninhydrin reagent (A2): 0.8, 1.2% w/v; concentration of sodium hydroxide (B2): 0.2, 0.6 M; heating time (C2): 5, 15 min; on the response (Y2) *i.e.* absorbance of Ruhemann's purple, measured at 585 nm in a spectrophotometer.

Statistical analysis

Statistical analysis was performed together with the experimental design (BBD/CCD) in Design-Expert software.

The significance of variables was studied through (*p* values) ANOVA. Multiple regression analysis was performed and estimated the correlation coefficient (r^2) for response studied. The main and interaction effects of variables were detected *via* best-fitted models, selected based on various parameters like predicted error sum of squares (PRESS), R^2 (adjusted, predicted), % coefficient of variation (CV), adequate precision and lack of fit analysis. Contour plots (2D) and response surface plots (3D) were employed for quantitative identification of influence of each variable (along with interaction) on the response (Y). The design space was generated as a multi-dimensional combination between variables and response for the maximum desirability function.

Validation of methods

The proposed methods were validated[26] for linearity, accuracy, precision, limit of detection (LOD), and limit of quantification (LOQ) as *per* the International Conference on Harmonization (ICH) guidelines.

Linearity

Method-1: Aliquots (0.01, 0.05, 0.1, 0.15 ,0.2, 0.25 mL) of standard solution (10 µg/mL) of saxagliptin were taken into a series of 10 mL volumetric flasks. To these 0.5 mL of 1.1% MBTH solution and 0.5 mL of 3.5% $FeCl_3$ were added, shaken vigorously and kept a side for 20 min. Then volume was then made up to the mark with water to prepare a series of standard solutions containing 0.01-0.25 µg/mL of saxagliptin. Then, the absorbance of the blue-green colored chromogen was measured at 600 nm against corresponding reagent blank. The amount of saxagliptin was computed from the Beer-Lambert's plot.

Method-2: Aliquots (0.1, 0.2, 0.4, 0.6, 0.8, 1 mL) of standard drug solution (100 µg/mL) of saxagliptin were taken into a series of 10 mL volumetric flasks. To these 2 mL of 1% ninhydrin reagent, 2 mL of 0.4 M NaOH was added, shaken vigorously and heated for 13 min. The volume was then made up to the mark with water to prepare a series of standard solutions containing 1-10 µg/mL of saxagliptin. Then, the absorbance of the yellow-purple colored chromogen was measured at 585 nm against corresponding reagent blank. The amount of saxagliptin was computed from the Beer-Lambert's plot.

Precision

The intra-day and inter-day precision of the proposed colorimetric methods were determined for three different concentrations of saxagliptin within the linearity range. Estimated the corresponding response of solutions prepared three times on the same day and three different days of a week. The results were reported in terms of relative standard deviation (% RSD).

Accuracy

The accuracy of the method was determined by calculating recoveries of saxagliptin using the method of standard additions. Known concentration of saxagliptin solutions were added at 80, 100, and 120% levels to pre-quantified sample solutions of saxagliptin and analyzed through proposed methods. Each sample was prepared in triplicate at each level. The amount of saxagliptin was estimated by applying the obtained values to regression equation.

Sensitivity

The LOD and LOQ of saxagliptin by proposed methods were derived from the standard calibration curve using 3.3 σ/s and 10 σ/s, formulae, respectively, where s is the slope of the calibration curve and σ is standard deviation of the y-intercept of regression equation.[27]

Assay of saxagliptin marketed dosage form

Twenty tablets of saxagliptin (Onglyza®) were weighed and powdered. The powder quantity equivalent to 10 mg of the drug was dissolved in 10 mL ethanol, filtered (using Whatman's filter paper) into 100 mL volumetric flask and made the volume up to the mark with distilled water. From this 1 mL was transferred into a 10 mL volumetric flask, added 2 mL of 1% ninhydrin reagent and 2 mL of 0.4 M sodium hydroxide, shaken vigorously and heated for 13 min (method-2). For method-1, further filtrate (1 mL diluted to 10 mL with water) was diluted. To this 0.1-mL solution, added 0.5 mL each 1.1% MBTH and 3.5% $FeCl_3$, shaken vigorously and kept aside for 20 min. The volume was made up to the mark with distilled water. The absorbance of the resulting colored solution was measured at 600 (method-1)/585 nm (method-2) against the corresponding reagent blank. The amount of saxagliptin was calculated from the Beer-Lambert's plot.

RESULTS AND DISCUSSION

Basis for color development

Direct spectroscopy method for analysis of a saxagliptin in pharmaceutical formulation may prone interferences due to matrix effect. Chemical derivatization of drug enhances selectivity and sensitivity of the method. The proposed methods subjugated the saxagliptin to chemical derivatization using chromogenic reagents (MBTH and ninhydrin) for its visible spectroscopic analysis.

In method-1, saxagliptin undergoes an oxidative coupling reaction with MBTH in the presence of oxidizing agent (ferric chloride) to produce bluish-green colored chromogen. Initially, oxidation (loss of 2 electrons and 1 proton) of MBTH by ferric chloride occurs to give an electrophilic intermediate, which coupled at the most nucleophilic site of saxagliptin and forms a bluish-green colored chromogen (Figure 1), which absorbs visible light maximally at a wavelength of 600 nm in a spectrophotometer.

In method-2, ninhydrin undergoes tautomerism (with loss of water) to 1,2,3-indane trione, which actively reacts with the primary amine group of saxagliptin and forms a Schiff base. In this reaction attack of the nucleophile (amine) on the electrophile (carbonyl group) of 1,2,3-indane, followed by dehydration occurs. Further hydrolysis gives an intermediate amine due to isolation of carbonyl compound. A deep blue/purple color compound (diketohydrindylidene-diketohydrindamine) extensively known as Ruhemann's purple produces upon

condensation of an intermediate amine with another molecule of ninhydrin (Figure 2), exhibiting absorption maxima at 585 nm in a spectrophotometer.

Evidence of chemical derivatization

Saxagliptin chemical derivatization with proposed reagents was evidenced by the thin layer chromatography (TLC) analysis of reaction mixture. Pre-coated TLC plates were spotted separately for method-1 and 2 with a freshly prepared solution of saxagliptin, reagent blank solution and chromogen produced using that method. Plates were developed in saturated chromatographic tanks using ethyl acetate: acetonitrile (7:3) as a mobile phase and spots were visualized in the UV chamber at 254 nm. Three spots were observed with different retention factor values on both plates (method-1 and method-2), indicates three different compounds. Higher retardation factor values were observed for derivatives (Supplementary 1), denotes the formation of a new compound by the proposed reaction mechanism.

Method optimization via AQbD approach

Optimization of reagent concentration, diluting solvent and time for color development was established to accomplish

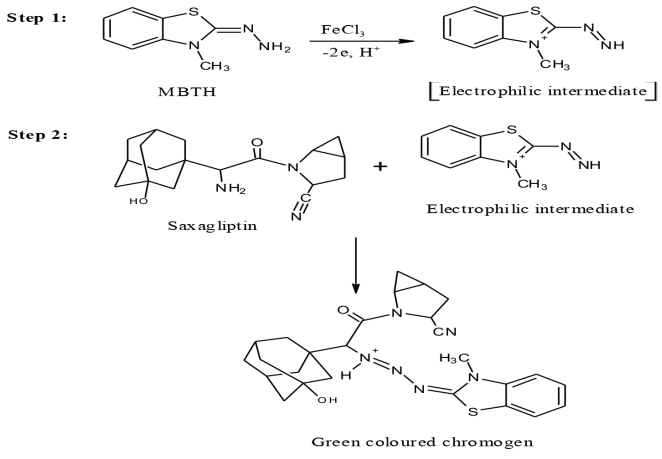

Figure 1. Oxidative coupling reaction between saxagliptin and MBTH
MBTH: 3-methyl-2-benzothiazolinone hydrazone

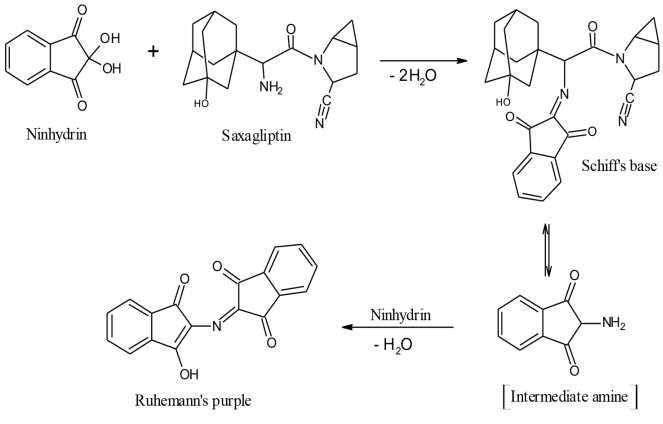

Figure 2. Schiff's base formation and condensation of saxagliptin with ninhydrin

maximum absorbance and stability. The influence of variables on absorption values of colored species was studied by multivariate approach.

The matrix of BBD, CCD and results of experimental runs performed on UV-visible spectrophotometer are provided in Table 1. ANOVA was performed for experimental observations to evaluate the significant effect of variables on the response, summarized in Table 2. The experimental results are fitted to a second-order polynomial (quadratic) model for the response Y being studied (absorbance), given by the following equations:

$$Y1=0.5830+0.0426\,A_1+0.0413\,B_1+0.0106\,C_1+0.0032\,A_1B_1+0.0040\,A_1C_1+0.0062\,B_1C_1-0.0390\,A_1^2-0.0593\,B_1^2-0.0190\,C_1^2$$

$$Y2=+0.9808+0.0788\,A_2+0.0198\,B_2+0.0431\,C_2-0.0444\,A_2B_2+0.0438\,A_2C_2+0.0433\,B_2C_2-0.0726\,A_2^2-0.0824\,B_2^2-0.0379\,C_2^2$$

Statistical analysis data of both methods reveal the significant effect of three variables (A, B, C) on the response under study as their *p* values (probability) found below the considered value ($p<0.05$) at 95% confidence levels. The high values of regression co-efficient ($r^2>0.999$) obtained, indicates the good correlation between the experimental data and the selected models. CV found to be less than 5%, indicates the reproducibility of model. The values of low PRESS, high adequate precision (>4), agreement between the predicted and adjusted R^2 (difference <0.2) denoted the model aptness.

The sensitiveness of a specific response by the perturbation of an individual factor from its reference value (while other factors kept constant) was studied through the construction of perturbation plots. The steepest slope of perturbation plots (Supplementary 2a) observed, indicates that the response (absorbance) in method-1 is highly influenced by the concentration of MBTH (A1) followed by the concentration of ferric chloride (B1). Curvature in plots (Supplementary 2b) indicate the response (absorbance) in method-2 is highly affected by the concentration of ninhydrin (A2) and followed by reaction heating time (C2). Variable-response relationship was visualized through contour (2D) and response surface (3D) graphs. These plots can be used to find the response for a given set of input variables, the non-linear trend in response surfaces (Supplementary 3, 4) was observed, reveals the existence of a high degree of interaction (among variables) that effects the method response. Optimization of variables for maximum spectrophotometric absorbance at respective wavelengths was carried out using Derringer's desirability function. The solution with maximum desirability value is selected as an optimized one, out of different solutions provided by the software. The design space generated is portrayed in Figure 3, indicated high performance owing to maximum desirability value (equal to 1) for both methods and unveiled method operable design region with the location of the optimized solution for the design studied.

The optimized conditions interpreted from statistical and response surface analysis are as follows. Method-1: 1.1% w/v MBTH (A1), 3.5% w/v ferric chloride (B1) and reaction time 20 min (C1). Method-2: 1% w/v ninhydrin reagent (A2), 0.4 M sodium hydroxide (B2) and reaction heating time 13 min (C2). These reaction conditions are adequate for

Table 1. Box-Behnken design, central composite design and experimental results

Box-Behnken design					Central composite design				
Run	Factors			Response	Run	Factors			Response
	A1	B1	C1	Y1		A2	B2	C2	Y2
1	1	3	20	0.584	1	1.2	0.2	15	0.934
2	0.8	5	20	0.477	2	1.2	0.6	5	0.711
3	1	3	20	0.586	3	1	0.4	10	0.979
4	1	5	10	0.529	4	1.28	0.4	10	0.948
5	1.2	3	10	0.554	5	0.72	0.4	10	0.725
6	0.8	3	10	0.479	6	0.8	0.2	5	0.688
7	1	3	20	0.582	7	1	0.4	17	0.967
8	0.8	3	30	0.488	8	1	0.4	10	0.977
9	1.2	1	20	0.486	9	0.8	0.6	15	0.815
10	1	1	30	0.468	10	1	0.4	10	0.981
11	1.2	5	20	0.571	11	1	0.4	03	0.845
12	1.2	3	30	0.579	12	1	0.68	10	0.845
13	1	3	20	0.582	13	1	0.4	10	0.983
14	0.8	1	20	0.405	14	1	0.18	10	0.789
15	1	1	10	0.455	15	1	0.4	10	0.982
16	1	5	30	0.567	-				
17	1	3	20	0.581					

A1: MBTH (%), B1: Ferric chloride (%), C1: Reaction time (min), Y1: Absorbance of blue-green complex, A2: Ninhydrin (%), B2: NaOH (M), C2: Heat time (min), Y2: Absorbance of Ruhemann's purple, MBTH: 3-methyl-2-benzothiazolinone hydrazone

Table 2. ANOVA and regression analysis of selected models

Response	Y1	Y2		Y1	Y2
Fit model	Quadratic	Quadratic	SD	0.0037	0.0026
Sum of squares	0.0541	0.1698	Mean	0.5278	0.8779
df	9	9	% CV	0.6952	0.2919
Mean square	0.0060	0.0189	R^2	0.9983	0.9998
F value	446.60	2873.81	Adjusted R^2	0.9960	0.9995
p value	<0.0001	<0.0001	Predicted R^2	0.9764	0.9937
Lack of fit (*p* value)	0.0509	0.2670	Adequate precision	63.56	139.48
			PRESS	0.0013	0.0011

SD: Standard deviation, CV: Coefficient of variation, PRESS: Predicted error sum of squares

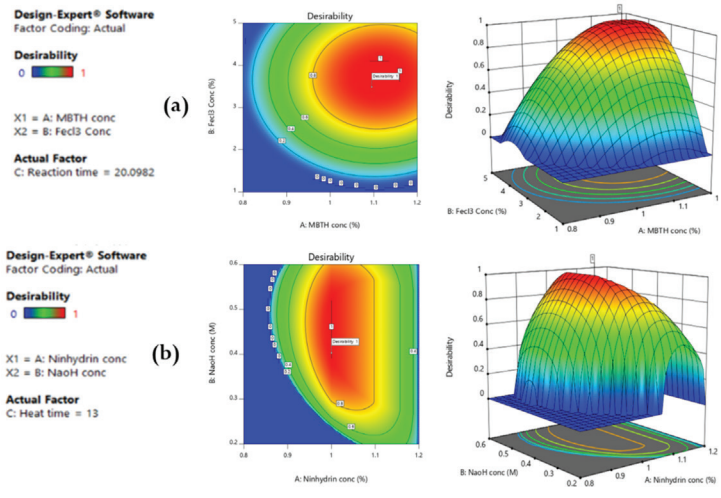

Figure 3. Desirability study (2D, 3D plot), (a): Design space for method-1, (b): Design space for method-2

reproducible, maximum color development for spectroscopic estimation of saxagliptin and were verified through practical experimentation. The UV-visible absorbance spectrum of saxagliptin under optimized conditions was recorded (Supplementary 5) for method-1 and 2.

Effect of solvents

Diluting solvent plays an important role in the stability of the colored complex. The effects of different diluting solvents, such as acetone, acetonitrile, ethanol, methanol, and distilled water have been studied (Figure 4) for measurement under optimized reaction conditions. The best sensitivity, maximum

UV absorption, and product stability were attained when water was used as a solvent for both the methods. Both reagents were freely soluble in water. Hence, distilled water was selected as a diluting solvent for proposed methods that dwindle the cost of experiment and considered as a green approach for spectrophotometric method development.

The stoichiometry of the reaction

The stoichiometry of the reaction in method-1 and method-2 was studied by Job's continuous variation method. Equimolar solutions ($3.174x10^{-6}$ M) of saxagliptin and reagents (MBTH and ninhydrin) were prepared in distilled water. The drug and reagent (MBTH: method-1/ninhydrin: method-2) were mixed in various proportions to produce different mole ratio values (0, 0.2, 0.4, 0.5, 0.6, 0.8, 1). These solutions were analyzed through the proposed methods. The stoichiometric relationship displayed in Figure 5. A mole ratio of 0.5 gave the highest absorbance value for method-1 whereas 0.7 for method-2. This mole ratio values indicates that saxagliptin has one center (primary amino group) available for the chromogenic reaction with MBTH (1 molecule) and ninhydrin (2 molecules) reagents at their optimum wavelengths.

Validation of the proposed methods

The proposed methods were statistically validated as *per* ICH guidelines and results are provided in Table 3. Linear regression analysis was performed for the Beer's Law data (Supplementary 6), and calibration plots (Supplementary 7) were drawn (correlation co-efficient 0.999). A linear increase in the absorbance was found with an increase in saxagliptin concentration at a range of 0.01-0.25 µg/mL and 1-10 µg/mL of saxagliptin by method-1 and 2, respectively. Overlaid UV-visible spectra of saxagliptin in the linearity range is shown in Figure 6. Precision studies evinced the reproducibility of proposed method (Supplementary 8), where no significant difference between intra and inter-day precision values was observed and % RSD values were less than 2. The % recoveries of saxagliptin (Supplementary 9) denote the fair accuracy of proposed methods with no interference of tablet excipients. A high value of the molar absorptivity and low values of Sandell's sensitivity, LOD, and LOQ signposts the good sensitivity of proposed methods.

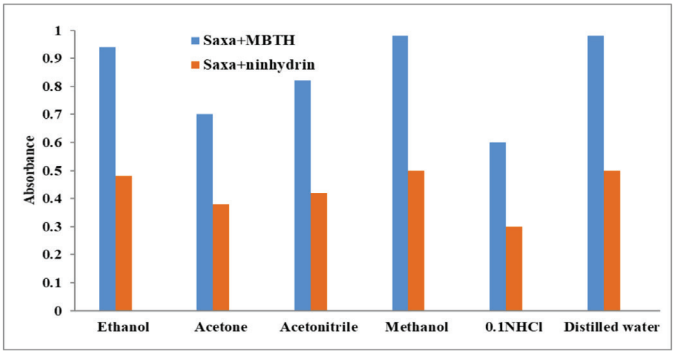

Figure 4. Effect of solvent on saxagliptin reaction with MBTH and ninhydrin
MBTH: 3-methyl-2-benzothiazolinone hydrazone

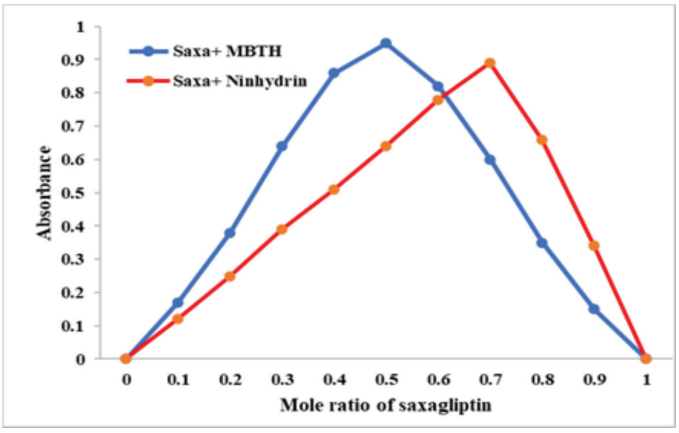

Figure 5. Job's continuous variation plot for method-1 and method-2
MBTH: 3-methyl-2-benzothiazolinone hydrazone

Assay of saxagliptin marketed dosage form

The proposed methods were applied for the assay of marketed dosage forms containing saxagliptin (label claim 5 mg). The

Table 3. Optimized characteristics of saxagliptin

Parameters	Value	
	Method-1	Method-2
Absorption wavelength (nm)	600	585
Beers law range (µg/mL)	0.01-0.25 µg/mL	1-10 µg/mL
Regression equation	Y=2.7709x+0.307	Y=0.0704x+0.2494
Correlation coefficient (r^2)	0.999	0.999
Limit of detection (µg/mL)	0.002	0.328
Limit of quantification (µg/mL)	0.007	0.994
Molar absorptivity (L $mole^{-1}$ cm^{-1})	$0.189x10^7$	$0.302x10^5$
Sandell's sensitivity (µg cm^{-2})	$1.66x10^{-3}$	$1.04x10^{-7}$
Stability of colored species	7 hr	5 hr

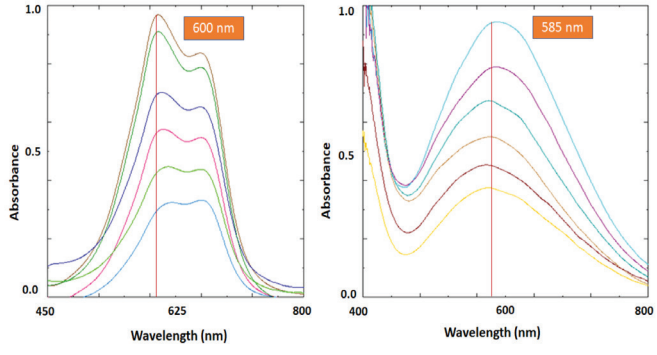

Figure 6. Overlaid UV-visible spectra (a): Saxagliptin (0.01-0.25 µg/mL) with MBTH, (b): Saxagliptin (0.1-10 µg/mL) with ninhydrin
UV: Ultraviole, MBTH: 3-methyl-2-benzothiazolinone hydrazone

Table 4. Comparison of proposed method with literature methods of saxagliptin

Parameter	Reported method[21]		Reported method[20]		Proposed method	
Chromogenic reagent	DDQ	TCNQ	NQS	NBD-Cl	MBTH	Ninhydrin
λ_{max} (nm)	461	838	475	470	600	585
LOD (µg/mL)	2.53	2.79	1.0	0.56	0.002	0.328
LOQ (µg/mL)	7.68	8.46	3.01	1.68	0.007	0.994
Linearity range	50-300	10-110	5-30	3-20	0.01-0.25	1-10
Time of reaction (min)	40	30	10	15	20	13
Reaction stability	50 min	1 hr	4 hr	4 hr	7 hr	5 hr
Diluting solvent	Methanol	Methanol	Water	Methanol	Water	Water

DDQ: (2,3-dichloro-5,6-dicyano-1,4-benzoquinone), TCNQ: (7,7,8,8-tetracyanoquinodimethane), NQS: (1,2-Naphthoquinone-4-sulfonic acid), NBD-Cl: (4-chloro-7-nitrobenzofurazan), MBTH: (3-methyl-2-benzothiazolinone hydrazone), LOD: Limit of detection, LOQ: Limit of quantification, max: Maximum

% assay of saxagliptin was found to be 100.27 and 99.86 by method-1 and method-2, respectively. There was no interference of formulation excipients during the estimation of saxagliptin in tablets. The assay values were found to be within the limits and % RSD was less than 2.

Comparison with reported analytical methods

The proposed AQbD method is found to be superior to literature methods due to its ability to predict interactive effects of parameters on the performance of the method. The literature methods have limitations such as less robust, less feasibility for method transfer, no variable- interaction study and required a high number of experiments.

Study limitations

These limitations were eliminated using RSM in this investigation. Two chromogenic reagents (MBTH and ninhydrin) were employed for chemical derivatization of saxagliptin, which were not reported earlier. From Table 4, this method was found to be highly sensitive than literature methods, owed to linearity at lower concentration range, LOD and LOQ values (0.007, 0.994). The proposed methods rely on the use of distilled water as a solvent, which point to an economical and eco-friendly method for drug analysis.

CONCLUSION

In this study, two spectrophotometric methods were developed which evaded the use of organic solvents for the analysis of saxagliptin in bulk and pharmaceutical dosage forms. Chemical derivatization mechanisms for saxagliptin with MBTH and ninhydrin were proposed. The optimization of reaction conditions for visible spectroscopic estimation of the drug was performed through AQbD approach, where experimental design (BBD, CCD), statistical analysis and response surface analysis were employed. The proposed methods obeyed validation criterion of ICH. The assay values agreed well with the label claim and suggested that no interference of formulation excipients during the estimation of the drug. Contemplated methods are more sensitive, less chemical hazardous and versatile over reported methods. Hence, the proposed eco-friendly and economical methods can be routinely employed in quality control for the analysis of saxagliptin in the pharmaceutical dosage forms.

Conflict of interest: No conflict of interest was declared by the authors. The authors are solely responsible for the content and writing of this paper.

REFERENCES

1. Rosenstock J, Sankoh S, List JF. Glucose-lowering activity of the dipeptidyl peptidase-4 inhibitor saxagliptin in drug-naive patients with type 2 diabetes. Diabetes Obes Metab. 2008;10:376-386.
2. Jadzinsky M, Pfützner A, Paz-Pacheco E, Xu Z, Allen E, Chen R; CV181-039 Investigators. Saxagliptin given in combination with metformin as initial therapy improves glycaemic control in patients with type 2 diabetes compared with either monotherapy: a randomized controlled trial. Diabetes Obes Metab. 2009;11:611-622.
3. Rosenstock J, Aguilar-Salinas C, Klein E, Nepal S, List J, Chen R; CV181-011 Study Investigators. Effect of saxagliptin monotherapy in treatment-naïve patients with type 2 diabetes. Curr Med Res Opin. 2009;25:2401-2411.
4. Koli SN, Belvotagi AV, Mudke RP, Patil SA. UV spectrophotometric method development and validation for estimation of saxagliptin in API and in pharmaceutical dosage form. Int J Pharm Pharm Res. 2019;14:166-179.
5. Zameeruddin M, Bundel SS, Bharkad VB, Khan HN, Sandip TT. Development and validation of UV spectroscopic method for simultaneous estimation of dapagliflozin and saxagliptin in synthetic mixture. Int J Pharm Anal Res. 2019;8:59-66.
6. Bhadauria RS, Agarwal V. Development and validation of UV spectroscopic method for simultaneous estimation of dapagliflozin and saxagliptin in marketed formulation. J Drug Deliv Ther. 2019;9:1160-1164.
7. Raveendra BG, Kumar RA, Shaheen SD, Greeshma A, Satyanarayana M, Manikanta RSHT, Syam CPB. A novel stability-indicating method for the simultaneous estimation of saxagliptin and dapagliflozin in rat serum by using UV spectroscopy. Pharm Anal Acta. 2018;9:3.
8. Suthar AS, Prajapati L, Joshi A, Patel J, Kharofiya ML, Sahah SBM. Estimation of saxagliptin hydrochloride and dapagliflozin propendiol monohydrate in combined dosage form. J Innov Appl Pharm Sci. 2018;3:1-7.

9. Sisode PS, Raj HA, Jain VC. Simultaneous determination of saxagliptin hydrochloride and glibenclamide in synthetic mixture using spectrophotometric technique (first order derivative method). Asian J Pharm Anal. 2016;6:77-82.
10. Nyola N, Jeyebalan G. Development and validation of UV-Vis spectroscopy method for simultaneous estimation of saxagliptin hydrochloride and metformin hydrochloride in active pharmaceutical ingredient. J Pharm Edu Res. 2012;3:19-23.
11. Kalaichelvi R, Jayachandran E. Validated spectroscopic method for estimation of saxagliptin in pure and from tablet formulation. Int J Pharm Pharm Sci. 2011;3:179-180.
12. Veeresham C, Srividya S, Swetha E. Development and validation of high-performance thin layer chromatographic method for quantitative analysis of saxagliptin. Am J Analyt Chem. 2015;6:797-806.
13. Donepudi S, Achanta S. Simultaneous estimation of saxagliptin and dapagliflozin in human plasma by validated high performance liquid chromatography - ultraviolet method. Turk J Pharm Sci. 2019;16:227-233.
14. Aswini R, Eswarudu MM, Babu PS. A novel RP-HPLC method for simultaneous estimation of dapagliflozin and saxagliptin in bulk and pharmaceutical dosage form. Int J Pharm Sci Res. 2018;9:5161-5167.
15. Adegoke OA, Babalola CP, Kotila OA, Obuebhor O. Simultaneous spectrophotometric determination of trimethoprim and sulphamethoxazole following charge-transfer complexation with chloranilic acid. Arab J Chem. 2017;10:S3848-S3860.
16. Sunil Kumar AVVNK. Reddy TV, Sekharan CB. Utility of picric acid and 2,4 dinitrophenol as chromogenic reagents for visible spectrophotometric quantification of alogliptin. Bull Fac Pharm Cairo Univ. 2017;55:177-184.
17. Pani Kumar AD, Archana G, Sunitha G, Rachel Paul K, Harika R, Sowndarya NSKR. Simplistic application of 3-methy-2-benzothiazoline hydrazone (MBTH), an oxidative coupling chromogenic reagent for quantification of metaxalone and dabigatran etexilate mesylate bulk drug and their dosage forms. Pharm Anal Acta. 2015;6:5.
18. Varsha MS, Babu NR, Padmavathi Y, Kumar PR. Development of new spectrophotometric method for estimation of tenofovir disoproxil fumarate using MBTH reagent. Int Curr Pharm J. 2015;4:378-381.
19. Ismail NBS, Narayana B. Spectrophotometric determination and spectroscopic studies on Schiff base and charge transfer complex of ketorolac tromethamine. J Anal Sci Technol. 2015;6:32.
20. Moneeb MS. Spectrophotometric and spectrofluorimetric methods for the determination of saxagliptin and vildagliptin in bulk and pharmaceutical preparations. Bull Fac Pharm Cairo Univ. 2013;51:139-150.
21. El-Bagary RI, Elkady EF, Ayoub BM. Spectrophotometric methods based on charge transfer complexation reactions for the determination of saxagliptin in bulk and pharmaceutical preparation. Int J Biomed Sci. 2012;8:204-208.
22. Abd-alaah HJ, Hamody AS. Design of experiments model for optimization of spectrophotometric determination of phenylephrine hydrochloride in pure and pharmaceutical formulations using p-bromanil. J Pharm Sci Res. 2019;11:501-507.
23. Wani YB, Patil DD. An experimental design approach for optimization of spectrophotometric method for estimation of cefixime trihydrate using ninhydrin as derivatizing reagent in bulk and pharmaceutical formulation. J Saudi Chem Soc. 2017;21:S101-S111.
24. Papanna RK, Gowda JBK, Nagaraja P. An experimental design approach for optimization of spectrophotometric estimation of mirabegron in bulk and pharmaceutical formulations. J Anal Chem. 2018;73:884-893.
25. Demirkaya-Miloglu F, Polatdemir E, Senol O, Kadioglu Y. Design and optimization of a novel spectrophotometric method using response surface methodology for the determination of losartan potassium in pharmaceuticals. Curr Pharm Anal. 2017;13:552-558.
26. International conference on harmonization (ICH) of technical requirements for registration of pharmaceuticals for human use, Validation of analytical procedures: Text Q2 (R1) Geneva, 2005:1-5.
27. International conference on harmonization (ICH) of technical requirements for registration of pharmaceuticals for human use, Validation of analytical procedures: Methodology. Q2 (R1) Geneva, 2005:6-13.

Supplementary 1. TLC analysis of saxagliptin and reaction products

Sample	Method-1	Method-2
	R_f value	R_f value
Saxagliptin standard	0.11±0.004	0.12±0.003
Reagent blank	0.34±0.02	0.46±0.03
Saxagliptin-chemical derivative	0.59±0.02	0.72±0.04

TLC: Thin layer chromatography

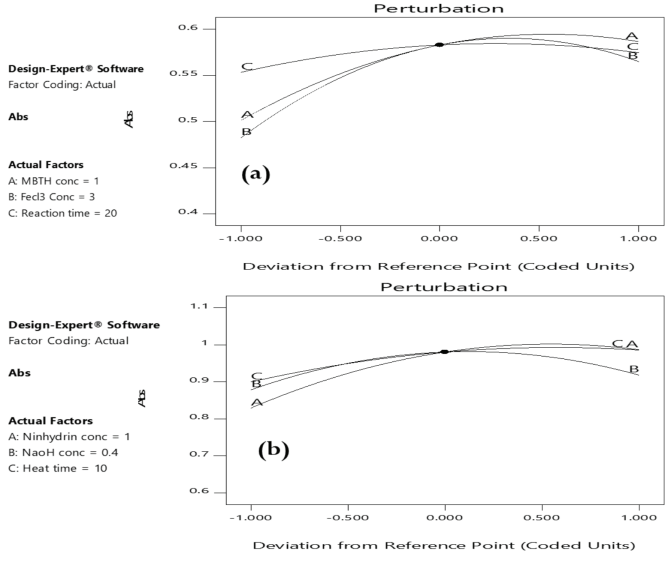

Supplementary 2. Perturbation plots of variables (a) method-1 (b) method-2

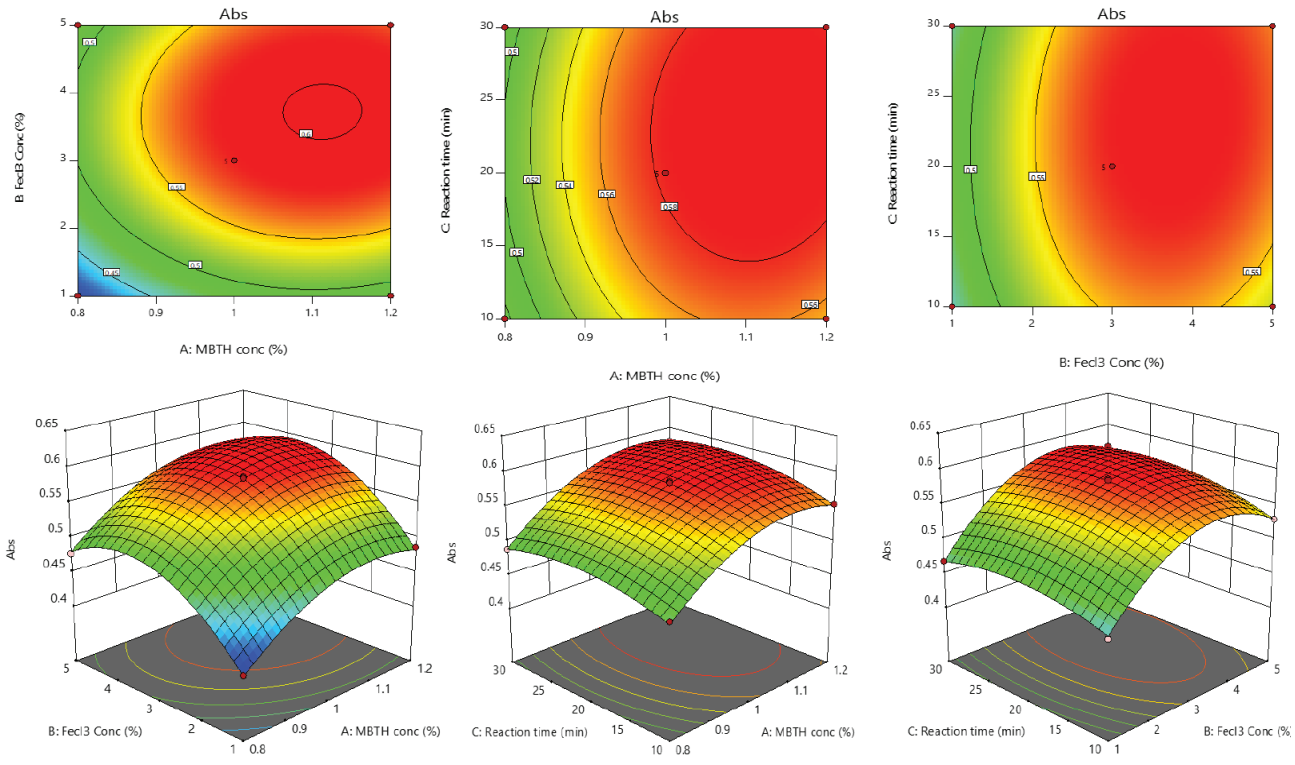

Supplementary 3. Contour (2D), response surface plots (3D) of two variable interactions in method-1

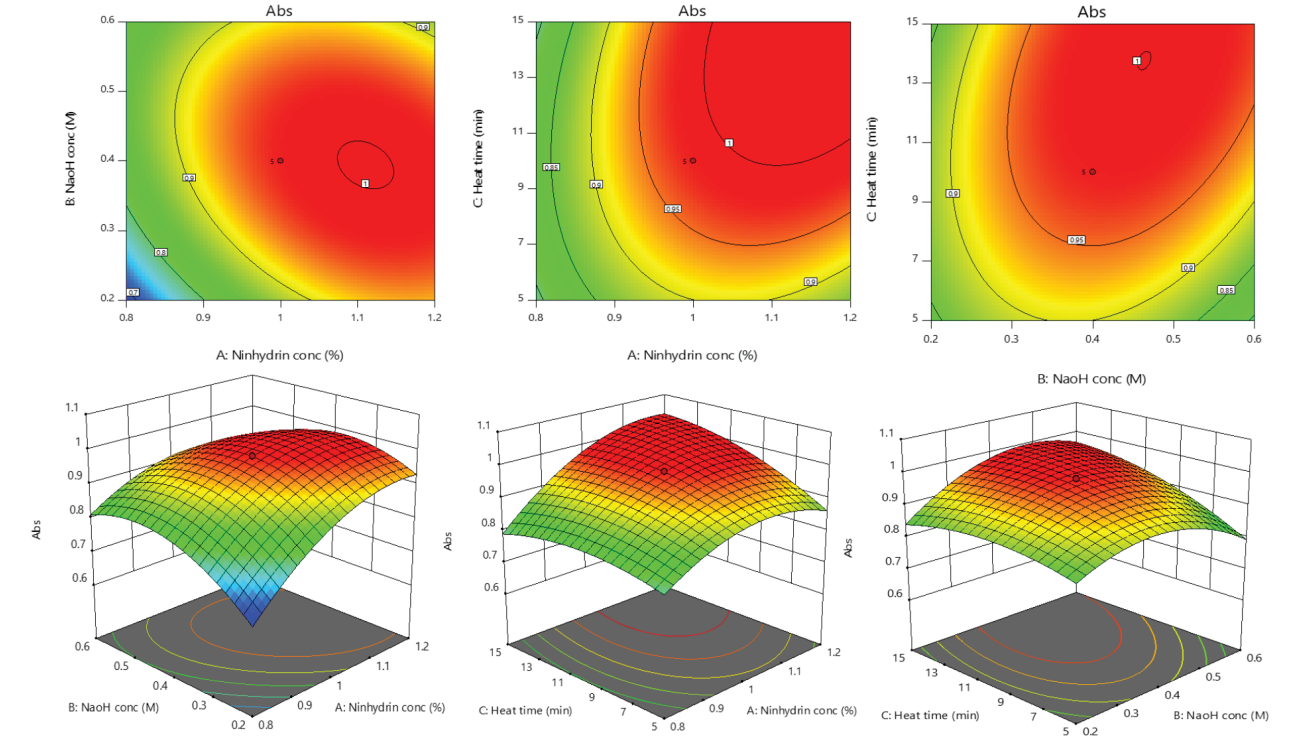

Supplementary 4. Contour (2D), response surface plots (3D) of two variable interactions in method-2

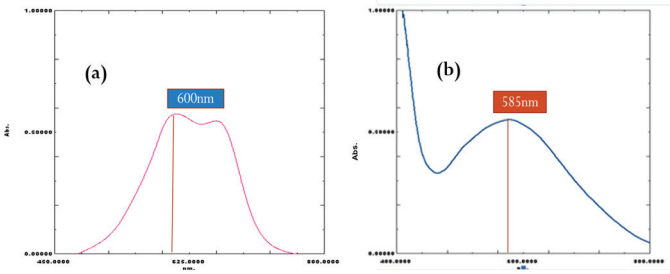

Supplementary 5. UV-visible spectrum, (a): Saxagliptin (0.1 µg/mL) with MBTH, (b): Saxagliptin (5 µg/mL) with ninhydrin

UV: Ultraviole, MBTH: 3-methyl-2-benzothiazolinone hydrazone

Supplementary 6. Data of linearity studies

S. no	Method-1		Method-2	
	Concentration (µg/mL)	Absorbance (AM ± SD) n=6	Concentration (µg/mL)	Absorbance (AM ± SD) n=6
1	0.01	0.331±0.002	1	0.315±0.007
2	0.05	0.445±0.007	2	0.402±0.011
3	0.1	0.587±0.011	4	0.525±0.015
4	0.15	0.722±0.014	6	0.669±0.018
5	0.2	0.874±0.015	8	0.811±0.017
6	0.25	0.989±0.015	10	0.957±0.019

AM: Arithmetic mean, SD: Standard deviation, n: Number of determinations

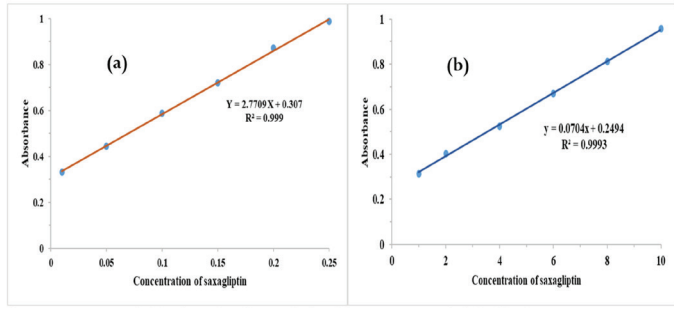

Supplementary 7. Calibration plot of saxagliptin with MBTH (a) and ninhydrin (b)

MBTH: 3-methyl-2-benzothiazolinone hydrazone

Supplementary 8. Results of precision studies

Method	Concentration saxagliptin (µg/mL)	Intra-day analysis		Inter-day analysis	
		Concentration found (AM ± SD), n=3	% RSD	Concentration found (AM ± SD), n=3	% RSD
Method-1	0.1	0.098±0.001	1.02	0.109±0.002	1.8
	0.15	0.153±0.002	1.30	0.159±0.003	1.88
	0.2	0.206±0.002	0.97	0.212±0.003	1.46
Method-2	2	2.06±0.011	0.53	2.08±0.021	1.0
	6	5.95±0.028	0.47	6.01±0.032	0.53
	10	9.97±0.033	0.33	9.95±0.024	0.24

AM: Arithmetic mean, SD: Standard deviation, n: Number of determinations, RSD: Relative standard deviation

Supplementary 9. Results of accuracy studies of proposed methods with tablets

Method	Level of recovery (%)	Theoretical content (µg/mL)	Amount recovery (AM ± SD), n=3 (µg/mL)	% Recovery	% RSD
Method-1	80	0.18	0.178±0.003	98.88	1.7
	100	0.2	0.203±0.003	101.5	1.5
	120	0.22	0.222±0.004	100.9	1.8
Method-2	80	7.2	7.16±0.07	99.44	0.98
	100	8	8.07±0.08	100.87	0.99
	120	8.8	8.77±0.05	99.65	0.57

AM: Arithmetic mean, SD: Standard deviation, n: Number of determinations, RSD: Relative standard deviation

Turk J Pharm Sci 2022;19(1):19-27
DOI: 10.4274/tjps.galenos.2021.63903

ORIGINAL ARTICLE

Influence of Vehicles and Penetration Enhancers on the Permeation of Cinnarizine Through the Skin

Taşıyıcıların ve Penetrasyon Artırıcıların Sinarizinin Deriden Permeasyonuna Etkisi

Şükran DAMGALI[1], Samet ÖZDEMİR[2], Asli BARLA DEMİRKOZ[3,4], Melike ÜNER[1]*

[1]Istanbul University, Faculty of Pharmacy, Department of Pharmaceutical Technology, Istanbul, Turkey
[2]Istanbul Health and Technology University, Faculty of Pharmacy, Department of Pharmaceutical Technology, Istanbul, Turkey
[3]Aromsa Flavours and Food Additives Inc. Co., Department of Research and Development Center, Kocaeli, Turkey
[4]Halic University, Faculty of Health Sciences, Department of Nutrition and Dietetics, Istanbul, Turkey

ABSTRACT

Objectives: The aim of this study was to determine the influence of vehicles and penetration enhancers on the penetration and permeation of cinnarizine (CNZ) through the skin.

Materials and Methods: Topical formulations based on hydrogel, o/w emulsion and oleaginous cream were prepared. After determination of physical properties of formulations, the penetration and permeation of CNZ through the *stratum corneum* and *full-thickness* skin was investigated by an *ex vivo* study.

Results: The cumulative amount of CNZ permeated from the base hydrogel formulation was about 5 times higher than the base o/w emulsion and base oleaginous cream formulations. The incorporation of penetration enhancers to the base hydrogel and o/w emulsion formulations generally increased CNZ penetration through the skin. Transcutol® was confirmed to provide the highest penetration in the hydrogel formulation. Propylene glycol was found to be the most suitable penetration enhancer for CNZ in the oleaginous cream. Glycerol and oleic acid displayed the highest effect in the o/w emulsion.

Conclusion: It was concluded that the hydrogel containing Transcutol® provided the highest penetration through the skin among all formulations and this formulation could be an alternative to the oral route in the treatment of Ménière's disease and motion sickness. Thus, the risk of systemic side effects caused by oral medication can be reduced or eliminated.

Key words: Cinnarizine, Ménière's disease, motion sickness, penetration enhancers, skin permeation

ÖZ

Amaç: Bu çalışmanın amacı taşıyıcıların ve penetrasyon artırıcıların sinarizinin (CNZ) deriden penetrasyonu ve permeasyonu üzerindeki etkisini tayin etmektir.

Gereç ve Yöntemler: Hidrojel, y/s emülsiyonu ve yağlı krem bazlı topikal formülasyonlar hazırlandı. Formülasyonların fiziksel özelliklerinin tayininden sonra, CNZ'nin *stratum corneum* ve tam kalınlıkta deriye penetrasyon ve permeasyonu bir *ex vivo* çalışma ile incelendi.

Bulgular: Baz hidrojel formülasyonundan nüfuz eden kümülatif CNZ'nin miktarı, baz y/s emülsiyonu ve baz yağlı krem formülasyonlarından yaklaşık 5 kat daha yüksekti. Baz hidrojel ve y/s emülsiyon formülasyonlarına penetrasyon artırıcıların ilavesi, genellikle CNZ'nin deriden penetrasyonunu artırdı. Transcutol®'un hidrojel formülasyonunda en yüksek pentrasyonu sağladığı doğrulandı. CNZ için yağlı kremde en uygun penetrasyon artırıcı propilen glikol olarak bulundu. Gliserol ve oleik asit y/s emülsiyonunda en yüksek etkiyi gösterdi.

Sonuç: Transcutol® içeren hidrojelin tüm formülasyonlar arasında deriden en yüksek CNZ geçişi sağladığı ve bu formülasyonun Meniere hastalığı ile hareket hastalığının tedavisinde oral yola bir alternatif olabileceği sonucuna varıldı. Böylece ağızdan alınan ilacın neden olduğu sistemik yan etki riski azaltılabilir veya ortadan kaldırılabilir.

Anahtar kelimeler: Sinarizin, Meniere hastalığı, hareket hastalığı, penetrasyon artırıcılar, deri geçirgenliği

A part of this study was presented as a poster in International Multidisciplinary Symposium on Drug Research and Development in Erzurum, Turkey in 5-7 October 2017.

***Correspondence:** melikeuner@yahoo.com, **Phone:** +90 212 440 00 00, **ORCID-ID:** orcid.org/0000-0003-2786-5947

Received: 28.11.2020, **Accepted:** 06.04.2021

INTRODUCTION

Cinnarizine (CNZ) is a piperazine derivative histamine H1-antagonist and a selective calcium channel blocker drug.[1,2] It is commonly prescribed for peripheral and cerebral disorders, vertigo, tinnitus, nystagmus, motion sickness and Ménière's disease. There are only oral formulations in the pharmaceutical market of CNZ. The oral bioavailability of CNZ is low and variable. Many side effects of CNZ have been reported. Side effects of CNZ range from mild to quite severe. Its more common side effects are drowsiness and blurred vision, sweating, dry mouth, headache, skin problems, lethargy, gastrointestinal irritation, hypersensitivity reactions, muscle rigidity and tremor. CNZ can easily pass blood-brain barrier and it displays a sedative activity. Thus, its use by pilots and aircrew who must be dependably alert due to increased levels of drowsiness caused by the medication, is generally limited. Long-term CNZ therapy may cause weight gain, depressive conditions and several extrapyramidal syndromes, including tremor, acute and chronic Parkinsonism. CNZ can cause a tardive dyskinesia similarly to neuroleptic agents.

An alternative route to oral administration can provide an effective drug therapy. The transdermal route can be stated as one of the most reliable routes of application. Transdermal dosage forms are an alternative for the delivery of actives that have low oral bioavailability and systemic side effects. Moreover, transdermal delivery allows for the avoidance of the first-pass metabolism. There are various strategies to accelerate the drug passing through the skin. Thus, immediate and moderate action can also be observed. Penetration enhancers are required to enhance permeation through the skin by different penetration mechanisms for optimization of well-formulating topical products. Thus, to obtain an efficient treatment can be provided *via* the transdermal route. Penetration enhancers essentially improve transdermal delivery of both lipophilic and hydrophilic actives by decreasing barrier resistance of the skin.[3,4] Polyols, fatty acids and terpenes are commonly used as penetration enhancers. Diethyleneglycol monoethylether [Transcutol® (Tc)], propylene glycol (PG), glycerol (Gl), oleic acid (OA) and limonene (L) are some of the most generally used penetration enhancers. They can carry drug delivery further through the skin displaying different mechanisms, through upper layers of the skin, mainly the *stratum corneum*. Tc and PG alter thermodynamic activity of permeants in their vehicles after permeating through tissues themselves at first. Afterwards, permeants diffuse into the skin by modification of driving forces for diffusion.[5-7] The activity of PG is also pronounced to result from solvatation of α-keratin within the *stratum corneum*, herewith promoting permeation by reducing drug-tissue binding. L promotes the permeation of lipophilic and amphiphilic penetrants by increasing their diffusion in the *stratum corneum*.[8,9] OA, a long-chain fatty acid, enhances percutaneous drug absorption by decreasing the phase transition temperatures of the skin lipids. A polar head group attached to the alkyl chain of OA conducts its potential enhancement function. However, Gl displays its penetration enhancing effect when along with water.[10]

In this study, it was prepared topical formulations of CNZ to overcome side effects caused by oral administration of the drug and to provide an alternative therapy in Ménière's disease and motion sickness. For this purpose, effects of various traditional vehicles and penetration enhancers on the permeation of CNZ were investigated. Topical formulations based on a hydrogel (G), o/w emulsion (E) and oleaginous cream (OC) were prepared and their physical characteristics were determined. Penetration and permeation of CNZ through the *stratum corneum* and skin were investigated with an *ex vivo* study. This study was conducted on the abdominal skin of Wistar Albino rats since the rat skin can be used as a model for investigation of transdermal drug delivery through the human skin as reported in earlier studies. *In vivo* and *ex vivo* tests on rats have been demonstrated that can be used for searching properties required from actives and/or vehicles for skin delivery.[11-14]

MATERIALS AND METHODS

CNZ was kindly provided from Nobel Ilaç San. ve Tic. A.Ş., Turkey. Hydroxypropyl methylcellulose (Methocel™ K15M) (HPMC) was kindly provided by Colorcon (Turkey). PG, OA, polyethylene glycol (PEG 400), Gl and Tween® 80 were purchased from Merck (Germany). Polyvinylpyrrolidone® K90 (PVP K90), cetyl alcohol and liquid paraffine were purchased from Sigma-Aldrich (Germany). Stearic acid and glyceryl monostearate were purchased from Doğa İlaç Hammaddeleri Tic. Ltd. Şti. (Turkey). Tc was provided by Gattéfosse (France). All other reagents and chemicals were of analytical grade.

Preparation of topical formulations

The composition of base CNZ formulations (G, E, and OC) is presented in Table 1. Penetration enhancers (Tc, PG, Gl and OA) were added to these formulations (Table 2). L was also added to base formulations at the rate of 5%. However, they went to the phase separation or they lost their homogeneity within one week. Thus, they were excluded from the study. As an addition, Tc was confirmed to be incompatible with the base formulation OC.

Quantification of CNZ

The high performance liquid chromatography (HPLC) method was verified for analytical quantification of the drug in samples obtained during experiments. International Council for Harmonisation (ICH) guideline for the method validation procedure was considered for this purpose.[15] Linearity, intra-day and inter-day precision, accuracy, recovery and specifity were determined for verification of the method. Each verification analysis was replicated 6 times.

For this purpose, a HPLC apparatus (Shimadzu LC-20AT) was equipped with an ultraiole/visible detector (Shimadzu SPD-20A) and autosampler (Shimadzu SIL-20A HT). The separation was carried out using a TC-C_{18} column (5 µm, 4.6x250 mm) (Agilent Tech, Germany) at 40 °C. Samples were detected under 1 mL/min flow rate of acetonitrile: ammonium phosphate monobasic solution (pH: 4.5) (6:4, v/v) as the mobile phase at 253 nm. 0.24 mg/mL stock standard solution of CNZ in methanol was prepared to evaluate the linearity of the method under the

Table 1. Constituents of the base formulations

Constituents (%, w/w)	G	E	OC
CNZ	2.5	2.5	2.5
HPMC	3.15	-	-
PVP K90	0.35	-	-
PEG 400	15	-	-
Vaseline	-	8	75
Liquid paraffine	-	19	12.5
Stearic acid	-	2	10
Cetyl alcohol	-	2	-
Tween® 80	-	4	-
GMS	-	1	-
Saline	22.5	-	-
Distilled water	56.5	61.5	-
Methylparaben	0.15	0.15	-
Propylparaben	-	0.15	0.15

G: Hydrogel, E: o/w emulsion, OC: Oleaginous cream, CNZ: Cinnarizine, HPMC: Hydroxypropyl methylcellulose, PVP: Polyvinylpyrrolidone, PEG: Polyethylene glycol, GMS: Glyceryl monostearate

Table 2. Formulations containing penetration enhancers

Formulations	Enhancers (%)			
	Tc	PG	Gl	OA
G*	-	-	-	-
G-Tc	5	-	-	-
G-PG	-	5	-	-
G-Gl	-	-	5	-
G-OA	-	-	-	2
E*	-	-	-	-
E-Tc	5	-	-	-
E-PG	-	5	-	-
E-Gl	-	-	5	-
E-OA	-	-	-	5
OC*	-	-	-	-
OC-PG	-	5	-	-
OC-Gl	-	-	5	-
OC-OA	-	-	-	5

*G, E, and OC are base formulations. G: Hydrogel, E: o/w emulsion, OC: Oleaginous cream, Tc: Transcutol®, PG: Propylene glycol, Gl: Glycerole, OA: Oleic acid, G: Hydrogel

selected conditions. Drug determination was carried out at six concentrations (4–24 µg/mL) for providing the calibration curve.

Solubility of CNZ in various mediums

The solubility of CNZ was determined in various media according to the method reported in USP XIX.[16] 15 mL of the dissolution medium was placed in four 25-mL flasks for this purpose. A quantity of CNZ was added to each flask that was greater than the quantity expected to dissolve in the medium. Flasks were closed and they were fixed in a constant temperature water bath (Daihan Scientific, Korea) adjusted to 25±1°C. The apparatus was maintained under 200 rpm continuous agitation. Dispersions were filtered through S & S[5893] blue ribbon papers (2 µm pore size, Schleicher & Schuell, Germany) after 24 h agitation. Measured portions of clear supernatants were removed and the solubility of CNZ was determined with HPLC.

Partition coefficient

The partition coefficient of CNZ between isopropyl myristate and distilled water was determined using the shake flask method, following the guidelines of the European Chemical Bureau (European-Chemical-Bureau, Dir 92/69/EEC).

In vitro drug release of formulations

0.45 µm cellulose acetate membranes (Sartorius, Germany) were kept in the receptor phase, a physiological saline solution (PSS): PEG 400 mixture (6:4, v/v) over night. Membranes were placed between two halves of Franz-type diffusion cells with 3.15 cm^2 surface area and 33.2 mL volume containing the receptor phase. 1 g topical formulation was placed on to the membrane in the donor phase. The receptor phase was maintained at 37±0.5°C constant temperature during this study for 6 h. Samples were taken from the receptor phase at certain time intervals. Cumulative amounts of CNZ released (mg/cm^2) determined by HPLC after samples were filtered through S & S[5893] blue ribbon papers. Six replicates were conducted for each formulation. Drug release profiles were obtained by plotting cumulative amounts of the drug as the function of time and release profiles were evaluated using different kinetic models (zero order, first order and Higuchi square-root model).[17,18] The exponent value (n) of the Korsmeyer-Peppas kinetic model was considered for specifying drug release mechanism well un-known or for more than one type of release mechanisms comprised.

Ex vivo skin penetration and permeation studies

2.5-3 months aged male Wistar Albino rats (200-250 g) were provided from Aziz Sancar Institute of Experimental Medicine. The experimental protocol the Local Ethical Committee approved the experimental protocol of Animal Experiments (17.12.2013, no: 2013/131). Animals were housed in plastic cages at 22±1°C and 60±1% humidity under 12 h light-dark cycle. They were given standard laboratory diet and tap water *ad libitum*. Precisely shaved full-thickness abdominal rat skins were taken after they were sacrificed for *ex vivo* skin penetration and permeation assessments. The underlying fatty tissue was removed with blunt dissection without damaging the epidermal surface. Skins were placed between two halves of Franz-type diffusion cells. 1 g formulation was applied on the skin in the donor chamber of cells. PSS: PEG 400 (6:4, v/v), was

used as the receptor phase. This study was continued for 6 h at 37±1°C constant temperature. The cumulative amount of CNZ permeated was verified in samples collected from the receptor phase at predetermined time intervals by HPLC. Three replicates were conducted for each formulation. The cumulative amount (Q_n, mcg/cm^2) of CNZ permeated through the skin was calculated and cumulative drug amounts were plotted as the function of time (t, h).[19-21] The steady state flux of the drug (J_s, mcg/cm^2/h) was ascertained from the slope of linear part of plot using the linear regression analysis (r>0.99) and then the efficiency of the penetration enhancers were determined.

The penetration of CNZ was assayed through the skin. A tape stripping study was conducted. For this purpose, abdominal rat skins over receptor chambers of Franz-type diffusion cells were used. Excess formulation in contact with the *stratum corneum* was carefully expunged using cotton swabs.[22] Circular PVC tape strip sticking plaster pieces in 1 cm semidiameter (Ve-ge®, İzmir, Turkey) was applied with a light pressure over the diffusion area. Then, it was removed with forceps. The first two strips were thrown away, because they collected residue of the formulation within crevices of the skin surface. The next 10 sticking plaster pieces were then applied using uniform firm pressure to obtain the formulation residue deposited within the skin tissue. They were then removed with uniform force rapidly using forceps. All tape strip sticking plaster pieces were collected in a 25 mL flask for extracting the drug content. For extracting CNZ, 10 mL ethanol was added to flasks and all flasks were tightly closed. They were fixed in a water bath at 25±1°C. The apparatus was adjusted to 160 rpm continuous agitation for 24 h. Flasks' contents were then filtered through S & S^{5893} blue ribbon papers. Measured portions of clear supernatants were removed from each flask for determination of CNZ content by HPLC. Subsequently, the solubility constraint (σ_{sc}) of CNZ in the *stratum corneum* was also calculated [log σ_{sc}: 1.911 (10^3/melting point as Kelvin) - 2.956].[23] The melting point of CNZ was obtained by differential scanning calorimetry (DSC) analysis. For this purpose, a DSC apparatus (Universal V4.5A TA Instruments, U.S.A.) was employed. 9.7-mg sample was weighted into aluminum pans of the apparatus and heated with 10°C/min heating rate under 50 mL/min N_2 flow. Thermogram of the sample was obtained indicating its melting point and enthalpy.

Statistical analyses

Drug release and permeation profiles of the formulations obtained from *in vitro* and *ex vivo* experiments and data obtained from the tape stripping experiment were compared using One-Way ANOVA test and subsequent Tukey post hoc pairwise tests. The Minitab® 18 Statistical Software was used for this purpose by setting the significance level as α: 0.05.

RESULTS AND DISCUSSION

Analytical quantification

The analytical quantification of CNZ by HPLC was verified according to the instructions of the ICH Tripartite Guideline.[15] The representative linear equation was A=aC + b, where A is the absorbance, a is the slope, C is the concentration and b is the intercept. The regression equation was A=81417.9C+3405.3 (correlation coefficient, r=0.9999). The retention time of CNZ was found as 5.8 min (Figure 1A). Limits of detection and quantification of the quantification method were determined as 5.929 ng/mL and 17.968 ng/mL, respectively. Relative standard deviations for accuracy, intra-day and inter-day precision of the methods were below 2%. The recovery of CNZ was found to be 99.87±0.06-100.74±0.03%. Chromatograms of the receptor phase and placebo base formulations demonstrated the specifity of the method (Figure 1B-E). Chromatograms of the formulations containing penetration enhancers (TC, PG, GL and

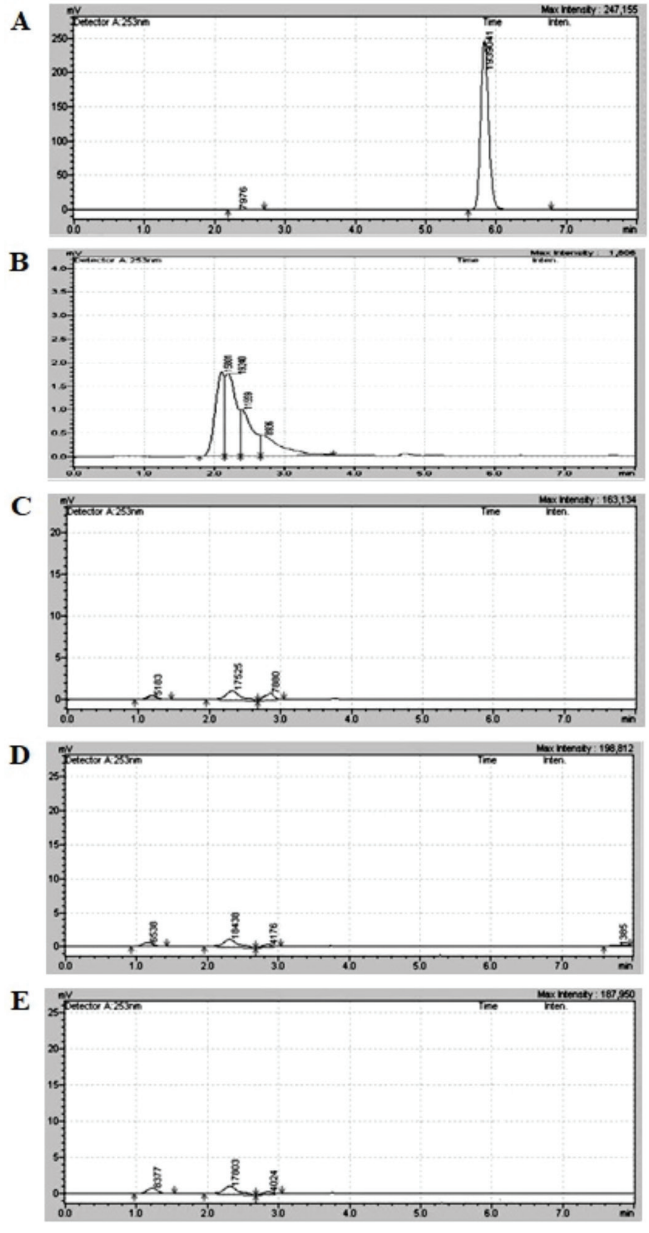

Figure 1. HPLC chromatograms - (A) CNZ, (B) receptor phase and placebo base formulations [(C) G, (D) E and (E) OC]

HPLC: High performance liquid chromatography, CNZ: Cinnarizine, G: Hydrogel, E: o/w emulsion, OC: Oleaginous cream

OA, individually at the 5% rate in the formulations) were also verified the specificity of the method (they are not presented). Peaks of ingredients in the formulations were observed not to interfere with the drug peak.

Solubility of CNZ

The solubility of CNZ in various media at 25°C are represented in Table 3. PSS:PEG 400 mixture (6:4, v/v) was decided to be used as the receptor phase since the solubility of CNZ was found to be the highest in it.

In vitro drug release of formulations

Table 3. Solubility of CNZ in different media at 25±1°C

Mediums	Solubility (mg/mL)	
pH 7.4 PBS	0.017±0.004	*p.i.*
pH 6.8 PBS	0.027±0.008	*p.i.*
5% bovine serum albumin in PSS (w/v)	0.024±0.006	*p.i.*
PSS: PEG 400 (8:2)	0.601±0.013	*vss*
Water	0.749±0.005	*vss*
PSS: PEG 400 (6:4)	1.406±0.010	*s.s.*

According to the European and the United States Pharmacopeias, pi: Practically in soluble, vss: Very slightly soluble, ss: Slightly soluble, PBS: Phosphate buffered saline, PSS: Physiological saline solution, PEG: Polyethylene glycol, CNZ: Cinnarizine

To achieve the sink condition, the receptor phase must have a high capacity to dissolve or carry away the drug. An acceptable sink condition has been reported to be one where the maximum concentration of the drug in the receptor phase reached during the experiment does not exceed 30% of its maximum solubility in the receptor phase.[24] It is provided in a volume of the medium that is at least 3-10 times the saturation volume. The solubility of CNZ at 37±1°C was also determined and it was found to be 2.352±0.012 mg/mL. Thus, the volume of the receptor phase allowed to maintain the sink condition.

Permeation characteristics of a drug through the skin can't be judged with *in vitro* drug release experiments. But it avail researchers to reckon some reasons for low drug penetration rate, including the affinity of the drug to the vehicle.[25,26] CNZ was confirmed to display the highest affinity to OC compared to G and E ($p<0.05$). The emulsion formulation E was confirmed to display the highest drug release rate among base formulations up to 6th hours ($p<0.05$) (Figure 2, Table 4). G (0.293 mg/cm^2/h) and OC (0.151 mg/cm^2/h) respectively, followed E (0.326 mg/cm^2/h). It was determined that the incorporation of penetration enhancers to the base formulations led to a significant increase in drug release rate of the vehicles in the case of formulations E and G ($p<0.05$) while an opposite situation was occurring for OC with all penetration enhancers. Tc and Gl addition to formulation E and PG addition to formulation G provided the highest release rate of drug from vehicles ($p>0.05$). Due to the lipophilic character of CNZ resulted in its retention in the base OC formulation.[27] Moreover, the incorporation of penetration enhancers (PG, Gl and OA) to OC statistically insignificantly

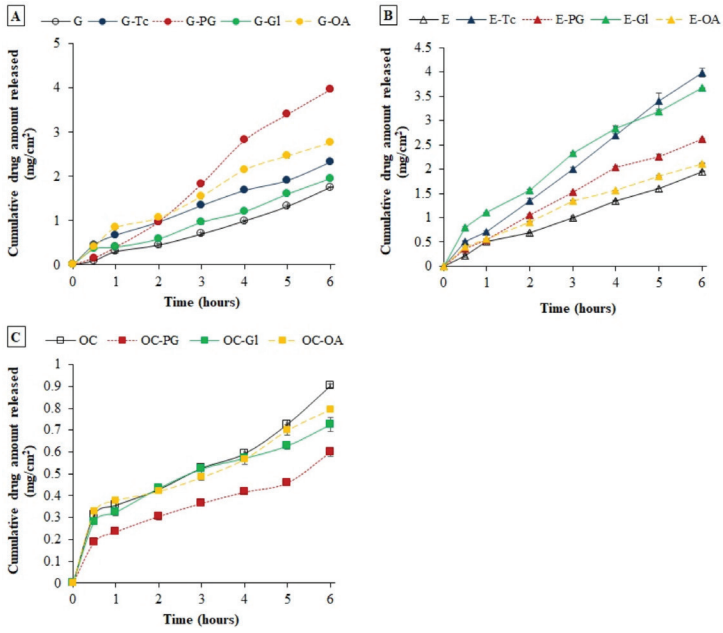

Figure 2. CNZ release profiles of topical formulations in PSS:PEG 400 (6:4, v/v). (A) hydrogel based formulations, (B) o/w emulsion based formulations and (C) oleaginous cream based formulations

CNZ: Cinnarizine, PSS: Physiological saline solution, PEG: Polyethylene glycol, G: Hydrogel, E: o/w emulsion, OC: Oleaginous cream, Tc: Transcutol®, PG: Propylene glycol, Gl: Glycerole, OA: Oleic acid

changed the drug release rate and slower drug release profiles were obtained from formulations OC-OA, OC-Gl, and OC-PG ($p>0.05$) compared to the emulsion and hydrogel formulations. Thus, it was affirmed that increase in the solubility of the drug in the vehicle resulted in slower drug release.[25] Emulsion and hydrogel based formulations displayed anomalous transport of drug release because of kinetic modeling (Table 4). This phenomena can be attributed to two mechanisms conducted drug release, diffusion and polymer relaxation in hydrogel formulations or drug release free from concentration in emulsion formulations.

Ex vivo skin permeation and penetration studies

CNZ permeation from topical formulations through rat skin was ascertained to involve in the polarity of the formulations and type of penetration enhancers as reported earlier studies conducted on skin permeation of lipophilic drugs.[27] Polar hydrogel structure provided the highest drug permeation rates among other vehicles (Figure 3, Table 5). This phenomena can be attributed to the high partition coefficient of CNZ (log P: 5.74±0.03 in isopropyl myristate/water). G significantly displayed the highest permeation rate followed by E and OC ($p<0.05$), respectively. Tc was found as the most effective penetration enhancer compared to PG, GL and OA for hydrogel based formulations ($p<0.05$). The highest drug permeation rate was obtained in formulation G-Tc (0.110±0 mg/cm^2/h) followed by G-Gl (0.062±0.002 mg/cm^2/h), G-PG (0.057±0.001 mg/cm^2/h) and G-OA (0.050±0.001 mg/cm^2/h). Although emulsion based formulations followed G formulations in the same penetration enhancer order, differences between emulsion and oleaginous cream based formulations were insignificant ($p>0.05$). Tc

Table 4. Release parameters of CNZ from the formulations for 6 h and kinetic modeling of release profiles

			Zero order $[Q_t=Q_0 + k_0t]$		First order $[Q_t=Q_\infty (1 - e^{-kt})]$		Higuchi model $(Q_t=Q_0 + k_H t^{1/2})$		Korsmeyer-Peppas model $[\log (Q_t/Q_\infty) = \log k + n\log t]$	
Formulations	**Q (mg/cm²)**	**The release rate (mg/cm²/h)**	**r**	**k_o**	**r**	**k_1**	**r**	**D**	**r**	**n, dominant release mechanism**
G	1.754±0.004	0.293±0.001	0.9910	0.286	0.9468	0.456	0.9642	0.887	0.9915	1.08 (non-Fickian), An.T.
G-Tc	2.325±0.010	0.388±0.002	0.9984	0.331	0.9715	0.279	0.9895	1.046	0.9957	0.65 (non-Fickian), An.T.
G-PG	3.966±0.024	0.662±0.004	0.9962	0.729	0.9395	0.555	0.9824	2.294	0.9986	1.33 (non-Fickian), An.T.
G-Gl	1.952±0.022	0.326±0.004	0.9918	0.296	0.9914	0.322	0.9624	0.916	0.9650	0.71 (non-Fickian), An.T.
G-OA	2.771±0.013	0.463±0.002	0.9932	0.430	0.9472	0.317	0.9880	1.363	0.9911	0.75 (non-Fickian), An.T.
E	1.951±0.011	0.326±0.002	0.9966	0.303	0.9427	0.353	0.9852	0.956	0.9914	0.84 (non-Fickian), An.T.
E-Tc	3.988±0.087	0.666±0.015	0.9991	0.649	0.9726	0.372	0.9831	2.036	0.9931	0.86 (non-Fickian), An.T.
E-PG	2.616±0.021	0.437±0.004	0.9945	0.422	0.9503	0.354	0.9942	1.346	0.9970	0.83 (non-Fickian), An.T.
E-Gl	3.674±0.011	0.614±0.002	0.9953	0.530	0.9683	0.271	0.9919	1.684	0.9929	0.63 (non-Fickian), An.T.
E-OA	2.113±0.012	0.353±0.002	0.9956	0.316	0.9592	0.297	0.9949	1.008	0.9967	0.70 (non-Fickian), An.T.
OC	0.902±0.008	0.151±0.001	0.9860	0.101	0.9979	0.186	0.9554	0.313	0.9547	0.40 (Fickian), diffusion
OC-PG	0.600±0.021	0.100±0.004	0.9869	0.068	0.9832	0.191	0.9714	0.213	0.9816	0.43 (Fickian), diffusion
OC-Gl	0.725±0.034	0.121±0.006	0.9934	0.078	0.9752	0.166	0.9942	0.249	0.9906	0.38 (Fickian), diffusion
OC-OA	0.796±0.010	0.133±0.002	0.9874	0.083	0.9965	0.158	0.9567	0.258	0.9450	0.34 (Fickian), diffusion

Q: Cumulative amount of drug released, Q_t *and* Q_0: Quantity of drug released at time t and in the release medium at t=0, respectively, r: Correlation coefficient, k_1, k_0, and k_H rate constants of the zero order, first order and Higuchi kinetic models, respectively, Q_t/Q_∞: fractional release of drug, *k* and *n*: Kinetic constant and diffusion exponent of the release mechanism (slope) according to the Korsmeyer-Peppas model, An.T.: Anomalous transport, Tc: Transcutol®, PG: Propylene glycol, Gl: Glycerole, OA: Oleic acid, OC: Oleaginous cream, CNZ: Cinnarizine, G: Hydrogel, E: o/w emulsion

and PG possibly contributed to their own permeation through tissues and modified the thermodynamic activity of CNZ before modification of driving forces for drug diffusion as reported earlier.[19,28] Solvatation of *a*-keratin within the *stratum corneum* by PG was additionally be claimed to improve the permeation of CNZ by reducing drug-tissue binding. OA and Gl enhanced percutaneous absorption of CNZ by decreasing phase transition temperatures of skin lipids and displaying the occulusion effect on the skin, respectively.[19,29] All formulations were affirmed to reach the steady-state flux (Js) at the 1st hour, except for the base formulation G (3rd hour).

CNZ percent in the *stratum corneum* and the receptor phase that was determined for each formulation at the 6th hour are presented in Figure 4. It was found that amount of CNZ accumulated in the *stratum corneum* was significantly higher than determined in the receptor compartment. As can be seen in the figure, G-Tc displayed the highest skin penetration of the drug followed by formulations G-Gl, G-OA, G-PG and, o/w emulsion based and oleaginous cream based formulations, respectively (p<0.05). Formulations displayed high drug accumulation in the *stratum corneum* were expected to exhibit continuous drug permeation of most of the retained drug by steady state flux in time.

The melting point of CNZ was found as 121.94°C (121.16°C onset melting temperature and 98.18 J/g melting enthalpy) according to its DSC thermogram indicating a sharp melting peak (Figure 5).

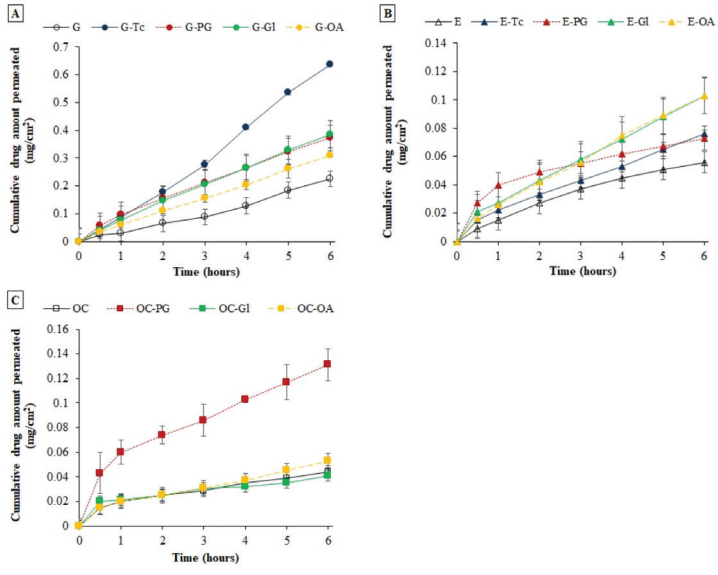

Figure 3. Permeation profiles of CNZ through rat skins. (A) Hydrogel based formulations, (B) o/w emulsion based formulations and (C) oleginous cream based formulations

CNZ: Cinnarizine, G: Hydrogel, E: o/w emulsion, OC: Oleaginous cream, Tc: Transcutol®, PG: Propylene glycol, Gl: Glycerole, OA: Oleic acid

Table 5. Permeation parameters of CNZ through the skin

Formulations	Q_n (mg/cm²)	J_s (mg/cm²/h)	K_p (cm/h)	r	ER
G	0.250±0.002	0.046±0.002	1.86x10-3±8.00x10-5	0.9976	-
G-Tc	0.638±0.007	0.113±0.002	4.52x10-3±6.63x10-5	0.9976	2.46
G-PG	0.373±0.011	0.056±0.001	2.22x10-3±0.87x10-5	0.9991	1.22
G-Gl	0.386±0.028	0.061±0.001	2.45x10-3±3.52x10-5	0.9993	1.33
G-OA	0.309±0.013	0.050±0.001	2.00x10-3±1.69x10-5	0.9995	1.09
E	0.056±0.021	0.008±0.004	0.33x10-3±15.48x10-5	0.9879	-
E-Tc	0.076±0.003	0.011±0.002	0.43x10-3±7.25x10-5	0.9994	1.38
E-PG	0.073±0.013	0.006±0.002	0.26x10-3±9.49x10-5	0.9961	0.75
E-Gl	0.103±0.012	0.015±0.002	0.60x10-3±6.06x10-5	0.9998	1.88
E-OA	0.103±0.017	0.016±0.003	0.62x10-3±11.72x10-5	0.9991	2.00
OC	0.044±0.005	0.005±0.001	0.20x10-3±3.01x10-5	0.9962	-
OC-PG	0.131±0.013	0.014±0.001	0.57x10-3±2.97x10-5	0.9992	2.80
OC-Gl	0.041±0.004	0.004±0.001	0.15x10-3±1.59x10-5	0.9889	0.80
OC-OA	0.053±0.003	0.007±0	0.27x10-3±0.36x10-5	0.9970	1.40

Eqs. $$Q_n = \frac{C_n V_0 + \sum_{i=1}^{n-1} C_i V_i}{A} \qquad J_s = C_0 \frac{KD}{L} \qquad K_p = \frac{J_s}{C_0} \qquad ER = \frac{J_s \text{ (with the enhancer)}}{J_s \text{ (without the enhancer)}}$$

Q_n: Cumulative amount of the drug permeated, C_n: Drug concentration in the receptor phase at the n^{th} sampling interval, A: Effective diffusion area (surface of the sample cell), V_0 and V_i: Volumes of the receptor phase in the individual Franz cell and the sample, respectively, $\sum_{i=1}^{n-1} C_i$: Sum of drug concentration determined at sampling intervals 1 through n-1, J_s: Steady state flux of the drug, C_0: Constant drug concentration in the donor phase, D: Diffusion coefficient, L: Thickness of the membrane, K: partition coefficient of the drug and the vehicle, K_p: Permeability coefficient, r: Correlation coefficient, ER: The enhancement ratio, CNZ: Cinnarizine, G: Hydrogel, E: o/w emulsion, OC: Oleaginous cream, Tc: Transcutol®, PG: Propylene glycol, Gl: Glycerole, OA: Oleic acid

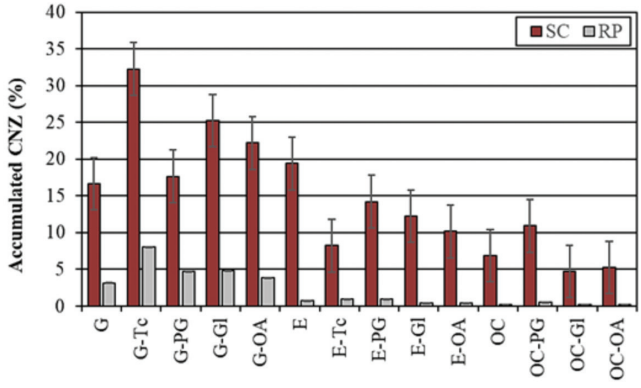

Figure 4. The cumulative amount of CNZ (%) retained in the *stratum corneum* (SC) of rat skins and remained in the receptor compartment (RC) after 6 h of application of the formulations

CNZ: Cinnarizine, G: Hydrogel, E: o/w emulsion, OC: Oleaginous cream, Tc: Transcutol®, PG: Propylene glycol, Gl: Glycerole, OA: Oleic acid

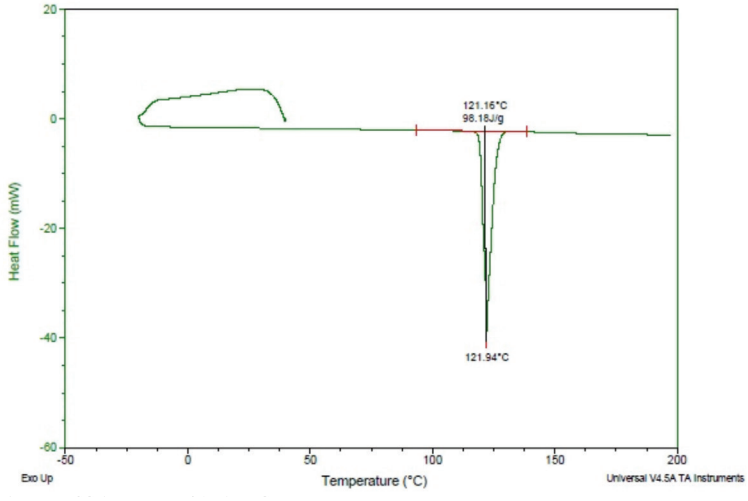

Figure 5. DSC thermogram of the drug (CNZ)

CNZ: Cinnarizine, DSC: Differential scanning calorimetry

The solubility constraint (σ_{sc}) of CNZ was calculated as 1.88 in the *stratum corneum* indicating the potential of this compound that forms a reservoir in the *stratum corneum*. Organic substances with high melting points and enthalpies have lower aqueous solubility in general since solvents cannot pass into the crystalline structure of such molecules to dissolve them.[30,31] Thus, an indirect relationship exists between the melting point and the solubility of a drug.[32] In other words, a decrease in the melting point of a drug would lead to an increase in its solubility in the *stratum corneum* and consequently its penetration and then permeation through the skin.

CONCLUSION

Formulations that were studied in this research introduce various advantages over many transdermal drug delivery

systems. They are suitable for large-scale production and cost-effective dosage forms produced with excipients used in pharmaceuticals and cosmetics for years. *Ex vivo* study conducted on rats gave information about the influence of the polarity of vehicles and penetration enhancer on skin penetration of CNZ. It was concluded that skin penetration increased as the lipophilicity of the vehicle decreased. The hydrogel formulation without a penetration enhancer provided about five times higher drug permeation compared to an o/w emulsion and oleaginous cream. Furthermore, when Transcutol® was introduced to the HPMC hydrogel, it displayed the highest penetration enhancer activity. As a result, the HPMC hydrogel containing Tc can be suggested as a suitable carrier for CNZ intended to be used topically for relief of various conditions.

ACKNOWLEDGEMENTS

This study was supported by the Research Fund of Istanbul University (project number: 40188) and TUBITAK (The Scientific and Technological Research Council of Turkey) (grant number: TEYDEB 1649B031305845).

Conflict of interest: No conflict of interest was declared by the authors. The authors are solely responsible for the content and writing of this paper.

REFERENCES

1. Sweetman SC. Martindale: The complete drug reference (36th ed). New York; Pharmaceutical Press; 2009.
2. Haress NG. Cinnarizine: Comprehensive Profile. Profiles Drug Subst Excip Relat Methodol. 2015;40:1-41.
3. Lopes LB, Garcia MT, Bentley MV. Chemical penetration enhancers. Ther Deliv. 2015;6:1053-1061.
4. Trommer H, Neubert RH. Overcoming the *Stratum corneum*: the modulation of skin penetration. A review. Skin Pharmacol Physiol. 2006;19:106-121.
5. Remon JP. Absorption Enhancers. In: Swarbrick J, ed. Encyclopedia of pharmaceutical technology, Vol. 1 (3rd ed). New York; Informa Healthcare. 2007:13-18.
6. Patwardhan S, Patil M, Sockalingam A. Development and evaluation of naproxen sodium gel using piper cubeba for enhanced transdermal drug delivery and therapeutic facilitation. Recent Pat Drug Deliv Formul. 2017;11:28-35.
7. Dahlizar S, Futaki M, Okada A, Yatomi C, Todo H, Sugibayashi K. Combined Use of *N*-palmitoyl-glycine-histidine gel and several penetration enhancers on the skin permeation and concentration of metronidazole. Pharmaceutics. 2018;10:163.
8. Koyama Y, Bando H, Yamashita F, Takakura Y, Sezaki H, Hashida M. Comparative analysis of percutaneous absorption enhancement by d-limonene and oleic acid based on a skin diffusion model. Pharm Res. 1994;11:377-383.
9. Prasanthi D, Lakshmi PK. Effect of chemical enhancers in transdermal permeation of alfuzosin hydrochloride. ISRN Pharm. 2012;2012:965280.
10. Vijaya C, Bingi M, Vigneshwaran LV. Transdermal delivery of venlafaxine hydrochloride: the effects of enhancers on permeation across pig ear skin. Indian J Pharm Sci. 2011;73:456-459.
11. Liu X, Quan P, Li S, Liu C, Zhao Y, Zhao Y, Fang L. Time dependence of the enhancement effect of chemical enhancers: Molecular mechanisms of enhancing kinetics. J Control Release. 2017;248:33-44.
12. Moghimipour E, Salimi A, Zadeh BSM. Effect of the various solvents on the *in vitro* permeability of vitamin B12 through excised rat skin. Trop J Pharm Res. 2013;12:671-677.
13. Maurya A, Murthy SN. Pretreatment with skin permeability enhancers: importance of duration and composition on the delivery of diclofenac sodium. J Pharm Sci. 2014;103:1497-1503.
14. Monti D, Egiziano E, Burgalassi S, Chetoni P, Chiappe C, Sanzone A, Tampucci S. Ionic liquids as potential enhancers for transdermal drug delivery. Int J Pharm. 2017;516:45-51.
15. ICH Harmonised Tripartite Guideline: Validation of Analytical Procedures: Text and Methodology Q2 (R1). Harmonization Co, Editor. 2005.
16. Üner M, Karaman EF. Preliminary studies on solid lipid microparticles of loratadine for the treatment of allergic reactions *via* the nasal route. Trop J Pharm Res. 2013;12:287-293.
17. Higuchi T. Mechanism of sustained action medication. Theoretical analysis of rate of release of solid drugs dispersed in solid matrices. J Pharm Sci. 1963;52:1145-1149.
18. Korsmeyer RW, Gurny R, Doelker E, Buri P, Peppas NA. Mechanisms of solute release from porous hydrophilic polymers. Int J Pharm. 1983;15:25-35.
19. Williams AC, Barry BW. Penetration enhancers. Adv Drug Deliv Rev. 2004;56:603-618.
20. Haq A, Michniak-Kohn B. Effects of solvents and penetration enhancers on transdermal delivery of thymoquinone: permeability and skin deposition study. Drug Deliv. 2018;25:1943-1949.
21. Sloan KB, Koch SA, Siver KG, Flowers FP. Use of solubility parameters of drug and vehicle to predict flux through skin. J Invest Dermatol. 1986;87:244-252.
22. Houston DM, Bugert J, Denyer SP, Heard CM. Anti-inflammatory activity of *Punica granatum* L. (Pomegranate) rind extracts applied topically to *ex vivo* skin. Eur J Pharm Biopharm. 2017;112:30-37.
23. Hadgraft J, Brain KR. Xenobiotic experimentation: predicting percutaneous penetration. In: Marks R, Plewig G, eds. The environmental threat to the skin. London; CRC Press, Taylor & Francis Group; 1992:179-184.
24. European Medicine Agency, Draft Guideline on quality and equivalence of topical products (EMA/CHMP/QWP/708282/2018).
25. Surber C, Smith E. The vehicle: The pharmaceutical carrier of dermatological agents. In: Gabard B, Surber C, Elsner P, Surber C, Treffel P, editors. Dermatopharmacology of topical preparations. A product development-oriented approach. Berlin; Springer-Verlag; 2000:5.
26. Salerno C, Carlucci AM, Bregni C. Study of *in vitro* drug release and percutaneous absorption of fluconazole from topical dosage forms. AAPS PharmSciTech. 2010;11:986-993.
27. Watkinson RM, Guy RH, Oliveira G, Hadgraft J, Lane ME. Optimisation of cosolvent concentration for topical drug delivery III--influence of

lipophilic vehicles on ibuprofen permeation. Skin Pharmacol Physiol. 2011;24:22-26.

28. Harrison JE, Watkinson AC, Green DM, Hadgraft J, Brain K. The relative effect of Azone and Transcutol on permeant diffusivity and solubility in human *Stratum corneum*. Pharm Res. 1996;13:542-546.

29. Pathan IB, Setty CM. Chemical penetration enhancers for transdermal drug delivery systems. Trop J Pharm Res. 2009;8:173-179.

30. N'Da DD. Prodrug strategies for enhancing the percutaneous absorption of drugs. Molecules. 2014;19:20780-20807.

31. Lipinski CA, Lombardo F, Dominy BW, Feeney PJ. Experimental and computational approaches to estimate solubility and permeability in drug discovery and development settings. Adv Drug Deliv Rev. 2001;46:3-26.

32. Stott PW, Williams AC, Barry BW. Transdermal delivery from eutectic systems: enhanced permeation of a model drug, ibuprofen. J Control Release. 1998;50:297-308.

Turk J Pharm Sci 2022;19(1):28-34
DOI: 10.4274/tjps.galenos.2021.70745

ORIGINAL ARTICLE

Ameliorative Potential of Rosuvastatin on Doxorubicin-induced Cardiotoxicity by Modulating Oxidative Damage in Rats

Sıçanlarda Oksidatif Hasar Modülasyonuyla Doksorubisinin İndüklediği Kardiyotoksisite Üzerine Rosuvastatinin İyileştirici Potansiyeli

Jayaraman RAJANGAM[1]*, Navaneetha KRISHNAN S[1], Narahari N PALEI[2,3], Shvetank BHATT[4], Manas Kumar DAS[5], Saumya DAS[6], Krishnapillai MATHUSOOTHANAN[7]

[1]Sree Vidyanikethan College of Pharmacy, Department of Pharmacology, Andhra Pradesh, India
[2]Sree Vidyanikethan College of Pharmacy, Department of Pharmaceutics, Andhra Pradesh, India
[3]The Neotia University School of Pharmacy, Department of Pharmaceutics, West Bengal, India
[4]Amity University Amity Institute of Pharmacy, Department of Pharmacology, Madhya Pradesh, India
[5]Orlean College of Pharmacy, Department of Pharmacology, Uttar Pradesh, India
[6]NIET College of Pharmacy, Department of Pharmacology, Uttar Pradesh, India
[7]Grace College of Pharmacy, Department of Pharmaceutics, Kerala, India

ABSTRACT

Objectives: The study aimed to explore the *in vivo* protective potential of rosuvastatin (ROSS), an oral antihyperlipidemic drug against doxorubicin (DOXO) induced cardio toxicity in rats.

Materials and Methods: Cardiac toxicity was induced by DOXO injection (10 mg/kg, *i.p.*), once on the 20th day of the experiment. Except for the control rats, all were received DOXO and the study was continued for up to 21 days. The influence of ROSS on acute treatment was analyzed by quantification of cardiac marker enzymes such as creatine kinase-MB (CK-MB), lactate dehydrogenase (LDH) and liver marker enzymes like aspartate aminotransferase (AST), alanine aminotransferase (ALT) along with the measurement of *in vivo* antioxidants like superoxide dismutase and catalase. To observe histological changes of myocardial tissue hematoxylin and eosin staining were used.

Results: Acute administration of DOXO resulted in a marked rise of cardiac marker enzymes that confirms the myocardial damage compared to control animals whereas administration of ROSS (10 mg/kg, *p.o.*) resulted in the significant reduction of CK-MB, LDH levels ($p<0.05$) and AST, ALT levels to a remarkable extent. Moreover, ROSS administration significantly increased the activities of various *in vivo* antioxidant levels.

Conclusion: From the results, the acute administration of ROSS showed significant cardioprotective property, which was evidenced by a significant reduction of cardiac and liver marker enzymes along with significant improvement of *in vivo* antioxidant activities. Furthermore the results were supported with histopathological observations. Hence, it can be concluded that cardioprotective potential of ROSS may be through attenuation of oxidative stress by modulating oxidative damage in rats.

Key words: Cardioprotection, rosuvastatin, doxorubicin, cardiotoxicity, cardiac markers, antioxidants

ÖZ

Amaç: Çalışma, sıçanlarda doksorubisin (DOXO) indüklediği kardiyotoksisiteye karşı oral antihiperlipidemik bir ilaç olan rosuvastatinin (ROSS) *in vivo* koruyucu potansiyelini araştırmayı amaçlamıştır. Kardiyak toksisite, deneyin 20. gününde bir kez DOXO enjeksiyonu (10 mg/kg, *i.p.*) ile indüklenmiştir. Kontrol sıçanları hariç tümüne DOXO verildi ve çalışmaya 21 güne kadar devam edilmiştir. Akut uygulamada ROSS'nin etkisi, süperoksit dismutaz ve katalaz gibi *in vivo* antioksidanların ölçümü ile birlikte kreatin kinaz-MB (CK-MB), laktat dehidrojenaz (LDH) gibi kardiyak

*Correspondence: jayaraam81@gmail.com, Phone: +0877-2236711, ORCID-ID: orcid.org/0000-0002-6367-0365
Received: 17.09.2020, Accepted: 09.04.2021

gösterge enzimlerin ve aspartat aminotransferaz (AST), alanin aminotransferaz (ALT) gibi karaciğer gösterge enzimlerinin kantitatif tayini ile analiz edilmiştir. Miyokardiyal dokudaki histolojik değişiklikleri gözlemlemek için hematoksilen ve eozin boyaması kullanılmıştır. DOXO'nun akut uygulaması, kontrol hayvanlarına kıyasla miyokardiyal hasarı doğrulayan kardiyak gösterge enzimlerinde belirgin bir artışa neden olurken, ROSS (10 mg/kg, *p.o.*) uygulaması CK-MB, LDH düzeylerinde (p<0,05) ve AST, ALT düzeylerinde dikkate değer ölçüde önemli bir azalmaya neden olmuştur. Dahası, ROSS uygulaması, çeşitli *in vivo* antioksidan düzeylerinin aktivitelerini önemli ölçüde artırmıştır. Sonuçlardan, ROSS'nin akut uygulaması, kardiyak ve karaciğer gösterge enzimlerinde önemli bir azalmanın yanı sıra *in vivo* antioksidan aktivitelerde önemli bir iyileşme ile kanıtlanan önemli kardiyoprotektif özellik göstermiştir. Ayrıca sonuçlar histopatolojik gözlemlerle desteklenmiştir. Bu nedenle, ROSS'un kardiyoprotektif potansiyelinin, sıçanlarda oksidatif hasarı modüle ederek oksidatif stresin azaltılması yoluyla olabileceği sonucuna varılabilir.

Anahtar kelimeler: Kardiyoproteksiyon, rosuvastatin, doksorubisin, kardiyotoksisite, kardiyak göstergeler, antioksidanlar

INTRODUCTION

Incidence rates of cardiovascular disorders (CVDs) are increasing day by day around the globe, particularly developing countries like India, most mortality rates are due to CVDs despite several advances in medical treatments. Among all CVDs, ischemic heart disease (IHD) like angina pectoris, myocardial infarction (MI) is the most alarming clinical conditions and is the main principle cause of mortality even in developed countries also.[1]

According to the current status of estimation by 2030, around 23.6 million people will die from only CVDs. Moreover, MI is considered as one of the common forms of IHD leads to irreversible necrosis of cardiac myocytes or myocardial tissue damage due to the failure of vasoregulatory or auto regulatory mechanisms.[2]

In addition to this, despite advances in the management of CVDs, MI remains the leading cause of mortality around the globe with high incidence rates around the age of 35 years was noticed in male patients who may be due to chronic stress, lack physical activity and lifestyle modifications, etc.[3,4] Hence, there is a high demand for research, and innovations were in progress in the field of cardioprotection by employing various animal models. In this study, the doxorubicin (DOXO)-induced cardiotoxicity model was used to screen the cardioprotective potential in Wistar Albino rats.

DOXO is a potent broad-spectrum antibiotic used for treating various cancers. However, the clinical usage has been limited due to serious side effects such as myocardial injury, mainly due to mitochondrial dysfunction, apoptosis and the excess generation of free radical leads to cardio toxicity.[5-7] Free radical-mediated myocardial damage is an important etiological mechanism that is associated with an increased level of reactive oxygen species and inadequate antioxidant defense system.[8,9] Hence, DOXO induced MI is the most widely used model to evaluate the cardioprotective effect of various drugs, and the administration of DOXO in high doses produces myocardial lesions similar to MI in humans.

However, the test drug of this study rosuvastatin (ROSS) is a well-known inhibitor of the rate-limiting enzyme i.e 3-hydroxy-3-methylglutaryl-CoA (HMG-CoA reductase) for *in vivo* cholesterol biosynthesis. As *per* the data, apart from antihyperlipidemic effects, statins possess diverse pharmacological effects, including lowering the CVDs and exerts neuroprotective and antioxidant actions.[10-13] However, the potential of statins on cardioprotection remains to be explored in different animal models. Therefore, we decided to put some effort to screen the cardioprotective effect of ROSS on DOXO induced cardiotoxicity in Wistar Albino rats.

MATERIALS AND METHODS

Animal care and handling

Wistar albino rats with a weight range of 140-180 g were used and housed at 25°±5°C until the acclimatization period of about one week at Sree Vidyanikethan College of Pharmacy, A. Rangampet, Tirupati. All the animals were maintained under standard experimental conditions according to the guidelines of the Committee for control and supervision on experiments on Animals (CPCSEA) and the experimental protocols were duly approved by IAEC (Institutional Animal Ethics Committee-SVCP/IAEC/I-003/2019-20).

Drugs, chemicals, and instruments

DOXO was procured from Sigma-Aldrich, U.S.A whereas assay kits like LDH & creatine kinase-MB (CK-MB) were supplied by Crest Biosystems, Coral clinical systems, Goa, India. ROSS was received as a gift sample from Dr.N.N.Palei, Faculty of Pharmacy, Sree Vidyanikethan College of Pharmacy. All biochemical estimation was done using a semi-automatic analyzer (Mispa-VIVA, Agappe Diagnostics, Kerala, India) following the methods and stepwise procedures described by the manufacturers.

Experimental design

Morphometric analysis

Body weight of all experimental animals was recorded at regular intervals, whereas relative organ weight was calculated post-experimental period after sacrificing the animals. Heart weight was measured after washing it in ice-cold saline after removal from the body, squeezing out the blood, and blotted on the filter paper.

Induction of cardiotoxicity

A total of 24 Albino rats (150±10 gm) were divided by following a random sampling technique into four groups of six animals each (n=6). All the experimental animals were treated as *per* the study design and the duration of the treatment was continued up to 21 days.

Group I - Rats were given normal saline (1 mL/kg.*s.c*), Group II - Rats were given DOXO on 20th day (10 mg/kg, *i.p.*),

Group III - Rats were given ROSS (10 mg/kg, *p.o*),

Group IV - Rats were given ROSS (10 mg/kg, *p.o*) + DOXO (10 mg/kg, *i.p.*).

Cardiac toxicity was induced by a single intraperitoneal injection of DOXO at a dose of 10 mg/kg on the 20th day of the experiment.[14] At the end of the experimental period, After 48 h of DOXO injection, rats were anesthetized with mild ether anesthesia and blood samples were collected from retro-orbital plexus, and serum was separated by centrifugation at 10000 rpm for 10 min using a centrifuge (REMI, India).

Estimation of cardiac and liver marker enzymes

The separated serum sample was used to estimate the creatinine kinase-MB (CK-MB, measured by immune inhibition method by determining the rate of NADPH formation at 340 nm) and liver markers enzymes such as aspartate aminotransferase (AST), alanine aminotransferase (ALT) and lactate dehydrogenase (LDH), measured using ultraviolet kinetic method by observing the rate of nicotinamide adenine dinucleotide reduced form formation at 340 nm) using an semi-automatic analyzer (Mispa-Viva-Agappe Diagnostics) with respective assay kits by following stepwise procedures given by the manufacturer.[15-18]

Estimation of marker enzymes using post mitochondrial supernatant (PMS)

Animals were sacrificed and the vital organ like heart was harvested for preparation of PMS. In brief, the harvested heart was *per* fused with ice-cold normal saline solution and homogenized using a phosphate buffer (0.1 M, pH 7.4) and KCl (1.17%, w/v) solution. Then the homogenate was centrifuged (800 rpm for 5 min at 4˚C) to separate the nuclear debris from the mixture. After that, the obtained supernatant was centrifuged at 10,500 rpm for 20 min at 4˚C to obtain PMS. Collected PMS was used for analyzing for the presence of different enzymes related to MI, such as CK-MB fraction and LDH using an semi-automatic analyzer (Mispa-Viva-Agappe Diagnostics).[15-18]

Antioxidant activity

Collected PMS solution from the heart tissue was used for measuring superoxide dismutase (SOD)[19] and catalase (CAT)[20] following standard procedures.

Histopathological study

The collected heart tissue was washed with ice-cold normal saline and fixed in formalin (10% neutral) solution followed by embedding in paraffin. Then, it was sectioned (5 µm thickness) and stained with hematoxylin and eosin for histopathological examination under a light microscope.[21]

Statistical analysis

The statistical analysis was performed by ANOVA under One-Way classification followed by Dunnett's test. $p<0.05$ was considered statistically significant. Values are expressed as mean ± standard error of the mean.

RESULTS

Morphometric analysis

Morphometric analysis of all experimental animals is tabulated in Table 1. Results depict that the body weight of experimental animals was recorded on a weekly interval of drug treatment. From the results, the administration of DOXO had shown significant changes in the body weight of animals, whereas acute administration of ROSS has shown a remarkable increase (185.39±1.63, $p<0.05$) in body weight compared to control (171.29±1.36) and DOXO (164.45±2.49) treated group on day 21. However, heart weight and relative heart weight of experimental animals are summarized in Table 2. As *per* the results, heart weight followed by relative heart weight of rats received DOXO was statistically higher than control and ROSS received animals. But, treatment with ROSS significantly ($p<0.05$) inhibited these weight variation changes influenced by DOXO administration and the obtained results were significantly ($p<0.05$) comparable with control groups.

Cardiac marker enzymes

The results presented in Figure 1 and Table 3 depicts the effect of ROSS on serum CK-MB levels against DOXO-induced cardiotoxicity in rats. Results indicate that DOXO received group 2 animals showed a significant raise of CK-MB levels ($p<0.05$) compared to control animals. However, animals treated along with ROSS showed inhibitory action (**$p<0.01$) on the raising level of CK-MB induced by DOXO in rats. Similarly, the same trend was noticed in LDH levels too. The results of the effect of ROSS on serum LDH levels are presented in Figure 2 and Table 3. After injection of DOXO, we observe that the rats in group II animals showed a marked rise in LDH levels ($p<0.05$) compared with control groups. But the results from groups 3 and 4 show inhibitory action on the toxicity induced by DOXO in rats and the results were comparable with control animals.

Table 1. Effect of ROSS on morphometric analysis on DOXO induced cardiotoxicity

Treatments (mg/kg, b.w)	Body weight (gr)		
	Day 7	Day 14	Day 21
CON (1 mL/kg, *s.c.*)	143.39±1.67	162.58±3.29	171.29±1.36
DOXO (10 mg/kg, *i.p.*)	154.81±3.78	157.928±2.18	164.45±2.49
ROSS (10 mg/kg, *p.o.*)	152.68±2.62	165.37±1.79	172.29±1.39
ROSS (10 mg/kg, *p.o.*) + DOXO (10 mg/kg, *i.p.*)	145.73±2.45	173.42±2.56	185.39±1.63*

Values are mean ± SEM, n=5: *$p<0.05$, when compared to the control group, SEM: Standard error of the mean, DOXO: Doxorubicin, ROSS: Rosuvastatin, CON: Control

Post mitochondrial supernatant

The results of the effect of ROSS on heart tissue homogenate CK-MB levels are shown in Figure 3 and Table 3. After the injection of DOXO, we observe that rats in group II animals showed a remarkable rise in CK-MB levels ($p<0.05$) in tissue homogenate compared with control groups. But the results from groups III and IV show the inhibitory action ($p<0.05$) on the toxicity induced by DOXO in rats and the results were comparable with control animals.

Table 2. Effect of ROSS on relative organ weight on DOXO-induced cardiotoxicity

Treatments (mg/kg, b.w)	Heart weight (mg)	
	Absolute heart weight	Relative heart weight
CON (1 mL/kg, *s.c.*)	755±3.29	0.44±0.06
DOXO (10 mg/kg, *i.p.*)	908±2.53	0.55±0.08
ROSS (10 mg/kg, *p.o.*)	771±1.49	0.44±0.04
ROSS (10 mg/kg, *p.o.*) + DOXO (10 mg/kg, *i.p.*)	774±4.56	0.41±0.03

Values are mean ± SEM, n=5. SEM: Standard error of the mean, DOXO: Doxorubicin, ROSS: Rosuvastatin, CON: Control

Liver marker enzymes

The effects of ROSS on serum AST, ALT levels are summarized in Table 4. As *per* the obtained results, DOXO received animals showed marked rise of both AST (240.34±5.53; ***$p<0.001$) and ALT (103.67±3.44; ***$p<0.001$) whereas acute administration of ROSS significantly reversed these biochemical alterations to a significant extent incase of AST (87.85±4.56; **$p<0.01$) and ALT (53.72±0.33**, **$p<0.01$) compared to DOXO and control animals.

Antioxidant activity

The effects of ROSS on antioxidant levels are presented in Table 5, Figure 4, 5. The results reveal that SOD and CAT levels were reduced in PMS solution of heart tissue of DOXO treated group II animals. Administration of DOXO showed marked reduction in SOD ($p<0.05$) and CAT ($p<0.05$) at dose of

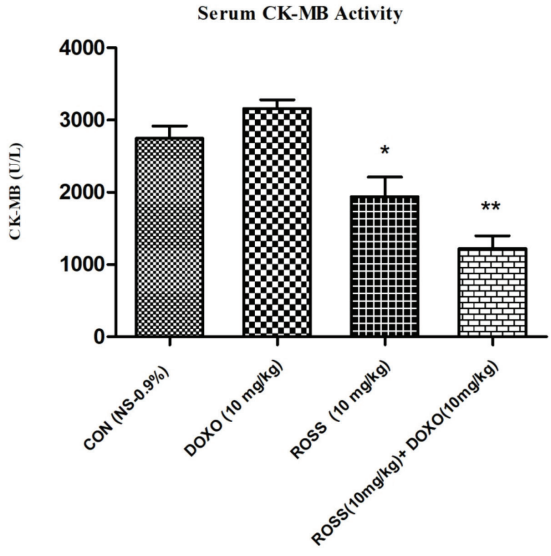

Figure 1. Effect of ROSS on serum CK-MB levels on DOXO-induced cardiotoxicity in rats

ROSS: Rosuvastatin, CK-MB: Creatine kinase-MB, DOXO: Doxorubicin, CON: Control

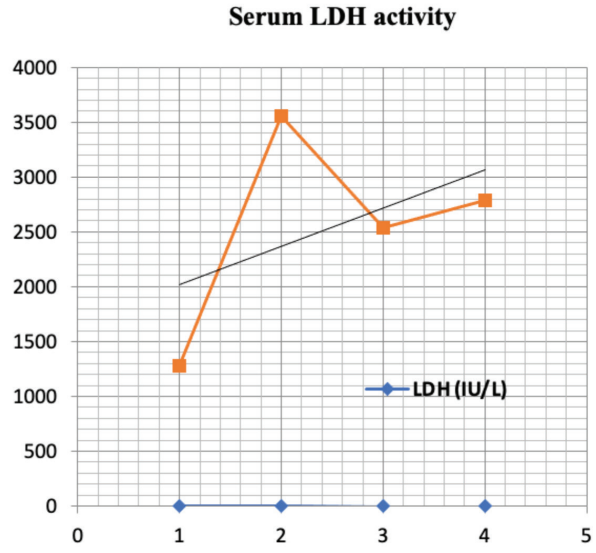

Figure 2. Effect of ROSS on serum LDH levels on DOXO-induced cardiotoxicity in rats

ROSS: Rosuvastatin, DOXO: Doxorubicin, LDH: Lactate dehydrogenase

Table 3. Effect of ROSS on creatine kinase-MB and lactate dehydrogenase levels on DOXO-induced cardio toxicity

Treatments (mg/kg, b.w)	Marker enzymes		
	CK-MB (U/L) (serum)	CK-MB (U/L) (heart tissue homogenate)	LDH (IU/L) (serum)
CON (1 mL/kg, *s.c.*)	2912.05±4.59	222.05± 2.47	1277±3.47
DOXO (10 mg/kg, *i.p.*)	3157.32±3.62	317.32±4.16	3560±5.29
ROSS (10 mg/kg, *p.o.*)	1973.37±7.48*	299.37±1.49	2541±4.58*
ROSS (10 mg/kg, *p.o.*) + DOXO (10 mg/kg, *i.p.*)	1091.62±2.39**	235.62±2.36*	2789±4.39*

Values are mean ± SEM, n=5, *$p<0.05$, **$p<0.01$, when compared to control and toxic control group, ROSS: Rosuvastatin, CK-MB: Creatine kinase-MB, LDH: Lactate dehydrogenase, DOXO: Doxorubicin, ROSS: Rosuvastatin, SEM: Standard error of the mean, CON: Control

Table 4. Effect of ROSS on liver marker enzymes on DOXO-induced cardiotoxicity

Treatments (mg/kg, b.w)	Liver marker enzymes	
	AST (IU/mL)	ALT (IU/mL)
CON (1 mL/kg, *s.c.*)	64.23±3.45	43.48±2.57
DOXO (10 mg/kg, *i.p.*)	240.34±5.53***	103.67±3.44***
ROSS (10 mg/kg, *p.o.*)	131.67±3.49*	73.43±1.29*
ROSS (10 mg/kg, *p.o.*) + DOXO (10 mg/kg, *i.p.*)	87.85±4.56**	53.72±0.33**

Values are mean ± SEM, n=5, *p<0.05, **p<0.01, when compared to control and toxic control group, ROSS: Rosuvastatin, CK-MB: Creatine kinase-MB, DOXO: Doxorubicin, ROSS: Rosuvastatin, AST: Aspartate aminotransferase, ALT: Alanine aminotransferase, SEM: Standard error of the mean, CON: Control

Table 5. Effect of ROSS on Antioxidant levels on DOXO-induced cardiotoxicity

Treatments (mg/kg, b.w)	Antioxidant enzymes	
	SOD (µg/mg of protein)	CAT (U/mg of protein)
CON (1 mL/kg, *s.c.*)	45.86±1.49	1.37±0.69
DOXO (10 mg/kg, *i.p.*)	32.6±2.32	0.77±0.54
ROSS (10 mg/kg, *p.o.*)	58.7±1.56*	1.41±0.48*
ROSS (10 mg/kg, *p.o.*) + DOXO (10 mg/kg, *i.p.*)	60.9±1.58*	1.67±0.53*

Values are mean ± SEM, n=5. *p<0.05, when compared to control and toxic control group, SEM: Standard error of the mean, DOXO: Doxorubicin, ROSS: Rosuvastatin, SOD: Superoxide dismutase, CAT: Catalase

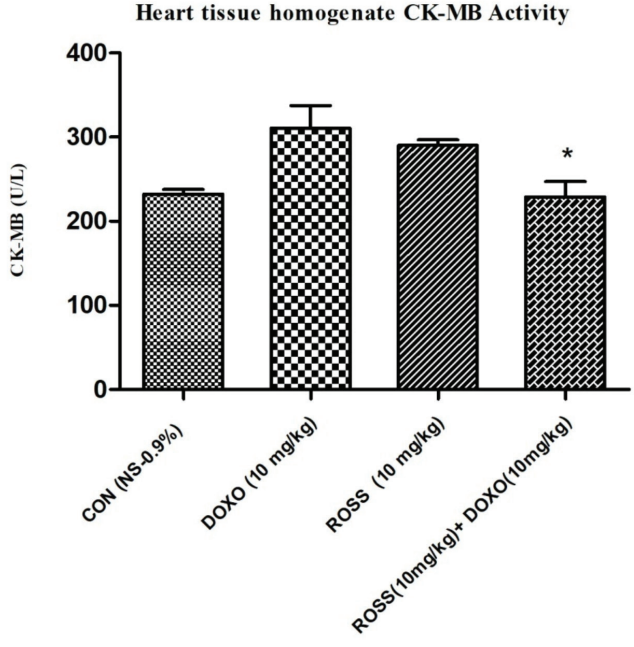

Figure 3. Effect of ROSS on CK-MB in heart tissues homogenate on DOXO-induced cardiotoxicity in rats

ROSS: Rosuvastatin, CK-MB: Creatine kinase-MB, DOXO: Doxorubicin, CON: Control

10 mg/kg. However, ROSS administration caused a reversal of depleted antioxidants to near normal levels, which indicated its protective and antioxidant capabilities.

Histopathological study

Histopathological observations of the cardiac tissues of all experimental groups are shown in Figure 6. From these results, cross-section of cardiac tissues of control animals showed normal myocardial architecture without inflammatory cell infiltration whereas necrotic cardiac tissue damage and like proliferated granulation tissues were seen in DOXO received animals. However, the administration of ROSS reversed these cellular changes to a remarkable significant extent with mild granulation tissue and restored normal cellular architecture, which reflects its protective potential against cardiotoxicity induced by DOXO.

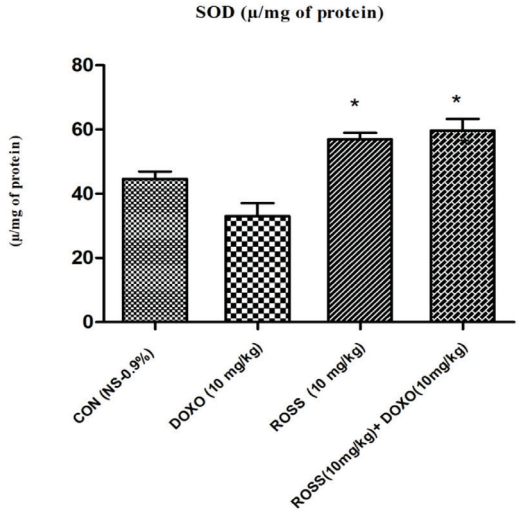

Figure 4. Effect of ROSS on SOD levels on DOXO-induced cardiotoxicity

ROSS: Rosuvastatin, DOXO: Doxorubicin, SOD: Superoxide dismutase, CON: Control

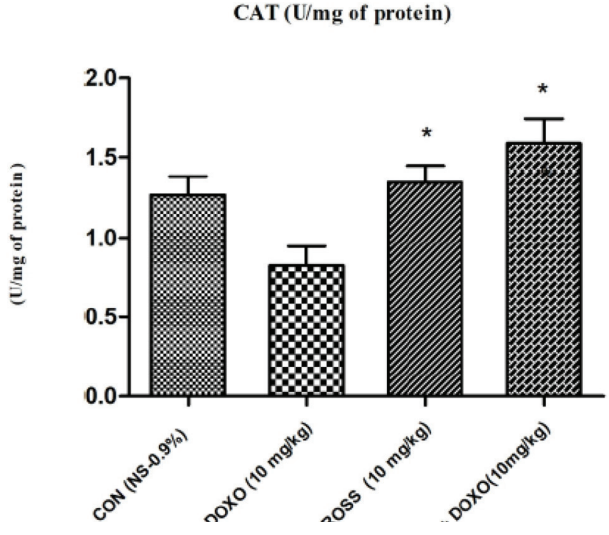

Figure 5. Effect of ROSS on CAT levels on DOXO-induced cardiotoxicity

ROSS: Rosuvastatin, CAT: Catalase, DOXO: Doxorubicin, CON: Control

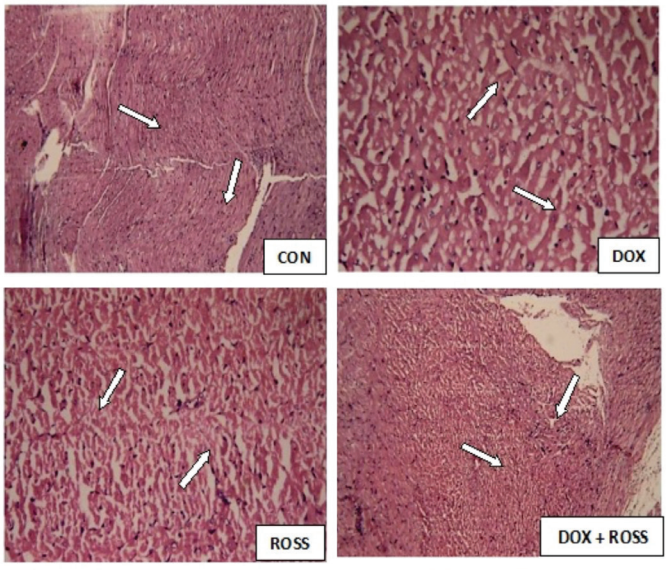

Figure 6. Histopathological observations of different experimental animals using hematoxylin and eosin staining (CON: Control animals showed normal myocardial cellular architecture, DOXO: Doxorubicin received groups showed noticeable necrotic cellular tissue damage, ROSS: Rosuvastatin treated groups; DOXO + ROSS: Doxorubicin plus rosuvastatin treated groups showed significant reversal of necrotic tissue damage caused by doxorubicin)

DISCUSSION

MI is an acute necrotic disorder of the heart and one of the most commonly diagnosed forms of CVD in industrialized nations like India. It is a common and life-threatening manifestation of IHD leads to mortality.[22] MI is the technical name for a heart attack, occurring due to myocardial ischemia resulting from irreversible myocardial tissue necrosis because of complete occlusion of blood vessel (coronary artery) supplying blood to the myocardium. Therefore, the development of cardioprotective agents to improve myocardial function is of great clinical importance.

ROSS has shown significant organ protective properties with diverse pharmacological effects, including anti-inflammatory and antioxidative properties.[23,24] Furthermore, according to studies, ROSS reduces oxidative stress by mediating many antioxidant effects, including decreased NADPH oxidase, suppression of endothelial nitric oxide synthase uncoupling, up regulation of antioxidant enzymatic defense mechanisms, and inhibition of hydrogen peroxide-induced DNA harm.[25,26] But the experimental background found to be fertile or seem to have more gap to support the scientific background of diverse pharmacological profile of ROSS. Hence, the study elucidated the possible *in vivo* ameliorative influence of ROSS in DOXO-induced cardiotoxicity in rats.

DOXO is a well-known cardiotoxic agent capable of inducing cardiac injury in experimental animals and it is widely used model to induce cardiotoxicity.[27] DOXO destroys the myocardial cells, causing it to release cytosolic enzymes such as CK-MB, LDH, AST, and ALT into extra cellular fluid and in serum which indicates the myocardial tissue damage which was reflected in the study.

Results of this study indicate that, DOXO caused significant myocardial tissue damage, as indicated by a marked raise in the levels of cardiac injury markers, oxidative stress, heart weight, and histological changes in myocardial tissue, etc.

The same trend was noticed in heart tissue homogenate of DOXO treated animals compared with the control animals demonstrating the necrotic damage of the myocardial membrane by DOXO. Whereas ROSS-treated groups at doses of 10 mg/kg alone and in combination demonstrated a significant decline in CK-MB and LDH levels ($p<0.05$), which ultimately reflects its protective activity against DOXO-induced cardiotoxicity in rats.

However, in the pathogenesis of various cardiovascular diseases, reports from earlier studies indicated the involvement of reactive oxygen species and the reduction of antioxidants. In this connection, it is well known that SOD is one of the important antioxidant enzymes to control many pathological progress in vast disease and disorders. In this study, increased levels of SOD to a significant extent ($p<0.05$), which in turn reflects the protective role of ROSS. The same trend was observed in CAT too. CAT is also considered as one of the vital enzymes made of hemeprotein and used to scavenge the formed ROS, prevents the tissue damage against free radicals.[28,29] Additionally, histopathological reports further corroborated the obtained results of the present investigations. As *per* the results,the administration of ROSS reversed cellular changes caused by DOXO to a significant extent and restored the normal cellular architecture, which reflects its protective potential against cardiotoxicity induced by DOXO.

CONCLUSION

Results from this study demonstrate that ROSS has shown promising potent cardioprotective effects on DOXO-induced cardiotoxicity in rats, as evidenced by the significant reduction of cardiac marker enzymes like CK-MB and LDH both in serum and in heart tissue homogenate along with significant reduction of liver marker enzymes like ALT, AST along with significant beneficial effects were seen in morphometric analysis. However, it is well recognized that various radical scavengers, such as CAT, SOD, and GPX, as well as GSH, serve as the first line of defense against oxidative damage, including cardiotoxicity. Reactive oxygen species can cause oxidative damage due to the lack of an appropriate endogenous antioxidant defense mechanism. The same were reflected in this study, which clearly indicated the diminishment of antioxidants such as SOD, CAT in DOXO treated animals. Thus, from the results, oxidative damage was clearly involved in DOXO-induced cardiotoxicity. However, the treatment of ROSS remarkably restored DOXO-induced cardiotoxicity by up-regulating the antioxidants. Thus, results from *in vivo* antioxidant study reflect that administration of ROSS significantly raised the level of SOD and CAT along with significant reversal of necrotic tissue damage caused by DOXO. Hence, it can be concluded that the cardioprotective potential of ROSS may be due to attenuation of cardiac, liver marker enzymes and oxidative stress by modulating oxidative damage by up-regulating the antioxidant defense mechanism.

ACKNOWLEDGMENTS

The authors are grateful to the Principal and Management of Sree Vidyanikethan College of Pharmacy for providing the necessary facilities, and this research received no particular funding from any government, commercial, or non-profit organization.

Conflict of interest: No conflict of interest was declared by the authors. The authors are solely responsible for the content and writing of this paper.

REFERENCES

1. Ianaro A, Ialenti A, Maffia P, Sautebin L, Rombolà L, Carnuccio R, Iuvone T, D'Acquisto F, Di Rosa M. Anti-inflammatory activity of macrolide antibiotics. J Pharmacol Exp Ther. 2000;292:156-163.
2. Singal PK, Pierce GN. Adriamycin stimulates low-affinity Ca2+ binding and lipid peroxidation but depresses myocardial function. Am J Physiol Heart Circ Physiol. 1986;250:H419-H425.
3. Thillaivanan S, Parthiban P, Kanakavalli K, Sathiyarajeshwaran P. A review on "Kapa Sura Kudineer"-a Siddha formulary prediction for swine flu. Int J Pharm Sci Drug Res. 2015;7:376-383.
4. Arya V, Gupta VK. Chemistry and pharmacology of plant cardio protective: a review. Int J Pharm Sci. 2011;2:1156-1167.
5. Nazish J, Ur-Rahman, Shoukat A. Cardioprotective, and antilipidemic potential of *Cyprus rotundas* in chemically induced cardiotoxicity. Int J Agric Biol. 2012;14:989-992.
6. Geisberg CA, Sawyer DB. Mechanisms of anthracycline cardiotoxicity and strategies to decrease cardiac damage. Curr Hypertens Rep. 2010;12:404-410.
7. Octavia Y, Tocchetti CG, Gabrielson KL, Janssens S, Crijns HJ, Moens AL. Doxorubicin-induced cardiomyopathy: from molecular mechanisms to therapeutic strategies. J Mol Cell Cardiol. 2012;52:1213-1225.
8. Minotti G, Menna P, Salvatorelli E, Cairo G, Gianni L. Anthracyclines: molecular advances and pharmacologic developments in antitumor activity and cardiotoxicity. Pharmacol Rev. 2004;56:185-229.
9. Konorev EA, Kotamraju S, Zhao H, Kalivendi S, Joseph J, Kalyanaraman B. Paradoxical effects of metalloporphyrins on doxorubicin-induced apoptosis: scavenging of reactive oxygen species versus induction of heme oxygenase-1. Free Radic Biol Med. 2002;33:988.
10. Monetti M, Canavesi M, Camera M, Parente R, Paoletti R, Tremoli E, Corsini A, Bellosta S. Rosuvastatin displays anti-atherothrombotic and anti-inflammatory properties in apoE-deficient mice. Pharmacol Res. 2007;55:441-449.
11. Funderburg NT, Jiang Y, Debanne SM, Labbato D, Juchnowski S, Ferrari B, Clagett B, Robinson J, Lederman MM, McComsey GA. Rosuvastatin reduces vascular inflammation and T-cell and monocyte activation in HIV-infected subjects on antiretroviral therapy. J Acquir Immune Defic Syndr. 2015;68:396-404.
12. Miida T, Takahashi A, Ikeuchi T. Prevention of stroke and dementia by statin therapy: experimental and clinical evidence of their pleiotropic effects. Pharmacol Ther. 2007;113:378-393.
13. Duarte T, da Cruz IB, Barbisan F, Capelleto D, Moresco RN, Duarte MM. The effects of rosuvastatin on lipid-lowering, inflammatory, antioxidant and fibrinolytics blood biomarkers are influenced by Val16Ala superoxide dismutase manganese-dependent gene polymorphism. Pharmacogenomics J. 2016;16:501-506.
14. Khatib NA, Mediswathi, Patel Jignesh. Evaluation of concomitant treatment of simvastatin and Zingiber Officinale in doxorubicin induced cardio toxicity in waster rats. IJRAP. 2011;2:660-664.
15. Reitman S, Frankel S. A colorimetric method for the determination of serum glutamic oxalacetic and glutamic pyruvic transaminases. Am J Clin Pathol. 1957;28:56-63.
16. Young DS. Effects of drugs on clinical laboratory tests. 3rd ed. Washington, DC: AACC Press; 1990:356-357.
17. Tsung SH. "Creatine kinase activity and isoenzyme pattern in various normal tissues and neoplasms. Clin Chem. 1983;2040-2043.
18. Lorentz K, Klauke R, Schmidt E. Recommendation for the determination of the catalytic concentration of lactate dehydrogenase at 37 degrees C. Standardization Committee of the German Society for Clinical Chemistry, Enzyme Working Group of the German Society for Clinical Chemistry. Eur J Clin Chem Clin Biochem. 1993;31:897-899.
19. Kakkar P, Das B, Viswanathan PN. A modified spectrophotometric assay of superoxide dismutase. Indian J Biochem Biophys. 1984;21:130-132.
20. Aebi H. Catalase. In: Methods of enzymatic analysis. Bergmeyer HU (ed). Verlag, Chemic Academic Press Inc; 1974:673-685.
21. Talib VH. A handbook of medical laboratory technology. 2nd ed. New Delhi: CBS Publisher and Distributors; 2007:155-167.
22. Patel V, Upaganlawar A, Zalawadia R, Balaraman R. Cardioprotective effect of melatonin against isoproterenol induced myocardial infarction in rats: a biochemical, electrocardiographic and histoarchitectural evaluation. Eur J Pharmacol. 2010;644:160-168.
23. Shen P, Zhang RN, Li F, et al. Diagnostic value of serum cystatin C in early contrast nephropathy after coronary intervention. Laboratory Medicine and Clinic. 2018;15:2475-2478.
24. Chen Z, Cao Y, Qian J, Ma J, Zou Y, Ge J. Cardio protection of rosuvastatin against cardiac dysfunction after coronary micro-embolization via alleviating inflammatory induced micro infarctions. Circulation. 2015;132:A13434.
25. Grosser N, Erdmann K, Hemmerle A, Berndt G, Hinkelmann U, Smith G, Schröder H. Rosuvastatin upregulates the antioxidant defense protein heme oxygenase-1. Biochem Biophys Res Commun. 2004;325:871-876.
26. Habibi J, Whaley-Connell A, Qazi MA, Hayden MR, Cooper SA, Tramontano A, Thyfault J, Stump C, Ferrario C, Muniyappa R, Sowers JR. Rosuvastatin, a 3-hydroxy-3-methylglutaryl coenzyme a reductase inhibitor, decreases cardiac oxidative stress and remodeling in Ren2 transgenic rats. Endocrinology. 2007;148:2181-2188.
27. Doroshow JH. Doxorubicin-induced cardiac toxicity. N Engl J Med. 1991;324:843-845.
28. Chance B, Greenstein DS, Roughton RJW. The mechanism of catalase action1-steady-state analysis. Arch Biochem Biophys. 1952;37:301-321.
29. Yan H, Harding JJ. Glycation-induced inactivation and loss of antigenicity of catalase and superoxide dismutase. Biochem J. 1997;328:599-605.

Turk J Pharm Sci 2022;19(1):35-47
DOI: 10.4274/tjps.galenos.2021.77177

ORIGINAL ARTICLE

Quantitative Determination of Related Substances in Formoterol Fumarate and Tiotropium in Tiomate Transcaps® Dry Powder Inhaler

Tiomate Transcaps® Kuru Toz İnhalerde Formoterol Fumarat ve Tiotropiumdaki İlgili Maddelerin Kantitatif Tayini

Priyanka Satish GONDHALE*, Binoy VARGHESE CHERIYAN

Department of Pharmaceutical Chemistry and Analysis, School of Pharmacy, Vels Institute of Science, Technology and Advanced studies (VISTAS), Tamil Nadu, India

ABSTRACT

Objectives: Tiotropium (TIO) and formoterol fumarate (FF) combination in dry powder inhaler (DPI) dosage form used for treating asthma, bronchospasm, chronic bronchitis, emphysema and chronic obstructive pulmonary diseases. Aim to develop an analytical method for estimating emerging and advancing dry powder inhaler combination toward enhanced therapeutics for the estimation of related substances but for this it is foremost to have a sensitive, simple, robust and validated method therefore, a new reverse phase-high performance liquid chromatography (HPLC) method has been developed for the determination of related substances in FF and TIO DPI.

Materials and Methods: The analytical method was performed on schimadzu HPLC with a quaternary pump, the separation achieved using BDS Hypersil C18 (250×4.6 mm, 5 µm) column with mobile phase consisting of sodium phosphate buffer pH 3.2 and acetonitrile 1.0 mL min^{-1} flow rate in the gradient elution. Diluent consists of a mixture of buffer pH 3.2 and acetonitrile in the ratio of (70:30) %v/v. 30˚C column temperature and photodiode-array detection detector at a wavelength 240 nm. The run time was 50 min. The Retention time of FF and TIO was found to be at 7.8 and 10.3 min respectively.

Results: Both the analyte peaks were found to be free from interference. The method was validated as *per* the International Council on Harmonisation guidelines, the linearity was performed on 0.015 to 1.089 ppm for TIO and 0.01 to 0.728 ppm for FF concentration with correlation coefficient of 1,000. The precision and accuracy were also performed at the limit of quantification level were within the limits. Forced degradation study was also conducted.

Conclusion: The recommended method for the related substance determination of FF and TIO is simple, selective, specific and precise. It also demonstrates the study of the degradation pattern. Moreover, the above developed related substance analytical method was applied to the bulk analysis and pharmaceutical dosage form for routine analysis and stability study.

Key words: Dry powder inhaler, forced degradation study, LOD & LOQ determination, ICH guidelines, asthma, COPD (chronic obstructive pulmonary diseases)

ÖZ

Amaç: Kuru toz inhaler (KTİ) dozaj formunda olan tiotropium (TIO) ve formoterol fumarat (FF) kombinasyonu, astım, bronkospazm, kronik bronşit, amfizem ve kronik obstrüktif akciğer hastalıklarının tedavisinde kullanılmaktadır. Amaç, kuru toz inhaler kombinasyonları olarak ortaya çıkan ve gelişmekte olan dozaj formlarındaki ilgili maddelerin tespitine yönelik analitik bir yöntem geliştirmektir. KTİ'de bulunan FF, TIO ve ilgili maddelerin belirlenebilmesi için öncelikle hassas, basit, sağlam ve valide edilmiş yeni bir ters faz yüksek performanslı sıvı kromatografisi (HPLC) yöntemi geliştirilmiştir.

Gereç ve Yöntemler: Analitik yöntem, dörtlü pompalı Shimadzu HPLC cihazı ile gerçekleştirilmiştir; ayırım BDS Hypersil C18 (250x4,6 mm, 5 µm) kolonu, 1,0 mL dk^{-1} akış hızında sodyum fosfat tamponu pH 3,2 ve asetonitrilden oluşan mobil faz kullanılarak gradient elüsyon ile sağlanmıştır. Mobil faz pH 3,2 tampon ve asetonitril karışımından (70:30; % h/h) oluşmaktadır. Analiz, kolon sıcaklığı 30˚C, fotodiyot dizi detektörü 240 nm dalga boyunda gerçekleştirilmiştir. Analiz süresi 50 dk olmuştur. FF ve TIO'nun retansiyon zamanları sırasıyla 7,8 ve 10,3 dk olarak bulunmuştur.

Bulgular: Her iki analitin herhangi bir girişimde bulunmadığı saptanmıştır. Yöntem, Uluslararası Harmonizasyon Konseyi yönergelerine göre valide edilmiştir; doğrusallık TIO için 0,015-1,089 ppm ve FF için 0,01-0,728 ppm konsantrasyon aralıklarında, 1,000 korelasyon katsayısı ile

*Correspondence: gondhalepriyanka@gmail.com, Phone: +08097313283, ORCID-ID: orcid.org/0000-0003-3156-5306

Received: 04.12.2020, Accepted: 10.04.2021

gerçekleştirilmiştir. Kesinlik ve doğruluk, tayin limiti seviyesinde gerçekleştirilmiş, sınırlar içinde bulunmuştur. Zorlamalı bozunma çalışması da gerçekleştirilmiştir.

Sonuç: FF, TIO ve ilgili maddelerin tespiti için önerilen yöntem basit, seçici, spesifik ve kesindir. Aynı zamanda zorlamalı degradasyon çalışmasını da göstermektedir. Ayrıca, geliştirilen analitik yöntem yığın analizi ve farmasötik dozaj formunun rutin analizlerinde ve stabilite çalışmasına uygulanmıştır.

Anahtar kelimeler: Kuru toz inhaler, zorlamalı degradasyon çalışması, LOD & LOQ belirleme, ICH kılavuzu, astım, KOAH (kronik obstrüktif akciğer hastalığı)

INTRODUCTION

Chronic bronchitis and emphysema are the two existing lung diseases in which the airway become narrow and is collectively named as chronic obstructive pulmonary disease (COPD).[1]

Essential management approaches are stopping smoking habit, vaccinations, rehabilitation and treatment by using inhalers. The combination of formoterol fumarate (FF) and tiotropium (TIO) is used in targeting various characteristics of COPD as bronchodilation and the inflammations.[1,2]

FF dihydrate is a directly acting sympathomimetic with beta-adrenoceptor stimulant activity. FF is prescribed for its long acting beta 2 agonist effect for treating airway obstruction, asthma and COPD.[3] The pharmacological effect of beta 2 agonist is to stimulate intracellular adenyl cyclase enzyme that catalyzes the conversion of adenosine triphosphate to cyclic-3',5'-adenosine monophosphate (cyclic AMP). Increased cyclic AMP levels causes relaxation in the release of immediate hypersensitivity mediators from mast cells. Chemically, it is *N*-2-hydroxy-5-(1*RS*)-1-hydroxy-2-(1*RS*)-2(4methoxyphenyl)1methy lethylaminoethyl phenyl formamide(*E*)-butenedioatedihydrate with molecular formula $C_{42}H_{52}N_4O_{12}\cdot 2H_2O$ and molecular weight of 840.92.[1,2]

TIO bromide monohydrate is an anticholinergic, antimuscarinic bronchodilator used in the airway obstruction, COPD conditions.[1-3] TIO shows its pharmacological effects by inhibiting M3 receptors in the smooth muscle, which leads to bronchodilation. Chemically it is (1*R*,2*R*,4*S*,5*S*,7*s*)-7-(2-hydroxy-2,2-dithiophen-2-ylacetyl)oxy-9,9-dimethyl-3-oxa-9-azoniatricyclo3.3.1.02,4 non-anebromidemonohydrate with molecular formula $C_{19}H_{22}BrNO_4S_2\cdot H_2O$ and molecular weight of 490.40.[1]

A complete literature survey reveals that TIO is determined by spectrophotometric method.[4] TIO in bulk and dry powder inhalation (DPI) form is determined by high performance thin-layer chromatography.[5] Methods are available to determine TIO and related substances by high performance liquid chromatography (HPLC).[6] For the biological estimation of TIO in human plasma; three methods illustrated.[7-9] Estimation of FF in various pharmaceutical dosage forms by spectrophotometry with charge transfer complexation technique,[10,11] Q absorbance ratio and solving simultaneous equation,[12] and zero order spectrophotometric method and area under curve technique.[13] FF also estimated along with other drug moieties by thin layer chromatography densitometry methods.[14-17] FF also estimated along with other drug moieties in HPLC,[14,17-24] also in plasma, urine and biological samples.[25,26] TIO has been determined by either FF[27-29] or ciclesonide or olodaterol[30-33] in various dosage forms by HPLC methods, but the focus was found to be on a single drug compound. In FF the hydrazine hydrate content is determined by gas chromatography-mass spectrometry method.[34] Moreover, no related substances analytical method available in any of the pharmacopeias.

To the best of the author's knowledge, no simple, sensitive and robust related substances analytical method, which focused on both the drug moieties reported till now for the simultaneous evaluation of TIO and FF in DPI dosage form and validated according to International Council for Harmonisation (ICH) guidelines.[35] The proposed validated reversed-phase-HPLC method can therefore be applied for simultaneous evaluation of TIO and FF QC testing and stability studies for the determination of related substances. To perform this study Tiomate Transcaps® DPI manufactured by Lupin ltd. India is used.

MATERIALS AND METHODS

Instrumentation

The Dionex HPLC system consists of dionex ultimate 3,000 UHPLC system equipped with a quaternary gradient pump dionex ultimate 3,000 pumps, dionex ultimate 3,000 auto sampler, dionex ultimate 3,000 column compartment and a dionex ultimate 3,000 UV-Photo Diode Array detector. Separation and quantitation were carried out using a C18 Hypersil BDS column (250 mmx4.6 mm, 5 µm) Chromeleon 7.2 SR5 software used for data acquisition.

Chemicals and reagents

Pharmaceutical respiratory-grade TIO was provided and qualified by Vamsi lab Ltd (India) as such assay was found to be 101.79%. Pharmaceutical-grade FF was provided and qualified by Vamsi lab Ltd (India) as such assay was found to be 100.12%. HPLC grade acetonitrile (Rankem), Milli-Q water (Milli-Q® CLX 7000), sodium dihydrogen phosphate monohydrate, triethylamine, orthophosphoric acid (Rankem), 0.45 µm Buffer filter (mdi) was used.

Chromatographic conditions

The chromatographic separation utilizes a gradient elution in which buffer consists of 1.38 mg of sodium dihydrogen phosphate monohydrate in 1,000 mL of water, add 2 mL of triethylamine, adjust pH 3.2 with dilute orthophosphoric acid, filter and degas through 0.45 µm filter. Mobile phase A is buffer solution pH 3.2 and mobile phase B is acetonitrile 1.0 mL min^{-1} flow rate and BDS Hypersil C18 (250×4.6 mm, 5 µm). Diluent consists of a mixture of buffer pH 3.2 and acetonitrile in the

ratio of 70:30 v/v. Analysis was carried out at 30˚C column temperature and photodiode-array detection (PDA) detector at wavelength 240 nm for both TIO and FF. The injection volume was 100 µL and run time was 50 min. The Retention time of FF and TIO was found to be at 7.8 and 10.3 min, respectively.

The gradient program is as follows:

Time (minutes)	% Mobile phase: A (mL/min)	% Mobile phase: B (mL/min)
0	80	20
30	60	40
40	30	70
45	30	70
50	80	20

Standard preparation

TIO standard stock solution

Standard solutions of TIO were prepared by taking 36-mg TIO separately in each 100 mL volumetric flask, added 70 mL of diluent sonicate to dissolve and make volume with diluent and mix. Further dilute 5 mL of this solution to 100 mL with the diluent.

FF standard stock solution

Standard solutions of FF were prepared by taking 24-mg FF separately in each 50 mL volumetric flask, added 35 mL of diluent sonicate to dissolve and make volume with diluent and mix. Further dilute 1 mL of this solution to 100 mL with the diluent.

Mix standard solution

Pipette out 5 mL of TIO standard stock solution and 10 mL of FF standard stock solution to 100 mL with diluent.

Sample preparation

Tiomate Transcaps® (Lupin ltd..) preparation, carefully open and collect the sample powder equivalent to 0.72-mg TIO in to 10 mL volumetric flask, added about 7 mL diluent sonicate for 15 minutes with intermediate shaking, cool and dilute to volume with diluent and mix well and filter the solution through 0.45 µm filter by discarding the first few mL of the filtrate and use.

Procedure

Separately inject equal volume of the diluent, placebo solution, standard and sample solutions, record the peak responses. Disregard any peak area due to diluent, FF and placebo solution in the sample solution. Calculate the % of each impurity present in the sample solution by following formulae:

Calculation:

$$\text{Similarity factor} = \frac{\text{Area of standard -1}}{\text{Area of standard -2}} \times \frac{\text{Wt. of standard -2}}{\text{Wt. of standard -1}} \times 100$$

$$\textbf{\% Impurity} = \frac{AT}{AS} \times \frac{\text{Wt. std}}{100} \times \frac{5}{100} \times \frac{5}{100} \times \frac{10}{\text{Wt. spl}} \times \frac{P}{100} \times \frac{\text{Avg. Wt}}{\text{L.C.}} \times \frac{392.5}{490.4} \times 100 \times 1000$$

where,

AT: Area of each impurity in the sample solution, As: The following: Area of standard solution 1, Wt. std.: Weight of standard in mg, Wt. spl.: Weight of sample in mg, Avg. Wt: Average weight of net content in mg, L.C.: Label claim in mcg, P: Potency of standard, 392.5: Molecular weight of tiotropium, 490.4: Molecular weight of tiotropium bromide monohydrate

Analytical method development and optimization

The milli-Q water in different proportions of methanol and acetonitrile tried in both isocratic and gradient elution as well by using various C8 and C18 columns but no proper separations were achieved. Different proportions of potassium and sodium salt buffer (10 mMol to 30 mMol) with methanol and/or acetonitrile were used in various proportions in both isocratic and gradient elution patterns but no proper peak shape, tailing factor and theoretical plates of TIO and FF were observed; also resolution between TIO and FF was not good.

Various ranges of pH were tried from pH 2.5 to pH 6.5 and found that the best results were obtained with sodium dihydrogen phosphate monohydrate buffer pH 3.2 and acetonitrile 1.0 mL min^{-1} flow rate and BDS Hypersil C18 (250×4.6 mm, 5 µm). Diluent consists of a mixture of buffer pH 3.2 and acetonitrile in the ratio of 70:30 v/v. Analysis was carried out at 30˚C column temperature and PDA detector at a wavelength 240 nm for both TIO and FF. The injection volume was 100 µL and run time was 50 min. The retention time of FF and TIO was found to be at 7.8 and 10.3 min respectively.

Analytical method validation parameters

The comprehensive and systematic method validation was carried out as *per* ICH guidelines. The analytical method was validated for system suitability, system precision, method precision, intermediate precision, ruggedness, specificity, selectivity, forced degradation, linearity & range, accuracy, limit of detection (LOD) & limit of quantification (LOQ) determination, precision at LOQ level, filter validation, robustness (change in chromatographic conditions) and stability of an analytical solution.

System suitability and system precision were determined by injecting two and six replicate injections of the standard solutions, respectively. The responses of peaks were recorded.

In LOD and LOQ determination, a series of standard preparations of FF and TIO standard over the range starting from 1% to at least 50% of standard concentration was prepared. Plotted linearity graph of average area at each level against the concentration (ppm) and determine the correlation coefficient, slope and intercept of analyte for LOQ determination. The concentrations for LOD & LOQ from linearity study were determined.

Method precision may be defined as the precision of an analytical procedure expressing the closeness of agreement between a series of measurements obtained from multiple sampling of the same homogeneous sample under the prescribed conditions. In method precision six samples were prepared as *per* the analytical method representing a single batch; % impurities of these samples were determined for both the analytes and the analytical method precision was assessed by the % relative standard deviation (RSD).

Intermediate precision (ruggedness) expresses the ability of an analytical method to remain unaffected and produce reliable results within the laboratory variations such as different days, different equipment, different analysts. Six samples were prepared as *per* the analytical method representing the same batch used for method precision. % impurities of these samples were determined for both the analytes. The method precision and intermediate precision was assessed by the overall % RSD.

The specificity (selectivity) study is conducted to prove the ability of an analytical method to assess unequivocally the analyte in the presence of components which may be expected to be present in the sample. The diluent, placebo solution, FF dihydrate selectivity solution, TIO selectivity solution, fumaric acid selectivity solution, standard and sample solution were prepared as mentioned in the analytical method, injected and recorded the observations for both TIO and FF.

In forced degradation study, the sample and placebo were exposed under relevant stress conditions such as temperature, oxidation, photolytic, humidity, acid hydrolysis and base hydrolysis. Samples of these stress conditions were analyzed as *per* the analytical method described. The experiment was performed to achieve 5-30% of degradation in at least one stress condition.

Linearity & range; the linearity of an analytical procedure is its ability within a given range to find test results that are directly proportional to the analyte concentration in the sample solution. TIO and FF standards were prepared in a range of LOQ to 150% of the working standard concentration. Linearity graph of concentration vs. average peak area of the analyte was plotted separately. The correlation co-efficient, slope, and y intercept were evaluated.

The accuracy expresses the closeness of agreement between the value which is accepted either as a conventional true value or an accepted reference value and the value obtained using the method. The samples for accuracy were prepared as *per* spiking the TIO and FF standard solution in the placebo at LOQ level, 50%, 100%, and 150% concentration level of standard in triplicate for 50, 100, 150% and six times for LOQ level of working concentration and analysed as *per* the described method.

For the filter study, the sample solution was prepared as described in the analytical method. The solution was centrifuged at 4,000 rpm for 10 minutes. Decanted supernatant solution was injected as centrifuged sample solution. From the remaining half portion of the solution, filtered the solution through 0.45 µm nylon filter and filled the vials by discarding 0 mL, 2 mL and 5 mL solution. These solutions were injected as a sample solution. The peak responses were recorded for both the analytes for all centrifuged and filtered solution in single sequence.

The robustness of an analytical procedure is a measure of its capacity to remain unaffected by small, but deliberate variations in the analytical method parameters and provides an indication of its reliability. In this study, parameters like change in detection wavelength, flow rate, column oven temperature, mobile phase organic composition (acetonitrile) and mobile phase buffer pH were performed and peak responses were recorded for both analytes.

For solution stability, the standard and sample solutions for both FF and TIO were prepared and injected against freshly prepared standard solution on day-0, day-1, day-2, and day-3.

RESULTS AND DISCUSSION

System suitability & system precision

System suitability is demonstrated by preparing duplicate standard solution of TIO and FF and injecting the same. System precision is demonstrated by injecting standard solution of TIO and FF in six replicate injections according to the analytical method described above. For system suitability the similarity factor for both standard solution 1 and standard solution 2 should be between 95.0% to 105.0% for both TIO and FF. For system precision, the similarity factor for six replicate injections of standard solution 1 should be between 95.0% to 105.0% for both TIO and FF. The number of theoretical plates should not be less than 2,000, tailing factor should not be more than 2.0 and capacity factor should be more than 1.0 for both FF and TIO peaks (Table 1, 2).

LOD and LOQ determination

Prepare a series of standard preparations of FF and TIO standard over a range starting from 1% to at least 50% of standard concentrations (Figure 1). A series of low concentrations

Table 1. System suitability

		Area	Similarity factor	Tailing factor	Theoretical plates	Capacity factor
Formoterol fumarate	Standard solution-1	66680	100.0	1.0	3905	1.58
	Standard solution-2	66567		1.0	3973	1.57
Tiotropium	Standard solution-1	165363	100.1	1.1	10526	2.51
	Standard solution-2	165256		1.1	10647	2.51

Table 2. System precision

System precision FF					System precision TIO				
Inj. no	**FF area**	**Similarity factor**	**TF**	**NTP**	**Inj. no**	**TIO area**	**Similarity factor**	**TF**	**NTP**
1	66680	100.0	1.0	3905	1	165363	100.0	1.1	10526
2	66769	99.9	1.0	3969	2	165007	100.2	1.1	10569
3	66800	99.8	1.0	3980	3	165529	99.9	1.1	10553
4	66518	100.2	1.0	3969	4	165026	100.2	1.1	10641
5	66114	100.9	1.0	3971	5	165902	99.7	1.1	10533
6	66422	100.4	1.0	3990	6	166040	99.6	1.1	10656
Avg.	**66551**				**Avg.**	**165478**			
SD	258.7908				STDEV	433.0337			
% RSD	**0.39**				**% RSD**	**0.26**			

FF: Formoterol fumarate, TIO: Tiotropium, SD: Standard deviation, RSD: Relative standard deviation, TF: Tailing factor, NTP: Number of theoretical plates, Inj. no: Injection number, Avg: Average

ranges from 0.007 ppm to 0.365 ppm for TIO and 0.005 ppm to 0.243 ppm for FF has been prepared on the basis of standard response and injected in triplicate injections. The calibration curves were prepared for area vs. concentration for TIO and FF is given below. From these calibration curve slope; intercept and correlation coefficient from the Microsoft Excel along with the STEYX were determined and the LOD & LOQ were calculated as *per* below formula (Table 3, Figure 2, 3).

For TIO,

LOD = 3.3 x STEYX/slope
=3.3 x 0.00241
=0.008 PPM

Reported value in PPM = NA

LOQ =10 x STEYX/slope
= 10 x 0.00241
= 0.024 PPM

Reported value in PPM = 0.015

From the prediction linearity study statistically calculated LOD and LOQ values are, LOD is 0.008 ppm and LOQ is 0.024 ppm and reported LOQ = 0.015 ppm *i.e.* 0.02%.

For FF,

LOD =3.3 x STEYX/slope
=3.3 x 0.00210
=0.007 PPM

Reported value in PPM = NA

LOQ =10 x STEYX/slope
=10 x 0.00210
=0.021 PPM

Reported value in PPM = 0.01

From the prediction linearity study statistically calculated LOD and LOQ values are, LOD is 0.007 ppm and LOQ is 0.021 ppm and reported LOQ = 0.01 ppm *i.e.* 0.02%.

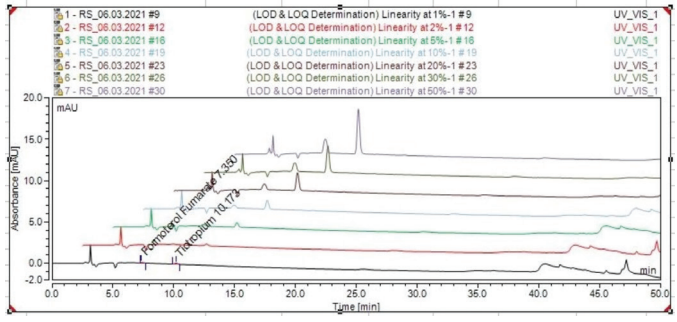

Figure 1. Overlaid chromatogram of TIO & FF for LOD & LOQ determination 1% to 50%

TIO: Tiotropium, FF: Formoterol fumarate, LOD: Limit of detection, LOQ: Limit of quantification

Method precision & intermediate precision (ruggedness)

In method precision, as *per* the analytical method, six sample preparation were prepared representing a single batch. The intermediate precision or ruggedness was verified by performing precision study as *per* the analytical method six sample preparation of a single batch sample by different analyst, on different day, using different column and on different instrument. As *per* ICH guideline Q2 (R1), The % single maximum impurity (above LOQ level), % total impurity, the mean of % single maximum impurity (above LOQ level), and intermediate precision were calculated the % RSD of results of % single maximum impurity (above LOQ level) & % total impurity of six sample preparations should not be more than 15.0 (Table 4).

Specificity (selectivity)

Prepared diluent, placebo solution, FF selectivity solution, TIO selectivity solution, fumaric acid selectivity solution standard and sample solution, as mentioned in analytical method and injected and recorded the observations. The diluent and placebo should not give any interfering peak at the retention time of

Table 3. Linearity data for LOD & LOQ determination

FF LOD & LOQ determination		FF precision at LOQ level	
Conc. in ppm	**Average area**	**Preparation**	**% Impurity**
0.005	707	1	0.0190
0.010	1366	2	0.0199
0.024	3366	3	0.0190
0.049	6586	4	0.0191
0.097	13923	5	0.0196
0.146	20410	6	0.0180
0.243	33292	**Average**	**0.0190**
Slope	**137743.1890**	Standard deviation	0.0007
Intercept	**83.6299**	**% RSD**	**3.68**
Correlation coefficient	**1.000**		
STEYX	**289.66**		
STEYX/slope	**0.00210**		
TIO LOD & LOQ determination		**TIO precision at LOQ level**	
Conc. in ppm	**Average area**	**Preparation**	**% Impurity**
0.007	1777	1	0.0160
0.015	3611	2	0.0166
0.036	8390	3	0.0164
0.073	16835	4	0.0161
0.146	34770	5	0.0157
0.219	49835	6	0.0158
0.365	83173	**Average**	**0.0160**
Slope	**227482.0383**	Standard deviation	0.0003
Intercept	**361.2807**	**% RSD**	**1.88**
Correlation coefficient	**1.000**		
STEYX	**582.95**		
STEYX/slope	**0.00256**		

LOD: Limit of detection, LOQ: Limit of quantification, FF: Formoterol fumarate, RSD: Relative standard deviation, STEYX: Standard error of estimates, TIO: Tiotropium, Conc.: Concentration

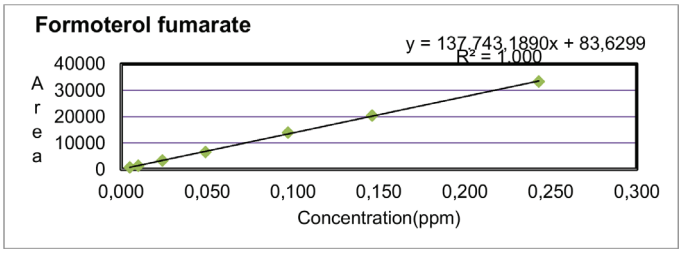

Figure 2. LOD & LOQ determination of FF

FF: Formoterol fumarate, LOD: Limit of detection, LOQ: Limit of quantification

FF and TIO peaks. The peak purity should pass for the analyte peaks in the standard and sample solution. FF is a fumarate salt prepared from arformoterol, in a chemical reaction for every two molecules of formoterol one molecule of fumaric acid is released. Aim to inject fumaric acid selectivity solution is to identify the retention time of fumaric acid and to confirm that it is not interfering with the retention time of FF and TIO peaks and based on the above observations the method is found to be selective (Table 5, Figure 4a-f).

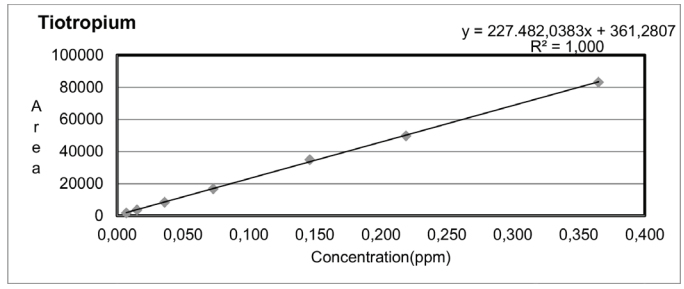

Figure 3. LOD & LOQ determination of TIO

TIO: Tiotropium, LOD: Limit of detection, LOQ: Limit of quantification

Table 4. Method precision, intermediate precision

Preparation		% Single maximum impurity	% Total impurity
Method precision	1	0.109	0.207
	2	0.122	0.223
	3	0.142	0.267
	4	0.129	0.244
	5	0.135	0.255
	6	0.133	0.261
Average (A)		**0.128**	**0.243**
Standard deviation		0.0116	0.0234
% RSD		**9.06**	**9.63**
Intermediate precision	7	0.101	0.194
	8	0.123	0.239
	9	0.131	0.258
	10	0.121	0.233
	11	0.134	0.257
	12	0.126	0.245
Average (B)		**0.123**	**0.238**
Standard deviation		0.0117	0.0235
% RSD		**9.51**	**9.87**
Overall average (A + B)		**0.126**	**0.240**
Overall standard deviation		0.0115	0.0225
% RSD		**9.13**	**9.38**

RSD: Relative standard deviation

Table 5. Selectivity

Sr. no.	Solution preparation	Observation at retention time of product	Peak purity match (TIO)	Peak purity match (FF)	Peak purity results
1	Diluent	No interference is observed at the retention time of formoterol and tiotropium peaks	NA		
2	Placebo solution	No interference is observed at the retention time of formoterol and tiotropium peaks	NA		
3	Formoterol fumarate dihydrate selectivity solution	Peak purity passes & no interference observed at the retention time of tiotropium peak and impurity peaks	1000	1000	Passes
4	Tiotropium selectivity solution	Peak purity passes & no interference observed at the retention time of formoterol fumarate peak and impurity peaks	1000	1000	Passes
5	Fumaric acid selectivity solution	Peak purity passes & no interference observed at the retention time of formoterol fumarate and tiotropium peak and impurity peaks	1000	1000	Passes
6	Standard solution	Peak purity of formoterol and tiotropium peaks passes	999	NA	Passes
7	Sample solution	Peak purity of formoterol and tiotropium peaks passes. % Single maximum impurity (above LOQ level): 0.093. % Total impurity: 0.167	1000	999	Passes

TIO: Tiotropium, LOQ: Limit of quantification, FF: Formoterol fumarate, Sr.: Serial number, NA: Not applicable

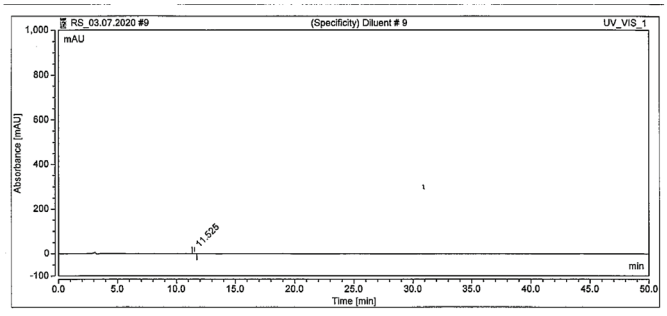

No	Ret. Time min	Peak Name	Area µAU*sec	Peak Type	RRT	Height µAU	Area %	Match
1	11.525		2232	BMB	n.a.	175	100.000	730
	Total		2232				100	

Figure 4a. Chromatogram of (specificity) diluent

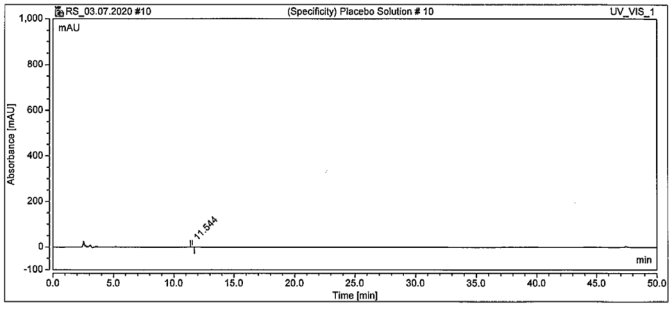

No	Ret. Time min	Peak Name	Area µAU*sec	Peak Type	RRT	Height µAU	Area %	Match
1	11.544		1532	BMB	n.a.	138	100.000	625
	Total		1532				100	

Figure 4b. Chromatogram of (specificity) placebo solution

Forced degradation

Forced degradation study is conducted to generate the data for estimating finished drug product stability. The forced degradation study consists of an appropriate solid and solution state stress conditions as *per* ICH guidelines. Intact capsules

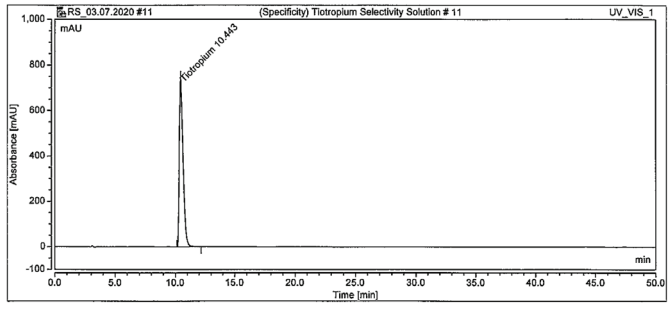

No	Ret. Time min	Peak Name	Area µAU*sec	Peak Type	RRT	Height µAU	Area %	Match
1	10.443	Tiotropium	16214683	BMB	1.000	744630	100.000	1000
	Total		16214683				100	

Figure 4c. Chromatogram of (specificity) tiotropium selectivity solution

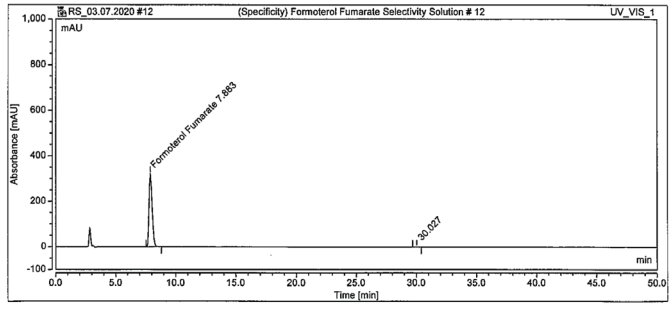

No	Ret. Time min	Peak Name	Area µAU*sec	Peak Type	RRT	Height µAU	Area %	Match
1	7.883	Formoterol Fumarate	5864148	BMB	n.a.	322421	99.855	1000
2	30.027		8490	BMB	n.a.	389	0.145	800
	Total		5872637				100	

Figure 4d. Chromatogram of (specificity) formoterol fumarate selectivity solution

were kept at different stress conditions and were withdrawn at the exact time and samples were prepared according to each condition mentioned. The entire runtime was about double the retention times of both FF and TIO peaks. The degradant peaks

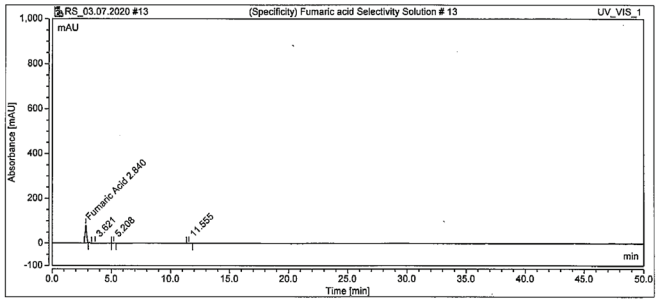

No	Ret. Time min	Peak Name	Area µAU*sec	Peak Type	RRT	Height µAU	Area %	Match
1	2.840	Fumaric Acid	632702	BMB	n.a.	79544	86.926	1000
2	3.621		87584	BMB	n.a.	1629	12.033	990
3	5.208		4370	BMB	n.a.	415	0.600	934
4	11.555		3204	BMB	n.a.	195	0.440	650
	Total		727861				100	

Figure 4e. Chromatogram of (specificity) fumaric acid selectivity solution

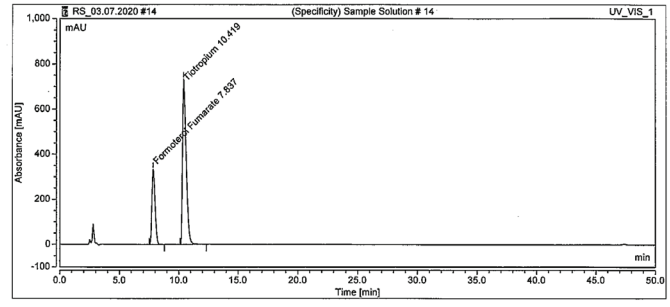

No	Ret. Time min	Peak Name	Area µAU*sec	Peak Type	RRT	Height µAU	Area %	Match
1	7.837	Formoterol Fumarate	6240826	BMB	0.752	333107	28.762	999
2	10.419	Tiotropium	15457260	BMB	1.000	734295	71.238	1000
	Total		21698086				100	

Figure 4f. Chromatogram of (specificity) sample solution

should be well separated from the FF and TIO peaks also peak purity should pass for the FF and TIO peaks in the degradation samples as shown in (Figure 5a-h). The sample and placebo were degraded in the following manner mentioned in (Table 6).

Linearity & range

The linearity of related substance analytical method for FF and TIO in FF and TIO DPI was performed in standard concentrations over the concentration levels ranging from LOQ to 150% of the standard solution standard concentration for each TIO and FF is considered 100% that is 0.015 ppm to 1.089 ppm for TIO and 0.01 ppm to 0.728 ppm for FF. Linearity graph of concentration vs. average peak area of analytes plotted. The correlation coefficient between concentration (ppm), peak area slope and y intercept evaluated. The correlation coefficient should not be less than 0.999 for both analytes (Table 7, Figure 6, 7).

Accuracy

FF and TIO standards were spiked in placebo at different concentration levels *i.e.* LOQ level, 50%, 100% and 150% of targeted concentration and analyzed as *per* method described that is 0.0148 ppm to 1.1129 ppm for TIO and 0.01 ppm to 0.7464 ppm for FF. % recovery obtained at concentration levels LOQ, 50%, 100% and 150% is reported in (Table 8).

At LOQ-level % recovery should be between 80.0% to 120.0% and % RSD of recovery at LOQ level should not more than

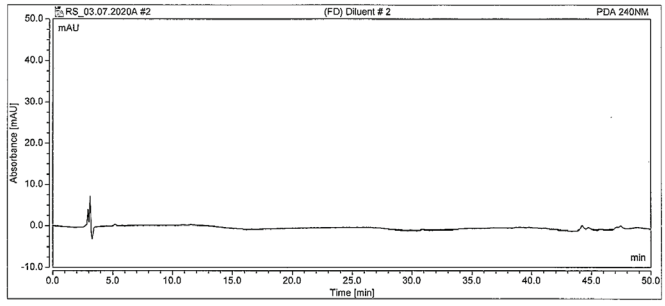

No	Ret. Time min	Peak Name	Area µAU*sec	Peak Type	RRT	Height µAU	Area %	Match
	Total		0				0	

Figure 5a. Typical chromatogram of diluent

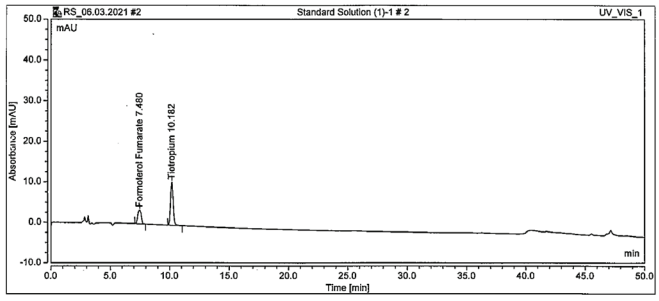

No	Peak Name	Ret.Time min	Area µAU*sec	Peak Type	RRT	Area %	S/N Ratio
1	Formoterol Fumarate	7.480	66680	BMB	0.735	28.736	n.a.
2	Tiotropium	10.182	165363	BMB	1.000	71.264	n.a.
	Total		232043			100	

No	Peak Name	Ret.Time min	Height µAU	Resolution (USP)	Theoretical Plates	Asymmetry
1	Formoterol Fumarate	7.480	3319	n.a.	3905	1.0
2	Tiotropium	10.182	10631	6.2	10526	1.1

Figure 5b. Typical chromatogram of standard solution

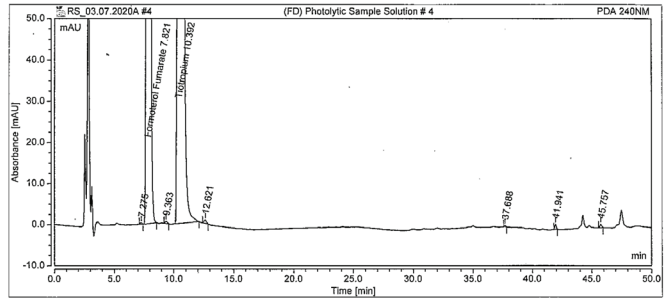

No	Ret. Time min	Peak Name	Area µAU*sec	Peak Type	RRT	Height µAU	Area %	Match
1	7.275		3981	BMB	0.700	375	0.018	940
2	7.821	Formoterol Fumarate	6121462	BMB	0.753	330534	27.975	999
3	9.363		7282	BMB	0.901	570	0.033	918
4	10.392	Tiotropium	15713808	BMB	1.000	777249	71.812	1000
5	12.621		11968	BMB	1.215	886	0.055	941
6	37.688		2826	BMB	3.627	394	0.013	809
7	41.941		10838	BMB	4.036	1275	0.050	895
8	45.757		9722	BMB	4.403	920	0.044	839
	Total		21881888				100	

Figure 5c. Chromatogram of photolytic degraded sample solution

15.0 and at 50%, 100%, and 150% level, % recovery should be between 85.0% to 115.0% and % RSD of recovery should not more than 15.0. The result observed are within the acceptance criteria, therefore the method is accurate throughout the selected range.

Filter study

The prepared sample solution and analysed centrifuged and filtered sample solution through nylon filter 0.45 µm in single

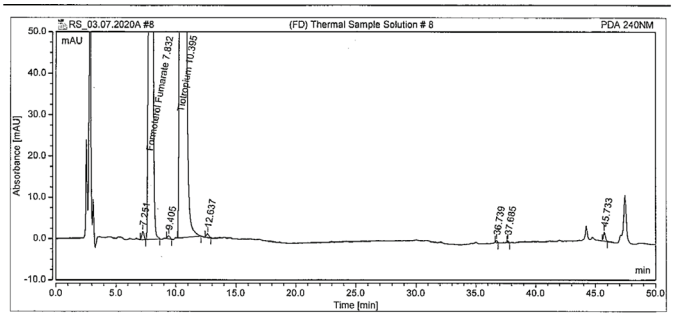

No	Ret. Time min	Peak Name	Area µAU*sec	Peak Type	RRT	Height µAU	Area %	Match
1	7.251		26342	BMB	0.698	2049	0.122	999
2	7.832	Formoterol Fumarate	5875643	BMB	0.753	358268	27.134	999
3	9.405		9267	BMB	0.905	774	0.043	929
4	10.395	Tiotropium	15698262	BMB	1.000	781496	72.495	1000
5	12.637		13434	BMB	1.216	1000	0.062	954
6	36.739		3837	BMB	3.534	452	0.018	805
7	37.685		3220	BMB	3.625	463	0.015	802
8	45.733		24339	BMB	4.400	2152	0.112	981
	Total		21654344				100	

Figure 5d. Chromatogram of thermal degraded sample solution

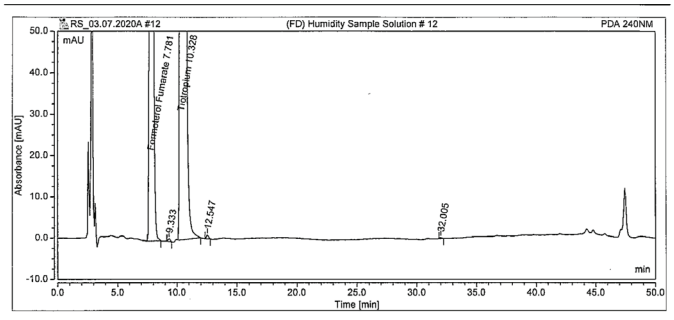

No	Ret. Time min	Peak Name	Area µAU*sec	Peak Type	RRT	Height µAU	Area %	Match
1	7.781	Formoterol Fumarate	5737688	BMB	0.753	352290	27.170	999
2	9.333		8407	BMB	0.904	703	0.040	876
3	10.328	Tiotropium	15355160	BMB	1.000	776204	72.713	1000
4	12.547		12603	BMB	1.215	963	0.060	910
5	32.005		3551	BMB	3.099	281	0.017	659
	Total		21117409				100	

Figure 5e. Chromatogram of humidity degraded sample solution

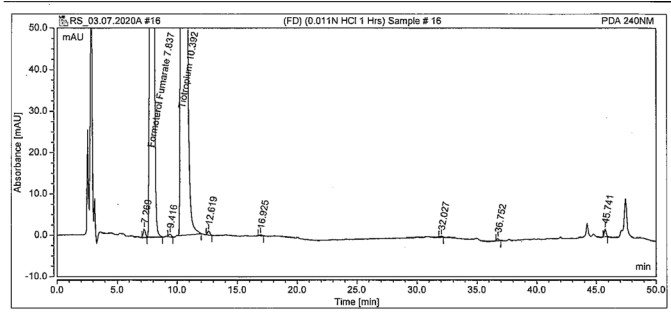

No	Ret. Time min	Peak Name	Area µAU*sec	Peak Type	RRT	Height µAU	Area %	Match
1	7.269		27152	BMB	0.700	2129	0.127	998
2	7.837	Formoterol Fumarate	5848700	BMB	0.754	352096	27.334	999
3	9.416		9554	BMB	0.906	744	0.045	843
4	10.392	Tiotropium	15465666	BMB	1.000	775429	72.279	1000
5	12.619		12987	BMB	1.214	1021	0.061	954
6	16.925		4217	BMB	1.629	344	0.020	775
7	32.027		3490	BMB	3.082	318	0.016	684
8	36.752		6379	BMB	3.537	594	0.030	751
9	45.741		19004	BMB	4.402	1876	0.089	977
	Total		21397150				100	

Figure 5f. Chromatogram of acid degraded sample solution

sequence. The absolute % difference for % single maximum impurity (above LOQ level) and % total impurity between filtered and centrifuged sample solution should not be more than 2.0. hence 0.45 µm nylon membrane filters can be used, and it is

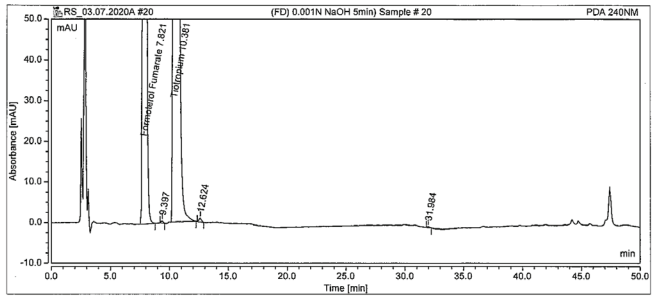

No	Ret. Time min	Peak Name	Area µAU*sec	Peak Type	RRT	Height µAU	Area %	Match
1	7.821	Formoterol Fumarate	5900413	BMB	0.753	352475	27.534	999
2	9.397		6766	BMB	0.905	635	0.032	901
3	10.381	Tiotropium	15504439	BMB	1.000	768777	72.352	1000
4	12.624		13516	BMB	1.216	981	0.063	945
5	31.984		4167	BMB	3.081	325	0.019	747
	Total		21429302				100	

Figure 5g. Chromatogram of base degraded sample solution

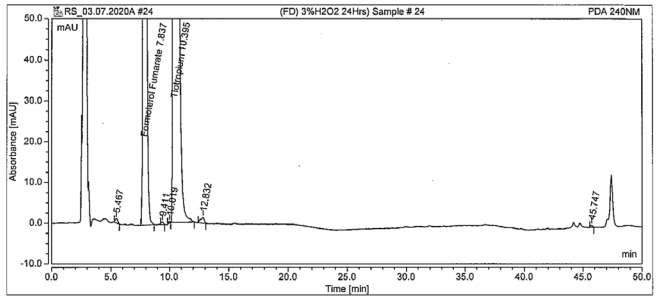

No	Ret. Time min	Peak Name	Area µAU*sec	Peak Type	RRT	Height µAU	Area %	Match
1	5.467		16460	BMB	0.526	1139	0.080	996
2	7.837	Formoterol Fumarate	5527781	BMB	0.754	370706	26.730	999
3	9.411		7501	BMB	0.905	698	0.036	893
4	10.019		4729	BMB	0.964	489	0.023	810
5	10.395	Tiotropium	15088954	BMB	1.000	750783	72.964	1000
6	12.832		28505	BMB	1.234	1478	0.138	872
7	45.747		6163	BMB	4.401	572	0.030	822
	Total		20680091				100	

Figure 5h. Chromatogram of hydrogen peroxide degraded sample solution

recommended to discard the first 5 mL of the sample solution in the routine analysis (Table 9).

Robustness

The % RSD of the area of five replicate standard injections, theoretical plates and tailing factor of TIO peak in each replicate injection were recorded and reported (Table 10).

Solution stability

The standard and sample solutions for FF and TIO were prepared on day 0 of experiment, stored these solutions at room temperature for every time interval up to 3 days and analyzed these solutions on subsequent days. The standard solution was prepared freshly and calculated the assay of analyte in the standard solution and % impurities in the sample solution.

The cumulative % RSD of % assay of the stored standard solution should not be more than 5.0.

The % single maximum impurity (above LOQ level) & % total impurity for samples should comply with the specification limits. The cumulative% RSD of impurity results (above LOQ level) obtained using stored sample solutions should not be more than 5.0.

Table 6. Forced degradation

Sr. no.	Degradation condition	Degrading agents/ condition	Exposure period	% Single maximum impurity	% Total degraded impurities	Peak purity match (TIO)	Peak purity match (FF)	Peak purity result
1	Thermal	60°C	For 2 days	0.189	0.575	1000	999	Passes
2	Photolytic	1.2 million lux hours; 200 watt hrs./m^2	For 7 days	0.086	0.336	1000	999	Passes
3	Humidity	40°C/75% RH	For 7 days	0.092	0.179	1000	999	Passes
4	Acid	0.01N HCl	For 1 hr at RT	0.196	0.597	1000	999	Passes
5	Base	0.001N NaOH	For 5 min at RT	0.098	0.177	1000	999	Passes
6	Peroxide	3% H_2O_2	For 24 hr at RT	0.206	0.458	1000	999	Passes

TIO: Tiotropium, FF: Formoterol fumarate, NA: Not applicable, RH: Relative humidity, Sr. no: Serial number

Table 7. Linearity

Linearity FF				Linearity TIO			
Linearity level	Conc. (%)	Conc. (ppm)	Area	Linearity level	Conc. (%)	Conc. (ppm)	Area
1	LOQ	0.010	1386	1	LOQ	0.015	3489
2	20	0.097	13138	2	20	0.145	35978
3	50	0.243	34008	3	50	0.363	83211
4	80	0.388	53406	4	80	0.581	135688
5	100	0.485	69004	5	100	0.726	167367
6	120	0.582	79151	6	120	0.872	195637
7	150	0.728	101903	7	150	1.089	245102
Slope		139302.5901		Slope		224043.3645	
Intercept		-122.4944		Intercept		2446.2293	
Correlation coefficient		1.000		Correlation coefficient		1.000	

FF: Formoterol fumarate, LOQ: Limit of quantification, Conc.: Concentration

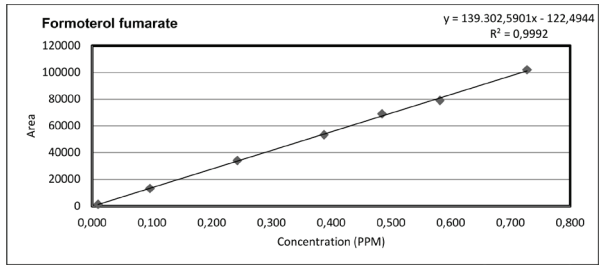

Figure 6. Linearity of formoterol fumarate

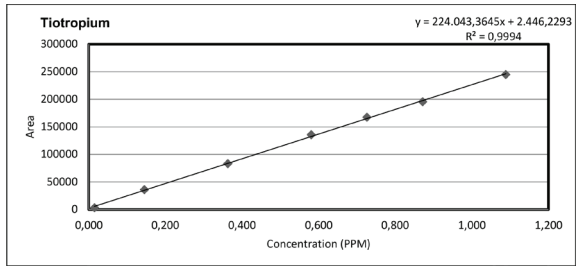

Figure 7. Linearity of tiotropium

Table 8. Accuracy

Accuracy at LOQ Level FF				Accuracy at LOQ level TIO			
Preparation	Amount added (ppm)	Amount recovered (ppm)	% Recovery	Preparation	Amount added (ppm)	Amount recovered (ppm)	% Recovery
1	0.0100	0.0094	94.0	1	0.0148	0.0150	101.4
2	0.0100	0.0099	99.0	2	0.0148	0.0155	104.7
3	0.0100	0.0094	94.0	3	0.0148	0.0153	103.4
4	0.0100	0.0095	95.0	4	0.0148	0.0151	102.0
5	0.0100	0.0098	98.0	5	0.0148	0.0147	99.3
6	0.0100	0.0089	89.0	6	0.0148	0.0148	100.0
Average			94.8	Average			101.8
SD			3.5449	SD			2.0327
% RSD			3.74	% RSD			2.00

Inj. no.	FF accuracy 50% level			FF accuracy 100% level			TIO accuracy 150% Level		
	Amount added (ppm)	Amount recovered (ppm)	% Recovery	Amount added (ppm)	Amount recovered (ppm)	% Recovery	Amount added (ppm)	Amount recovered (ppm)	% Recovery
1	0.2488	0.2500	100.5	0.4976	0.5035	101.2	0.7464	0.7305	97.9
2	0.2488	0.2408	96.8	0.4976	0.4822	96.9	0.7464	0.7330	98.2
3	0.2488	0.2360	94.9	0.4976	0.4903	98.5	0.7464	0.7502	100.5
Average			97.4			98.9			98.9
SD			2.8478			2.1733			1.4224
% RSD			2.92			2.2			1.44

Inj. no.	TIO accuracy 50% level			TIO accuracy 100% level			TIO accuracy 150% Level		
	Amount added (ppm)	Amount recovered (ppm)	% Recovery	Amount added (ppm)	Amount recovered (ppm)	% Recovery	Amount added (ppm)	Amount recovered (ppm)	% Recovery
1	0.3710	0.3673	99.0	0.7419	0.7532	101.5	1.1129	1.0847	97.5
2	0.3710	0.3816	102.9	0.7419	0.7298	98.4	1.1129	1.1073	99.5
3	0.3710	0.3762	101.4	0.7419	0.7371	99.4	1.1129	1.1067	99.4
Average			101.1			99.8			98.8
SD			1.9672			1.5822			1.1269
% RSD			1.95			1.59			1.14

SD: Standard deviation, RSD: Relative standard deviation, LOQ: Limit of quantification, TIO: Tiotropium, FF: Formoterol fumarate

Table 9. Filter validation

Sample solution	% Impurity		Absolute % difference	
	% Single maximum impurity	% Total impurity	% Single maximum impurity	% Total impurity
Centrifuged	0.105	0.201	NA	NA
0 mL discarded	0.106	0.343	0.95	70.65
2 mL discarded	0.106	0.202	0.95	0.50
5 mL discarded	0.105	0.201	0.00	0.00

NA: Not applicable

The solution is considered stable, until the time point where the % RSD of the stored standard and sample solution is not more than 5.0; thus, the solution is stable up to 2 days at room temperature is proved (Table 11).

Table 10. Robustness

Parameters	Wavelength (nm) (+/-3)		Flow rate (mL/min) (+/0.1 mL/min)		Column temperature (°C) (+/- 5°C)		Gradient composition (+/- 5%)		Buffer pH (+/- 0.2)	
	237	243	0.9	1.1	25°C	35°C	-5%	+5%	3.0	3.4
Similarity factor	98.5	96.9	100.1	100.7	99.0	99.3	98.6	99.3	99.6	99.0
T.F.	1.2	1.2	1.2	1.2	1.3	1.3	1.3	1.3	1.3	1.3
NTP	10063	9990	10951	8797	10828	9817	10952	10082	9638	9110

T.F.: Tailing factor, NTP: Number of therotical plates, °C: Degree celsius

Table 11. Solution stability

Stability data for standard solution					Stability data for sample solution						
Time point	% TIO	Cumulative			% Single maximum impurity	Cumulative			% Total impurity	Cumulative		
		Avg.	SD	% RSD		Avg.	SD	% RSD		Avg.	SD	% RSD
Day 0 (initial)	100.0	NA	NA	NA	0.109	NA	NA	NA	0.207	NA	NA	NA
Day 1	101.5	100.8	1.0607	1.05	0.104	0.107	0.0035	3.27	0.205	0.206	0.0014	0.68
Day 2	96.1	99.2	2.7875	2.81	0.102	0.105	0.0036	3.43	0.191	0.201	0.0087	4.33

TIO: Tiotropium, SD: Standard deviation, RSD: Relative standard deviation, Avg: Average

CONCLUSION

The recommended analytical method for the related substance determination of Tiomate Transcaps® DPI is simple, robust, selective, specific and precise. It also demonstrates the study of degradation pattern; therefore, can be used for quality control testing, routine analysis and for stability studies.

ACKNOWLEDGMENTS

The authors are grateful to SAVA Healthcare Ltd.; Pune India, for providing the facilities to conduct this work.

Conflict of interest: No conflict of interest was declared by the authors. The authors are solely responsible for the content and writing of this paper.

REFERENCES

1. Rabe KF, Hurd S, Anzueto A, Barnes PJ, Buist SA, Calverley P, Fukuchi Y, Jenkins C, Rodriguez-Roisin R, van Weel C, Zielinski J; Global Initiative for Chronic Obstructive Lung Disease. Global strategy for the diagnosis, management, and prevention of chronic obstructive pulmonary disease: GOLD executive summary. Am J Respir Crit Care Med. 2007;176:532-555.
2. British Pharmacopoeia (BP). The stationary office on behalf of The Medicines and Healthcare Products Regulatory Agency, London, UK, 2016.
3. Sweetman S. Martindale: the complete drug reference, 40th ed. Pharmaceutical, London; 2016.
4. Ahmed HM, Clark BJ. Spectrofluorometric determination of tiotropium bromide by ion pair extraction using 9,10 dimethoxyanthracene-2-sulphonate sodium. J Ion Exch. 2007;18:402-405.
5. Nevse AS, Yadav S, Purohit RN, Rao JR. Development and validation of HPTLC method for estimation of tiotropium bromide monohydrate in dry powder inhalation dosage form. World J Pharm Pharm Sci. 2016;5:795-802.
6. Zhou YM, Zhou B. Determination of tiotropium bromide and its related substances by HPLC. Chin J Pharm. 2015;46:1327-1329.
7. Ding L, Tan W, Zhang Y, Shen J, Zhang Z. Sensitive HPLC-ESI-MS method for the determination of tiotropium in human plasma. J Chromatogr Sci. 2008;46:445-449.
8. Wang J, Jiang Y, Wang Y, Li H, Fawcett JP, Gu J. Highly sensitive assay for tiotropium, a quaternary ammonium, in human plasma by high-performance liquid chromatography/tandem mass spectrometry. Rapid Commun Mass Spectrom. 2007;21:1755-1758.
9. Chi J, Li F, Jenkins R. Ultrasensitive sub-pg/ml determination of tiotropium bromide in human plasma by 2D-UHPLC-MS/MS: challenges and solutions. Bioanalysis. 2016;8:385-95.
10. Gousuddin M, Raju SA, Sultanuddin Manjunath S. Development and validation of spectrophotometric methods for estimation of formoterol bulk drug and its pharmaceutical dosage forms. Int J Pharm Pharm Sci. 2011;3:306-309.
11. Taşkın D, Erensoy G, Sungur S. A validated spectrophotometric method for determination of formoterol fumarate dihydrate in bulk and dosage form using methyl orange as ion pair reagent. Marmara Pharm J. 2016;20:275-279.
12. Prasad A. Simultaneous spectrophotometric determination of formoterol fumarate and budesonide in their combined dosage form. Indian J Chem Technol. 2006;13:81-83.
13. Aashish SP, Sandip DF, Sanjay JS. Validated UV spectrophotometric area under curve method for determination of formoterol fumarate dihydrate in bulk and pharmaceutical formulation using hydrotropic solubilization technique. Anal Chem Indian J. 2016;16:1-7.
14. Gowekar NM, Wadher SJ. Simultaneous estimation of formoterol fumarate dihydrate and fluticasone propionate in dry powder inhalation formulation by HPTLC. Der Pharma Chem. 2016;8:27-32.

15. Merey HA, El-Mosallamy SS, Hassan NY, El-Zeany BA. Validated chromatographic methods for the simultaneous determination of mometasone furoate and formoterol fumarate dihydrate in a combined dosage form. Bull Fac Pharm Cairo Univ. 2016;54:99-106.

16. Parmar VK, Patel HN, Patel BK. Sensitive and robust methods for simultaneous determination of beclomethasone dipropionate and formoterol fumarate dihydrate in rotacaps. J Chromatogr Sci. 2014;52:1255-1266.

17. Patil AS. Stability-indicating high performance thin layer chromatography/densitometry estimation of formoterol fumarate dihydrate in bulk and capsules. Int J Adv Pharm Anal. 2015;5:80-84.

18. Akapo SO, Asif M. Validation of a RP-HPLC method for the assay of formoterol and its related substances in formoterol fumarate dihydrate drug substance. J Pharm Biomed Anal. 2003;33:935-945.

19. Assi KH, Tarsin W, Chrystyn H. High performance liquid chromatography assay method for simultaneous quantitation of formoterol and budesonide in Symbicort Turbuhaler. J Pharm Biomed Anal. 2006;41:325-328.

20. Gujarati PZ, Thula KC, Maheshwari DG. Stability indicating hplc method for simultaneous estimation of mometasone furoate and formoterol fumarate in combined dosage form. Pharmacophore. 2014;5:219-230.

21. Kale NR, Pingle AP, Mirza JA, Dhongade GN. Development and validation of stability-indicating RP-HPLC method for simultaneous estimation of formoterol fumarate and budesonide in metered dose inhaler formulation. World J Pharm Res. 2014;3:1386-1399.

22. Malik K, Kumar D, Tomar V, Kaskhedikar S, Soni L. Simultaneous quantitative determination of formoterol fumarate and fluticasone propionate by validated reversed-phase HPLC method in metered dose inhaler. Der Pharmacia Sinica. 2011;2:77-84.

23. Srinivasarao K, Gorule V, Ch VR, Krishna V. Validated method development for estimation of formoterol fumarate and mometasone furoate in metered dose inhalation form by high performance liquid chromatography. J Anal Bioanal Tech. 2012;3:1-4.

24. Salem YA, Hammouda MEA, Abu El-Enin MA, El-Ashry SM. Multiple analytical methods for determination of formoterol and glycopyrronium simultaneously in their novel combined metered dose inhaler. BMC Chemistry. 2019. doi: org/10.1186/s13065-019-0592-9.

25. Kakubari I, Dejima H, Miura K, Koga Y, Mizu H, Takayasu T, Yamauchi H, Takayama S, Takayama K. Determination of formoterol in rat plasma by liquid chromatography-electrospray ionisation mass spectrometry. Pharmazie. 2007;62:94-95.

26. Nadarassan DK, Chrystyn H, Clark BJ, Assi KH. Validation of high-performance liquid chromatography assay for quantification of formoterol in urine samples after inhalation using UV detection technique. J Chromatogr B Analyt Technol Biomed Life Sci. 2007;850:31-37.

27. Pulla RP, Sastry BS, Prasad YR, Raju NA. RP-HPLC method for simultaneous estimation of formoterol fumarate, tiotropium bromide and Ciclesonide in pharmaceutical metered dose inhalers. Asian J Res Chem. 2011;4:585-590.

28. Shah BD, Kumar S, Yadav YC, Seth AK, Ghelani TK, Deshmukh GJ. Analytical method development and method validation of tiotropium bromide and formoterol fumarate metered dose inhaler (MDI) by using RP-HPLC method. Asian J Biochem Pharma Res. 2011;1:145-158.

29. Srinivasu K, Rao JV, Appalaraju N, Mukkanti K. Simultaneous RP-HPLC method for the estimation of formoterol fumarate and tiotropium bromide in pharmaceutical dosage forms. Asian J Chem. 2010;22:3943-3948.

30. Sule S, Ambadekar S, Singh AK, Naik PP. A rapid and stability indicating RP-HPLC method for simultaneous determination of tiotropium, formoterol and ciclesonide in a dry powder inhaler. World J Pharm Res. 2014;3:819-830.

31. Trivedi RK, Chendake DS, Patel MC. A rapid, stability-indicating rp-hplc method for the simultaneous determination of formoterol fumarate, tiotropium bromide, and ciclesonide in a pulmonary drug product. Sci Pharm. 2012;80:591-603.

32. Bhoomaiah B, Jayasree A. Simultaneous quantification of olodaterol and tiotropium bromide by high performance liquid chromatography. Asian J Chem. 2017;29:145-148.

33. Elkady EF, Tammam MH, Elmaaty AA. Development and validation of RP- HPLC method for simultaneous estimation of tiotropium bromide, Formoterol fumarate, and Olodaterol HCl in Bulk and metered dose aerosol: application to olodaterol HCl forced degradation study and degradation kinetics. Chromatographia. 2017;80:1749-1760.

34. Rani SS, CA. Sri Ranjani CA. Quantitative determination of hydrazine hydrate content in formoterol fumarate dihydrate by GC-MS method. J Sci Res Pharm. 2017;6:112-116.

35. ICH Harmonized Tripartite Guidelines (2013) validation of analytical procedures: text and methodology Q2 (R1), international conference on harmonization, 2005.

Turk J Pharm Sci 2022;19(1):48-53
DOI: 10.4274/tjps.galenos.2021.52284

ORIGINAL ARTICLE

Analysis of Changes in Serum Levels and Gene Expression Profiles of Novel Adipocytokines (Omentin, Vaspin, Irisin and Visfatin) and Their Correlation with Serum C-reactive Protein Levels in Women Diagnosed with Endometriosis

Endometriozis Tanısı Alan Kadınlarda Yeni Adipositokinlerin (Omentin, Vaspin, İrisin ve Visfatin) Serum Seviyelerindeki ve Gen Ekspresyon Profillerindeki Değişimlerinin Analizi ve Bu Adipositokinlerin Serum C-reaktif Protein Düzeyleri ile Korelasyonu

Ecem KAYA SEZGİNER[1]*, Ömer Faruk KIRLANGIÇ[2], Merve Didem EŞKİN TANRIVERDİ[3], Hasan Onur TOPÇU[4], Serap GÜR[5]

[1]Ankara University Faculty of Pharmacy, Department of Biochemistry, Ankara, Turkey
[2]University of Health Sciences Turkey, Gülhane Faculty of Medicine, Department of Medical Biochemistry, Ankara, Turkey
[3]University of Health Sciences Turkey, Ankara City Hospital, Department of Obstetrics and Gynecology, Ankara, Turkey
[4]Memorial Ankara Hospital, Department of Obstetrics and Gynecology, Ankara, Turkey
[5]Ankara University Faculty of Pharmacy, Department of Pharmacology, Ankara, Turkey

ABSTRACT

Objectives: This study aimed to investigate the role of new adipocytokines (omentin, vaspin, irisin and visfatin) in the development of endometriosis and the relationship of these adipocytokines with the inflammatory marker, C-reactive protein (CRP) levels in serum.

Materials and Methods: In this study, endometriosis (n=16) and control groups (n=14) were determined *via* ultrasound. Serum omentin, vaspin and irisin levels were measured by ELISA method. CRP levels in serum and the gene expression of visfatin and vaspin in whole blood samples were determined by clinical analyzer and the real-time polymerase chain reaction, respectively.

Results: Serum irisin and CRP levels in the endometriosis group were significantly higher than in the control group. Irisin protein levels demonstrated a positive correlation with body mass index and CRP in women diagnosed with endometriosis. No statistically significant difference was found in serum omentin and vaspin levels between groups. The visfatin and vaspin gene expression in whole blood samples from the endometriosis group was found to be significantly lower than the control group.

Conclusion: Increased levels of serum irisin and decreased visfatin and vaspin gene expressions in blood may be considered as a potential biomarker in endometriosis. The identification of new adipocytokines, which demonstrate an alteration in the presence of endometriosis and the relationship between these adipocytokines and inflammation will facilitate the detection of mechanisms involved in endometriosis and will lead to the development of targeted therapy.

Key words: Endometriosis, adipocytokines, inflammation

ÖZ

Amaç: Bu çalışmanın amacı, yeni adipositokinlerin (omentin, vaspin, irisin ve visfatin) endometriozis gelişimindeki rolünü ve bu adipositokinlerin inflamatuvar belirteç olan serumdaki C-reaktif protein (CRP) düzeyi ile ilişkisini araştırmaktır.

***Correspondence:** ecemkaya@ankara.edu.tr, **Phone:** +90 312 203 30 54, **ORCID-ID:** orcid.org/0000-0002-8490-6293
Received: 21.01.2021, **Accepted:** 18.04.2021

Gereç ve Yöntemler: Bu çalışmada endometriozis (n=16) ve kontrol grupları (n=14) ultrason aracılığı ile belirlenmiştir. Serum omentin, vaspin ve irisin seviyeleri ELISA yöntemi ile ölçülmüştür. Serumda CRP seviyeleri ile tam kan örneklerinde visfatin ve vaspin gen ekspresyonu sırası ile klinik analiz cihazı ve gerçek zamanlı-polimeraz zincir reaksiyonu ile belirlenmiştir.

Bulgular: Endometriozis grubunda, serum irisin ve CRP seviyeleri kontrol grubuna göre anlamlı olarak yüksek bulunmuştur. Endometriozis tanısı alan kadınlarda irisin protein düzeyleri, vücut kitle indeksi ve CRP ile pozitif korelasyon göstermiştir. Serum omentin ve vaspin düzeylerinde gruplar arasında istatistiksel olarak anlamlı fark bulunmamıştır. Endometriozis grubundan alınan tam kan örneklerinde, visfatin ve vaspin gen ekspresyonu, kontrol grubuna göre anlamlı derecede düşük bulunmuştur.

Sonuç: Serum irisin düzeylerinde artma ve kanda visfatin ve vaspin gen ekspresyonunda azalma endometrioziste potansiyel bir biyobelirteç olarak düşünülebilir. Endometriozis varlığında değişiklik gösteren yeni adipositokinlerin ve bu adipositokinler ile inflamasyon arasındaki ilişkinin tanımlanması, endometrioziste rol oynayan mekanizmaların tespitini kolaylaştıracak ve hedeflendirilmiş tedavinin geliştirilmesine yol açacaktır.

Anahtar kelimeler: Endometriozis, adipositokinler, inflamasyon

INTRODUCTION

Endometriosis is a painful disorder identified by the growth of endometrium-like tissue such as endometrial glands and stroma, outside the uterus.[1] Endometriosis reduces the quality of life among women due to dysmenorrhea, chronic pelvic pain, irregular uterine bleeding, infertility and affects about 5%-10% of women of reproductive age.[2,3] Previous studies have reported that 30%-40% of infertile women have endometriosis, and they are more likely to have endometriosis than fertile women.[4,5]

A standardized approach for the definite diagnosis of endometriosis is laparoscopic visualization of lesions together with histological examination.[2] Besides, transvaginal ultrasound is an alternative technique to diagnose pelvic endometriosis.[6] The current gold standard for the definitive treatment of endometriosis involves surgical removal of ectopic lesions and/or hormonal suppression.[1] The identification of mechanisms in the pathogenesis of endometriosis remains critical for reducing various side effects of these treatment options and a high incidence of relapses.[7]

Chronic inflammation plays a considerable role in the development and progression of endometriosis in the peritoneal cavity.[8] Adipocytokines are proteins secreted from white adipose tissue and affect metabolism, immunity, endocrine system and inflammation regulation and play different and even opposing roles.[9,10] Accumulating evidence suggests that pro- or anti-inflammatory actions of adipocytokines and inflammatory markers are partly responsible for the pathogenesis of endometriosis.[11,12]

Omentin-1 is a circulating novel hydrophilic adipokine with extensive protective effects in various diseases.[13] Vaspin known as visceral adipose tissue-derived serine protease inhibitor, is a member of the serine protease inhibitor family and was first identified as an adipokine that is expressed mainly in the visceral adipose tissue of Zucker fatty rats.[14] Irisin has been identified as a novel myokine which is involved in white adipose tissue browning and anti-inflammatory pathways.[15] A ubiquitous intracellular enzyme, visfatin is known also as nicotinamide phosphoribosyltransferase and pre-B-cell colony-enhancing factor.[16]

This study was conducted to investigate a possible role of "omentin, vaspin, irisin and visfatin" adipocytokines called "new adipocytokines" and their association with the inflammatory marker C-reactive protein (CRP) levels in endometriosis.

MATERIALS AND METHODS

Study subjects

Thirty women attending Dr. Zekai Tahir Burak Women's Health Care Education and Research Hospital were enrolled in this study. The women were divided into two groups as control (n=14) and endometriosis (n=16) *via* ultrasound examination. Blood samples of all participants were collected and divided into test tubes containing K3EDTA and serum-separating tubes after overnight fasting to perform biochemical analysis. Serum was obtained by centrifugation at 400× g for 10 min and both whole blood and serum samples were stored at -70°C until further analysis. This study was conducted with the approval of Ankara University Faculty of Medicine Clinical Research Ethics Committee (19-1296-18) and standard informed consent was obtained from women involved in this study.

Measurement of adipocytokines (omentin, vaspin, irisin) and inflammatory marker (CRP) concentrations in serum

The circulating levels of omentin in the serum were assayed using commercially available ELISA kits (catalog no. E-EL-H2028, Elabscience, Houston, Texas, United States). Serum vaspin and irisin concentrations in the serum were detected by a commercially available ELISA kit [catalog no. CSB-E09771h (vaspin) and CSB-EQ027943HU (irisin), Cusabio Biotechnology, Wuhan, China]. The minimum detectable concentration of omentin, vaspin, and irisin was 0.38 ng/mL, 7.8 pg/mL, and 0.78 ng/mL, respectively. For the omentin ELISA, the intra-assay coefficient of variation (CV) was <4.05%; the inter-assay CV was <3.12%. For the vaspin and irisin ELISA kits, the intra-assay CV was <8%; the inter-assay CV was <10%. A biomarker of inflammation, CRP levels were measured by Beckman Coulter AU680 clinical chemistry analyzer (Beckman Coulter Inc., Brea CA, USA).

RNA isolation and complementary DNA (cDNA) synthesis

Total RNA was isolated from whole blood samples using the RNA isolation kit (Macherey-Nagel, Düren, Germany) according to the manufacturer's instructions. The concentration of each total RNA was determined by spectrophotometer (NanoDrop ND-1000 spectrophotometer; Thermo Scientific, Wilmington, DE, USA). Equal amounts of total RNA (200 ng) from each sample were used for the production of complementary DNA (cDNA) using the ProtoScript II first strand cDNA synthesis

kit (New England Biolabs, Ipswich, MA,USA) according to the manufacturer's protocol.

Each transcription was performed in a reaction buffer containing 200 ng of total RNA (2 µL for each sample), 50 µM $d(T)_{23}VN$ (2 µL), 10 µL reaction mix (dNTPs and optimized buffer), 2 µL enzyme mix (reverse transcriptase and RNase inhibitor) and 4 µL RNase-free water for a total volume of 20 µL. After brief centrifugation, the reaction mixture was incubated at 42˚C for 10 min, and then heated at 80˚C for 5 min.

Quantitative real-time polymerase chain reaction (RT-PCR) assay

For the analysis of mRNA level of visfatin and vaspin, the newly synthesized cDNA was quantified on RT-PCR using CFX384 touch RT-PCR System (Bio-rad, Hercules, CA, USA) and Luna Universal qPCR Master Mix (New England Biolabs, Ipswich, MA, USA) according to the manufacturer's protocol. Each qRT-PCR reaction was carried out in 20 µL buffer, containing the same volume of the newly synthesized cDNA (2 µL) from each sample, 10 µL master mix, 1 µL forward and reverse primer (0,25 µM), and 7 µL DNA-free water. The oligonucleotide sequences of the primer pairs which were designed using the ensemble genome browser and primer 3 input programs are summarized in Table 1. The thermocycling protocol was performed as follows in duplicate: Initial denaturation at 95˚C for 1 min, followed by 40 cycles of PCR at 95˚C for 15 s and 60˚C for 30 s. After 40 cycles, a melting step was performed at 60˚C for 15 s. The relative mRNA expression was quantified by comparison with β-actin as a housekeeping gene from the same sample as an internal control. The relative gene expressions of visfatin and vaspin were computed using the $2^{-\Delta\Delta CT}$ as fold changes relative to those in controls.[17] At the end of the RT-PCR, product specificity was verified using a melting curve.

Statistical analyses

The statistical analyses were conducted using the SPSS software version 18.0. Mean values between the groups were compared by Student's *t*-test. Pearson's correlation coefficient was used to identify the relationship between parameters. A $p<0.05$ was considered statistically significant.

RESULTS

A total of 30 women between the ages of 25-40 years old participated in this study, including sixteen diagnosed with endometriosis and fourteen healthy women. Among the patients in the endometriosis group, the presence of dysmenorrhea was documented in 10 (35.8%) patients, while rest of 6 (64.2%) patients with endometriosis did not have dysmenorrhea.

There were no statistically significant differences in the serum omentin and vaspin concentrations between control and endometriosis groups (p values 0.861; 0.213, respectively; Figure 1). However, serum irisin levels were statistically higher in the endometriosis group than in the control group (p=0.024, Figure 2A) and significantly positively correlated with both body mass index (BMI) (r=0.65, p=0.021) and CRP levels (r=0.714, p=0.023) in women with endometriosis (Table 2). Serum CRP level was significantly increased in women with endometriosis compared to the control group (p=0.022, Figure 2B). Additionally, we measured the gene expression of vaspin and visfatin in whole blood samples of women with and without

Table 1. Sequences of primers used in RT-PCR

Gene	Primer sequences (5'-3')
Vaspin	Forward: TACTGGGGATGTGGGGAGAG
	Reverse: TGTAGGGCCGATGAGTCAGA
Visfatin	Forward: TCGGTTCTGGTGGAGGTTTG
	Reverse: CAAAATTCCCTGCTGGCGTC
β-actin	Forward: ACCTGCATTTCCTGGGAGTG
	Reverse: GACAGCCACGATCCCATAGG

RT-PCR: Real-time polymerase chain reaction

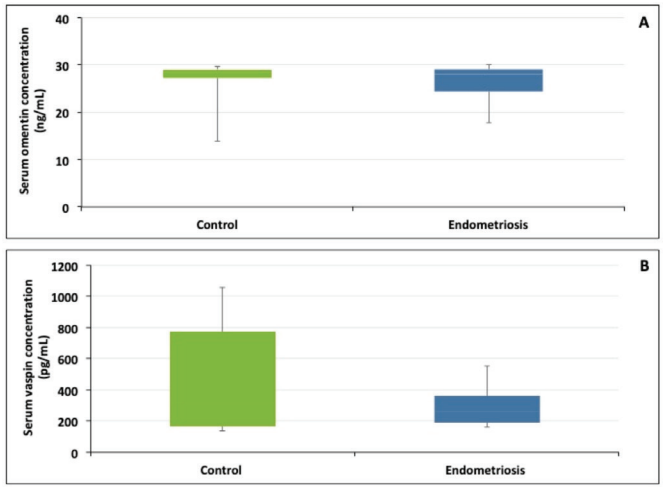

Figure 1. (A) Omentin and (B) vaspin concentration in serum from controls (n=14) and patients with endometriosis (n= 16). Data are expressed as the median and range

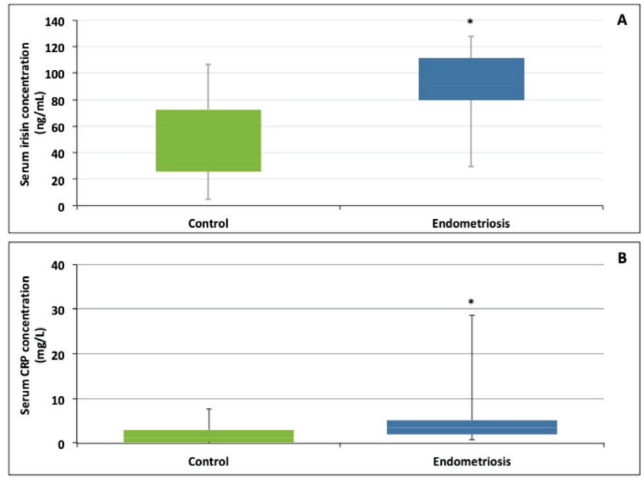

Figure 2. (A) Irisin and (B) CRP concentration in serum from controls (n=14) and patients with endometriosis (n=16). Data are expressed as the median and range

*$p<0.05$ compared to controls. CRP: C-reactive protein

endometriosis. Our results revealed that the mRNA expression levels of vaspin and visfatin in whole blood from endometriosis patients were significantly lower than the control group (*p* values 0.042; *p*=0.00097, respectively; Figure 3). While no significant association between the levels of vaspin, visfatin and clinical parameters was found in the endometriosis, the visfatin mRNA expression tended to positively correlate with BMI in patients with endometriosis, though without statistical significance (r=0.5, *p*=0.059, Table 2).

DISCUSSION

In this study, we firstly demonstrated that serum irisin and CRP concentrations were significantly higher in women with endometriosis than those without the disease. A significant positive correlation between serum irisin levels and both BMI and CRP levels was observed. In particular, decreased visfatin and vaspin gene expressions in whole blood samples were remarkable for women with endometriosis compared to healthy controls. There was a trend toward a positive correlation between BMI and visfatin mRNA expression, which was statistically non-significant.

Based on our results, serum omentin and vaspin concentrations did not differ between endometriosis and control groups and were not correlated with any parameter. However, vaspin mRNA expression levels were decreased in patients with endometriosis compared to healthy controls. Omentin and vaspin are anti-inflammatory mediators,[18-21] and decreased expression of these adipocytokines was detected in various chronic inflammatory diseases.[22,23] In this study, a non-significant partial decrease in vaspin protein level with significantly decreased vaspin mRNA expression may be related to the small number of subjects and severity of endometriosis in patients. In accordance with the growing evidence suggesting anti-inflammatory effects of vaspin,[14] endometriosis occurrence may be associated with decreased vaspin mRNA levels and vaspin could serve as a novel biomarker of endometriosis.

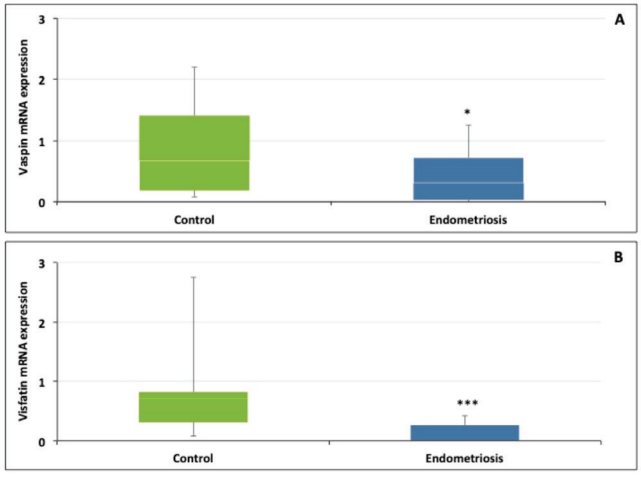

Figure 3. (A) Vaspin and (B) visfatin mRNA expression in whole blood from controls (n=14) and patients with endometriosis (n=16). Data are expressed as the median and range

*p<0.05, ***p<0.001 compared to controls

This study showed that circulating irisin levels were increased in patients with endometriosis compared to control subjects and were correlated with BMI and CRP. Some authors support our findings with reports of higher irisin levels in women with gestational diabetes and polycystic ovary syndrome.[24,25] These findings are in contrast to other studies, which indicated lower serum irisin levels compared to control in inflammation-related diseases.[15,26,27] Similarly, there was a significant positive correlation between serum irisin concentrations and BMI,[25,28,29] although other studies suggested an inverse association between irisin levels and BMI.[15,30] Previous preclinical and clinical studies suggested that irisin has anti-inflammatory properties, reducing secretion of inflammatory cytokines like interleukin-6 and tumor necrosis factor-α.[31,32] It is well established that increased levels of various proinflammatory cytokines play an important role in the pathogenesis of endometriosis.[33] The current results led us to speculate that increased circulating irisin may be an adaptive response to compensate for increased inflammation in endometriosis, which was also supported by a positive association between irisin and CRP and its anti-inflammatory properties. We can suggest an "irisin-proinflammatory/anti-inflammatory axis" to elucidate the role of irisin as a possible indicator in endometriosis.

CRP levels were increased in women with endometriosis in this study. Results reporting CRP levels in peripheral blood of endometriosis patients compared to controls are relatively contradictory due to differences in the severity of endometriosis, different measurement techniques, the sample size of studies.[34-36] We suggest that CRP could reveal subclinical inflammation in serum of women with endometriosis and serve as a biomarker of endometriosis which is considered a chronic inflammatory disease as reported previously.[37,38]

Visfatin is considered a new marker of inflammation, which is in line with reports suggesting that visfatin induces nuclear factor kappa B activity and the synthesis of other related pro-inflammatory molecules.[16,39,40] Since higher relative visfatin

Table 2. Correlations between BMI, CRP and adipocytokines in patients with endometriosis

	Serum omentin concentration (ng/mL)		Serum vaspin concentration (pg/mL)		Serum irisin concentration (ng/mL)		Vaspin gene expression		Visfatin gene expression	
	r	p	r	p	r	p	r	p	r	p
BMI	-0.316	0.101	0.422	0.086	0.65	0.021*	0.405	0.109	0.5	0.059
CRP	0.175	0.266	0.005	0.495	0.714	0.023*	-0.546	0.081	0.079	0.427

*p<0.05 demonstrates the significance of the correlation, BMI: Body mass index, CRP: C-reactive protein

mRNA levels in peripheral mononuclear cells from patients with a common inflammatory disease such as polycystic ovary syndrome and diabetes have been reported,[41,42] we suggested that visfatin contributes to endometriosis. Our findings demonstrated that visfatin mRNA expression in whole blood from the women with endometriosis was significantly lower than in the controls and tended to positively associate with the BMI, but not statistically significant. Similarly, a study by Seow et al.[42] found a non-significant correlation between visfatin and BMI in patients with polycystic ovary syndrome, which might be attributed to an insufficient sample size that might negatively affect the statistical power. Visfatin with its inflammatory properties might be involved in the pathogenesis of endometriosis. New insight into the role of visfatin may be attractive for novel therapeutic strategies targeting endometriosis-related chronic inflammation.

Moreover, there is no adipocytokine known as non-invasive biomarkers of endometriosis. Further studies with larger population will be required to determine whether these novel adipocytokines are involved in a particular developmental stage of the endometriosis and to clarify the mechanism of action of these inflammatory/anti-inflammatory adipocytokines under endometriotic conditions. The imbalance between pro- and anti-inflammatory adipocytokines may be an important causative factor in the pathogenesis of endometriosis.

CONCLUSION

Our study revealed, for the first time, decreased visfatin and vaspin gene expressions together with increased serum irisin and CRP levels were observed in endometriosis patients compared to control subjects. Our findings suggest that these adipocytokines may play a potential role in the development of endometriosis. Although this study has provided helpful information, many unknown aspects regarding the mechanisms and markers of endometriosis warrant further investigation. Finally, all the data suggest that additional studies are needed to define the significance of novel adipocytokines as prognostic markers and therapeutic targets in the etiology of endometriosis.

ACKNOWLEDGMENTS

This study was supported by Ankara University Scientific Research Project (19H0237003).

Conflict of interest: No conflict of interest was declared by the authors. The authors are solely responsible for the content and writing of this paper.

REFERENCES

1. Yoo JY, Kim TH, Fazleabas AT, Palomino WA, Ahn SH, Tayade C, Schammel DP, Young SL, Jeong JW, Lessey BA. KRAS activation and over-expression of SIRT1/BCL6 contributes to the pathogenesis of endometriosis and progesterone resistance. Sci Rep. 2017;7:6765.
2. Zondervan KT, Becker CM, Koga K, Missmer SA, Taylor RN, Viganò P. Endometriosis. Nat Rev Dis Primers. 2018;4:9.
3. Ozkan S, Murk W, Arici A. Endometriosis and infertility: epidemiology and evidence-based treatments. Ann NY Acad Sci. 2008;1127:92-100.
4. Kennedy S, Bergqvist A, Chapron C, D'Hooghe T, Dunselman G, Greb R, Hummelshoj L, Prentice A, Saridogan E; ESHRE Special Interest Group for Endometriosis and Endometrium Guideline Development Group. ESHRE guideline for the diagnosis and treatment of endometriosis. Hum Reprod. 2005;20:2698-2704.
5. Opøien HK, Fedorcsak P, Omland AK, Abyholm T, Bjercke S, Ertzeid G, Oldereid N, Mellembakken JR, Tanbo T. *In vitro* fertilization is a successful treatment in endometriosis-associated infertility. Fertil Steril. 2012;97:912-918.
6. Fraser MA, Agarwal S, Chen I, Singh SS. Routine vs. expert-guided transvaginal ultrasound in the diagnosis of endometriosis: a retrospective review. Abdom Imaging. 2015;40:587-594.
7. Bulun SE. Endometriosis. N Engl J Med. 2009;360:268-279.
8. Oh YK, Ha YR, Yi KW, Park HT, Shin JH, Kim T, Hur JY. Increased expression of resistin in ectopic endometrial tissue of women with endometriosis. Am J Reprod Immunol. 2017;78.
9. Juge-Aubry CE, Henrichot E, Meier CA. Adipose tissue: a regulator of inflammation. Best Pract Res Clin Endocrinol Metab. 2005;19:547-566.
10. Maijer KI, Neumann E, Müller-Ladner U, Drop DA, Ramwadhdoebe TH, Choi IY, Gerlag DM, de Hair MJ, Tak PP. Serum vaspin levels are associated with the development of clinically manifest arthritis in autoantibody-positive individuals. PLoS One. 2015;10:e0144932.
11. Choi YS, Oh HK, Choi JH. Expression of adiponectin, leptin, and their receptors in ovarian endometrioma. Fertil Steril. 2013;100:135-41.e1-2.
12. Jin CH, Yi KW, Ha YR, Shin JH, Park HT, Kim T, Hur JY. Chemerin expression in the peritoneal fluid, serum, and ovarian endometrioma of women with endometriosis. Am J Reprod Immunol. 2015;74:379-386.
13. Yang RZ, Lee MJ, Hu H, Pray J, Wu HB, Hansen BC, Shuldiner AR, Fried SK, McLenithan JC, Gong DW. Identification of omentin as a novel depot-specific adipokine in human adipose tissue: possible role in modulating insulin action. Am J Physiol Endocrinol Metab. 2006;290:E1253-E1261.
14. Hida K, Wada J, Eguchi J, Zhang H, Baba M, Seida A, Hashimoto I, Okada T, Yasuhara A, Nakatsuka A, Shikata K, Hourai S, Futami J, Watanabe E, Matsuki Y, Hiramatsu R, Akagi S, Makino H, Kanwar YS. Visceral adipose tissue-derived serine protease inhibitor: a unique insulin-sensitizing adipocytokine in obesity. Proc Natl Acad Sci USA. 2005;102:10610-10615.
15. Huerta-Delgado AS, Roffe-Vazquez DN, Gonzalez-Gil AM, Villarreal-Calderón JR, Tamez-Rivera O, Rodriguez-Gutierrez NA, Castillo EC, Silva-Platas C, Garcia-Rivas G, Elizondo-Montemayor L. Serum irisin levels, endothelial dysfunction, and inflammation in pediatric patients with type 2 diabetes mellitus and metabolic syndrome. J Diabetes Res. 2020;2020:1949415.
16. Kang YS, Song HK, Lee MH, Ko GJ, Cha DR. Plasma concentration of visfatin is a new surrogate marker of systemic inflammation in type 2 diabetic patients. Diabetes Res Clin Pract. 2010;89:141-149.
17. Livak KJ, Schmittgen TD. Analysis of relative gene expression data using real-time quantitative PCR and the 2(-Delta Delta C(T)) method. Methods. 2001;25:402-408.
18. Yamawaki H, Kuramoto J, Kameshima S, Usui T, Okada M, Hara Y. Omentin, a novel adipocytokine inhibits TNF-induced vascular inflammation in human endothelial cells. Biochem Biophys Res Commun. 2011;408:339-343.

19. Zhong X, Li X, Liu F, Tan H, Shang D. Omentin inhibits TNF-α-induced expression of adhesion molecules in endothelial cells *via* ERK/NF-κB pathway. Biochem Biophys Res Commun. 2012;425:401-406.
20. Li H, Peng W, Zhuang J, Lu Y, Jian W, Wei Y, Li W, Xu Y. Vaspin attenuates high glucose-induced vascular smooth muscle cells proliferation and chemokinesis by inhibiting the MAPK, PI3K/Akt, and NF-κB signaling pathways. Atherosclerosis. 2013;228:61-68.
21. Phalitakul S, Okada M, Hara Y, Yamawaki H. Vaspin prevents TNF-α-induced intracellular adhesion molecule-1 *via* inhibiting reactive oxygen species-dependent NF-κB and PKCθ activation in cultured rat vascular smooth muscle cells. Pharmacol Res. 2011;64:493-500.
22. Watanabe T, Watanabe-Kominato K, Takahashi Y, Kojima M, Watanabe R. Adipose tissue-derived omentin-1 function and regulation. Compr Physiol. 2017;7:765-781.
23. Li HL, Peng WH, Cui ST, Lei H, Wei YD, Li WM, Xu YW. Vaspin plasma concentrations and mRNA expressions in patients with stable and unstable angina pectoris. Clin Chem Lab Med. 2011;49:1547-1554.
24. Ebert T, Stepan H, Schrey S, Kralisch S, Hindricks J, Hopf L, Platz M, Lossner U, Jessnitzer B, Drewlo S, Blüher M, Stumvoll M, Fasshauer M. Serum levels of irisin in gestational diabetes mellitus during pregnancy and after delivery. Cytokine. 2014;65:153-158.
25. Li M, Yang M, Zhou X, Fang X, Hu W, Zhu W, Wang C, Liu D, Li S, Liu H, Yang G, Li L. Elevated circulating levels of irisin and the effect of metformin treatment in women with polycystic ovary syndrome. J Clin Endocrinol Metab. 2015;100:1485-1493.
26. Gamal RM, Mohamed ME, Hammam N, El Fetoh NA, Rashed AM, Furst DE. Preliminary study of the association of serum irisin levels with poor sleep quality in rheumatoid arthritis patients. Sleep Med. 2020;67:71-76.
27. Ali EY, Hegazy GA, Hashem EM. Evaluation of irisin, retinol-binding protein 4, and leptin serum levels as biomarkers of macrovascular complications involvement in Saudi type 2 diabetes mellitus. A case-control study. Saudi Med J. 2020;41:1369-1374.
28. Zhang R, Fu T, Zhao X, Qiu Y, Hu X, Shi H, Yin X. Association of circulating irisin levels with adiposity and glucose metabolic profiles in a middle-aged chinese population: a cross-sectional study. Diabetes Metab Syndr Obes. 2020;13:4105-4112.
29. Stengel A, Hofmann T, Goebel-Stengel M, Elbelt U, Kobelt P, Klapp BF. Circulating levels of irisin in patients with anorexia nervosa and different stages of obesity--correlation with body mass index. Peptides. 2013;39:125-130.
30. Huang W, Liu Y, Xu H, Zhu H, Guan J, Yi H, Zou J. Association of the serum irisin level with obstructive sleep apnea: a body mass index- and physical activity-matched study. Endocr J. 2020;67:607-612.
31. Mazur-Bialy AI, Bilski J, Pochec E, Brzozowski T. New insight into the direct anti-inflammatory activity of a myokine irisin against proinflammatory activation of adipocytes. Implication for exercise in obesity. J Physiol Pharmacol. 2017;68:243-251.
32. Park MJ, Kim DI, Choi JH, Heo YR, Park SH. New role of irisin in hepatocytes: the protective effect of hepatic steatosis *in vitro*. Cell Signal. 2015;27:1831-1839.
33. Wu MY, Ho HN. The role of cytokines in endometriosis. Am J Reprod Immunol. 2003;49:285-296.
34. Xavier P, Belo L, Beires J, Rebelo I, Martinez-de-Oliveira J, Lunet N, Barros H. Serum levels of VEGF and TNF-alpha and their association with C-reactive protein in patients with endometriosis. Arch Gynecol Obstet. 2006;273:227-231.
35. Lermann J, Mueller A, Körber F, Oppelt P, Beckmann MW, Dittrich R, Renner SP. Evaluation of high-sensitivity C-reactive protein in comparison with C-reactive protein as biochemical serum markers in women with endometriosis. Fertil Steril. 2010;93:2125-2129.
36. Mihalyi A, Gevaert O, Kyama CM, Simsa P, Pochet N, de Smet F, de Moor B, Meuleman C, Billen J, Blanckaert N, Vodolazkaia A, Fulop V, D'Hooghe TM. Non-invasive diagnosis of endometriosis based on a combined analysis of six plasma biomarkers. Hum Reprod. 2010;25:654-664.
37. Vodolazkaia A, Bossuyt X, Fassbender A, Kyama CM, Meuleman C, Peeraer K, Tomassetti C, D'Hooghe TM. A high sensitivity assay is more accurate than a classical assay for the measurement of plasma CRP levels in endometriosis. Reprod Biol Endocrinol. 2011;9:113.
38. Fassbender A, Burney RO, O DF, D'Hooghe T, Giudice L. Update on biomarkers for the detection of endometriosis. Biomed Res Int. 2015;2015:130854.
39. Brentano F, Schorr O, Ospelt C, Stanczyk J, Gay RE, Gay S, Kyburz D. Pre-B cell colony-enhancing factor/visfatin, a new marker of inflammation in rheumatoid arthritis with proinflammatory and matrix-degrading activities. Arthritis Rheum. 2007;56:2829-2839.
40. Adya R, Tan BK, Chen J, Randeva HS. Nuclear factor-kappaB induction by visfatin in human vascular endothelial cells: its role in MMP-2/9 production and activation. Diabetes Care. 2008;31:758-760.
41. Tsiotra PC, Tsigos C, Yfanti E, Anastasiou E, Vikentiou M, Psarra K, Papasteriades C, Raptis SA. Visfatin, TNF-alpha and IL-6 mRNA expression is increased in mononuclear cells from type 2 diabetic women. Horm Metab Res. 2007;39:758-763.
42. Seow KM, Hwang JL, Wang PH, Ho LT, Juan CC. Expression of visfatin mRNA in peripheral blood mononuclear cells is not correlated with visfatin mRNA in omental adipose tissue in women with polycystic ovary syndrome. Hum Reprod. 2011;26:2869-2873.

Turk J Pharm Sci 2022;19(1):54-62
DOI: 10.4274/tjps.galenos.2021.77010

ORIGINAL ARTICLE

Assessment of the Appropriateness of Prescriptions in a Geriatric Outpatient Clinic

Geriatri Polikliniğinde Reçete Uygunluğunun Değerlendirilmesi

Burcu KELLECİ ÇAKIR[1]*, Muhammet Cemal KIZILARSLANOĞLU[2], Mustafa Kemal KILIÇ[2], Rana TUNA DOĞRUL[2], Mehmet Emin KUYUMCU[2], Aygin BAYRAKTAR EKİNCİOĞLU[1], Merve BAŞOL[3], Meltem HALİL[2], Kutay DEMİRKAN[1]

[1]Hacettepe University Faculty of Pharmacy, Department of Clinical Pharmacy, Ankara, Turkey
[2]Hacettepe University Faculty of Medicine, Department of Internal Medicine, Division of Geriatric Medicine, Ankara, Turkey
[3]Hacettepe University Faculty of Medicine, Department of Biostatistics, Ankara, Turkey

ABSTRACT

Objectives: Appropriateness of the geriatric outpatients' medications needs special attention due to risks of falls, fractures, depression, hospital admissions and mortality. This study aimed to identify current practice on medication usage by using the 2nd version of "Screening Tool of Older People's Potentially Inappropriate Prescriptions" and "Screening Tool to Alert Doctors to Right Treatment" criteria and affecting factors for the Turkish population.

Materials and Methods: This cross-sectional study was conducted between September 2015 and May 2016 at a university research and training hospital's geriatric outpatient clinic. Patients aged ≥65 years and had ≥5 different prescribed medications (considered as polypharmacy) were recruited. The main outcome measure was the frequency of inappropriate medications identified by clinical pharmacist in the outpatient clinic according to the 2nd version of the criterion sets.

Results: A total of 700 patients (440 female) were included in this study. According to the results, 316 patients (45.1%) with at least one potentially inappropriate medication and 668 patients (98.3%) with at least one potential prescription omission were detected. Potentially inappropriate medications were associated with the number of medications used per patient [odds ratio (OR): 1.20 $p<0.001$], living alone (OR: 4.12 $p=0.02$), and having congestive heart failure (OR: 2.41 $p<0.001$). Twenty-two (27.5%) out of 80 criteria and 4 (11.8%) out of 34 criteria did not apply to the study population.

Conclusion: Detecting inappropriate medications to maintain treatment effectiveness is necessary to provide the optimum therapy. Despite the awareness of polypharmacy in outpatient clinics it is still one of the important causes of inappropriate prescription followed by vaccination rate. Therefore, with the contribution of clinical pharmacist using these available criteria is important, moreover modification of these criteria according to the local needs to be considered to achieve better outcomes.

Key words: Clinical pharmacist, older adults, outpatients, polypharmacy, STOPP/START criteria

ÖZ

Amaç: Geriatri polikliniğinde reçete uygunluğu düşme, kırık, depresyon, hastaneye yatış ve mortalite riskini artırdığı için dikkat edilmesi gereken önemli bir konudur. Bu çalışmanın amacı STOPP/START kriterlerinin 2. versiyonu kullanılarak geriatri polikliniğindeki reçete uygunsuzluklarının ve uygunsuzluğu etkileyen faktörlerin belirlenmesidir.

Gereç ve Yöntemler: Bu çalışma kesitsel olarak Eylül 2015 ve Mayıs 2016 tarihleri arasında bir eğitim ve araştırma hastanesinin geriatri polikliniğinde yürütülmüştür. Çalışmaya ≥65 yaşında ve ≥5 ilaç (polifarmasi) kullanımı olan hastalar dahil edilmiştir. Bir klinik eczacı tarafından uygulanan STOPP/START kriterlerinin 2. versiyonuna göre uygunsuz ilaçların tespit edilmesi birincil çıktı olarak belirlenmiştir.

Bulgular: Toplamda 700 hasta (440 kadın) çalışmaya dahil edilmiştir. Dahil edilen hastaların 316'sının (%45,1) durdurulması gereken ve 668'inin (%98,3) ihmal edilmiş en az bir uygunsuz ilacı bulunduğu tespit edilmiştir. Uygunsuz ilaçların bulunması durumu; kullanılan ilaç sayısı [odds oranı (OR): 1,20 $p<0,001$), hastaların yalnız yaşaması (OR: 4,12 $p=0,02$) ve konjestif kalp yetmezliği tanısı (OR: 2,41 $p<0,001$) ile ilişkili bulunmuştur. STOPP kriterinden 80 kriterin 22'si (%27,5) ve START kriterinden 34 kriterin 4'ü (%11,8) çalışma süresince herhangi bir hastaya uygulanamamıştır.

Sonuç: Hastalar için en uygun ve etkili ilaç tedavisinin sağlanabilmesi amacıyla ilaç uygunsuzluklarının tespit edilmesi önem taşımaktadır. Poliklinikte polifarmasi hakkında farkındalık yüksek olmasına rağmen uygunsuz reçetelemenin başlıca nedenlerinden biri olmaya devam etmektedir, bunu aşılanma oranı takip etmektedir. Klinik eczacının katkısı ile mevcut kriterlerin kullanımı, ek olarak mevcut kriterlerin popülasyona uygun hale getirilmesi ya da yerel kriterlerin geliştirilmesi önem taşımaktadır.

Anahtar kelimeler: Klinik eczacılık, yaşlı hastalar, poliklinik, polifarmasi, STOPP/START kriterleri

***Correspondence:** burcukelleci@hacettepe.edu.tr, **Phone:** +90 535 610 97 84, **ORCID-ID:** orcid.org/0000-0003-2547-8919

Received: 02.03.2021, **Accepted:** 26.04.2021

INTRODUCTION

During the aging process, pharmacokinetic and pharmacodynamic parameters (such as muscle and liver mass, cardiac blood circulation, total body fluid) also change concomitantly with physical, cognitive and psychomotor characteristics and can alter therapeutic response to medications in older adults.[1,2] It is well-known that the incidence of geriatric syndromes increases gradually[3] along with the presence of chronic diseases leading to polypharmacy.

According to the Turkish Statistics Institute, older adult population in Turkey expanded 21.9% during the last five years and reached 9.1% in 2019, having the 66th rank among 167 countries in the list of countries with older adult population.[4] An increase in the older adult population brings up several concerns such as special care needs and increased medication use. It was determined that 30% of prescribed drugs in Turkey was issued for older adult patients.[5]

Increased medication use leads to polypharmacy, which defined as the use of multiple medications for multiple indications. Different cut-offs for polypharmacy was mentioned such as using ≥3 medications, ≥5 medications or 7-10 medications, however 3 concurrent use of medications might increase adverse effects and deteriorate physical health.[6]

Polypharmacy, due to an increased amount of indications or presence of potentially inappropriate medications (PIM) and potential prescription omissions (PPO), generates risks of falls, fractures, depression, mortality and hospital admissions.[7] There have been some explicit and implicit criteria developed to determine PIMs and PPOs such as Beers criteria[8] or Turkish inappropriate medication use in elderly (TIME) criterion set.[9] Due to TIME criterion set has an ongoing validation process, its usage is limited.[9] Among the available explicit criteria, Screening Tool of Older People's Potentially Inappropriate Prescriptions (STOPP) and Screening Tool to Alert Doctors to Right Treatment (START) are prominent due to their ease of use, wide coverage (includes most of drug related conditions) and clinicians' preferences in Europe. According to the new studies and emerging evidence, updated criteria were released in 2015.[10,11] Along with these criteria, comprehensive geriatric assessment should be considered to assess general health status in older adults and appropriateness of prescriptions.[12]

It has been reported that pharmacists play affective role in reducing number of falls, the number of medications, medication costs, number of hospital admission and PIMs by determining and making intervention about inappropriate prescription.[13] In one study conducted in geriatric outpatient clinic indicating that polypharmacy was seen 47.6% among the patients[14] which is the leading cause of PIMs. This ratio is consistent with the literature conducted in European populations.[14]

The quality of prescriptions and provided care can be eased by ensuring a more effective treatment with appropriate and accurate medications and to achieve a multidisciplinary team including a clinical pharmacist must take part in the treatment.[15,16]

In this study, appropriateness of the geriatric outpatients' medications was assessed according to the 2nd version of STOPP/START criteria and the influencing factors such as group of prescribed drugs, chronic diseases, immunization status, living arrangements, comprehensive geriatric screening test results on prescriptions were evaluated.

MATERIALS and METHODS

Patient characteristics

Patients who were aged 65 years or older and had at least 5 different prescribed drugs (excluding topical medicines other than glaucoma medications) were recruited from the university research and training hospital's geriatric outpatient clinic prospectively between September 2015 and May 2016. All patients who met inclusion criteria during the study period were recruited. Therefore, the sample size calculation was not performed. Patients diagnosed with advanced dementia or Alzheimer's disease or receiving anti-cancer treatment were excluded. To minimize bias; standardized forms were used for data collection, the study population was clearly defined and collected data were analyzed by a statistician independently.

The main outcome measures were the frequency of inappropriate medications among Turkish older adult outpatients and determination of factors affecting inappropriate medication usage according to the 2nd version of the STOPP/START criteria assessed by a clinical pharmacist.

Data collection

Data on demographics (such as age, gender, educational status), comorbidities, medication usage (strength, dose, duration, dosage form), laboratory findings related to the prescribed medications were obtained from the patients, healthcare team and hospital information management system. The prescribed medications were classified according to the first four characters of Anatomical Therapeutic Chemical Classification System (ATC) codes recommended by the World Health Organization. A time required to apply STOPP/START criteria was also recorded for each patient. Informed consent to participate in this study taken from all participants when they arrived in the outpatient clinic. The appropriateness of the patients' medications was determined according to the 2nd version of the STOPP/START criteria by the clinical pharmacist with the collaboration of clinicians upon their outpatient clinic visits. Polypharmacy was defined as using five or more medications. The study was approved by the University, Non-Interventional Clinical Research Ethics Board (26.08.2015/GO 15/555) and the procedures used in this study adhere to the tenets of the Declaration of Helsinki. Informed consent to participate and publishing recorded data in this study taken from all participants when they arrived in the outpatient clinic.

In the literature female gender, older age, polypharmacy, having multiple prescribers, and having poor health status are more likely to be associated with PIMs.[17] The patient's characteristics has been given in comparison between genders since all of the study population, has older age and polypharmacy. The patient's characteristics also compared according to PIM presence to determine variables for logistic regression analyze.

Comprehensive geriatric assessment

A comprehensive geriatric assessment, which included the evaluation of functional status [by activities of daily living (ADL) and instrumental ADL (IADL) scales], nutritional status [by mini nutritional assessment-short form (MNA-SF)], cognitive status [by mini-mental state exam (MMSE) screening tests] and depressive symptoms [by geriatric depression scale (GDS) scores] was performed by physicians at outpatient clinics and data were recorded.

Statistical analysis

As descriptive statistics, mean and standard deviation (SD) or count and percentages are given for continuous variables and frequency and percentage are given for categorical variables. The normality of continuous variables was tested using the Shapiro-Wilk test. The difference between groups was analyzed with independent *t*-test or Mann-Whitney *U* test depends on parametric test assumptions. Chi-square tests are used to investigate whether a significant relationship between categorical variables exists or not. Univariate logistic regression analysis was used to determine which variable(s) are significant by using $p<0.20$. Then, the variable(s) found significant is (are) included in the logistic regression analysis. Analysis was performed using valid data only, patients with missing data were excluded from analysis. All the data analyzed using SPSS version 23®.

RESULTS

During the study period, 700 (52.63%) out of 1,330 patients who admitted to the outpatient clinic were included. The patients with the usage of less than 5 medications, diagnosed with advanced dementia or Alzheimer's disease or receiving anti-cancer treatment were excluded. Of those, 440 (62.8%) were female and the mean ± SD age was 75.75±6.56 years in the total study group.

The mean ± SD number of comorbidities was 4.46±1.58 and medications per patient was 7.46±2.38. Characteristics of the study population are given in Table 1. STOPP/START criteria were applied to each patient with the mean duration ± SD of 6.42±2.51 min.

A total of 5226 prescribed medications were evaluated and the most common medications according to the ATC codes were listed as A10B-blood glucose lowering drugs-excluding insulins (n=403, 7.7%), N02B-other analgesics and antipyretics (n=351, 6.7%), C07A-beta blocking agents (n=332, 6.3%), C10A-lipid modifying agents-plain (n=310, 5.9%) and A02B-drugs for peptic ulcer and gastroesophageal reflux disease (n=285, 5.4%).

Among the study participants, 384 patients (54.9%) without any PIM and 12 patients (1.7%) without any PPO were detected (Figure 1). The inapplicable STOPP/START criteria given in Table 2. A total of 441 PIM was identified in 316 patients (45.1%) and 1660 PPO were identified in 688 patients (98.3%). The most common PIM was "any drug prescribed without an evidence-based clinical indication" with 64 (9.1%) and PPO was "pneumococcal vaccine at least once after age 65 according to national guidelines" with 681 (97.3%) (Table 3).

When all variables were analyzed according to the presence of PIM (existence and non-existence), statistically significant variables were detected as age ($p=0.05$), comorbidities ($p=0.005$), number of medications ($p<0.001$), dyslipidemia ($p=0.03$), chronic obstructive pulmonary disease ($p=0.02$), gastritis ($p=0.03$), constipation ($p=0.03$), GDS score ($p=0.03$), congestive heart failure ($p<0.001$), MNA-SF scores ($p=0.05$), but not in others (cigarette smoking, gender, fall history, hypertension, diabetes mellitus, hypothyroidism, hyperthyroidism, incontinence, Parkinson disease).

The variable(s) influenced PIM presence were determined with $p<0.20$ by using univariate logistic regression analysis. After the variable(s) were chosen (such as age, gender, place of residence, geriatric syndromes per patient, comorbid diseases per patient), they were included in the multiple logistic regression analysis to evaluate their effects. The significant variables are given Table 4.

Additionally, when all variables were analyzed according to the presence of PPO (existence and non-existence), statistically significant relations were detected in variables such as number of medication ($p=0.03$), asthma ($p=0.005$) and rheumatoid arthritis ($p=0.01$). However, further analysis with multiple logistic regression analysis could not be performed as the results were unreliable due to imbalanced sample size in each group (688 *versus* 12).

DISCUSSION

Polypharmacy becomes an important issue with the aging in terms of increased risk of negative outcomes due to drug related problems. The implementation of STOPP/START criteria may play important role to determine inappropriate medication use and to modify the prescriptions for protecting older adult patients from negative outcomes of polypharmacy.

It is shown that with the collaboration of clinical pharmacist, appropriateness of prescription is improving in older adults.[13,16] Clinical pharmacist plays an important role in monitoring, dispensing and reviewing of the medications decided and initiated by the physicians.[13] Collaboration with physicians, detailed medication review and pharmaceutical care are resulting with less medication usage and costs.[16,18] Therefore, clinical pharmacists are encouraged to participate in wards and outpatients' clinics as a member of multidisciplinary team.[16] In this study by the clinical pharmacist assessments, 54.9% of the patients had no PIM and 1.7% had no PPO. However, 22 out of 80 (27.5%) STOPP criteria and 4 out of 34 (11.8%) START criteria were not applicable to any medication during the study period. At least one PIM was detected in 45.1% of the patients according to the STOPP criteria in our study that is similar to the other studies previously reported between 14.8%-49.1%.[5,19-21]

Concerns about special care needs and increased medication use is strongly related to each other. For older adult population; living arrangements as a part of special care needs (living alone or living with someone) can be decisive in situations such as medication use. Patients who are routinely monitored in outpatient clinics often need analgesics, diuretics, cardiovascular

Table 1. Characteristics of the study population

Variables (n=700)	Total n (%)	Female (440, 62.8%) n (%)	Male (260, 37.2%) n (%)	*p* value
Smokers	171 (24.4)	48 (28.1)	123 (71.9)	<0.001
Fall history	49 (7.0)	36 (73.5)	13 (26.5)	0.1
Level of education				
No education	229 (32.7)	211 (92.1)	18 (7.9)	
Primary school	257 (36.7)	159 (61.9)	98 (38.1)	
Middle school	56 (8.0)	23 (41.1)	33 (58.9)	<0.001
High school	81 (11.6)	18 (22.2)	63 (77.8)	
University	69 (9.9)	28 (40.6)	41 (59.4)	
Higher education	8 (1.1)	1 (12.5)	7 (87.5)	
Living arrangements				
Alone	121 (17.3)	90 (80.4)	22 (19.6)	<0.001
With partner/relative/caregiver	579 (82.7)	344 (59.4)	235 (40.5)	
Number of medications				
Medications *per* patient (mean ± SD)	7.46±2.38	7.47±2.44	7.46±2.30	0.95*
Total prescribed medication (n)	5226	3287	1941	
Person with polypharmacy (5-10 medication) (n, %)	570 (81.4)	365 (64)	205 (36)	0.17
Person with excessive polypharmacy (>10 medication) (n, %)	130 (18.6)	75 (57.7)	55 (42.3)	
Comprehensive geriatric tests results				
Katz score of ADL categoric (score ≤2/6)	85 (12.1)	61 (71.8)	24 (28.2)	0.06
MNA-SF categoric Malnutrition risk (score ≤11/14) Malnutrition (score ≤7/14)	 103 (14.7) 18 (2.6)	 70 (68) 11 (61.1)	 33 (32) 7 (38.9)	0.53
MMSE (score ≥18, ≤23)	138 (19.7)	102 (73.9)	36 (26.1)	0.01
GDS categoric (score ≥5/15)	187 (26.7)	138 (73.8)	49 (26.2)	0.001
Most common and significant comorbidities				
Hypertension	608 (86.9)	392 (64.5)	216 (35.5)	0.03
Diabetes mellitus	366 (52.3)	237 (64.8)	129 (35.2)	0.31
Dyslipidemia	251 (35.9)	160 (63.7)	91 (36.3)	0.71
Coronary artery disease	207 (29.6)	106 (51.2)	101 (48.8)	**<0.001**
Osteoporosis	181 (25.9)	151 (83.4)	30 (16.6)	**<0.001**

Data other than n (%) are given as mean ± SD. Pearson chi-square test used as statistical evaluation, Mann-Whitney *U* test had been used for parameters with * sign. ADL: Activities of daily living, MNA-SF: Mini nutritional assessment-short form, MMSE: The mini-mental state exam, GDS: Geriatric depression scale, SD: Standard deviation

medications. Furthermore, generally use acetaminophen, non-steroidal anti-inflammatory drugs (NSAIDs), anti-histamines and gastrointestinal system drugs for some minor symptoms that are contributing the inappropriate prescriptions.[22]

Like other studies, "inappropriate use of NSAID's",[5,19,20,22] "usage of medication that cause duplication"[5,20] and "inappropriate dosage of aspirin"[5] are some of the most common PIMs that were also identified in our patients. In this study, the most common PIM (presence of any medication prescribed without evidence-based indication) was associated mainly with proton pump inhibitors (PPI) usage. PPI treatment was continued for gastritis even though the disease was cured. "Drugs for peptic ulcer and gastroesophageal reflux disease" were also detected among most commonly used medications when listed according to their ATC codes. It has been reported that continuation of PPI at the maximum dose after relieved gastrointestinal

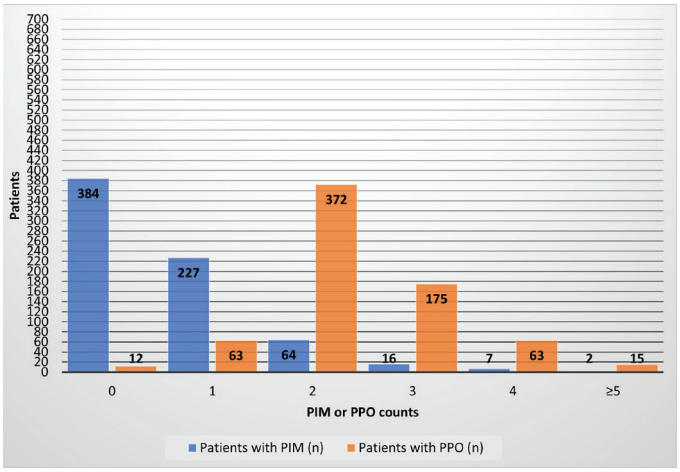

Figure 1. Number of PIM and PPO according to Screening Tool of Older Person's Prescriptions/Screening Tool to Alert Doctors to Right Treatment criteria

PIM: Potentially inappropriate medications, PPO: Potential prescribing omission

symptoms may lead to various problems such as increased risks of vitamin B12 deficiency, calcium and iron deficiency, osteoporosis, infection by bacteria such as *Clostridium difficile* and certain types of cancer.[12] Therefore, the necessity of PPI usage in patients should be assessed periodically.

One of the main findings of this study was that 98.3% of the patients had at least one PPO according to the START criteria, which is higher than the rates reported previously (28.1%-73.3%).[16,21,23] However consistent with the results of a study conducted in patients with falls and syncope.[24] "Calcium/vitamin D supplementation in patients with osteoporosis" is one of the most common PPO revealed in other studies[19,23-25] as in our study. Unlike other studies, the most frequent identified PPOs in this study were "pneumococcal vaccination at least once after 65 years of age according to national guidelines" (97.3%) and "annual influenza vaccination" (78.7%). Even though the vaccination is covered by the governmental health insurance the vaccinated older adult numbers were very low in this study.

The total time of the application of a criterion set might be an effective factor on its active usage in clinical practice. In this study, STOPP/START criteria were fully applied quickly with the mean duration ± SD of 6.42±2.51 min. Application time was found 3 min for STOPP criteria and 1 min for START criteria in a study by Ryan et al.[26] In another study, it was stated that the application time of START criteria did not exceed 5 min per patient and to apply STOPP criteria quickly, the results of the geriatric screening test of the patient and the detailed treatment history should be known previously.[27]

As expected in older adult patients, the number of comorbidities (median: 4, range: 1-10) and polypharmacy (median: 7, range: 5-20) was high in our study patients. Hypertension, diabetes mellitus and coronary artery diseases were the most common comorbidities in our study that is very similar to the results of Frankenthal et al.[23] (a study evaluated medications of 359 older adults according to the STOPP/START criteria) as well as the co-medications for these comorbidities. Those comorbid conditions interfere each other in most cases and it is well known in clinical practice that clinicians should pay more attention to those group of patients in terms of appropriate and safe prescribing.

Unlike the study of Frankenthal et al.[23] most of the patients in this study were independent in their daily life activities according to the Katz score (87.9% vs. 25%). This might be explained by both exclusion of the advanced stage dementia patients and inclusion of small number of dementia patients (seen only in 13.1% of the patients).

Previous studies reported that age, female gender, number of medications, falls, and hospitalization are the most common factors associated with PIM.[17,19,20,23,28,29] Besides the number of medications (OR: 1.20) was associated with PIM in our study. It was also found that detection of PIM is probably increased by having congestive heart failure (2.41-fold) and living alone (4.12-fold). The gender had relation with smoking status, level of education, some of the comprehensive geriatric screening test scores and some comorbidities but it didn't produce statistically significant result on PIM occurrence. Even though comprehensive geriatric screening test scores in this study were similar with that of Kara et al.[19] Such as Katz score of ADL (6 *vs.* 6), IADL (16 *vs.* 17), MMSE (28 *vs.* 27), MNA-SF (13 *vs.* 13) and GDS (1 *vs.* 0), these similarities did not produce the same outcomes when multivariate logistic regression analysis was performed. Kara et al.[19] Found that gender, osteoporosis, number of medications and Katz scores of ADL were independently associated with STOPP criteria, however only similar outcome of this study is the number of medications.

The association between PPOs and age, female gender, number of medications and comorbidities has been shown in previous studies.[19,25,30,31] However, due to the uneven distribution of the number of patients with and without PPOs (688 and 12), multivariate logistic regression analysis was not performed in our study.

The removal of 2 criteria and modification of 2 criteria in START criteria and the modification of 5 criteria in STOPP criteria were recommended by Castillo-Páramo et al.[32] While they used the 1st version of STOPP/START in Spain. In another study conducted in Sri-Lanka due to unavailability of some medicines or clinical information the necessity of modified version of the STOPP/START criteria has been indicated.[33] In the 2nd version of criterion set 8% reduction has been made with the two Delphi rounds.[33] In our study, with the 2nd version of STOPP/START, it was found that 22 of 80 STOPP criteria and 4 out of 34 START criteria have not been applicable for any medication at the study period. Since, medications and procedures are not universal, local modification of STOPP/START criteria or development of local criteria to evaluate the medication of geriatric patients is necessary. Therefore, local "TIME" criteria have been developed which originated from the STOPP/START and the CRIME criteria.[9]

Table 2. Inapplicable STOPP and START criteria

Inapplicable STOPP criteria
Cardiovascular system criteria 1. Centrally-acting antihypertensives (*e.g.* methyldopa, clonidine, moxonidine, rilmenidine, guanfacine), unless clear intolerance of, or lack of efficacy with, other classes of antihypertensives 2. Aldosterone antagonists (*e.g.* spironolactone, eplerenone) with concurrent potassium-conserving drugs (*e.g.* ACEI's, ARB's, amiloride, triamterene) without monitoring of serum potassium 3. Phosphodiesterase type-5 inhibitors (*e.g.* sildenafil, tadalafil, vardenafil) in severe heart failure characterised by hypotension *i.e.* systolic BP <90 mmHg, or concurrent daily nitrate therapy for angina
Coagulation system criteria 1. Ticlopidine in any circumstances
Central nervous system criteria 1. Tricyclic antidepressants with dementia, narrow angle glaucoma, cardiac conduction abnormalities, prostatism, or prior history of urinary retention 2. Neuroleptics as hypnotics, unless sleep disorder is due to psychosis or dementia 3. Phenothiazines as first-line treatment, since safer and more efficacious alternatives exist 4. First-generation antihistamines
Renal system criteria 1. Digoxin at a long-term dose greater than 125 µg/day if eGFR <30 mL/min/1.73 m^2 2. Factor Xa inhibitors (*e.g.* rivaroxaban, apixaban) if eGFR <15 mL/min/1.73 m^2 3. Colchicine if eGFR <10 mL/min/1.73 m^2
Respiratory system criteria 1. Systemic corticosteroids instead of inhaled corticosteroids for maintenance therapy in moderate-severe COPD 2. Benzodiazepines with acute or chronic respiratory failure *i.e.* pO_2 <8.0 kPa ± pCO_2 >6.5 kPa
Musculoskeletal system criteria 1. Corticosteroids (other than periodic intra-articular injections for mono-articular pain) for osteoarthritis 2. COX-2 selective NSAIDs with concurrent cardiovascular disease 3. NSAID with concurrent corticosteroids without PPI prophylaxis
Endocrine system criteria 1. Oestrogens with a history of breast cancer or venous thromboembolism. 2. Oestrogens without progestogen in patients with intact uterus 3. Androgens in the absence of primary or secondary hypogonadism
Drugs that predictably increase the risk of falls in older people 1. Hypnotic Z-drugs (*e.g.* zopiclone, zolpidem, zaleplon)
Analgesic drugs 1. Use of oral or transdermal strong opioids (morphine, oxycodone, fentanyl, buprenorphine, diamorphine, methadone, tramadol, pethidine, pentazocine) as first line therapy for mild pain. 2. Long-acting opioids without short-acting opioids for break-through pain
Total: 22 out of 80 (27.5%) criteria
Inapplicable START criteria
Cardiovascular system criteria. Aspirin (75 mg - 160 mg once daily) in the presence of chronic atrial fibrillation, where vitamin K antagonists or direct thrombin inhibitors or factor Xa inhibitors are contraindicated
Central nervous system & ophthalmic criteria Dopamine agonist (ropinirole or pramipexole or rotigotine) for restless legs syndrome, once iron deficiency and severe renal failure have been excluded
Musculoskeletal system criteria Folic acid supplement in patients taking methotexate.
Urogenital System criteria. Topical vaginal oestrogen or vaginal oestrogen pessary for symptomatic atrophic vaginitis
Total: 4 out of 34 (11.8) criteria

STOPP: Screening Tool of Older Person's Prescriptions, ACE: Angiotensin converting enzyme, ARB: Angiotensin II receptor blockers, BP: Blood pressure, eGFR: Estimated glomerular filtration rate, COPD: Chronic obstructive pulmonary disease, COX-2: Cyclooxigenase 2, NSAIDs: Non-steroidal anti-inflammatory drugs, START: Screening Tool to Alert doctors to Right Treatment

Table 3. Most common PIMs according to STOPP criteria and PPOs according to START criteria

STOPP screening criteria	n (%)
Any drug prescribed without an evidence-based clinical indication	88 (10.9)
Any duplicate drug class prescription *e.g.* two concurrent NSAIDs, SSRIs, loop diuretics, ACE inhibitors, anticoagulants	73 (9)
NSAID with established hypertension (risk of exacerbation of hypertension) or heart failure	33 (4.1)
ACE inhibitors or angiotensin receptor blockers in patients with hyperkalemia	27 (3.3)
Long-term aspirin at doses greater than 160 mg *per* day	26 (3.2)
START screening criteria	
Pneumococcal vaccine at least once after age 65, according to national guidelines	789 (97.5)
Seasonal trivalent influenza vaccine annually	553 (68.4)
Vitamin D supplement in patients with known osteoporosis and previous fragility fracture(s) and/or (bone mineral density T-scores more than -2.0 in multiple sites)	77 (9.5)
Bone anti-resorptive or anabolic therapy (*e.g.* bisphosphonate, strontium ranelate, teriparatide, denosumab) in patients with documented osteoporosis, where no pharmacological or clinical status contraindication exists (bone mineral density T-scores ->2.5 in multiple sites) and/or previous history of fragility fracture(s)	73 (9)
Statin therapy with a documented history of coronary, cerebral or peripheral vascular disease, unless the patient's status is end-of-life or age is >85 years	66 (8.2)

PIM: Potentially inappropriate medications, STOPP: Screening Tool of Older Person's Prescriptions, NSAID: Non-steroidal anti-inflammatory drug, ACE: Angiotensin converting enzyme, SSRI: Selective serotonin reuptake inhibitor, PPO: Potentially prescribing omissions, START: Screening Tool to Alert Doctors to Right Treatment

Table 4. Factors independently associated with STOPP criteria

Variables	No PIM n (%)	PIM	OR	95% CI	*p* value
Living arrangements (living alone)	57 (47.1)	64 (52.9)	4.12	2.03-12.08	0.02
Congestive heart failure (exist)	21 (28.4)	53 (71.6)	2.41	1.37-4.22	0.001
Medication *per* patient	6.98±1.96	8.05±2.71	1.20	1.11-1.29	<0.001

Data other than n (%) are given as mean ± SD.
Multivariate logistic regression analysis was performed to find the independent associates of STOPP criteria. All variables with $p<0.20$ in the univariate logistic regression analysis were included in multivariate regression analysis (age, gender, place of residence, geriatric syndromes *per* patient, comorbid diseases *per* patient, falls in the last months, hypertension, ischemic heart disease, diabetes mellitus, hyperlipidemia, chronic obstructive pulmonary disease, osteoporosis, constipation, number of medication, comprehensive geriatric screening tests). The parameters that were significantly associated are given in the table $p<0.005$ is statistically significant. STOPP: Screening Tool of Older Person's Prescriptions, PIM: Potentially inappropriate medication, OR: Odds ratio, CI: Confidence interval

Study limitations

This study also has some limitations. Even though many patients were involved in this study compared to other published studies,[11,26,29] a randomized controlled study design could not be implemented due to a restrictive period of master of science thesis. About non-applicable criteria; this can't generalize to the Turkish population but considering our sample size this still gives an idea about necessity of the unused criteria. Moreover, the physicians in the department that this study was conducted were familiar with the 1st version of the STOPP/START criteria therefore this might have influenced on the practice of prescribing.

CONCLUSION

Detecting inappropriate medications to maintain treatment effectiveness is necessary to provide the optimum therapy. Despite the awareness of many risk factors related to inappropriate prescription; living arrangements, having a congestive heart failure and increasing number of medications are seen as risk factors of inappropriate prescription. The vaccination section presents only in 2nd version of STOPP/START criteria has shown a valuable insight of older adult Turkish patients' vaccination status. STOPP/START criteria are still playing a pivotal role in the appropriateness of prescription in line with this valuable tool a local tool may be more beneficial to covering population characteristics.

ACKNOWLEDGMENTS

We are indebted to the members of Hacettepe University hospital department of geriatric medicine, Özgur Kara MD and Cafer Balcı MD for their precious help and advices in this study.

Conflict of interest: No conflict of interest was declared by the authors. The authors are solely responsible for the content and writing of this paper.

REFERENCES

1. Fried LP. Epidemiology of aging. Epidemiol Rev. 2000;22:95-106.
2. Schlender JF, Meyer M, Thelen K, Krauss M, Willmann S, Eissing T, Jaehde U. Development of a whole-body physiologically based pharmacokinetic approach to assess the pharmacokinetics of drugs in elderly individuals. Clin Pharmacokinet. 2016;55:1573-1589.
3. Flacker JM. What is a geriatric syndrome anyway? J Am Geriatr Soc. 2003;51:574-576.
4. Türkiye Istatistik Kurumu Istatistiklerle Yaşlılar, 2019; 33712. [cited 20 March 2020]; Available from: http://www.tuik.gov.tr/PreHaberBultenleri.do?id=33712
5. Yayla ME, Bilge U, Binen E, Keskin A. The use of START/STOPP criteria for elderly patients in primary care. Sci World J. 2013;2013:165873.
6. Linjakumpu T, Hartikainen S, Klaukka T, Veijola J, Kivelä SL, Isoaho R. Use of medications and polypharmacy are increasing among the elderly. J Clin Epidemiol. 2002;55:809-817.
7. Nascimento MMG, Ribeiro AQ, Pereira ML, Soares AC, de Loyola Filho AID, Dias-Junior CAC. Identification of inappropriate prescribing in a Brazilian nursing home using STOPP/START screening tools and the Beers' Criteria. Braz J Pharm Sci. 2014;50:911-918.
8. By the 2019 American Geriatrics Society Beers Criteria® Update Expert Panel. American Geriatrics Society 2019 Updated AGS Beers Criteria® for Potentially Inappropriate Medication Use in Older Adults. J Am Geriatr Soc. 2019;67:674-694.
9. Bahat G, Ilhan B, Erdogan T, Halil M, Savas S, Ulger Z, Akyuz F, Bilge AK, Cakir S, Demirkan K, Erelel M, Guler K, Hanagasi H, Izgi B, Kadioglu A, Karan A, Kulaksizoglu IB, Mert A, Ozturk S, Satman I, Sever MS, Tukek T, Uresin Y, Yalcin O, Yesilot N, Oren MM, Karan MA. Turkish inappropriate medication use in the elderly (TIME) criteria to improve prescribing in older adults: TIME-to-STOP/TIME-to-START. Eur Geriatr Med. 2020;11:491-498.
10. O'Mahony D, O'Sullivan D, Byrne S, O'Connor MN, Ryan C, Gallagher P. STOPP/START criteria for potentially inappropriate prescribing in older people: version 2. Age Ageing. 2015;44:213-218.
11. Anrys P, Boland B, Degryse JM, De Lepeleire J, Petrovic M, Marien S, Dalleur O, Strauven G, Foulon V, Spinewine A. STOPP/START version 2-development of software applications: easier said than done? Age Ageing. 2016;45:589-592.
12. Wahab MS, Nyfort-Hansen K, Kowalski SR. Inappropriate prescribing in hospitalised Australian elderly as determined by the STOPP criteria. Int J Clin Pharm. 2012;34:855-862.
13. Hashimoto R, Fujii K, Shimoji S, Utsumi A, Hosokawa K, Tochino H, Sanehisa S, Akishita M, Onda M. Study of pharmacist intervention in polypharmacy among older patients: non-randomized, controlled trial. Geriatr Gerontol Int. 2020;20:229-237.
14. Demircan C, Hasanzade U. Polypharmacy and potential inappropriate drug use in the elderly admitted to the general internal medicine outpatient clinic. Turk J Int Med. 2021;(Supplement 1):S46-S48.
15. Gillespie U, Alassaad A, Hammarlund-Udenaes M, Mörlin C, Henrohn D, Bertilsson M, Melhus H. Effects of pharmacists' interventions on appropriateness of prescribing and evaluation of the instruments' (MAI, STOPP and STARTs') ability to predict hospitalization--analyses from a randomized controlled trial. PLoS One. 2013;8:e62401.
16. Ryan C, O'Mahony D, Byrne S. Application of STOPP and START criteria: interrater reliability among pharmacists. Ann Pharmacother. 2009;43:1239-1244.
17. Alhawassi TM, Alatawi W, Alwhaibi M. Prevalence of potentially inappropriate medications use among older adults and risk factors using the 2015 American Geriatrics Society Beers criteria. BMC Geriatr. 2019;19:154.
18. Ammerman CA, Simpkins BA, Warman N, Downs TN. Potentially inappropriate medications in older adults: deprescribing with a clinical pharmacist. J Am Geriatr Soc. 2019;67:115-118.
19. Kara Ö, Arık G, Kızılarslanoglu MC, Kılıc MK, Varan HD, Sümer F, Esme M, Altıner S, Kuyumcu ME, Yesil Y, Yavuz BB, Cankurtaran M, Halil M. Potentially inappropriate prescribing according to the STOPP/START criteria for older adults. Aging Clin Exp Res. 2016;28:761-768.
20. Gallagher P, O'Mahony D. STOPP (screening tool of older persons' potentially inappropriate prescriptions): application to acutely ill elderly patients and comparison with Beers' criteria. Age Ageing. 2008;37:673-679.
21. Lozano-Montoya I, Vélez-Diaz-Pallarés M, Delgado-Silveira E, Montero-Errasquin B, Cruz Jentoft AJ. Potentially inappropriate prescribing detected by STOPP-START criteria: are they really inappropriate? Age Ageing. 2015;44:861-866.
22. Al-Azayzih A, Alamoori R, Altawalbeh SM. Potentially inappropriate medications prescribing according to Beers criteria among elderly outpatients in Jordan: a cross sectional study. Pharm Pract (Granada). 2019;17:1439.
23. Frankenthal D, Lerman Y, Kalendaryev E, Lerman Y. Potentially inappropriate prescribing among older residents in a geriatric hospital in Israel. Int J Clin Pharm. 2013;35:677-682.
24. de Ruiter SC, Biesheuvel SS, van Haelst IMM, van Marum RJ, Jansen RWMM. To STOPP or to START? Potentially inappropriate prescribing in older patients with falls and syncope. Maturitas. 2020;131:65-71.
25. Gallagher P, Lang PO, Cherubini A, Topinková E, Cruz-Jentoft A, Montero Errasquín B, Mádlová P, Gasperini B, Baeyens H, Baeyens JP, Michel JP, O'Mahony D. Prevalence of potentially inappropriate prescribing in an acutely ill population of older patients admitted to six European hospitals. Eur J Clin Pharmacol. 2011;67:1175-1188.
26. Ryan C, O'Mahony D, Kennedy J, Weedle P, Byrne S. Potentially inappropriate prescribing in an Irish elderly population in primary care. Br J Clin Pharmacol. 2009;68:936-947.
27. Borges EP, Morgado M, Macedo AF. Prescribing omissions in elderly patients admitted to a stroke unit: descriptive study using START criteria. Int J Clin Pharm. 2012;34:481-489.
28. Liu CL, Peng LN, Chen YT, Lin MH, Liu LK, Chen LK. Potentially inappropriate prescribing (IP) for elderly medical inpatients in Taiwan: a hospital-based study. Arch Gerontol Geriatr. 2012;55:148-151.
29. Lang PO, Hasso Y, Dramé M, Vogt-Ferrier N, Prudent M, Gold G, Michel JP. Potentially inappropriate prescribing including under-use amongst older patients with cognitive or psychiatric co-morbidities. Age Ageing. 2010;39:373-381.
30. San-José A, Agustí A, Vidal X, Formiga F, Gómez-Hernández M, García J, López-Soto A, Ramírez-Duque N, Torres OH, Barbé J; Potentially Inappropriate Prescription in Older Patients in Spain (PIPOPS) Investigators' project. Inappropriate prescribing to the oldest old patients admitted to hospital: prevalence, most frequently used medicines, and associated factors. BMC Geriatr. 2015;15:42.
31. Manias E, Kusljic S, Lam DL. Use of the screening tool of older persons' prescriptions (STOPP) and the screening tool to alert doctors to the right

treatment (START) in hospitalised older people. Australas J Ageing. 2015;34:252-258.

32. Castillo-Páramo A, Pardo-Lopo R, Gómez-Serranillos IR, Verdejo A, Figueiras A, Clavería A. Valoración de la idoneidad de los criterios STOPP/START en el ámbito de atención primaria en España por el método RAND [Assessment of the appropriateness of STOPP/START criteria in primary health care in Spain by the RAND method]. Semergen. 2013:413-420.

33. Samaranayake NR, Balasuriya A, Fernando GH, Samaraweera D, Shanika LGT, Wanigasuriya JKP, Wijekoon CN, Wanigatunge CA. 'Modified STOPP-START criteria for Sri Lanka'; translating to a resource limited healthcare setting by Delphi consensus. BMC Geriatrics. 2019;19:282.

Turk J Pharm Sci 2022;19(1):63-69
DOI: 10.4274/tjps.galenos.2021.47417

ORIGINAL ARTICLE

Novel Indole Derivative as the First P-glycoprotein Inhibitor from the Skin of Indian Toad *(Bufo melanostictus)*

P-glikoprotein İnhibitörü Olarak Hint Kurbağası *(Bufo melanostictus)* Derisinden İlk Kez Elde Edilen Yeni Bir İndol Türevi

Prasad NEERATI*, Sangeethkumar MUNIGADAPA

Kakatiya University College of Pharmaceutical Sciences, Department of Pharmacology, Division of Drug Metabolism and Pharmacokinetics, Telangana, India

ABSTRACT

Objectives: To study the inhibitory effect of novel indole derivative (NID) from Indian toad skin *(Bufo melanostictus)* on permeability glycoprotein (P-gp).

Materials and Methods: Dried Indian toad skin was used to isolate NID with column chromatography, and its structure was elucidated by infrared spectra, ^{13}C nuclear magnetic resonance (NMR), ^{1}H NMR spectra, and liquid chromatography-mass spectrometry. Female Wistar rats were used to determine LD_{50}, *in vitro* permeability studies were done with the intestinal sac method, and *in vivo* pharmacokinetic studies were carried out to prove the P-gp inhibition using the rat model.

Results: The NID has shown increased clear permeability P_{app} ($x10^{-6}$ cm/sec) significantly ($p<0.001$) from 1.04±0.11 to 2.90±0.08 in ileum 1.44±0.14 to 3.92±0.13 in jejunum this *in vitro* results confirmed that P-gp inhibited, this was further confirmed by *in vivo* studies in *in vivo* studies observed increased oral bioavailability of digoxin (DIG) significantly in NID treated groups from 3.26±0.25 to 7.47±0.18 ng/mL, the volume of distribution decreased from 232.56±64.59 to 86.57±7.04 L/kg. Area under the curve increased from 37.89±1.13 to 64.62±0.70 ng/mL/hr. This demonstrates NID increased the oral bioavailability of DIG significantly.

Conclusion: Many compounds were isolated from the Indian toad skin. This NID was not reported earlier. Results demonstrate NID increased the oral bioavailability of DIG significantly. The isolated NID from Indian toad skin proved as a potent P-gp inhibitor in both *in vitro* and *in vivo* studies, and further studies are needed to develop as a possible new drug candidate.

Key words: Clear permeability, bioavailability, novel indole derivative, permeability glycoprotein

ÖZ

Amaç: Hint kurbağa derisinden (*Bufo melanostictus*) elde edilen yeni indol türevinin (NID) permeabilite glikoproteini (P-gp) üzerindeki inhibitör etkisini incelemek.

Gereç ve Yöntemler: NID, kurutulmuş Hint kurbağası derisinden kolon kromatografisi ile elde edilmiş ve yapı tayini infrared spektoskopisi, ^{13}C nükleer magnetic rezonans (NMR), ^{1}H NMR spektroskopisi ve sıvı kromatografisi-kütle spektrometrisi ile gerçekleştirilmiştir. LD_{50}, dişi Witsar sıçanlar kullanılarak belirlenmiştir, *in vitro* permeabilite çalışmaları intestinal kese yöntemi ile, ve P-gp inhibisyonunu doğrulamak amacıyla *in vivo* farmakokinetik çalışmalar, rat modeli kullanılarak gerçekleştirilmiştir.

Bulgular: NID'nin, ileumda 1,04±0,11'den 2,90±0,08'e; jejunumda 1,44±0,14'ten 3,92±0,13'e önemli ölçüde ($p<0,001$) artan açık permeabilite göstermiştir P_{app} ($x10^{-6}$ cm/s) anlamlı bir şekilde göstermiştir ve bu *in vitro* sonuçlar P-gp'nin inhibe edildiğini doğrulamaktadır; bu sonuçlar NID ile tedavi edilen gruplarda digoksinin (DIG) oral biyoyararlınımının 3,26±0,25'ten 7,47±0,18 ng/mL'ye önemli ölçüde artmasının ve dağılım hacminin 232,56±64,59'dan 86,57±7,04 L/kg'ye düşmesinin gözlenmesi ile *in vivo* olarak da doğrulanmıştır. Eğrinin altındaki alan 37,89±1,13'ten 64,62±0,70 ng/mL/saate yükselmiştir. Bu, NID'nin DIG'nin oral biyoyararlanımını önemli ölçüde artırdığını gösterir.

*Correspondence: prasadneerati@gmail.com, Phone: +09494812120, ORCID-ID: orcid.org/0000-0002-7145-1699

Received: 16.03.2021, Accepted: 17.05.2021

Sonuç: Hint kurbağa derisinden birçok bileşik izole edilmiştir. NID bileşiği daha önce bildirilmemiştir. Sonuçlar, NID'nin DIG'nin oral biyoyararlanımını önemli ölçüde artırdığını göstermektedir. Hint kurbağa derisinden izole edilen NID'nin hem *in vitro* hem de *in vivo* çalışmalarda güçlü bir P-gp inhibitörü olduğu kanıtlanmıştır ve olası yeni bir ilaç adayı olarak geliştirmek için daha fazla çalışmaya ihtiyaç vardır.

Anahtar kelimeler: Açık permeabilite, biyoyararlınım, yeni indol türevi, permeabilite glikoprotein

INTRODUCTION

Toxic animals are widely distributed throughout the globe.[1,2] Venomous animals are recognized as a new emerging source of new drug discovery and therapeutics.[3] Recently many new bioactive compounds from different toads were reported.[4] Toads belong to amphibians and Anura family. The toad skin and parotid glands play an essential role in the survival of amphibians from diverse conditions and predators.[5,6] Toads possess two types of glands beneath their skin, mucous glands and granular glands. Mucous glands secrete thick mucus secretions, which are important to keep toad skin moist.[7] Granular glands secrete acrid, toxic substances, which provides protection from predators.[8] This acrid, toxic substance, when comes intact, induces inflammation, irritation, and vomiting sensations in toad predators.[9] This glandular secretion chemically belongs to potent substances like steroids, alkaloids, peptides, proteins, and biogenic amines.[10] New drug discovery is a challenge many active compounds extracted from plants, animals, fungi, other sources. There is still to discover new compounds from the above sources.[11] Toad skin extracts have been widely used for treating many types of ailments in China and other countries as traditional alternative medicine. The chemical composition and pharmacological activities of toad skin remain unclear.[12] Permeability glycoprotein (P-gp) is an important transporting protein present on the cell membrane that effluxes many xenobiotic substances like drug molecules out of cells.[13] P-gp has a significant impact on drug absorption, distribution, metabolism, excretion and is associated with drug-drug interactions.[14-16] P-gp is over-expressed on the surface of cancer cells and prevents drug entry into the tumor due to rapid and prolonged efflux mechanism.[17,18] P-gp induces resistance to anticancer drugs, which leads to therapeutic failure. There are many phytochemicals and drugs reported as P-gp inhibitors but associated with severe side effects.[19,20] An alternate approach is needed to overcome this issue by exploring new compounds from new sources,[21,22] in this study toad skin extract studies for inhibitory action on P-gp. In this study, digoxin (DIG) was used as probe substrate,[23] and verapamil (VER)[24] was taken as standard inhibitor. The isolated novel indole derivative (NID) inhibited P-gp and enhanced the oral bioavailability of DIG *in vivo* studies.

MATERIALS AND METHODS

Experimental

Sample collection and preparation

Adult live toads (45 to 50 g) were collected from the near places in Warangal and University surroundings. After collecting the toads, the skins were isolated carefully and shade dried at room temperature (27˚C); after complete dryness soaked in methanol for 30 days in an amber-colored bottle, the supernatant was collected, evaporated to dryness using rotary evaporator, at the end, dark brown solid mass methanolic extract (44 g) was obtained. The methanol extract was extracted further with ethyl acetate; this ethyl acetate fraction (EAF) was collected. EAF was subjected to column chromatography on silica gel (100-200 mesh-Merck), eluted slowly in increasing polarity mixture of solvents like *n*-hexane, chloroform, ethyl acetate, ethanol, methanol, and water to obtain different fractions. five fractions were collected; fraction-2 was obtained as a pale gray colored compound, which on TLC produced a single spot. Further purification was done with acetone and methanol.[25,26] The final isolated compound yield was found to be 800 mg.

Animals

Female and male Wistar rats were procured from Vyas Enterprises, Hyderabad, acclimatized for 10 days, then used housed in standard laboratory conditions.[27] All experimental animal protocols were approved by the Ethics Committee of IAEC (approval number: IAEC/02/UCPSc/KU/2016).

Chemicals and other requirements

Acetonitrile (Merck-Mumbai), methanol (Merck-Mumbai), EA (Merck-Mumbai), DIG (Sigma Aldrich-Bangalore), VER (Lupin Pvt Labs-Pune-India) Equipment used are, n-hexane (Merck-Mumbai), chloroform (Merck- Mumbai), ethanol (Merck-Mumbai), high-performance liquid chromatography (HPLC) (Schimadzu, with phenominex C-18 column), biofuge-centrifuge (Heraeus instrument- Germany), chromatography column-borosilicate made, TLC aluminum Plates-Sigma Aldrich, ultra sonicator (Ramsit scientific equipement-Hyd), rotavapor-R-300 (Mumbai-India), oral feeding needle, syringe filters-minisart (sartorius stedim Biotech-Germany).

Toxicity studies

According to the OECD-423 guidelines maximum, tolerated dose (MTD) was determined using 15 female Wistar rats. Rats were divided into 5 groups (n=3), control group treated with normal saline, the second group given NID (5 mg/kg, *p.o.*), third group NID (50 mg/kg, *p.o.*), the fourth group NID (300 mg/kg, *p.o.*), fifth group NID (2000 mg/kg, *p.o.*). Toxic effects were recorded for 14 days during the period observed for mortality, physiological parameters like body weight changes, food intake, water intake, and behavioral changes in each animal noted.[28]

Characterization of NID using spectral data

Spectral analysis was done using liquid chromatography-mass spectrometry (LC-MS) analysis 2.6.1. The components were identified using mass spectral libraries The ^{1}H spectra were

recorded at 300 K on a spectrometer operating at 600.13 MHz (14.1 T) using a 5 mm inverse probe equipped with a z-shielded gradient. Nuclear magnetic resonance (NMR) samples were prepared by dissolving extract in 500 µL dimethyl sulfoxide and 1 µL dimethyl formamide as an internal standard. ^{13}C NMR spectral reports were made by comparison of the observed chemical shift values with the reported values. An infrared (IR) spectrophotometer is used, and spectral data is used to find functional groups. ChemDraw pro 8.0 (Perkin Elmer) was used for structure assessment.

In vitro studies

Intestinal sac study was conducted according to the previously described methods.[29] Rats were grouped and sacrificed using anesthetic ether; the intestine was surgically removed, flushed with 50-mL saline (5%). The small intestine was cut into two segments jejunum and ileum of equal length (5 cm). The probe drug (DIG 500 µg/mL) was dissolved in pH 7.4 isotonic Dulbecco's phosphate buffered saline (D-PBS) containing 25 mM glucose. Similarly, DIG + VER (100 µg/mL), DIG + NID 2 mg/mL and DIG + NID 4 mg/mL loaded. And both ends of the sac were ligated tightly with surgical sutures. The sacs were placed in a beaker containing 40 mL of D-PBS, containing 25 mM glucose. The medium was pre-warmed at 37°C and pre-oxygenated with 5% CO_2/ 95% O_2 under bubbling with mixture gas, the transport of the DIG from apical to basolateral and basolateral to apical samples was collected periodically for 120 min periodically, the collected samples were stored at -20°C until analysis. The samples were analyzed by HPLC.

Calculation of clear permeability coefficient

The clear permeability coefficient (P_{app}) of DIG was calculated from the following equation:

Where dQ/dt: Transport rate of the drug in the serosal medium, A: is the surface area of the intestinal sacs, and C°: Initial concentration inside the sacs.[30]

Sample preparation for intestinal sac sample analysis

Samples were extracted using a simple protein precipitation method by adding acetonitrile (200 µL) to samples (100 µL). Samples were vortexed for 10 min and centrifuged at 6,000 rpm for 15 min. The resultant clean supernatant (20 µL) was injected and analyzed using HPLC (Supplementary Figure 1). The mobile phase consists of acetonitrile: Water 65:35. Flow rate: 1 mL/min, pressure: 115 kg.f/cm^2, ultraviolet-detection at the following: 220 nm.

In vivo studies

Male Wistar rats were used kept one week for acclimatization during the period supplied with normal *ad libitum* and free access for water. After one week they were divided into 4 groups (n=6) the first group treated with DIG (0.5 mg/kg, *p.o.*). Second group treated with DIG (0.5 mg/kg, *p.o.*) +VER (2 mg/kg, *p.o.*), third group treated with DIG (0.5 mg/kg, *p.o.*) + NID (2 mg/kg, *p.o.*) fourth group DIG (0.5 mg/kg, *p.o.*) + NID (4 mg/kg.p.o). Blood sample were collected by picturing lateral tail vein[31] at 0, 0.5, 1, 2, 4, 6, 8, 12 and 24 h time points. Samples were centrifuged and supernatant extracted with acetonitrile precipitation methods Samples were stored at -4°C until used for analyzed by HPLC (Supplementary Figure 2).[32]

Statistical analysis

All the pharmacokinetic parameters were analyzed using Phoenix WinNonlin version 8.3 kinetic software. The statistical analysis was performed using One-Way ANOVA followed by *Bonferroni post*-test and Graph Pad Prism version (8.0.2).

RESULTS

Structure assessment using spectral analysis

Based on the spectral analysis using LC-MS (Supplementary Figure 3), ^1H NMR (Supplementary Figure 4) (Table 1) ^{13}C NMR (Supplementary Figure 5) IR spectra (Supplementary Figure 6) and values the structure of NID is elucidated (Figure 1).

Toxicity assessment and determination of MTD

The mortality was found in three animals at 50 mg/kg treated groups, according to OECD-423 guidelines, comes under category-2,[33] (LD 50 cut-off dose 25 mg/kg). At 5 mg/kg, the animals remained alive after the administration of NID. Body weight slightly decreased in NID 5 mg/kg, compared to control. Water intakes decreased somewhat in NIA 5 mg/kg, compared to control, and locomotor activity was not changed significantly (Figure 2A-D) (Supplementary Table 1). The MTD found to be 25 mg/kg.

In vitro studies

The P_{app} (x10^{-6} cm/sec) significantly increased (p<0.001) in NID treated groups from 1.04±0.11 to 2.90±0.08 in ileum, and

Table 1. H^1 NMR, C^{13} Chemical shift in $CDCl_3$ data of NID

H^1	δppm	C^{13}	δct ppm
1	5.5 (S.H)	1	-
2	6.92 (S.H)	2	119
3	-	3	120
4	6.9 (S.H)	4	111
5	5.5 (S.H)	5	151
6	2.6 (S.H)	6	107
7	6.9 (S.H)	7	125
8	2.15 (δ 3H, *J*=7.4HZ)	8	123
9	2.4 (δ3H, *J*=7.2HZ)	9	129
10	-	10	103
11	2.6 (S,3H)	11	15
12	2.9 (S.3H)	12	66
	-	13	24
	-	14	47

NMR: Nuclear magnetic resonance, NID: Novel indole derivative, $CDCl_3$: Deuterated chloroform

1.44±0.14 to 3.92±0.13 in jejunum compare to control group (Table 2) (Supplementary Figure 1).

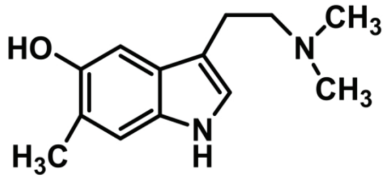

Figure 1. Chemical structure of NID
NID: Novel indole derivative

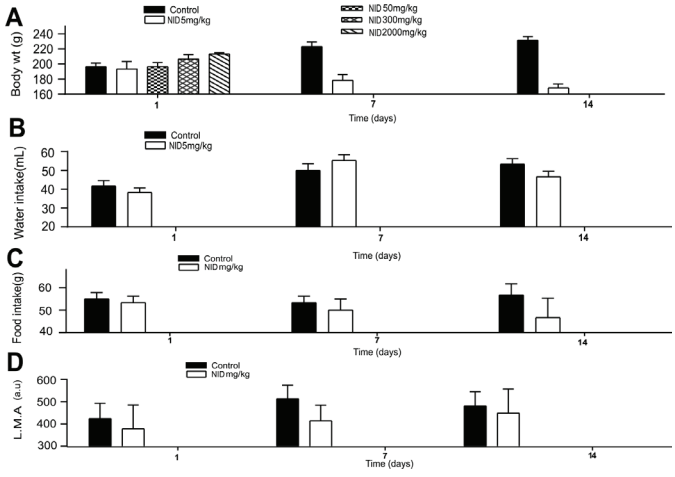

Figure 2. Toxicity studies of NID. NID: Novel indole derivative, A: Body weight, B: Food intake, C: Water intake, D: Locomotor activity

In vivo studies

The plasma drug concentration of DIG significantly increased in NID treated groups compared to control and positive control groups (Figure 3) (Supplementary Table 2). C_{max} increased from 3.26±0.254 to 7.47±0.186 ng/mL, T_{max} decreased from 27.17±13.85 to 9.88±1.13 h, AUMC from 371.27±18.16 to 530.57±16.52 ng.h^2/mL, area under the curve increased from 37.89±1.132 to 64.62±0.70 ng.h^2/mL, CL from 6.09±0.24 to 7.87±0.22 L/h/kg, volume of distribution decreased from 232.56±64.59 to 86.57±7.049 L/kg, mean residual time from 9.79±0.27 to 8.20±0.19 h significantly (p<0.001) (Table 3).

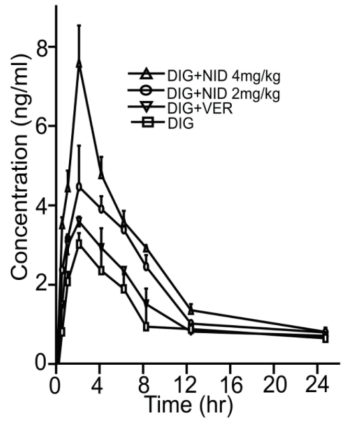

Figure 3. Effect novel indole derivative on pharmacokinetics of digoxin. Values mentioned in mean ± SD (n=6). NID: Novel indole derivative, DIG: Digoxin, VER: Verapamil, SD: Standard deviation

Table 2. *In vitro* clear permeability studies

Clear permeability	DIG	DIG + VER	DIG + NID 2 mg/mL	DIG + NID 4 mg/mL
Ileum	1.04±0.11	1.77±0.09**	2.42±0.12**	2.90±0.08**
Jejunum	1.44±0.14	2.00±0.17**	2.45±0.13**	3.92±0.13***

Data represent mean ± SD values, One-Way ANOVA was used for statistical analysis, **p<0.01, ***p<0.001 compared with the control (DIG). DIG: Digoxin, VER: Verapamil, NID: Novel indole derivative

Table 3. Effect of NID on pharmacokinetic parameters of digoxin

Pk parameter	DIG	DIG + VER	DIG + NID 2 mg/kg	DIG + NID 4 mg/kg
C_{max} (ng/mL)	3.26±0.254	3.79±0.117***	4.59±0.097****	7.47±0.186****
T_{max} (hr)	27.17±13.85	12.512±0.447**	10.70±0.430***	9.88±1.137***
$T_{½}$ (hr)	2.00±0.00	2.00±0.00	2.00±0.00	2.00±0.00
AUMC (ng.h^2/mL)	371.27±18.16	398.61±9.00*	468.92±13.79****	530.57±16.52****
AUC_{0-t} (ng/mL/hr)	37.89±1.132	43.01±0.43****	52.95±1. 31****	64.62±0.70****
CL (L/h/kg)	6.09±0.24	6.65±1.74	6.98±0.23	7.87±0.22**
K_{el} (h^{-1})	0.03±0.016	0.05±0.02***	0.065±0.003****	0.071±0.08****
V_d (L/kg)	232.56±64.59	141.99±12.94***	107.72±15.74****	86.57±7.04****
MRT (hr)	9.79±0.279	9.26±0.12***	8.85±0.10****	8.20±0.19****

Data represents mean ± SD values, One-Way ANOVA was used for statistical analysis followed by Bonferroni *post*-test. A significant difference ****, p<0.05, p<0.001, p<0.0001) compared with the control (DIG). DIG: Digoxin, VER: Verapamil, NID: Novel indole derivative, p: Probability value, C_{max}: Peak plasma concentration, T_{max}: Time to reach maximum concentration, $T_{½}$: Half-life, AUMC: Area under the first moment curve, AUC: Area under curve, CL: Clearance, Kel: Elimination rate constant, V_d: Volume of distribution, MRT: Mean residual time

DISCUSSION

In this study, we isolated a new compound from toad skin and spectral data accessed the structure. Some other studies reported different compounds from toad skin,[34] but this compound was not reported earlier. The MTD was determined according to OECD guidelines and found 5 mg/kg; others reported the LD_{50} of TSE as 400 mg/kg.[35] *In vitro* studies proved that NID inhibited P-gp and enhanced the clear permeability of DIG. Some plant extracts have shown P-gp inhibition in *in vitro* studies, and several studies are reported as P-gp inhibitors.[36] Few more studies reported that VER increases the oral bioavailability of DIG up to 60% but reported side effects;[37] in our study, NID has shown better oral bioavailability of DIG. In a similar study, the compound from the Asiatic toad (*Bufo gargarizans*) inhibited P-gp and decreased the expression.[38] Some studies explained that the herbal compounds inhibited P-gp and enhanced the oral bioavailability of its substrate drugs.[39] A similar study reported that toad parasitoid gland secretion inhibited P-gp and increased the bioavailability of substrate drug.[40] Our study also achieved P-gp inhibition and improved the bioavailability of DIG with NID.

CONCLUSION

The isolated compound from Indian toad skin is confined as a NID and unreported earlier; the compound significantly inhibited P-gp mediated transportation. *In vivo* studies revealed that NID increased the oral bioavailability of DIG. Co-administration of a drug with potent molecules like NID can alter transporter function to improve drug bioavailability.

ACKNOWLEDGMENTS

Thanks to director National Institute of Nutrition (NIN) -Hyd for formulation and supplying high fat diet; special thanks to Director-Indian Institute of Chemical Technology (IICT)-Hyd, A.Srinivas National Institute of Technology (NIT)-Wgl.

Conflict of interest: No conflict of interest was declared by the authors. The authors are solely responsible for the content and writing of this paper.

REFERENCES

1. Zhang Y. Why do we study animal toxins? Dongwuxue Yanjiu. 2015;36:183-222.
2. Utkin YN. Animal venom studies: Current benefits and future developments. World J Biol Chem. 2015;6:28-33.
3. Peigneur S, Tytgat J. Toxins in drug discovery and pharmacology. Toxins (Basel). 2018;10:126.
4. Qi J, Tan CK, Hashimi SM, Zulfiker AH, Good D, Wei MQ. Toad glandular secretions and skin extractions as anti-inflammatory and anticancer agents. Evid Based Complement Alternat Med. 2014;2014:312684.
5. Urban MC, Phillips BL, Skelly DK, Shine R. A toad more traveled: the heterogeneous invasion dynamics of cane toads in Australia. Am Nat. 2008;171:E134-E148.
6. Garg A, Hippargi R, Gandhare A. Toad skin-secretions: potent source of pharmacologically and therapeutically significant compounds. Int J Pharmacol. 2007;5:17.
7. Mills JW, Prum BE. Morphology of the exocrine glands of the frog skin. Am J Anat. 1984;171:91-106.
8. Jared C, Mailho-Fontana PL, Marques-Porto R, Sciani JM, Pimenta DC, Brodie Jr. ED, Antoniazzi MM. Skin gland concentrations adapted to different evolutionary pressures in the head and posterior regions of the caecilian siphonops annulatus. Sci Rep. 2018;1:3576.
9. Toledo RC, Jared C. Cutaneous granular glands and amphibian venom. Comp Biochem Physiol. 1995;1-29.
10. Zhang Y, Yuan B, Takagi N, Wang H, Zhou Y, Si N, Yang J, Wei X, Zhao H, Bian B. Comparative analysis of hydrophilic ingredients in toad skin and toad venom using the UHPLC-HR-MS/MS and UPLC-QqQ-MS/MS methods together with the anti-inflammatory evaluation of indolealkylamines. Molecules. 2018;24:86.
11. Ramana KV, Singhal SS, Reddy AB. Therapeutic potential of natural pharmacological agents in the treatment of human diseases. BioMed Res Int. 2014;573452.
12. Meng Q, Yau LF, Lu JG, Wu ZZ, Zhang BX, Wang JR, Jiang ZH. Chemical profiling and cytotoxicity assay of bufadienolides in toad venom and toad skin. J Ethnopharmacol. 2016;187:74-82.
13. Sharom FJ. The P-glycoprotein efflux pump: how does it transport drugs? J Membr Biol. 1997;160:161-175.
14. Lin JH, Yamazaki M. Role of P-glycoprotein in pharmacokinetics: clinical implications. Clin Pharmacokinet. 2003;42:59-98.
15. Hoosain FG, Choonara YE, Tomar LK, Kumar P, Tyagi C, du Toit LC, Pillay V. Bypassing P-glycoprotein drug efflux mechanisms: possible applications in pharmacoresistant schizophrenia therapy. Biomed Res Int. 2015;2015:484963.
16. Amin ML. P-glycoprotein inhibition for optimal drug delivery. Drug Target Insights. 2013;7:27-34.
17. Kong XB, Yang ZK, Liang LJ, Huang JF, Lin HL. Overexpression of P-glycoprotein in hepatocellular carcinoma and its clinical implication. World J Gastroenterol. 2000;6:134-135.
18. Kim SW, Md Hasanuzzaman, Cho M, Kim NH, Choi HY, Han JW, Park HJ, Oh JW, Shin JG. Role of 14-3-3 sigma in over-expression of P-gp by rifampin and paclitaxel stimulation through interaction with PXR. Cell Signal. 2017;31:124-134.
19. Lee CA, Cook JA, Reyner EL, Smith DA. P-glycoprotein related drug interactions: clinical importance and a consideration of disease states. Expert Opin Drug Metab Toxicol. 2010;6:603-619.
20. Glaeser H. Importance of P-glycoprotein for drug-drug interactions. Handb Exp Pharmacol. 2011;285-297.
21. Leopoldo M, Nardulli P, Contino M, Leonetti F, Luurtsema G, Colabufo NA. An updated patent review on P-glycoprotein inhibitors (2011-2018). Expert Opin Ther Pat. 2019;29:455-461.
22. Binkhathlan Z, Lavasanifar A. P-glycoprotein inhibition as a therapeutic approach for overcoming multidrug resistance in cancer: current status and future perspectives. Curr Cancer Drug Targets. 2013;13:326-346.
23. Akamine Y, Yasui-Furukori N, Uno T. Drug-drug interactions of P-gp substrates unrelated to CYP metabolism. Curr Drug Metab. 2019;20:124-129.
24. Wang L, Sun Y. Efflux mechanism and pathway of verapamil pumping by human P-glycoprotein. Arch Biochem Biophys. 2020;696:108675.

25. Sasidharan S, Chen Y, Saravanan D, Sundram KM, Yoga Latha L. Extraction, isolation and characterization of bioactive compounds from plants' extracts. Afr J Tradit Complement Altern Med. 2011;8:1-10.
26. Abubakar AR, Haque M. Preparation of Medicinal Plants: Basic extraction and fractionation procedures for experimental purposes. J Pharm Bioallied Sci. 2020;12:1-10.
27. Ottesen JL, Weber A, Gürtler H, Mikkelsen LF. New housing conditions: improving the welfare of experimental animals. Altern Lab Anim. 2004;(Suppl 1B):397-404.
28. Jonsson M, Jestoi M, Nathanail AV, Kokkonen UM, Anttila M, Koivisto P, Karhunen P, Peltonen K. Application of OECD Guideline 423 in assessing the acute oral toxicity of moniliformin. Food Chem Toxicol. 2013;53:27-32.
29. Barthe L, Woodley JF, Kenworthy S, Houin G. An improved everted gut sac as a simple and accurate technique to measure paracellular transport across the small intestine. Eur J Drug Metab Pharmacokinet. 1998;23:313-323.
30. Palumbo P, Picchini U, Beck B, van Gelder J, Delbar N, DeGaetano A. A general approach to the apparent permeability index. J Pharmacokinet Pharmacodyn. 2008;35:235-248.
31. Zou W, Yang Y, Gu Y, Zhu P, Zhang M, Cheng Z, Liu X, Yu Y, Peng X. Repeated blood collection from tail vein of non-anesthetized rats with a vacuum blood collection system. J Vis Exp. 2017:55852.
32. Mathies JC, Austin MA. Modified acetonitrile protein-precipitation method of sample preparation for drug assay by liquid chromatography. Clin Chem. 1980;26:1760.
33. Amuamuta A, Plengsuriyakarn T, Na-Bangchang K. Anticholangiocarcinoma activity and toxicity of the Kaempferia galanga Linn. Rhizome ethanolic extract. BMC Complement Altern Med. 2017;17:213.
34. Barnhart K, Forman ME, Umile TP, Kueneman J, McKenzie V, Salinas I, Minbiole KPC, Woodhams DC. Identification of bufadienolides from the boreal toad, *anaxyrus boreas*, active against a fungal pathogen. Microb Ecol. 2017;74:990-1000.
35. Manika D, Auddy B, Gomes A. Pharmacological study of the toad skin extract on experimental animals. Indian J Pharmacol. 1996;2:72-76.
36. Deferme S, Kamuhabwa A, Nshimo C, de Witte P, Augustijns P. Screening of Tanzanian plant extracts for their potential inhibitory effect on P-glycoprotein mediated efflux. Phytother Res. 2003;17:459-464.
37. Summers MA, Moore JL, McAuley JW. Use of verapamil as a potential P-glycoprotein inhibitor in a patient with refractory epilepsy. Ann Pharmacother. 2004;38:1631-1634.
38. Yuan Z, Shi X, Qiu Y, Jia T, Yuan X, Zou Y, Liu C, Yu H, Yuan Y, He X, Xu K, Yin P. Reversal of P-gp-mediated multidrug resistance in colon cancer by cinobufagin. Oncol Rep. 2017;37:1815-1825.
39. Athukuri BL, Neerati P. Enhanced oral bioavailability of domperidone with piperine in male wistar rats: involvement of CYP3A1 and P-gp inhibition. J Pharm Pharm Sci. 2017;20:28-37.
40. Madugula N, Neerati P. Influence of toad parotid gland secretion from Indian toad (*Bufo melanostictus*) in diabetic rats: an experimental evidence of P-glycoprotein inhibition. Int J Pharm Res. 2020;125-135.

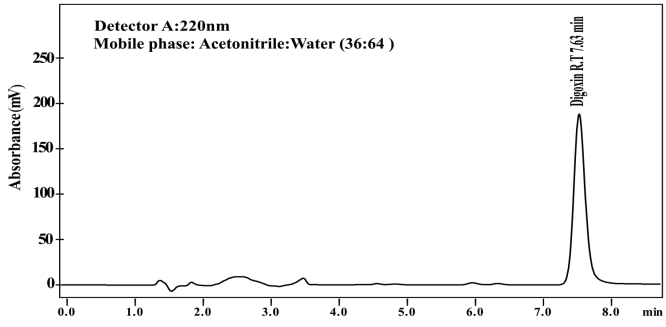

Supplementary Figure 1. Typical chromatogram of digoxin in rat plasma

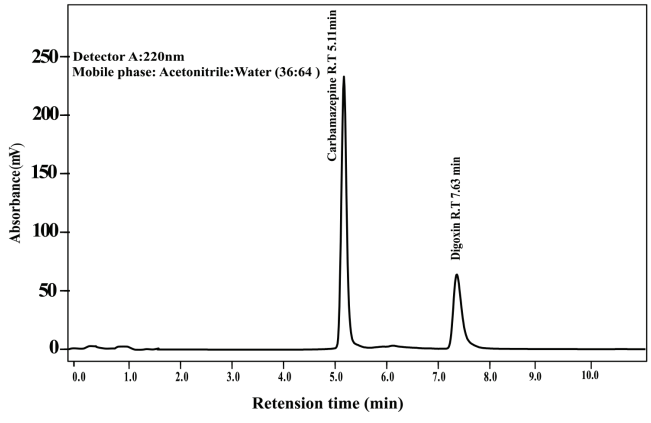

Supplementary Figure 2. Chromatogram of digoxin with internal standard in plasma

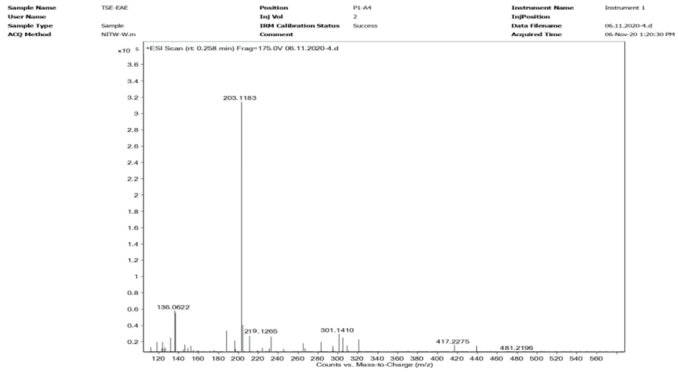

Supplementary Figure 3. LC-MS spectra of NID

LC-MS: Liquid chromatography-mass spectrometry, NID: Novel indole derivative

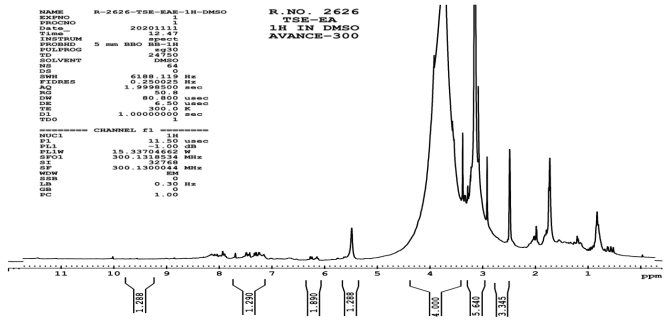

Supplementary Figure 4. ^{1}H NMR spectra of NID

NMR: Nuclear magnetic resonance, NID: Novel indole derivative

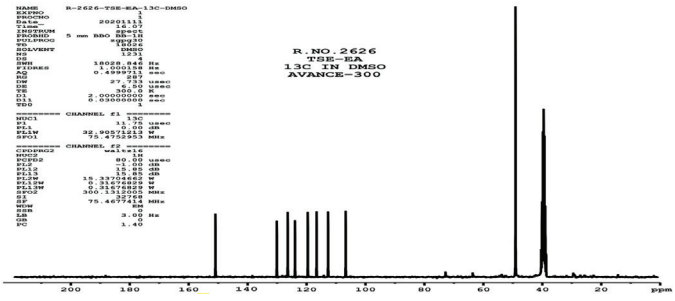

Supplementary Figure 5. ^{13}C NMR spectra of NID

NMR: Nuclear magnetic resonance, NID: Novel indole derivative

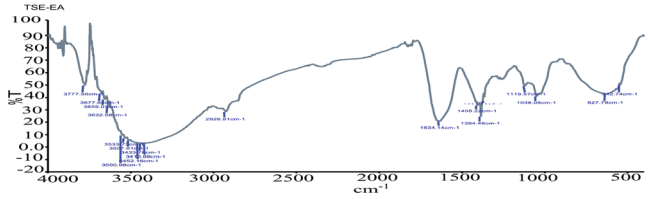

Supplementary Figure 6. FT-IR spectra of NID

FT-IR: Fourier-transform infrared spectroscopy, NID: Novel indole derivative

Supplementary Table 1. Toxicity studies and mortality rate

Group	Treatment	Sign of toxicity (TS/NS)	Mortality (D/S)
Control	Saline	0/3	0/3
NID	5 mg/kg	0/3	0/3
NID	50 mg/kg	3/3	3/3
NID	300 mg/kg	3/3	3/3
NID	2000 mg/kg	3/3	3/3

(n=3), NID: Novel indole derivative, TS: Toxicity sign, NS: No sign of toxicity, D: Death, S: Survival, L: Live

Supplementary Table 2. Plasma drug concentrations (µg/mL) of digoxin at different time points

Time (h)	DIG	DIG + VER	DIG + NID 2 mg/kg	DIG + NID 4 mg/kg
	Mean ± SD	Mean ± SD	Mean ± SD	Mean ± SD
0	0.0±0.0	0.0±0.0	0.0±0.0	0.0±0.0
0.5	1.226±0.160	1.85±0.078	2.666±0.081	3.716±0.172
1	2.393±0.231	3.236±0.213	3.391±0.100	4.576±0.040
2	3.265±0.253	3.793±0.116	4.596±0.096	7.476±0.186
4	2.65±0.187	3.183±0.081	4.08±0.295	4.88±0.414
6	2.228±0.336	2.65±0.063	3.6±0.057	3.78±0.261
8	1.343±0.089	1.868±0.044	2.743±0.265	3.18±0.078
12	1.293±0.116	1.235±0.057	1.416±0.0496	1.73±0.144
24	1.076±0.081	1.136±0.042	1.21±0.063	1.226±0.098

Data represents mean ± SD values. DIG: Digoxin, VER: Verapamil, NID: Novel indole derivative, SD: Standard deviation

Turk J Pharm Sci 2022;19(1):70-75
DOI: 10.4274/tjps.galenos.2021.86344

ORIGINAL ARTICLE

Determination of the Phototoxicity Potential of Commercially Available Tattoo Inks Using the 3T3-neutral Red Uptake Phototoxicity Test

Piyasada Satılan Dövme Boyalarının 3T3-nötral Kırmızısı Alım Fototoksisite Testi ile Fototoksisite Potansiyelinin Belirlenmesi

Elif Gözde UTKU TÜRK, Ayse Tarbin JANNUZZI, Buket ALPERTUNGA*

İstanbul University, Faculty of Pharmacy, Department of Pharmaceutical Toxicology, İstanbul, Turkey

ABSTRACT

Objectives: Tattooing is an ancient practice and its popularity has been increasing in the recent years. After tattooing, complications may occur related to compose tattoo inks. In this study, the phototoxicity potential of the blue, red and black colors of the most commonly used three different commercially-available tattoo ink brands have been examined by performing *in vitro* 3T3-neutral red uptake (NRU) phototoxicity test.

Materials and Methods: In the study, the phototoxicity of serial diluted concentrations of tattoo inks were evaluated with *in vitro* 3T3-NRU phototoxicity test method according to OECD guide 432. The data obtained from the NRU test result were uploaded to Phototox software (version 2.0) and the phototoxicity potentials of tattoo inks were determined *via* the calculation of the mean photo effect (MPE) and photo irritation factor (PIF) values.

Results: The red, black and blue colors of three different commercially available tattoo inks did not cause a cytotoxic activity on BALB/c 3T3 cells with 3T3-NRU test. The IC_{50} values could not be determined +ultraviolet (UV) and -UV conditions. PIF values could not be calculated and MPE values were <0.1, which predicts the absence of phototoxic effect for all of the tested tattoo inks.

Conclusion: All tested inks were evaluated as non-phototoxic according to the results of MPE values calculated using Phototox software. However, test results should be verified by other phototoxicity test methods to obtain a comprehensive evaluation of phototoxic complications of different tattoo inks.

Key words: Phototoxicity, *in vitro* phototoxicity, 3T3-NRU phototoxicity test, tattoo ink, BALB/c 3T3 cells

ÖZ

Amaç: Dövme yapmak eski zamanlardan beri süregelen bir uygulamadır ve popülaritesi son yıllarda artmaktadır. Dövme yapılmasından sonra dövme boyalarının bileşimine bağlı olarak çeşitli komplikasyonlar oluşabilir. Bu çalışmada, piyasada en çok kullanılan üç farklı dövme boyası markasının mavi, kırmızı ve siyah renklerinin fototoksisite potansiyeli *in vitro* 3T3-nötral kırmızı alım (NRU) fototoksisite testi yapılarak incelenmiştir.

Gereç ve Yöntemler: Çalışmada, dövme boyalarının seri olarak seyreltilmiş konsantrasyonlarının fototoksisitesi, OECD kılavuz 432'ye göre *in vitro* 3T3-NRU fototoksisite test yöntemi ile değerlendirilmiştir. NRU test sonucundan elde edilen veriler Phototox yazılımıyla (sürüm 2.0) değerlendirilmiştir. Dövme boyalarının fototoksisite potansiyelleri medyan foto etki (MPE) ve foto irritan faktör (PIF) değerlerinin hesaplanmasıyla belirlenmiştir.

Bulgular: Ticari olarak temin edilebilen üç farklı dövme boyasının kırmızı, siyah ve mavi renkleri, 3T3-NRU testi ile BALB/c 3T3 hücrelerinde sitotoksik aktiviteye neden olmamıştır. +Ultraviyole (UV) ve -UV koşullarında IC_{50} değerleri belirlenememiştir. PIF değerleri hesaplanamamıştır ve MPE değerleri <0,1 olarak belirlenmiştir. Bu sonuçlar test edilen tüm dövme boyalarının fototoksik etkilerinin olmadığını göstermektedir.

Sonuç: Phototox yazılımı ile hesaplanan MPE değerlerinin sonuçlarına göre test edilen tüm boyaların fototoksik olmadığı sonucuna ulaşılmıştır. Bununla birlikte, farklı dövme boyalarının fototoksik komplikasyonlarının kapsamlı bir değerlendirmesini yapabilmek için test sonuçlarının diğer fototoksisite test yöntemleriyle doğrulanması gerekmektedir.

Anahtar kelimeler: Fototoksisite, *in vitro* fototoksisite, 3T3-NRU fototoksisite testi, dövme boyası, BALB/c 3T3 hücreleri

***Correspondence:** tunga@istanbul.edu.tr, **Phone:** +90 532 251 48 88, **ORCID-ID:** orcid.org/0000-0001-6043-7560

Received: 02.05.2021, **Accepted:** 18.06.2021

INTRODUCTION

Tattooing has existed worldwide for many centuries and increases its popularity, especially among young people today. Tattooing is applied by injecting tattoo ink into the dermis layer that is 1.5-2 mm below the skin with the help of a needle.[1] Despite the increasing popularity of tattooing, the toxicity profile of tattoo inks and the potential risks of these inks remain unknown. Tattoo inks have different formulations. Generally, tattoo inks are prepared by suspending pigments in a solvent. Apart from pigments and solvents, tattoo inks contain additives such as binding agents, preservatives, thickeners, and antioxidants.[2] One of the most significant problems in the toxicological evaluation of tattoo inks is the lack of information about the ink compositions. Additionally, there is no regulation on their use in tattoo inks for organic/inorganic pigments, carbon black, and different chemicals used as coloring agents in tattoo inks.[3] Dermatological severe complications may occur during tattooing and there is a serious increase in the number of patients who apply to the dermatology doctor due to skin conditions caused by a tattoo. Allergic skin reactions caused by tattoos are the most common skin problem. Especially, red tattoo ink can cause allergic skin reactions.[4]

Phototoxicity describes the toxic response of the skin after light exposure due to chemicals present on the skin following cutaneous or systemic application. To produce a phototoxic effect, a chromophore or a photosensitizing molecule must absorb photons. The absorbed photon causes reactive oxygen species (ROS) formation and because of increased ROS level, symptoms such as edema, burning, and pain occur in the skin.[5,6] The European Union banned animal testing in cosmetic products in 2009 and their import and sale in 2013 to reduce the number of laboratory animals used and protect animals from unnecessary pain and injuries.[7,8] Subsequently, an increasing number of countries worldwide including Turkey have adopted the ban on animal testing for cosmetics.[9] Therefore, the need for validated relevant alternative *in vitro* test methods has increased to make the toxicologic evaluation of cosmetic products.[10] *In vivo* experiments to determine acute phototoxicity are not allowed in Europe since 2000. Instead, the validated and regulatory accepted 3T3-neutral red uptake (NRU) phototoxicity test is primarily used as an *in vitro* alternative method.[11] The 3T3-NRU allows users to test many factors such as different test material concentrations, exposure times, and ultraviolet (UV) irradiation dose. Also, it has been determined to be reliable as results obtained with *in vivo* acute phototoxicity tests in animals and humans.[12,13]

Therefore, the study aimed to evaluate the phototoxic potential of the black, blue, and red colors of three different commercially available tattoo ink brands that are widely used by *in vitro* 3T3-NRU according to the Organisation for Economic Cooperation and Development (OECD) 432 guideline.

MATERIALS AND METHODS

Cell culture

The BALB/c 3T3 fibroblasts were purchased from ATCC. The cells were cultured in Dulbecco's modified Eagle's medium (DMEM) supplemented with 10% heat-inactivated fetal bovine serum (FBS) and 1x antibiotic-antimycotic solution (all from Gibco) in a humidified atmosphere at 37°C.

Test compounds

The black, red and blue colors of three commercially available tattoo inks were used for the tests. Black-triple black, red-lipstick red, blue-muter earth (Eternal Tattoo Supply, Brighton, MI, USA), black-true black, red-bright red, blue-mario's light blue (Intenze Products Inc. NJ, USA), black, red, blue (Tang Dragon Tattoo, China) was used. Chlorpromazine was used as the positive control (Eczacıbaşı, Turkey).

The absorption spectrum of the tattoo inks

Before starting the phototoxicity test, the absorption spectra of the tattoo inks were measured in the 250-700 nm range (Epoc, Biotek). For this purpose, tattoo inks were dissolved in DMEM medium without phenol red at 1% final concentration, and this diluent was used as blank.

Photosensitivity of the BALB/c 3T3 fibroblasts

To determine the photosensitivity of the cells, the BALB/c 3T3 fibroblasts were seeded on clear 96-well plates at a seeding density of $1x10^4$ in DMEM without phenol red containing 10% FBS and 1x antibiotic antimycotic solution. The day after, cells were irradiated with 0-2.5-5-10-15 joule/cm^2 of UVA radiation. The UVA sensitivity of the cells was evaluated with NRU cell viability assay after 24 h, as mentioned in detail below.

Neutral red uptake phototoxicity assay

The BALB/c 3T3 fibroblast NRU assay was carried out as described using the OECD 432 guideline with minor modifications.[13] Extra washing steps due to the high coloring of tattoo inks were added to the assay. Briefly, the BALB/c 3T3 cells were seeded on clear 96-well plates at a seeding density of $1x10^4$ in DMEM without phenol red with 10% FBS and 1x antibiotic antimycotic solution (assay medium). After culturing the cells in the plate for 24 h, wells were washed with 1x PBS. Briefly, eight logarithmic dilution series of tattoo inks starting from 200 µg/mL to 1 µg/mL with assay medium was prepared. The prepared concentrations of tattoo inks were added to wells and allowed to incubate for 1 h. 2 different sets of plates (-UV and +UV) were prepared for the assay. Then, +UV plates were irradiated with 5 joule/cm^2 of UVA radiation from a Philips PL-L UVA lamp in a home-designed and constructed wooden box. UVA radiation calculation was made with a UVA light meter (lutron UVA-365SD, Taiwan). While +UV plates were irradiating, the -UV plates were kept in the dark. After irradiation, the solutions were discarded, and wells were washed with 1x PBS. Then, the cells were allowed to incubate overnight with the assay medium. To determine the phototoxic effects of the tattoo inks, the medium was replaced with 50 µg/mL-neutral red in assay medium and incubated for 3 h in a humidified atmosphere at 37°C. Then, the medium was discarded, and the uptaken neutral red was dissolved with a mixture of acetic acid, water and ethanol (1:49:50). The absorbance was read at 540 nm with a plate reader. Then, the phototoxicity of the tattoo inks was evaluated with Phototox version 2.0 software (ZEBET

Germany) by calculating the photo irritation factor (PIF) and the mean photo effect (MPE). Since the tattoo ink dilutions were prepared with DMEM without phenol red with 10% FBS and 1x antibiotic antimycotic solution (assay medium) and there was not any different solvent effect on the cells, only assay medium containing wells were used as the negative control. Therefore, negative control results used in the negative control sections in the Phototox program and IC_{50}, PIF, MPE values were not calculated for negative controls. According to the OECD guideline, MPE <0.1 predicts the absence of a phototoxic effect. MPE >0.1 and 0.15 predict a probable phototoxic effect and MPE >0.15 predicts a phototoxic effect.[13]

Statistical analysis

Phototox version 2.0 software (ZEBET Germany) was used for concentration-response analysis. Results are presented as mean standard deviation of three independent experiments run in triplicate.

RESULTS

According to OECD guideline 432, a substance must show absorption in the UV/visible area to be photoreactive.[13] For this reason, absorption spectra of each ink were taken before starting the 3T3-NRU phototoxicity test. Absorption peaks of inks were found to be between 410 and 420 nm in black inks, 610-640 nm in blue inks and 560-570 nm in red inks.

Photosensitivity study results showed that increasing doses of UVA had a phototoxic effect on the BALB/c 3T3 fibroblasts. The viability of the 5 joule/cm^2 of UVA irradiated cells was 95.7%±2.36 compared with non-irradiated cells (0 joule/cm^2) and >80% viability of the cells meets the quality criteria of OECD test guideline no: 432, (Figure 1).[13] To check the accuracy of the 3T3-NRU phototoxicity test under our laboratory conditions, an experiment was performed with chlorpromazine, which was selected as a positive control, in line with OECD guidelines. According to the OECD Guideline 432, chlorpromazine should have a PIF value greater than 14.4, and the MPE value should be in the range of 0.33-0.63. The IC_{50} values for +UV and -UV

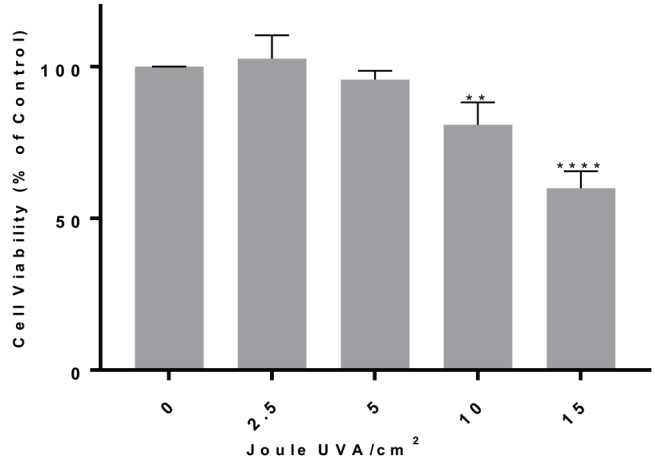

Figure 1. Photosensitivity of the BALB/c 3T3 fibroblast cells. ** p<0.01, **** p<000.1

should be 0.1-2.0 µg/mL and 7.0-90.0 µg/mL, respectively.[13] The results of the 3T3-NRU phototoxicity test with positive control showed that the PIF value for chlorpromazine is 27.7±4.2, the MPE value is 0.50±0.11, the IC_{50} values are 1.7±0.28 µg/mL at (+UV) and 47±6.9 µg/mL at (-UV). These values were found to comply with the OECD guideline 432 limits.

Tattoo inks phototoxicity evaluation with 3T3-NRU phototoxicity test is shown in Table 1. Based on our results, the red, black and blue colors of three different commercially available tattoo inks did not exhibit phototoxic potential with the 3T3-NRU phototoxicity test. The IC_{50} values could not be determined +UV and -UV conditions since tattoo inks did not show cytotoxic activity on BALB/c 3T3 cells. Consequently, PIF values could not be calculated, and MPE values were <0.1, which predicts the absence of phototoxic effect, (Table 1).

DISCUSSION

While tattooing has been practiced throughout the world for many centuries, the popularity of tattooing has increased significantly recently due to decorative reasons. Inflammatory, infectious and neoplastic complications may be seen after tattooing and a part of the beforementioned complications is related to allergy and hypersensitivity to tattoo inks.[14] Additionally, sensitivity to the sun around the tattooed area is common and 20% of individuals suffer from tattoo-associated complications.[6] Despite the increasing number of tattooed individuals, there are not sufficient toxicological and pharmacokinetic evaluations of the intradermal use of inks and colorants used for tattooing.[3]

Tattoo inks mainly contain pigments, dyes, water, solvent additives such as glycerin, alcohol, and ethylene glycol, preservatives, stabilizers, and pH regulators.[15] The coloring agents that are used in the inks can vary depending on the brand and the color.[2] The tattoo ink manufacturers not must disclose the chemical composition and exact ingredients in their inks that cause potential uncertainty in the evaluation of the toxic effects of the pigments, solvents, and binders that are used in the tattoo inks.[1]

The black tattoo inks mainly contain carbon. Besides, black tattoo inks may contain mutagenic and carcinogenic compounds such as carbon black, polyaromatic aromatic hydrocarbons (PAHs), and phenols. PAHs under UV irradiation can generate singlet oxygen, which can result in tattoo-associated complications.[15] The blue inks may contain elements such as cobalt, aluminum, copper, and it has been reported that cobalt-containing ink compositions cause more skin reactions and irritation than copper-containing ink compositions. Red tattoo inks may contain azo pigments and elements such as cadmium and iron for coloring.[16] Tattoo-related skin allergies are especially observed when red tattoo ink is used. Red tattoo-related skin allergies are supposed to be related to azo compounds.[17] The azo compounds that are used as pigments, under high energetic radiation and heat can cause the production of the aromatic amines and amines considered allergic sensitizers.[15] Also, often tattoo ink contains azo dyes with unknown compositions.[11,18] The

Table 1. Phototoxic evaluation of the red, black and blue colors of three different commercially available tattoo inks with Phototox version 2.0 software (ZEBET Germany)

Substance	IC_{50}		PIF ± SD	MPE ± SD	Evaluation
	-UV	+UV			
Clorpromazine (positive control)	47±6.9 µg/mL	1.7±0.28 µg/mL	27.7±4.2	0.50±0.11	Phototoxic
Eternal - black	-	-	1	-0.361±0.07	Non-phototoxic
Eternal - red	-	-	1	-0.351±0.02	Non-phototoxic
Eternal - blue	-	-	1	-0.229±0.01	Non-phototoxic
Intenze - black	-	-	1	-0.559±0.02	Non-phototoxic
Intenze - red	-	-	1	-0.159±0.01	Non-phototoxic
Intenze - blue	-	-	1	-0.126±0.01	Non-phototoxic
Tang dragon - black	-	-	1	-1.330±0.01	Non-phototoxic
Tang dragon - red	-	-	1	-1.155±0.04	Non-phototoxic
Tang dragon - blue	-	-	1	-0.535±0.03	Non-phototoxic

UV: Ultraviolet, PIF: Photo irritation factor, SD: Standard deviation, MPE: Mean photo effect

local metabolism of these unknown azo dyes into porphyrins may have photo-sensitizing effects on the skin.[19]

Phototoxicity describes the tissue reactions caused by light and it is the toxic response of the skin that develops due to the light exposure of a substance that is applied to the organism systemically or subcutaneously.[13] The phototoxic reactions are characterized by skin irritation or exaggerated sunburn-like symptoms such as erythema, tenderness, pruritus and edema in patients.[20]

The NRU test is based on the retention of the NRU dye in the viable cell's lysosomes, and the amount of the dye in the lysosomes is proportional to the cell viability.[21] However the alterations in the lysosomal membranes may affect the NRU test results and when the NRU test is used to evaluate the toxicity of substances that specifically target lysosomes, results may indicate artificially high cytotoxicity. This can be considered the main limitation of the NRU test for cytotoxicity studies.[22,23] The 3T3-NRU phototoxicity test is a validated and regulatory accepted test for predicting phototoxicity.[13] Therefore, the study aimed to evaluate the phototoxic potential of the black, blue and red colors of the most widely used three different commercially available tattoo ink brands by *in vitro* NRU phototoxicity test according to OECD 432 guideline. It has been reported that red, blue, and black tattoos cause more sun-related complaints than other colors.[19] A clear relationship between having tattoos and skin cancer development has not established today. There are case reports of the development of cancer types such as melanoma, basal cell carcinomas, squamous cell carcinomas, and keratoacanthomas in persons with tattoos. However, these cancer developments are most likely not only a result of having a tattoo but multifactorial.[24,25]

Our results showed that the black, blue and red colors of three different commercially available brands were not phototoxic by *in vitro* NRU phototoxicity test while the chlorpromazine (positive control) result was within the range recommended by OECD 432 guideline.

A recent study was conducted to evaluate the phototoxic effects of different tattoo pigments. In this study, cadmium sulfide, carbazole, cadmium selenide, mercury (II) sulfide, chromium oxide, and cobalt aluminate were examined using the 3T3-NRU phototoxicity test and 3D human reconstructed skin model. The results of this study showed that only carbazole and cadmium sulfide exhibited phototoxicity potential with the 3T3-NRU phototoxicity test, and this result could only be confirmed for carbazole with the 3D human skin model.[26] Similar to our study, the findings of this study do not address the phototoxicity potential of red [cadmium selenide and mercury (II) sulfide] and blue (cobalt aluminate) pigments.

Regensburger et al.[27] studied the 20 well-known PAHs content of 19 commercially available black tattoo inks. Many PAHs have been shown to be carcinogenic and have mutagenic activity. Furthermore, under UV irradiation they can generate singlet oxygen, which can contribute the tattoo-associated complications.[18,28,29] In the study, they evaluated the phototoxicity of PAH extracts from black tattoo inks through mitochondrial activity in human keratinocytes and found that some extracts caused singlet oxygen generation with UVA irradiation which might be indicative of phototoxic reactions.[27]

Another study is conducted to make *in vitro* and *in vivo* toxicological evaluations of the blue, green, red and black tattoo inks. According to the study, the red and green tattoo inks showed higher *in vitro* and *in vivo* toxicity due to containing azo compounds while black tattoo ink was found to be the safest.[30] Wamer and Yin[31] evaluated cytotoxic and photocytotoxic activity of eighteen TiO_2 containing permanent makeup inks in human dermal fibroblasts as inhibition of colony formation. They did not determine cytotoxicity among inks but did observe

eight inks were phototoxic under UVA irradiation. It has been reported that the higher the PIF values obtained from the 3T3-NRU phototoxicity test results in the higher the probability of finding phototoxic *in vivo*. Thus, guideline thresholds should be reconsidered for the better translation of the results to *in vivo.* Additionally, the lack of a barrier system is a known limitation of the 3T3-NRU phototoxicity test for testing topical agents.[32]

CONCLUSION

In conclusion, our study results do not indicate the phototoxic potential of examined black, blue, and red colors of three different commercially available brands. However, the 3T3-NRU phototoxicity test results should be verified by other phototoxicity test methods to evaluate the phototoxicity of tattoo inks correctly. Also, it should be considered that the data obtained because of the phototoxicity test do not provide information about other toxicological properties of tattoo inks. However, evidence from some studies suggests that tattoo ink compositions are variable, and some of this ink compositions can cause cytotoxic and phototoxic reactions. Thus, it is crucial to have better regulations on tattoo ink compositions to minimize their risk of complications.

Conflict of interest: No conflict of interest was declared by the authors. The authors are solely responsible for the content and writing of this paper.

REFERENCES

1. Grant CA, Twigg PC, Baker R, Tobin DJ. Tattoo ink nanoparticles in skin tissue and fibroblasts. Beilstein J Nanotechnol. 2015;6:1183-1191.
2. Dirks M. Making innovative tattoo ink products with improved safety: possible and impossible ingredients in practical usage. Curr Probl Dermatol. 2015;48:118-127.
3. Laux P, Tralau T, Tentschert J, Blume A, Dahouk SA, Bäumler W, Bernstein E, Bocca B, Alimonti A, Colebrook H, de Cuyper C, Dähne L, Hauri U, Howard PC, Janssen P, Katz L, Klitzman B, Kluger N, Krutak L, Platzek T, Scott-Lang V, Serup J, Teubner W, Schreiver I, Wilkniß E, Luch A. A medical-toxicological view of tattooing. Lancet. 2016;387:395-402.
4. Lerche CM, Heerfordt IM, Serup J, Poulsen T, Wulf HC. Red tattoos, ultraviolet radiation and skin cancer in mice. Exp Dermatol. 2017;26:1091-1096.
5. Mang R, Stege H, Krutmann J. Mechanisms of phototoxic and photoallergic reactions in Contact Dermatitis (5th ed). Berlin; Springer. 2011;6:97-104.
6. Serup J, Niels H, Linnet JT, Møhl B, Olsen O, Westh H. Tattoos—health, risks and culture. With introduction of the" seamless prevention" strategy. Copenhagen: The Council on Health and Disease Prevention. 2015.
7. Union P. Regulation (EC) no 1223/2009 of the European Parliament and of the Council. The OJEU. 2009;342:59.
8. EC (European Commission). Full EU ban on animal testing for cosmetics enters into force. Press release. 2013.
9. Sreedhar D, Manjula N, Pise SA, Ligade V. Ban of cosmetic testing on animals: a brief overview. Int J Cur Res Rev. 2020;12:113-116.
10. Vinken M. 3Rs toxicity testing and disease modeling projects in the European Horizon 2020 research and innovation program. EXCLI J. 2020;19:775-784.
11. Liebsch M, Spielmann H, Pape W, Krul C, Deguercy A, Eskes C. UV-induced effects. Altern Lab Anim. 2005;(Suppl 1):131-146.
12. Spielmann H, Balls M, Dupuis J, Pape WJ, Pechovitch G, de Silva O, Holzhütter HG, Clothier R, Desolle P, Gerberick F, Liebsch M, Lovell WW, Maurer T, Pfannenbecker U, Potthast JM, Csato M, Sladowski D, Steiling W, Brantom P. The International EU/COLIPA In Vitro Phototoxicity Validation Study: Results of Phase II (Blind Trial). Part 1: the 3T3 NRU phototoxicity test. Toxicol In Vitro. 1998;12:305-327.
13. OECD. Test Guideline 432: *In Vitro* 3T3 NRU Phototoxicity Test. OECD Guidel Test Chem. 2019.
14. Juhas E, English JC 3rd. Tattoo-associated complications. J Pediatr Adolesc Gynecol. 2013;26:125-129.
15. Savitha AS. Composition of Tattoo. TATTOO-The Invaluable Compendium for Dermatologists. New Delhi; The Health Sciences; 2017;24.
16. Forte G, Petrucci F, Cristaudo A, Bocca B. Market survey on toxic metals contained in tattoo inks. Sci Total Environ. 2009;407:5997-6002.
17. Serup J. Seamless prevention of adverse events from tattooing: integrated strategy emphasising the customer-tattooist interaction. Curr Probl Dermatol. 2015;48:236-247.
18. Shinohara MM. Complications of decorative tattoo. Clin Dermatol. 2016;34:287-292.
19. Hutton Carlsen K, Serup J. Photosensitivity and photodynamic events in black, red and blue tattoos are common: A 'Beach Study'. J Eur Acad Dermatol Venereol. 2014;28:231-237.
20. Kim K, Park H, Lim KM. Phototoxicity: Its Mechanism and Animal Alternative Test Methods. Toxicol Res. 2015;31:97-104. Erratum in: Toxicol Res. 2015;31:321.
21. Repetto G, del Peso A, Zurita JL. Neutral red uptake assay for the estimation of cell viability/cytotoxicity. Nat Protoc. 2008;3:1125-1131.
22. Clothier R. The FRAME modified neutral red uptake cytotoxicity test. Invittox Protocol (3a). 1991.
23. Cudazzo G, Smart DJ, McHugh D, Vanscheeuwijck P. Lysosomotropic-related limitations of the BALB/c 3T3 cell-based neutral red uptake assay and an alternative testing approach for assessing e-liquid cytotoxicity. Toxicol In Vitro. 2019;61:104647.
24. Høgsberg T, Loeschner K, Löf D, Serup J. Tattoo inks in general usage contain nanoparticles. Br J Dermatol. 2011;165:1210-1218.
25. Kluger N, Phan A, Debarbieux S, Balme B, Thomas L. Skin cancers arising in tattoos: coincidental or not? Dermatology. 2008;217:219-221.
26. Kim SY, Seo S, Choi KH, Yun J. Evaluation of phototoxicity of tattoo pigments using the 3 T3 neutral red uptake phototoxicity test and a 3D human reconstructed skin model. Toxicol In Vitro. 2020;65:104813.
27. Regensburger J, Lehner K, Maisch T, Vasold R, Santarelli F, Engel E, Gollmer A, König B, Landthaler M, Bäumler W. Tattoo inks contain polycyclic aromatic hydrocarbons that additionally generate deleterious singlet oxygen. Exp Dermatol. 2010;19:e275-e281.
28. Bao L, Xu A, Tong L, Chen S, Zhu L, Zhao Y, Zhao G, Jiang E, Wang J, Wu L. Activated toxicity of diesel particulate extract by ultraviolet a radiation in mammalian cells: role of singlet oxygen. Environ Health Perspect. 2009;117:436-441.

29. Nisbet ICT, LaGoy PK. Toxic equivalency factors (TEFs) for polycyclic aromatic hydrocarbons (PAHs). Regul Toxicol Pharmacol. 1992;16:290-300.

30. Arl M, Nogueira DJ, Schveitzer Köerich J, Mottim Justino N, Schulz Vicentini D, Gerson Matias W. Tattoo inks: Characterization and *in vivo* and *in vitro* toxicological evaluation. J Hazard Mater. 2019;364:548-561.

31. Wamer WG, Yin JJ. Photocytotoxicity in human dermal fibroblasts elicited by permanent makeup inks containing titanium dioxide. J Cosmet Sci. 2011;62:535-547.

32. Ceridono M, Tellner P, Bauer D, Barroso J, Alépée N, Corvi R, De Smedt A, Fellows MD, Gibbs NK, Heisler E, Jacobs A, Jirova D, Jones D, Kandárová H, Kasper P, Akunda JK, Krul C, Learn D, Liebsch M, Lynch AM, Muster W, Nakamura K, Nash JF, Pfannenbecker U, Phillips G, Robles C, Rogiers V, Van De Water F, Liminga UW, Vohr HW, Wattrelos O, Woods J, Zuang V, Kreysa J, Wilcox P. The 3T3 neutral red uptake phototoxicity test: practical experience and implications for phototoxicity testing--the report of an ECVAM-EFPIA workshop. Regul Toxicol Pharmacol. 2012;63:480-488.

Turk J Pharm Sci 2022;19(1):76-83
DOI: 10.4274/tjps.galenos.2021.86422

ORIGINAL ARTICLE

Essential Oil Content, Antioxidative Characteristics and Enzyme Inhibitory Activity of *Sideritis akmanii* Aytaç, Ekici & Dönmez

Sideritis akmanii Aytaç, Ekici & Dönmez Uçucu Yağ İçeriği, Antioksidatif Özellikleri ve Enzim İnhibitör Aktivitesi

Laçine AKSOY, İsmail GÜZEY, Mürüvvet DÜZ*

Afyon Kocatepe University, Faculty of Science and Arts, Department of Chemistry, Afyonkarahisar, Turkey

ABSTRACT

Objectives: Our research measures the essential oil analysis mineral substance profiles, total phenolic substance content, free radical scavenger properties, antioxidant capacity, and enzyme inhibitory activity of *Sideritis akmanii* Aytaç, Ekici & Dönmez, 1996.

Materials and Methods: A mixture of *S. akmanii* plant roots and stems were used. Essential fatty acid components of *S. akmanii* were determined by gas chromatography-mass spectrometry and bioelement concentrations by inductively coupled plasma optical emission spectrometry. The antioxidant activity of extracts was screened by 2,2-diphenyl-1-picrylhydrazyl (DPPH) radical scavenging activities, total phenolic content, total antioxidant status (TAS), total oxidant status (TOS) analysis. Cholinesterase (ChE), α-glucosidase, α-amylase, and tyrosinase inhibitory activity was determined.

Results: The results demonstrated that the phenolic substance content was higher in methanol extract (144.08±2.01 µg gallic acid equivalent/mg extract). DPPH scavenging effect of *S. akmanii* methanol extract (73.2%) was higher than acetone extract (60.1%). TAS values of extract methanol and acetone were 2.32±0.4 and 2.38±0.2 µmol trolox Eq/g, TOS values were 4.88±0.6 and 5.04±0.5 µmol H_2O_2 Eq/g, and oxidative stress index values were 2.1±0.3 and 2.11±0.24 arbitrary units, respectively. Hexadecanoic acid (17.9%) was found as the main component in the plant essential oil. *S. akmanii* species was prominent with high Mg and Al concentrations. Anti-ChE activity was determined that acetone extract (42.95%±0.90; 217.37±0.81 mg galantamine equivalents [(GALAEs)/g] exhibited higher than methanol (33.33%±1.81; 208.76±1.62 mg GALAE/g). α-Amylase inhibition was high in methanol extract [53.62±1.85 mmol angiotensin converting enzymes (ACEs)/g extract] compared to acetone (47.73±0.92 mmol ACEs/g extract). The tyrosinase inhibitory activity of *S. akmanii* was determined very low inhibition of the reference compound.

Conclusion: It has been determined that *S. akmanii* Aytaç, Ekici & Dönmez extracts have antioxidant properties and can inhibit acetylcholinesterase, α-glucosidase, α-amylase enzymes. This study is informative on future studies on *S. akmanii* a highly bioavailable species and very extensive studies should be carried out.

Key words: *Sideritis akmanii* Aytaç, Ekici & Dönmez, antioxidative activity, bioelement, essential oil, enzyme inhibitory activity

ÖZ

Amaç: Çalışmamız *Sideritis akmanii* Aytaç, Ekici ve Dönmez, 1996'nın antioksidan kapasitesini, toplam fenolik madde içeriğini, serbest radikal temizleyici özelliklerini, mineral madde profillerini, enzim inhibitör aktivitesini ve uçucu yağ analizini belirlenmiştir.

Gereç ve Yöntemler: *S. akmanii* bitki kökleri ve saplarından oluşan bir karışım kullanılmıştır. Bitkinin temel yağ asidi bileşenleri gaz kromatografisi-kütle spektrometresi ve bioelement konsantrasyonları indüktif eşleşmiş plazma optik emisyon spektrometresi ile belirlenmiştir. Metanol ve aseton ekstresinin antioksidan aktivitesi, 2,2-difenil-1-pikrilhidrazil radikali süpürücü etkisi, toplam fenolik içerik, toplam antioksidan durumu (TAS), toplam oksidan durumu (TOS) analizi ile incelenmiştir. Kolinesteraz (ChE), α-amilaz, α-glukozidaz, tirozinaz inhibitör aktivitesi belirlenmiştir.

Bulgular: Sonuçlar, metanol ekstresinde fenolik madde içeriğinin daha yüksek olduğunu göstermiştir. (144,08±2,01 µg gallik asit eşdeğeri/mg ekstre). *S. akmanii* metanol ekstresinin radikal süpürücü etkisi (%73,2) aseton ekstresinden (%60,1) daha yüksek bulunmuştur. Metanol ve aseton ekstrelerinin sırasıyla TAS değerleri 2,32±0,4 ve 2,38±0,2 µmol trolox Eq/g, TOS değerleri 4,88±0,6 ve 5,04±0,5 µmol H_2O_2 Eq/g ve oksidatif stres indeks değerleri 2,1±0,3 ve 2,11±0,24'tür. Uçucu yağda hekzadekanoik asit (%17,9) ana bileşen olarak tespit edilmiştir. *S. akmanii* türleri yüksek Mg

*Correspondence: duzmuruvvet@gmail.com, Phone: +90 506 298 05 18, ORCID-ID: orcid.org/0000-0001-7339-9858

Received: 26.03.2021, Accepted: 25.06.2021

ve Al konsantrasyonları ile öne çıkmıştır. Anti-ChE aktivitesi, aseton ekstresinin (%42,95±0,90; 217,37±0,81 mg GALAEs/g) metanol ekstresinden (%33,33±1,81; 208,76±1,62 mg GALAE/g) daha yüksek olduğu belirlenmiştir. α-amilaz inhibisyonu, aseton ekstresi ile [47,73±0,92 mmol anjiyotensin dönüştürücü enzim (ACE/g) ekstre] karşılaştırıldığında metanol ekstresinde (53,62±1,85 mmol ACE/g ekstre) daha yüksek tespit edilmiştir. *S. akmanii*'nin tirozinaz inhibe edici aktivitesi, referans bileşiğe göre çok düşük inhibisyon gösterdiği belirlenmiştir.

Sonuç: *S. akmanii* ekstrelerinin antioksidan özelliklere sahip olduğu ve asetilkolineesteraz, α-glukozidaz, α-amilaz enzimlerini inhibe edebildiği tespit edilmiştir. Bu çalışma, biyoyararlanımı yüksek bir tür olan *S. akmanii* ile ilgili gelecekte yapılacak çalışmalar hakkında bilgilendirici nitelikte olup, hücre kültürü ve hayvan deneylerini içeren çok kapsamlı çalışmaların yapılması gerekmektedir.

Anahtar kelimeler: *Sideritis akmanii* Aytaç, Ekici & Dönmez, antioksidatif aktivite, bioelement, uçucu yağ, enzim inhibitör aktivite

INTRODUCTION

Sideritis akmanii Aytaç, Ekici & Dönmez is an aromatic herbaceous plant with light green leafs and can grow up to 1 meter high. On the top, there are mucronate leaves and the leaves are 0.5 mm thick with a yellowish color. *Sideritis* species commonly known as mountain tea and clary has been used since ancient times in medicine due to their antibacterial, antifungal, antiviral, antiseptic, analgesic, antispasmodic, carminative, and antidiabetic properties. It is not exported and mostly used in the domestic market in Turkey. It is an endangered species due to its use in grazing and gathering in large quantities for animal feed production. Thus, the preservation and culturing of this economically significant species is necessary.[1]

The enzyme inhibition theory is very popular in the treatment strategies for universal health problems such as diabetes and Alzheimer's. According to this theory, the key enzymes that affect the pathology of diseases are inhibited to alleviate symptoms caused by disease.[2] α-Amylase and α-glucosidase enzymes are the main enzymes of sugar metabolism and their activity increases blood glucose level. In this sense, inhibition of these enzymes is an important mechanism in the control of blood glucose level in diabetes.[3] Tyrosinase is an oxidase that is the rate-limiting enzyme for controlling the production of melanin and the inhibition of this enzyme is the main way of controlling skin diseases.[4] Acetylcholine esterase catalyzes the breakdown of acetyl and choline in the synaptic space. Increased cognitive functions by inhibiting this enzyme in Alzheimer's patients and this are called a cholinergic hypothesis.[5]

This study determined determine the essential oil analysis mineral substance profiles, total phenolic substance content, free radical scavenger properties, antioxidant capacity, and enzyme inhibitory activity of methanol and acetone extracts of *S. akmanii* collected at Kumalar Mountain in Afyon province in Turkey.

MATERIALS AND METHODS

Plant material

S. akmanii was collected at 1880 m altitude at Kumalar Mountain, Çakmaktepe Pass, Şuhut/Afyonkarahisar (37 T 0719245, UTM 4511056) in August 2015, and it was identified by Dr. Mustafa Kargıoğlu. The samples of the plant locally known as "tail tea" are stored at Afyon Kocatepe University, Faculty of Sciences and Literature herbarium.

Preparation of extracts

A mixture of *S. akmanii* roots and stems were used. These parts were crushed into small pieces and dried at ambient temperature in the shade. To prepare the extracts, 20 g *S. akmanii* powder was mixed with 400 mL solvent.[6] Extracts were used to determine free radical scavenging activity and total phenolic content. For the antioxidant status analysis, 1 g dried and pulverized plant was sonicated after adding 10 mL solvent. The product was then filtered through paper and centrifuged. The obtained supernatant was centrifuged again for use in the analyses.[7] To determine *S. akmanii* mineral substance content, 0.5 g dried and pulverized plant was placed in a microwave to decompose the organic components.[8] Preparation of plant ethanol extracts for enzyme inhibition analysis was prepared at 100 µg/mL concentration. Acetone and methanol extracts were prepared by dissolving in ethanol for enzyme inhibition analyzes. 10 mg (0.01 g) of the extract was first dissolved in 1 mL ethanol and a 10 mg/mL stock was prepared. 100 µg/mL extracts were prepared from stock material.

Isolation of essential oil

For the extraction of essential oils from *S. akmanii* by hydrodistillation using a Clevenger type apparatus in 2.5 h. At the end of the distillation, the essential oil was collected, dried under anhydrous Na_2SO_4 and stored at 4°C in the dark until analysis.

Determination of 2,2-diphenyl-1-picrylhydrazyl (DPPH) radical scavenging activity

The DPPH radical scavenging activities of methanol and acetone extracts from root and stem parts of *S. akmanii* species were determined by the Blois[9] method. DPPH was used as free radical. Ethanol was added to samples at concentrations of 45, 90, and 135 µg/mL. Stock DPPH was added to the samples and allowed to incubate for 30 min in the dark and at room temperature. Absorbance measurements were recorded at 517 nm against ethanol blank.

Determination of total phenolic content

Total phenolic content of the extracts was determined using the Folin-Ciocalteu method. Folin-Ciocalteu reagent was added to the plant extracts and standard antioxidant solutions. Samples were stored in room for 2 h with the addition of Na_2CO_3. Absorbance measured against water at 760 nm.[10] The graph was plotted using the gallic acid standard. The total number of phenolic compounds in both extracts was calculated as gallic acid equivalent (GAE) using the formula obtained from the

graph (r^2: 0.9881). The standard gallic acid graph developed for this purpose is presented in Figure 1.

Total antioxidant status (TAS), total oxidant status (TOS) and oxidative stress index values (OSI)

Total antioxidant and TOS of *S. akmanii* was measured using commercial kits (Rel Assay, Gaziantep, Turkey).[7] The OSI index as an indicator of oxidative stress was calculated by dividing the TOS by the TAS.

Determination of the mineral substance content

A microwave oven (Speed Wave ERGHOF) was used to deform the organic compounds in the samples. Inductively coupled plasma-optical emission spectrometry (Spectro Genesis) bioelement concentrations were measured after the samples were ready for analysis.[8]

Gas chromatography-mass spectrometry (GC-MS) analysis

Volatile components in the 1 mL sample injected into the system were determined on the GC-MS device. The analysis conditions of the device are given in Table 1.

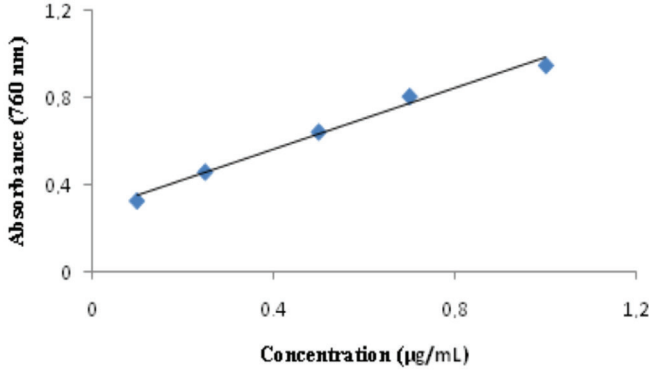

Figure 1. Gallic acid standard curves

Table 1. GC-MS analysis conditions

Features	Description
System	Agilent 7890 B GC5977B mass selective dedector system
Column	Agilent HP-Innowax (60 m, 0.25 mm inner diameter, 0.25 m film thickness)
Injection temperature	250°C
Ion source temperature	230°C
Ionization mode hand	E1
Electron energy	70 ev
Mass range	35-450 *m/z*
The temperature program	60°C (10 min), 4°C/min 220°C (10 min) 1°C/min 240°C (20 min)
Carrier gas	Helium (0.7 mL/min)
Definitions spectral database	Wiley 9-nist 11 nass

GC-MS: Gas chromatography-mass spectrometry

Enzyme inhibitory activity

Ellman method was used to determine the cholinesterase (ChE) inhibitory activity of the extracts and in a 96-well microplate using ELISA reader.[11] Sample solution (100 µg/mL, 50 µL) was mixed with DTNB (0,3 mM, 125 µL) and acetyl choline esterase (AChE) solution (0,026 U/mL, 25 µL) in Tris-HCl buffer (pH: 8.0) in a 96-well microplate and incubated for 15 min at 25°C. The reaction was initiated by the addition of 1.5 mM 25 µL of acetyl thio quinoline iodide substrate. Similarly, enzyme-free tube was prepared as a blank. Control sample for % inhibition calculation was prepared by the addition of ethanol instead of the sample. Sample, control, and blank absorbances were read at 405 nm after incubation at 25°C for 10 min. Galantamine was used as standard. Standard sample solutions of 0.5-0.0005 µmol/mL were prepared and the calibration graph is plotted. Results was expressed both equivalents of galanthamine (mg GALAEs/g extract) and % inhibition value. Equality is given below to calculate the percent inhibition value.

$\% I = (A_{control} - A_{sample})/A_{control} \times 100$

$A_{control}$: Absorption obtained by adding solvent used instead of plant extract

A_{sample}: absorbance of plant extract

α-amylase inhibitory activity was performed using Caraway-Somogyi iodide/potassium iodide (IKI) method.[12] Sample solution at 100 µg/mL concentration (25 µL) was mixed with α-amylase solution (50 µL) in phosphate buffer (pH 6.9 with 6 mM sodium chloride) in a 96-well microplate and incubated for 10 min at 37°C. After the pre-incubation, the reaction was started by adding 50 µL of 0.05% starch solution. Similarly, the enzyme-free blank solution and control samples containing solvent were prepared instead of samples. The reaction was stopped by the addition of HCl (25 µL, 1 M) and IKI solution (100 µL) was added. Acarbose was used as standard material.

Standard sample solutions of 2 µmol/mL, 1 µmol/mL, 0.1 µmol/mL, 0.01 µmol/mL, and 0.001 µmol/mL were prepared and a calibration graph was drawn. The results of α-amylase inhibitory activity were expressed as equivalent to both acarbose equivalent (mmol AKAE/g) and the % inhibition value used for the calculation.

α-Glucosidase inhibitory activity was performed according to the method.[13] Sample solution (100 µg/mL extracts, 50 µL) was mixed with glutathione (2 mg/mL, 50 µL), α-glucosidase solution (2 µ/mL, 50 µL) in phosphate buffer (pH 6.8) and 4-nitrofenil β-D-glukuronid (10 mM, 50 µL) in a 96-well microplate. Similarly, enzyme-free blank solution and control samples containing solvent instead of the sample were prepared. The reaction was stopped by adding 50 µL of 0.2 M Na_2CO_3 after incubating for 15 min at 37°C. Results was expressed to both acarbose (mmol AKAE/g) and the % inhibition value.

Dopacrome method modified with L-3.4-dihydroxyphenylalanine (L-DOPA) as substrate was used for determination of tyrosinase inhibitory activity.[14] Extracts were dissolved in 50% dimethyl sulfoxide and prepared at a concentration of 100 µg/mL. 40 µL of the sample solution, 20 µL of 480 µ/mL tyrosinase enzyme solution and 120 µL of phosphate buffer (20 mM pH 6.8

sodium phosphate buffer) were mixed in a 96-well microplate and incubated at 25˚C for 15 min. The reaction was initiated by addition of 20 µL of 2.5 mM L-DOPA. Control sample for % inhibition calculation prepared by the addition of ethanol instead of the sample. Samples and blank absorbances were read at 492 nm. Results are expressed as equivalent to both kojic acid (mg KAE/g) and % inhibition value.

Statistical analysis

The mean of four separate analysis results were presented as analysis results. The statistical analysis was performed using the software SPSS 15.0 (SPSS Inc.) and findings were recorded as mean ± standard deviation.

RESULTS AND DISCUSSION

S. akmanii is a perennial species that grows at 1520-1550 m high steppes. The species flowers in July and August. It is collected to Kumalar Mountains in Afyonkarahisar province. *S. akmanii* species is in the endangered species category due to overgrazing and consumption as herbal tea.

Total phenolic substance content

Phenolic compounds had anti-oxidative, free radical scavenging, enzymatic activity regulating, cell proliferation inhibitive, anti-inflammatory properties in previous studies.[15] *Sideritis* species are also a rich source of flavonoids. Major flavonoids found in *Sideritis* species were flavones, methoxyflavones, sideroflavones, cirsiliol and xanthomycin. Phytochemical studies on *S. akmanii* species reported sideridiol, sideroxol, linearol, isolinearol, folanol, and isofiolol content.[16,17]

The total phenolic content in the plants used in the study is presented in Table 2. As observed in Table 2, it was determined that *S. akmanii* plant methanol and acetone extract phenolic compound content was 144.08±2.01 and 117.72±6.4 µg GAE. We observed that the phenolic compounds in the plant and solvents used in the determination of antioxidant activity led to different results. It was found that the plant acetone extract contained higher phenolic compound levels compared to the methanol extract. This finding also provides information on higher antioxidant capacity due to the higher phenolic content of the species due to the procedures that would be conducted with an adequate solvent.

DPPH radical scavenging activity

The DPPH method is often used to determine radical scavenging activities of plants. There are also studies conducted with *Sideritis* species in the literature. A comprehensive study that all *Sideritis* species had high antioxidant and DDPH radical scavenging properties due to their high phenolic substance content.[18] *Sideritis caesarea*, which has a higher total phenolic substance and flavonol content, had DPPH radical scavenging properties.[19] In previous studies, it was determined that the high radical scavenging effect of methanol extracts was associated with the total amount of phenolic substance content in methanol extracts. Similarly, in this study, it was found that the radical scavenging properties of this extract were higher due to its high phenolic content.

Table 2. Total phenolic compound content in 1 mg *S. akmanii* methanol and acetone extracts

Extract	SAM	SAA
Total phenolic compound content (µg GAE/mg extract)	144.08±2.01	117.72±6.4

The results are presented as mean ± SD (n=4). SAM: *Sideritis akmanii* methanol extract, SAA: *Sideritis akmanii* acetone extract

DPPH radical scavenging activities of *S. akmanii* methanol and acetone extracts are presented in Figure 2. We observed that the DPPH radical scavenging activities of the extracts increased with the concentration. The DPPH radical scavenging activities of *S. akmanii* methanol and acetone extracts and the synthetic antioxidant butylated hydroxytoluene (BHT) and α-tocopherol and 135 µg/L concentration of the natural antioxidant α-tocopherol were determined as follows: α-Tocopherol > *S. akmanii* methanol extract (SAM) ~ BHT > *S. akmanii* acetone extract (SAA). The DPPH radical scavenging activities of *S. akmanii* methanol and acetone extracts were 78.7% in α-tocopherol, 73.2% in methanol extract, 72.7% in BHT and 60.1% in acetone extract. Results suggested that the SAM had similar activities with BHT.

TAS, TOS and OSI values

There are several methods to determine the total antioxidant activities in plant extracts or active substances isolated from plants.[20] Solitary measurement of antioxidants requires time consuming, expensive and complex techniques. For this reason, total antioxidant capacity or TAS measurement is the currently preferred and widely used methodology. TAS; TOS and OSI values for *S. akmanii* plant methanol and acetone extracts are presented in Figure 3. It was determined that *S. akmanii* plant methanol and acetone extract TAS values were 2.32±0.4 and 2.38±0.2 µmol trolox Eq/g, TOS values were 4.88±0.6 and 5.04±0.5 µmol H_2O_2 Eq/g, and OSI values were 2.1±0.3 and 2.11±0.24 arbitrary units, respectively. These results demonstrated that TAS values were similar in both plant

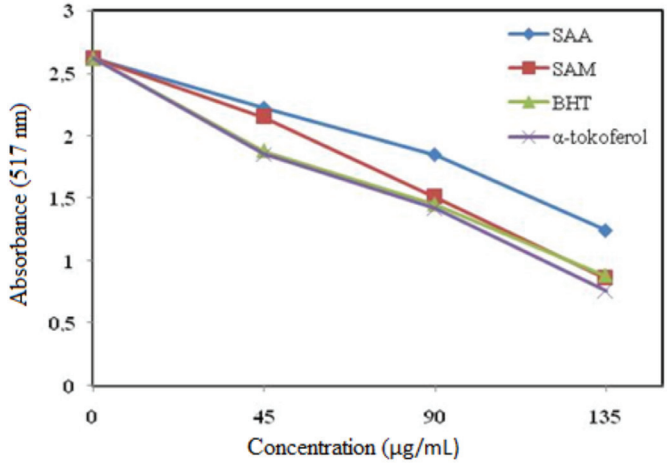

Figure 2. DPPH radical scavenging activities of plant extracts in different concentrations (45-135 µg/mL)

SAM: *Sideritis akmanii* methanol extract, SAA: *Sideritis akmanii* acetone extract, BHT: Butylated hydroxytoluene and α-tocopherol

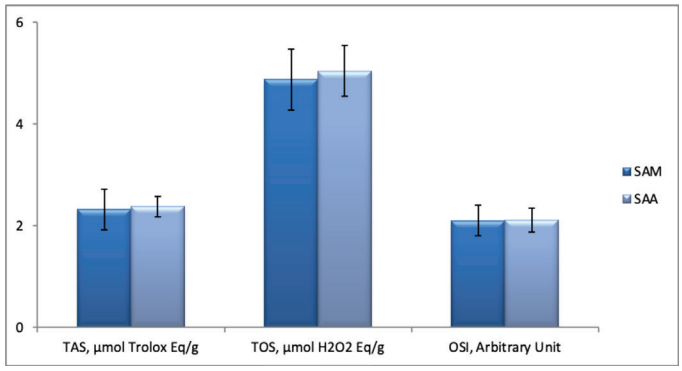

Figure 3. TAS, TOS and OSI data for *Sideritis akmanii*. The results are presented as mean ± SD (n=4)

SAM: *Sideritis akmanii* methanol extract, SAA: *Sideritis akmanii* acetone extract, TAS: Total antioxidant status, TOS: Total oxidant status, OSI: Oxidative stress index, SD: Standard deviation

extracts. The acetone extract TOS level was higher compared to the methanol extract, however it was found that the OSI, which is an indicator of the oxidative stress, was similar for both extracts.

Sideritis akmanii mineral substance content

In a study that determined the bio-element content in endemic *Sideritis* species (*S. germanico politana, S. galatica*, and *S. hispana*), it was determined that the heavy metal concentrations in *Sideritis* species were within the limits for human consumption without health risks and *Sideritis* species indigenous to Turkey could be considered a significant source for certain nutritional elements such as iron and potassium.[21]

In this study, the mineral substance profile of *S. akmanii* species was also examined. As is the case with other *Sideritis* species, *S. akmanii* species was prominent with high Mg and Al concentrations, in addition to Fe and K content. Furthermore, Zn, Mn and Cu concentrations in the antioxidant enzyme structure were also very high. However, since the concentration of Se element incorporated in the glutathione peroxidase structure was not within the measurable levels, it could not be recorded. Table 2 summarizes the mineral substance levels in *S. akmanii* species.

As shown in Table 3, Se, Be, and Co element concentrations were not within the detectable limits, so concentrations for these elements could not be determined. It was determined that all other minerals, which were identified as antioxidants, were observed at sufficient levels *S. akmanii* species, except Se.

GC-MS analysis results

S. akmanii collected from Afyonkarahisar province dry oil yield was determined as 0.13%. Palmitic acid (17.9%), myristic acid (11.0%) and spathulenol (8.0%) were found as the main components in the plant essential oil (Table 4).

The composition of *Sideritis* species volatile oil divided into 6 groups; rich in monoterpenes, rich in oxygenated monoterpenes, rich in sesquiterpenes, rich in oxygenated sesquiterpenes, rich in diterpenes and others.[22] Additionally, high oil yield of plants obtained from the essential oil composition monoterpene rich,

Table 3. Mineral substance and concentrations of *S. akmanii*

Mineral substance	Concentration (ppm)	Mineral substance	Concentration (ppm)
Al	891.64±46.78	K	1904.69±86.48
B	7.884±0.96	Li	0.619±0.28
Ba	31.02±0.98	Mg	907.26±35.96
Bi	3.634±0.64	Mn	32.05±3.46
Ca	1344.5±92.5	Na	461.68±28.59
Cr	2.13±0.17	Ni	1.23±0.16
Cu	6.23±1.82	Pb	3.21±0.83
Fe	1264.37±26.75	Zn	10.01±2.06

The results are presented as mean ± SD (n=4). SD: Standard deviation

Table 4. Essential oil composition of *S. akmanii*

No	Compound	Relative percentage (%)
1.	β-Burbone	0.5
2.	β-Caryophyllen	1.1
3.	α-Acoradiene	1.0
4.	Curcumen	4.5
5.	Caryophyllen oxide	5.7
6.	Hexahydrofarnesyl acetone	1.5
7.	Spatulenol	8.0
8.	Turmerol	1.3
9.	α-Bisabolol	1.5
10.	9-Geranyl-ρ-cymene	3.1
11.	Kaur-15-en	0.6
12.	Caryophylla-2(12),6-dien-5β-ol	1.3
13.	Manoyl oxide	1.3
14.	Dodecanoic acid (Lauric acid)	0.5
15.	(*E*)-9-octadecen-1-ol (*trans*-elaidyl alcohol)	0.7
16.	Tetradecanoic acid (myristic acid)	11.0
17.	8,12-epoxy-13-hydroxy-14-ene-labdien	1.1
18.	Pentadecanoic acid	0.6
19.	Hexadecanoic acid (palmitic acid)	17.9
20.	(*Z*)-Hexadecenoic acid (palmitoleic acid)	1.2
21.	(*Z*)-9-octadecenoik acid (oleic acid)	2.2

plants with low fat yield were found to be rich in sesquiterpene compounds.[23] Studies conducted with *Sideritis* genus demonstrated that the plants contain terpenes, flavonoids, iridoids, coumarins, lignans, and sterols. Diterpen and flavonoid structures are found in almost all species. It was considered that the pharmacological activity of the species originate from

these structures. While sesquiterpene and triterpene structures are uncommon in *Sideritis* species, diterpene structures are quite common. About 160 different diterpene species were found in these species.[24] Especially in Mediterranean countries (Turkey, Greece and Italy), it was observed that *Sideritis* species contained kauri diterpenes. Kauren diterpene derivatives, namely, folios, idol, linearol, sideridiol and isolinearol were identified in the species.[25-27]

In our study, the presence of pinene component in *S. akmanii* volatile oil was not detected and the presence of sesquiterpenes such as β-caryophylen (1.1%) caryophyllen oxide (5.7%) α-bisabolol (1.5%) were determined. More *ent*-kauren diterpenes are obtained from the plants grown in the Eastern Mediterranean region. Because of this study, only kaur-15-en diterpene was obtained.

Enzyme inhibitory activities

Anti-ChE activity

Alzheimer's disease (AD) is an age-related neurodegenerative disorder and the most common form of dementia in the elderly.[28] AChE inhibitors are used for treating AD and many researchers have attempted to identify novel AChE inhibitors from plant sources.[29,30] In this study, the anti-ChE activity of *S. akmanii* was investigated for the first time. It was determined that acetone extract (42.95%±0.90; 217.37±0.81 mg GALAEs/g) exhibited higher anti-ChE activity than methanol (33.33%±1.81; 208.76±1.62 mg GALAE/g) (Table 5). It has been reported that essential oil components such as oxygenated monoterpene compounds are the main agents responsible for the effect of anti-Alzheimer.[29] According to the GC-MS results, the fatty acid composition of *S. akmanii* contains terpene compounds such as β-caryophyllene and α-bisabolol. It has been reported that phenolic acids such as ferulic acid and p-coumaric acid exhibits strong anti-ChE activity in extracts.[31] Diterpenes isolated from *Sideritis arguta* showed no inhibition activity against acetylcholinesterase enzyme.[32] When our results are evaluated, AChE inhibitory activity of *S. amani* extracts perform quite well compared to the standard used galantamine. The higher activity of acetone extract than methanol reveals how the solvent used can alter the enzyme activity.

Antidiabetic activity

One of the therapeutic approaches for reducing blood sugar is to delay glucose absorption by inhibition of carbohydrate hydrolysis enzymes such as α-amylase and α-glucosidase in digestive organs.[33] Therefore, studies to develop new pharmacological agents are related to α-amylase and α-glucosidase inhibition.[5,34] It has been reported that some natural extract components containing phenolics, flavonoids and their glycosides exhibit α-glucosidase inhibitory effect. Polyphenolic compounds in plants inhibit the activity of digestive enzymes due to their ability to bind proteins.[35] Since these molecules have antioxidant effects, it is possible that the antioxidant and α-glucosidase inhibitory properties are due to their polyphenolic content.

In this study, α-amylase inhibition was high in methanol extract (53.62±1.85 mmol ACEs/g extract) compared to acetone (47.73±0.92 mmol ACEs/g extract (Table 6). Additionally, when we examined the percent inhibition, it was found that the results were very close to the acarbose and results of the methanol and acetone extracts were close to each other. α-Amylase inhibition value of the methanol extract of *Sideritis galatica*, 0.41±0.01 mmol ACEs/g, and the α-glucosidase inhibition value was 1.68±0.28 mmol ACEs/g. Simultaneously, *Sideritis galactica* petroleum ether and ethyl acetate extracts had higher α-amylase and α-glucosidase inhibition than methanol and water extracts.[13] The relatively low inhibitory potential of *Sideritis perfoliata* extracts prepared with increasing polarity.[36]

The inhibition of amylase and glucosidase enzymes close to the acarbose standard may indicate that the plant has significant potential for treating type 2 diabetes. In conclusion, it can be concluded that the species *S. akmanii*, which has antioxidant properties, may be a promising pharmacological agent for treating diabetes.

Tyrosinase inhibitory activity

Tyrosinase contains copper and is involved in melanin biosynthesis.it is also an enzyme that catalyzes the oxidation of tyrosine to DOPA and DOPA kinona.[36] Melanin plays an important role in protecting the skin from ionizing radiation such as ultraviolet. Tyrosinase has been researched for its use in the food industry along with cosmetics and agriculture for many years. Recently, its applications in the medical industry have gained considerable popularity because it affects protecting from pigmentation and other skin disorders such as vitiligo, malignant melanoma.[37] Common tyrosinase inhibitors, such as hydroquinone, kojic acid and arbutin, have some adverse effects on human health.[38]

In this study, the tyrosinase inhibitory activity of *S. akmanii* was determined *in vitro*. Methanol (4.24%±0.146) and acetone extracts (8.07%±0.29) were observed to exhibit very low inhibition of the reference compound, α-kojic acid (86.34%±1.46) (Table 7). The antityrosinase effect of the methanol extract was 80.42±0.95 mg KAE/g as the equivalent of the kojic acid, acetone extract was found as 105.42±1.91 mg KAE/g extracts. Our study is important because it is the first study on the tyrosinase enzyme inhibiting activity of *S. akmanii*. Different solvent extracts and different concentrations of the plant should be studied to determine the tyrosinase enzyme inhibition.

Table 5. Acetyl choline esterase enzyme inhibition results of *S. akmanii* methanol and acetone extract

Extract	AChE inhibition (mg GALAEs/g extract)	AChE inhibition (%)
SAM	208.76±1.62	33.33±1.81
SAA	217.37±0.81	42.95±0.90
Galantamine (0.5 µmol/mL)	-	51.28±0.01

Values expressed are means ± SD of four parallel measurements. GALAEs: Galantamine equivalents, AChE: Acetyl choline esterase, SAM: *S. akmanii* methanol extract, SAA: *S. akmanii* acetone extract

Table 6. α-Amylase and α-glucosidase enzyme inhibition results of *S. akmanii* methanol and acetone extract

Extract	α-Amylase inhibition (mmol ACAEs/g extract)	α-Amylase inhibition (%)	α-Glucosidase inhibition (mmol ACAEs/g extract)	α-Glucosidase inhibition (%)
SAM	53.62±1.85	45.39±0.22	59.23± 0.49	76.82±0.09
SAA	47.73±0.92	46.11±0.11	62.37±0.98	76.25±0.18
Acarbose (1 µmol/mL)	-	51.36±0.12	-	85.81±2.45

Results expressed are means ± SD of four parallel measurements. ACAE: Acarbose equivalent, SAM: *S. akmanii* methanol extract, SAA: *S. akmanii* acetone extract, SD: Standard deviation

Table 7. Tyrosinase enzyme inhibition results of *Sideritis akmanii* methanol and acetone extract

Extract	Tyrosinase inhibition (mg KAEs/g ekstre)	Tyrosinase inhibition (%)
SAM	80.42±0.95	4.24±0.146
SAA	105.42±1.91	8.07±0.29
Kojic acid (2 µmol/mL)	-	86.34±1.46

Values expressed are means ± SD of four parallel measurements. KAEs: Kojic acid equivalent, SAM: *Sideritis akmanii* methanol extract, SAA: *Sideritis akmanii* acetone extract, SD: Standard deviation

CONCLUSION

In conclusion, it can be suggested that *Sideritis akmanii* methanol, and acetone extracts possess antioxidant effects due to their phenolic substance content. The determined TAS, TOS and OSI values also support this suggestion. It was found that the radical scavenging activities in the methanol extract was similar to that of the synthetic antioxidant BHT and higher than that of the acetone extract. These findings indicated that the species, especially the methanol extract had antiradical effects. The mineral content of the species included important minerals (Mn, Zn, Fe, Cu) within the antioxidant enzyme structure. Due to the adverse effects of synthetic antioxidants, studies on natural antioxidant sources have increased during recent years. This is the first study to investigate the chemical composition and enzyme inhibitory potential of *S. akmanii*. As a result, methanol and acetone extracts of *S. akmanii* have enzyme inhibition activity and the data obtained will contribute to the search for new alternative drugs to be used for treating diseases such as diabetes, Alzheimer's and Parkinson's. Identification of antioxidant activities and active components in plants, identification and purification of their structures constitute the first step in these studies. Due to their total phenolic content, their effect on the radicals, TAS, TOS, OSI values and their mineral content, it is considered that *S. akmanii* could be used in phytotherapeutical studies and particularly in studies on antioxidant effect.

ACKNOWLEDGMENTS

This study was supported by the Scientific Research Projects Commission of the Afyon Kocatepe University, with the ID numbers 18. KARIYER.79 and 15.FEN.BIL.41.

Conflict of interest: No conflict of interest was declared by the authors. The authors are solely responsible for the content and writing of this paper.

REFERENCES

1. Gumuscu A, Tugay O, Kan Y. Comparison of essential oil compositions of some natural and cultivated endemic *Sideritis* species. Adv Environ Biol. 2011;5:222-226.
2. Chauhan PS, Puri N, Sharma P, Gupta N. Mannanases: microbial sources, production, properties and potential biotechnological applications. Appl Microbiol Biotechnol. 2012;93:1817-1830.
3. Etxeberria U, de la Garza AL, Campión J, Martínez JA, Milagro FI. Antidiabetic effects of natural plant extracts *via* inhibition of carbohydrate hydrolysis enzymes with emphasis on pancreatic alpha amylase. Expert Opin Ther Targets. 2012;16:269-297.
4. Kim YJ, Uyama H. Tyrosinase inhibitors from natural and synthetic sources: structure, inhibition mechanism and perspective for the future. Cell Mol Life Sci. 2005;62:1707-1723.
5. Murray AP, Faraoni MB, Castro MJ, Alza NP, Cavallaro V. Natural AChE inhibitors from plants and their contribution to Alzheimer's disease therapy. Curr Neuropharmacol. 2013;11:388-413.
6. Gülçin I, Beydemir Ş, Şat IG, Küfrevioğlu Ö. Evaluation of antioxidant activity of cornelian cherry (*Cornus mas L.*). Acta Aliment. 2005;34:193-202.
7. Dikilitas M, Guldur ME, Deryaoglu A, Erel O. Antioxidant and oxidant levels of pepper (*Capsicum annuum* cv. 'Charlee') infected with pepper mild mottle virus. Not Bot Horti Agrobo. 2011;39:58-63.
8. Aksoy L, Sözbilir NB. Trace and major element levels in rats after oral administration of diesel and biodiesel derived from opium poppy (*Papaver somniferum* L.) seeds. Toxicol Ind Health. 2015;31:890-897.
9. Blois MS. Antioxidant determinations by the use of a stable free radical. Nature. 1958;26:1199-1200.
10. Slinkard K, Singleton VL. Total phenol analysis: automation and comparison with manual methods. Am J Enol Viticult. 1977;28:49-55.
11. Ellman GL, Courtney KD, Andres V Jr, Feather-Stone RM. A new and rapid colorimetric determination of acetylcholinesterase activity. Biochem Pharmacol. 1961;7:88-95.
12. Yang XW, Huang MZ, Jin YS, Sun LN, Song Y, Chen HS. Phenolics from *Bidens bipinnata* and their amylase inhibitory properties. Fitoterapia. 201283:1169-1175.
13. Zengin G, Sarikurkcu C, Aktumsek A, Ceylan R, Ceylan O. A comprehensive study on phytochemical characterization of *Haplophyllum myrtifolium* Boiss. endemic to Turkey and its inhibitory

potential against key enzymes involved in Alzheimer, skin diseases and type II diabetes. Ind Crops Prod. 2014;53:244-251.

14. Masuda T, Yamashita D, Takeda Y, Yonemori S. Screening for tyrosinase inhibitors among extracts of seashore plants and identification of potent inhibitors from *Garcinia subelliptica*. Biosci Biotechnol Biochem. 200569:197-201.
15. Bravo L. Polyphenols: chemistry, dietary sources, metabolism, and nutritional significance. Nutr Rev. 1998;56:317-333.
16. Bondì ML, Bruno M, Piozzi F, Husnu Can Baser K, Simmonds MS. Diversity and antifeedant activity of diterpenes from Turkish species of *Sideritis*. Biochem Syst Ecol. 2000;28:299-303.
17. Şahin FP, Ezer N, Çalış İ. Terpenic and phenolic compounds from *Sideritis stricta.* Turk J Chem. 2006;30:495-504.
18. Tunalier Z, Kosar M, Ozturk N, Baser KHC, Duman H, Kirimer N. Antioxidant properties and phenolic composition of *Sideritis* species. Chem Nat Compd. 2004;40:206-210.
19. Sagdic O, Aksoy A, Ozkan G, Ekici L, Albayrak S. Biological activities of the extracts of two endemic *Sideritis* species in Turkey. Innov Food Sci Emerg. 2008;9:80-84.
20. Ku YS, Wong JW, Mui Z, Liu X, Hui JH, Chan TF, Lam HM. Small RNAs in plant responses to abiotic stresses: regulatory roles and study methods. int J Mol Sci. 2015;16:24532-24554.
21. Korkmaz K, Kara SM, Özkutlu F, Akgün M, Coşge Şenkal B. Profile of heavy metal and nutrient elements in some sideritis species. Int J Pharm. 2017;51:209-212.
22. Baser KHC. Aromatic biodiversity among the flowering plant taxa of Turkey. Pure Appl Chem. 2002;74:527-545.
23. Kirimer N, Baser KHC, Demirci B, Duman H. Essential oils of *Sideritis* species of Turkey belonging to the section Empedoclia. Chem Nat Compd. 2004;40:19-23.
24. González-Burgos E, Carretero ME, Gómez-Serranillos MP. *Sideritis* spp.: uses, chemical composition and pharmacological activities--a review. J Ethnopharmacol. 2011;135:209-225.
25. Fraga BM, Hernandez MG, Diaz CE. On the ent-kaurene diterpenes from *Sideritis athoa*. Nat Prod Res. 2003;17:141-144.
26. Kilic T. Isolation and biological activity of new and known isolation and biological activity of new and known diterpenoids from *Sideritis stricta* Boiss. & Heldr. Molecules. 2006;11:257-262.
27. Topçu G, Gören AC, Yildiz YK, Tümen G. Ent-kaurene diterpenes from *Sideritis athoa*. Nat Prod Lett. 1999;14:123-129.
28. Jukic M, Politeo O, Maksimovic M, Milos M, Milos M. *In vitro* acetylcholinesterase inhibitory properties of thymol, carvacrol and their derivatives thymoquinone and thymohydroquinone. Phytother Res. 2007;21:259-261.
29. Bahadori MB, Zengin G, Bahadori S, Maggi F, Dinparast L. Chemical composition of essential oil, antioxidant, antidiabetic, anti-obesity, and neuroprotective properties of *Prangos gaubae*. Nat Prod Commun. 2017;12:1945-1948.
30. Giacobini E. Cholinesterase inhibitors: new roles and therapeutic alternatives. Pharmacol Res. 2004;50:433-440.
31. Movahhedina N, Zengin G, Bahadori MB, Sarikurkcu C, Bahadoria S. Dinparast L. *Ajuga chamaecistus* subsp. *scoparia* (Boiss.) rech.f.: a new source of phytochemicals for antidiabetic, skin-care, and neuroprotective uses. Ind Crops Prod. 2016;94:89-96.
32. Szwajgier D, Borowiec K. Phenolic acids from malt are efficient acetylcholinesterase and butyrylcholinesterase inhibitors. J I Brewing. 2012;118:40-48.
33. Ertaş A, Oztürk M, Boğa M, Topçu G. Antioxidant and anticholinesterase activity evaluation of ent-kaurane diterpenoids from *Sideritis arguta*. J Nat Prod. 2009;72:500-502.
34. McCue P, Kwon YI, Shetty K. Anti-diabetic and anti-hypertensive potential of sprouted and solid-state bioprocessed soybean. Asia Pac J Clin Nutr. 2005;14:145-152.
35. Johnston BD, Ghavami A, Jensen MT, Svensson B, Pinto BM. Synthesis of selenium analogues of the naturally occurring glycosidase inhibitor salacinol and their evaluation as glycosidase inhibitors. J Am Chem Soc. 2002;124:8245-8250.
36. Loizzo MR, Saab AM, Tundis R, Menichini F, Bonesi M, Piccolo V, Statti GA, de Cindio B, Houghton PJ, Menichini F. *In vitro* inhibitory activities of plants used in Lebanon traditional medicine against angiotensin converting enzyme (ACE) and digestive enzymes related to diabetes. J Ethnopharmacol. 2008;119:109-116.
37. Souza PM, Elias ST, Simeoni LA, de Paula JE, Gomes SM, Guerra EN, Fonseca YM, Silva EC, Silveira D, Magalhães PO. Plants from Brazilian Cerrado with potent tyrosinase inhibitory activity. PLoS One. 2012;7:e48589.
38. Maeda K, Fukuda M. *In vitro* effectiveness of several whitening cosmetic components in human melanocytes. J Soc Cosmet Chem. 1991;42:361-368.

Turk J Pharm Sci 2022;19(1):84-92
DOI: 10.4274/tjps.galenos.2021.81905

ORIGINAL ARTICLE

The Nanosuspension Formulations of Daidzein: Preparation and *In Vitro* Characterization

Daidzein Nanosüspansiyon Formülasyonları: Hazırlanması ve *İn Vitro* Karakterizasyonu

Afife Büşra UĞUR KAPLAN[1]*, Naile ÖZTÜRK[2], Meltem ÇETİN[1], İmran VURAL[3], Tuba ÖZNÜLÜER ÖZER[4]

[1]Atatürk University Faculty of Pharmacy, Department of Pharmaceutical Technology, Erzurum, Turkey
[2]İnönü University Faculty of Pharmacy, Department of Pharmaceutical Technology, Malatya, Turkey
[3]Hacettepe University Faculty of Pharmacy, Department of Pharmaceutical Technology, Ankara, Turkey
[4]Atatürk University Faculty of Science, Department of Chemistry, Erzurum, Turkey

ABSTRACT

Objectives: Daidzein (DZ), a water-insoluble isoflavone, has many beneficial effects (anti-inflammatory, antioxidant, and anticancer effects, etc.) on human health. DZ has a very low oral bioavailability related to its physicochemical properties (low solubility, intense metabolism of DZ in the intestine and liver). This study aimed to prepare and *in vitro* characterize the nanosuspension formulations of DZ to improve the poor solubility and efficacy of DZ.

Materials and Methods: DZ nanosuspension formulations were prepared with media milling technique using zirconium oxide beads as milling media. Pluronic F127 and polyvinylpyrrolidone (PVP) K30 (formulation A; F-A) and sodium dodecyl sulfate (SDS) (SDS + pluronic F127 + PVP K30; formulation B; F-B) were used as stabilizers. The nanosuspension formulations were evaluated for morphological properties, particle sizes, zeta potential, DZ content, saturation solubility, dissolution, and their cytotoxic effects on RG2 glioblastoma tumor cells.

Results: F-A and F-B formulations were nanosized (in the range of about 181-235 nm) and had negative zeta potential values before and after lyophilization. The DZ content of F-A and F-B formulations were found to be 93.68±0.78% and 89.75±0.49%, respectively. Fourier transform infrared spectroscopy analysis showed that there was no significant interaction between DZ and the excipients. Differential scanning calorimetry and X-ray diffraction analyses confirmed no change in the crystal structure of DZ in F-A and F-B formulations.

Conclusion: In this study, the nanosuspension formulations were successfully prepared and characterized *in vitro*. Nanosuspension formulations increased the saturation solubility, dissolution rate, and cytotoxic effect of DZ.

Key words: Cytotoxicity, daidzein, FTIR analysis, nanosuspension, media milling

ÖZ

Amaç: Suda çözünmeyen bir izoflavon olan daidzein (DZ), insan sağlığı üzerinde pek çok faydalı etkiye (anti-inflamatuvar, antioksidan ve antikanser etkileri vb.) sahiptir. DZ, fizikokimyasal özelliklerine (düşük çözünürlük, bağırsakta ve karaciğerde DZ'nin yoğun metabolizasyonu) bağlı olarak çok düşük bir oral biyoyararlanıma sahiptir. Bu çalışmanın amacı, DZ'nin zayıf çözünürlüğünü ve etkinliğini iyileştirmek üzere DZ'nin nanosüspansiyon formülasyonunu hazırlamak ve *in vitro* olarak karakterize etmektir.

Gereç ve Yöntemler: DZ nanosüspansiyon formülasyonları, öğütme ortamı olarak zirkonyum oksit boncukları kullanılarak yaş öğütme tekniği ile hazırlandı. Stabilizan olarak pluronic F127 ve polivinilpirolidon (PVP) K30 (formülasyon A; F-A) ve sodyum dodesil sülfat (SDS) (SDS + pluronic F127 + PVP K30; formülasyon B; F-B) kullanıldı. Nanosüspansiyon formülasyonları, morfolojik özellikleri, partikül boyutları, zeta potansiyel, DZ içeriği, doygunluk çözünürlüğü, çözünme ve RG2 glioblastoma tümör hücreleri üzerindeki sitotoksik etkileri açısından değerlendirildi.

Bulgular: Liyofilizasyon öncesi ve sonrası, F-A ve F-B formülasyonları nano-boyutluydular (yaklaşık 181-235 nm aralığında) ve ayrıca negatif zeta potansiyel değerlerine sahiptiler. F-A ve F-B formülasyonlarının DZ içeriği sırasıyla; %93,68±0,78 ve %89,75±0,49 olarak bulundu. Fourier dönüşümlü kızılötesi analizi, DZ ve yardımcı maddeler arasında önemli bir etkileşim olmadığını gösterdi. Diferansiyel taramalı kalorimetre ve X-ışını difraktometresi analizleri, F-A ve F-B formülasyonlarında DZ'nin kristal yapısında hiçbir değişiklik olmadığını doğruladı.

Sonuç: Bu çalışmada, nanosüspansiyon formülasyonları başarıyla hazırlandı ve *in vitro* olarak karakterize edildi. Nanosüspansiyon formülasyonları DZ'nin doygunluk çözünürlüğünü, çözünme hızını ve sitotoksik etkisini artırdı.

Anahtar kelimeler: Sitotoksisite, daidzein, FTIR analizi, nanosüspansiyon, yaş öğütme

***Correspondence:** afife.busra.ugur@gmail.com, **Phone:** +90 442 231 53 15, **ORCID-ID:** orcid.org/0000-0003-2222-8789

Received: 05.03.2021, **Accepted:** 30.06.2021

INTRODUCTION

About 10% of the drugs in the clinical use and 40% of the newly developed drugs are poorly water-soluble. The poor solubility of active substances leads to poor bioavailability and limits their potential pharmacological effects. Therefore, increasing the aqueous solubility of poorly soluble active substances is critical. There are many approaches such as the use of co-solvents, salt formation, pH adjustment and the preparation of solid dispersions, inclusion complexes, nanosized dosage forms (nanosuspension, micelles, nanoliposome, microemulsion, etc.) to overcome the problem.[1,2] Nanosizing is a promising and popular approach to improve the solubility and bioavailability of hydrophobic active substances.[3,4] According to the Noyes-Whitney equation, the dissolution rate and bioavailability of a hydrophobic active substance increases with reducing the particle size and hence increasing the surface area of the particle.[1] Additionally, as theoretically confirmed by the Ostwald-Freundlich equation, the surface area and the saturation solubility of the particle increase with decreasing the particle size to the nanometer range.[2]

Nanosuspensions are colloidal dispersions of nanosized-particles (generally, the mean particle size: 200-600 nm), stabilized with stabilizers (surfactants, polymers, or their combination).[3,5] Especially, nanosuspensions are convenient formulations for the active substances with high log P value, high dose, and high melting point to increase the bioavailability of such active substances, reduce their dose and, obtain stable formulations as the selection of proper *stabilizers*.[6,7] Nanosuspension formulation leads to reduce the administered dose of active substance and its side effects/toxicity by improving the bioavailability of the active substances. Nanoscale size and hence greatly increased surface area of particles are responsible for the physical instability of nanosuspensions. The increased surface area leads to high interfacial tension, increasing the free energy of the system. Therefore, nanosuspension is not essentially thermodynamically stable system.[7,8] To reduce the system's free energy by decreasing interfacial tension, stabilizers are used in the formulation. The stabilizers [polyvinylpyrrolidone (PVP), Tween 80, polyvinyl alcohol, sodium lauryl sulfate, poloxamers, etc.] prevent nanoparticle aggregation by steric or electrostatic stabilization.[8] Currently, there are many nanosuspension products of poorly soluble active substances in the market, and many nanosuspension formulations are also under development.[9]

DZ(7-hydroxy-3-(4-hydroxyphenyl)-4H-chromen-4-one) mainly present in soy bean and soy products. DZ, a water-insoluble isoflavone, is a potent antioxidant and enzyme inhibitor. It also inhibits cytokines, cell adhesion proteins and platelet aggregation, induces nitric oxide production and reduces low-density lipoprotein cholesterol levels.[10,11] DZ has many beneficial effects (anti-inflammatory activities, anticancer effect, prevention of the onset of diabetes, prevention and treatment of cardiovascular diseases and prevention of bone loss after menopause, etc.) on human health as mentioned in previous studies.[10-13] The cytotoxic effects of DZ were investigated in different cancer cells (neuroblastoma, glioma, melanoma, and pancreatic carcinoma cells, colon, prostate, cervical cancer cells, etc.) and it has anti-carcinogenic properties.[10,14-17] DZ has very low oral bioavailability related to its physicochemical properties (low solubility, intense metabolism of DZ in the intestine, and liver), limiting its potential bioactivities for human health. It was reported that the absolute bioavailability of DZ was 6.1% after the oral administration of the suspension of DZ to rats.[11,18] DZ-loaded poly(lactide-co-glycolide) nanoparticles, or lipid nanocarriers, or chitosan microspheres for different application routes, DZ-cocrystals, and DZ-cyclodextrin-polymer complexes were prepared to resolve the problems such as the poor solubility and low bioavailability of DZ.[11-13,19-21]

Glioblastoma (GBM), the most common primary malignant tumor, accounts for about 30% of all central nervous system tumors. GBM constitutes 2.3% of all cancer-related deaths each year. In spite of some clinical trials in the past decade, improvement in the therapy of GBM has been insufficient. Although there is a multimodal approach consisting of surgery followed by radiotherapy and chemotherapy for GBM treatment, the average *overall* survival time of all patients with GBM is 12-15 months; only, the survival time of <5% of patients with GBM is longer than 5 years.[22]

In a study, the antitumor effects of DZ on neuroblastoma cells were investigated, and it was found that DZ inhibits cell proliferation by preventing cell cycle progression.[14] The intrinsic apoptotic pathway is modulated by DZ, and Bcl-2 plays a fundamental role in malignant glioma cell death mediated by the combination of tumor necrosis factor-related apoptosis-inducing ligand (TRAIL) and DZ.[23]

Zhang et al.[24] evaluated the inhibitory effects of daid002, a novel DZ derivative, on GBM cells (U87MG) proliferation. They reported that GBM growth was inhibited by daid002, and it induced G0/G1 phase arrest.

This study aimed to prepare and *in vitro* characterize nanosized-DZ for nanosuspension formulation to improve the poor solubility and efficacy of DZ. Also, its cytotoxic effect was evaluated using rat glioma 2 (RG2) GBM tumor cells.

MATERIALS AND METHODS

Materials

In this study, DZ (LC Laboratories, USA), pluronic F127 (BASF, Brenntag Canada Inc., Canada), PVP-K30 (Santa-Farma İlaç Sanayi A.Ş., Turkey), sodium dodecyl sulfate (SDS) (Santa-Farma İlaç Sanayi A.Ş., Turkey), thiazolyl blue tetrazolium bromide (MTT) (AppliChem GmbH, Darmstadt, Germany), *N,N*-dimethylformamide (DMF) (Sigma-Aldrich, Taufkirchen, Germany), dimethylsulfoxide (DMSO) (Lab-Scan, Ireland), *Dulbecco's modified Eagle's medium* (DMEM)/Ham's F12 (Biochrom, Berlin, Germany), L-glutamine (Biochrom, Berlin, Germany), fetal bovine serum (Biochrom, Berlin, Germany), penicillin (Biochrom, Berlin, Germany) and streptomycin (Biochrom, Berlin, Germany) were used.

Preparation of formulations

DZ nanosuspension formulations were prepared with media milling technique from coarse DZ using zirconium oxide beads as milling media and pluronic F127 and PVP K30 (formulation A; F-A) and SDS (SDS + pluronic F127 + PVP K30; formulation B; F-B) as stabilizers (Table 1).

Table 1. Content of the formulations

Ingredients	Formulation A (F-A)	Formulation B (F-B)
DZ	50 mg	50 mg
Pluronic F127	1% (w/v)	1% (w/v)
PVP K30	1% (w/v)	1% (w/v)
SDS	-	0.5% (w/v)
Ultrapure water	5 mL	5 mL

DZ: Daidzein, PVP: Polyvinylpyrrolidone, SDS: Sodium dodecyl sulfate

Coarse DZ was dispersed in a 10 mL glass vial containing the stabilizers' aqueous solution and zirconium oxide beads (diameter: 0.3-0.4 mm). Comminution was carried out on a magnetic stirrer at 1200 rpm for 24 h at room temperature as determined by preliminary studies. After the beads were removed by decantation, the obtained nanosuspensions were centrifuged at 12,500 rpm for 40 min. Then, the prepared DZ nanosuspension formulations were lyophilized for 24 h (-55˚C, 0.021 mbar; Martin Christ, Alpha 1-2 LD plus).

Characterization of the prepared formulations

Particle size and zeta potential

The mean particle size, polydispersity index (PDI) and, zeta potential of the formulations (F-A and F-B) were determined by Zetasizer Nano ZSP (Malvern Ins. Ltd, UK). Measurements were performed before and after lyophilization at 25°C. Samples (n=6) were diluted with ultrapure water to obtain a suitable concentration for measurement. Moreover, Mastersizer Hydro 2000 MU (Malvern Ins. Ltd., UK) was used to determine the particle size of coarse DZ due to its micron size. The results were expressed in mean ± standard error (SE).

Morphological analysis

The morphological features of coarse DZ and the lyophilized nanosuspension formulations (F-A and F-B) were examined using scanning electron microscope [(SEM), Zeiss Sigma 300, Germany] at an acceleration voltage of 5 kV and different magnifications. Before analysis, samples were fixed to metal plates and coated with gold under vacuum to increase conductivity.

Fourier transform infrared spectroscopy (FTIR) analysis

FTIR analysis of coarse DZ, stabilizers (pluronic F127, PVP K30, and SDS), the lyophilized nanosuspension formulations (F-A and F-B) was carried out in the region of 4000-400 cm^{-1} and under vacuum by using FTIR (Perkin Elmer Spectrum One FTIR spectrometer, Germany).

Differential scanning calorimetry (DSC) analysis

DSC analyzes of coarse DZ, stabilizers (pluronic F127, PVP K30, and SDS), the lyophilized nanosuspension formulations (F-A and F-B) were performed at 25-400°C with a heating rate of 10°C/min in air atmosphere using DSC (Netzsch STA 409 PC Luxx®, Germany) to determine their thermal properties. Alumina pans were used for samples.

X-ray diffraction (XRD) analysis

XRD analysis of coarse DZ, stabilizers (pluronic F127, PVP K30, and SDS), the lyophilized nanosuspension formulations (F-A and F-B) were carried out using Rigaku Miniflex diffractometer (Japan) using Cu Kα radiation (1.5406 Å) with a divergence slit 1.25˚. The XRD data for the samples were collected between 5˚ and 90˚. Percentage crystallinity of the materials was calculated using XRD deconvolution method using origin software.

DZ content

The lyophilized formulations (F-A and F-B) was dissolved in DMSO by mixing for 15 min to determine the DZ content. Later, the samples were filtered using a membrane filter [polytetrafluoroethylene (PTFE); pore size:220 nm], and DZ content was determined using a validated high performance liquid chromatography (HPLC)-ultraviolet (UV) method [HPLC conditions: Stationary phase: C_{18} column (Diamonsil 5 μm, 200x4.6 mm) and guard column (EasyGuard C_{18} 10x4 mm), mobile phase: methanol: ultrapure water (60:40), flow rate: 1 mL/min, UV detection: 249 nm, injection volume: 10 μL].

Saturation solubility

Saturation solubility of coarse DZ and the lyophilized nanosuspension formulations (F-A and F-B) were evaluated in six different media [HCl - pH 1.2; phosphate buffer (PB) - pH 6.8, and 7.4; HCl + 5% Tween 80 - pH 1.2; PB + 5% Tween 80 - pH 6.8, and 7.4 (PB)]. An excess amount of coarse DZ and the formulations (F-A and F-B) were dispersed in the suitable medium and shaken continuously for 24 h in a water bath at 37±0.5˚C. After centrifugation at 12,500 rpm for 15 min, the obtained supernatants were filtered using a membrane filter [polyvinylidene fluoride (PVDF); pore size: 220 nm]. Then, DZ concentration in samples was determined using a validated HPLC-UV method (at 249 nm).

Dissolution studies

Dissolution studies for coarse DZ and the lyophilized nanosuspension formulations (F-A and F-B) were conducted in 500 mL of three different dissolution media (HCl + 5% Tween 80 - pH 1.2; PB + 5% Tween 80 - pH 6.8, and 7.4) using USP dissolution apparatus 2 (paddle method) (Pharma Test PTWS IIIE/CE, Germany). During the dissolution experiment, the temperature was maintained at 37±0.5˚C, using a paddle speed of 100 rpm. 5-mL samples were withdrawn at predetermined time intervals, and an equal volume of fresh dissolution medium was added to the dissolution vessel to maintain Sink condition. After centrifugation at 12,500 rpm for 15 min, the obtained supernatants were filtered using a membrane filter (PVDF, pore size: 220 nm). Then, DZ concentration in samples was determined using a validated HPLC-UV method (at 249 nm).

Cell culture study

To evaluate the effects of coarse DZ and the nanosuspension formulations (F-A and F-B) on the viability of RG2 cell line (American Type Culture Collection, Manassas, VA, USA), MTT assay was used. 1:1 mixture of DMEM/Ham's F12 supplemented with 2.5 mM L-glutamine, 10% fetal bovine serum, penicillin (50 units/mL), and streptomycin (50 µg/mL) was used as culture medium. RG2 cells were seeded in 96-well plates (5×10^3 cells per well) and were incubated overnight at 37°C in 5% CO_2. After incubation, the cells were treated with DZ solution in a culture medium containing 0.5% DMSO (AppliChem GmbH, Darmstadt, Germany), the suspension of coarse DZ and the nanosuspensions of F-A, and F-B formulations prepared in the culture medium, and the solutions of the excipients (Exp F-A: Pluronic F127, and PVP K30) used in formulation A and formulation B (Exp F-B: Pluronic F127, PVP K30, and SDS) prepared in the culture medium. In this experiment, DZ concentrations were used in the range of 50-400 µM. After 24 and 48 h incubation, 25 µL of MTT solution (5 mg/mL) was added per well. 4 h later, 80 µL of 23% SDS solution in DMF: water (45:55, v/v) was added to each well and the plates were incubated overnight at 37°C in 5% CO_2. After incubation, absorbance (at 570 nm) was measured using a microplate reader to assess cell viability.

Statistical analysis

SPSS Statistics Version 22.0 (SPSS Inc., Chicago, USA) was used to perform statistical analysis. An independent t-test was used to evaluate the significance of the difference between two independent groups. The difference was accepted to be significant if $p<0.05$.

RESULTS AND DISCUSSION

Nanosuspension formulation has been developed to improve the poor solubility and low bioavailability of poorly water-soluble active substances/compounds by reducing their particle size. Consequently, the formulation alters the pharmacokinetics of these active substances/compounds and improve their efficacy and safety.[7,25] In our study, we prepared and characterized DZ nanosuspension formulations (F-A and F-B).

The particle sizes of coarse DZ, F-A, and F-B formulations

The mean particle sizes, and PDI values of F-A and F-B are shown in Figure 1. Also, the d10, d50, d90, and span values of coarse DZ are given in Table 2. Coarse DZ was micron in size, and d50 and d90, which correspond to the particle diameter at 50% and 90% of the total volume, were found to be 55.545±1.473 and 164.561±7.941 µm, respectively (Table 2). However, it was found that both formulations (F-A and F-B) were nanosized (in the range of about 181-235 nm) (Figure 1a). The mean particle size of the F-A formulation was smaller than those of the F-B formulation. Before lyophilization, the difference between particle sizes of F-A and F-B was significant ($p<0.05$), but after lyophilization, the difference was not significant ($p>0.05$). Also, the particle sizes of both formulations increased significantly after lyophilization ($p<0.05$), but their particle sizes were still nanosize range (Figure 1a). Lyophilization without *cryo-* and

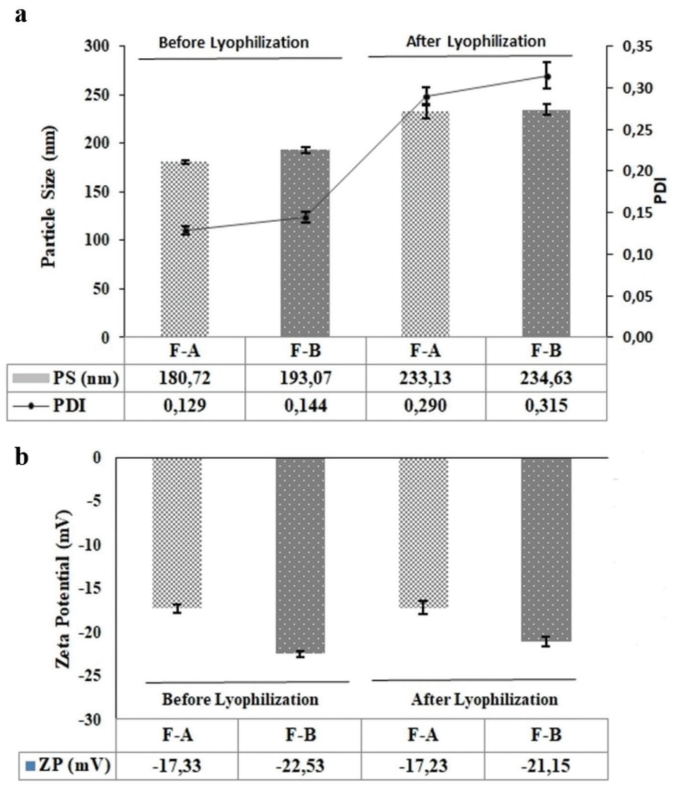

Figure 1. The particle size (PS), PDI and zeta potential (ZP) values of F-A and F-B formulations (n=6, mean ± SE). SE: Standard error, PDI: Polydispersity index

Table 2. Mean droplet size and span values of coarse DZ

Mean Diameter (µm)			Span
d_{10}	d_{50}	d_{90}	
18.490±0.617	55.545±1.473	164.561±7.941	2.633±0.162

(n=3, mean ± SE). DZ: Daidzein, SE: Standard error

lyoprotectant or in the presence of a low concentration of cryo- and lyoprotectant increases particle size due to aggregation.[26,27]

Furthermore, the PDI values of formulations (F-A and F-B) were less than 0.2 before lyophilization and approximately 0.3 after lyophilization; therefore, the prepared formulations (F-A and F-B) have narrow particle size distribution. The particle size, and PDI are very critical factors for the physical stability of colloidal dispersions. PDI value less than 0.3 is acceptable and indicates monodispersity for colloidal dispersions.[23]

The zeta potentials of F-A and F-B formulations

Zeta potential is an essential parameter for the physical stability of colloidal dispersions. Non-ionic surfactants/stabilizers and negative zeta potential prevent the aggregation of the particles by creating steric and electrostatic hindrances. Hence, the physical stability of nanosized dispersions is increased.[28,29] In the case of a combined steric and electrostatic stabilization, a zeta potential of at least about ±20 mV is acceptable.[30]

In this study, it was found that F-A and F-B had negative zeta potential values [in the range of (-) 17.23- (-) 22.53 mV] before

and after lyophilization (Figure 1b). Due to the presence of SDS (anionic surfactant) in the F-B formulation, the zeta potential of F-B was greater than the zeta potential of F-A ($p<0.05$). Besides, lyophilization did not cause a significant change in the zeta potential values of both formulations ($p>0.05$).

The morphological analyzes of coarse DZ, F-A and F-B formulations

SEM images were obtained for the morphological analysis of coarse DZ and F-A and F-B formulations (Figure 2). We observed that the coarse DZ particles were non-uniform and rod-like micron-sized particles (Figure 2a), in contrast, the F-A and F-B formulations had an approximately uniform shape and nano-sized distribution (Figure 2b, 2c).

The results of FTIR, DSC, and XRD analyze

FTIR analysis is performed to identify the compound's structural properties by determining the vibration characteristics of functional groups. It is also used to determine the interactions among the active compound(s) and other formulation components.[29]

FTIR spectra of coarse DZ, pluronic F127, PVP K30, SDS, and F-A and F-B formulations are given in Figure 3. In the FTIR spectrum of DZ, several characteristics peaks at about 3225 cm^{-1} (assigned to -OH group (intermolecular) stretching vibration), 2834 cm^{-1} (due to -CH stretching vibrations), 1630 cm^{-1} (assigned to -C=O stretching vibrations) and 1598 cm^{-1} (corresponding to -C=C vibration) (Figure 3). Similar data were reported by Bhalla et al.[21] When the FTIR spectra of coarse DZ, F-A and F-B formulations were examined, the FTIR spectra of F-A and F-B formulations (characteristic peaks related to DZ with different intensities were seen) were similar to the spectrum of coarse DZ. It showed that there was no significant interaction between DZ and the excipients. Consequently, the chemical structure of the DZ was preserved in the F-A and F-B formulations.

In this study, DSC analysis was performed to determine the thermal properties of the active compound and to examine the possible interactions among active compound and excipients in the formulation. The thermograms of the coarse DZ, pluronic F127, PVP K30, SDS, F-A, and F-B formulations are given in Figure 4. A sharp endothermic peak at about 338°C was seen in the thermogram of DZ (Figure 4). This characteristic peak is related to DZ's melting point (in the range of 330-340°C).[10,31,32] The thermograms of F-A and F-B formulations exhibited the characteristic peak related to the melting point of DZ (Figure 4); as a result, DSC analysis showed that the crystallinity of DZ was maintained in both formulations.

Besides, XRD analysis of the coarse DZ, pluronic F127, PVP K30, SDS, F-A, and F-B formulations were performed, and the results are given in Figure 5. This analysis was used to identicate the structure at the crystalline lattice level.[33] There were peaks at 2θ values of 6.9°, 8.5, 10.4, 12.9, 15.9, 17.0, 24.6, 25.3, 26.5, 28.1, and 28.8 in the XRD patterns of coarse DZ (Figure 5). These results are consistent with a previously published study.[33] The XRD patterns of F-A and F-B formulations were similar to the XRD patterns of coarse DZ (Figure 5). In our study, it was shown that the crystal structure of DZ was preserved in both formulations.

As a result, DSC and *XRD* analyzes *confirmed no change* in the crystal structure of DZ in F-A and F-B formulations.

DZ content of F-A and F-B formulations

The DZ content of F-A and F-B formulations were found to be 93.68±0.78% and 89.75±0.49% (mean ± SE, n=6), respectively. The negligible loss of DZ might be associated with the loss occurring during the preparation process of nanosuspension.[34] There was a slight reduction in the DZ content of F-B

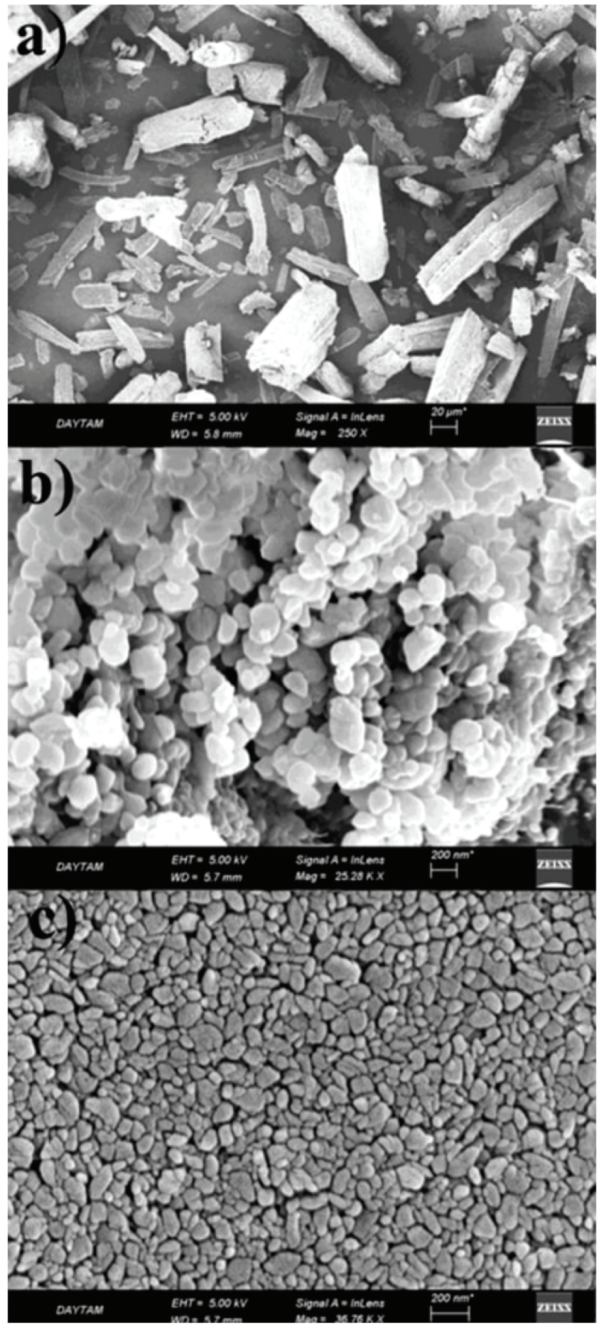

Figure 2. SEM images of coarse DZ (a), F-A (b) and F-B (c) formulations
SEM: Scanning electron microscope, DZ: Daidzein

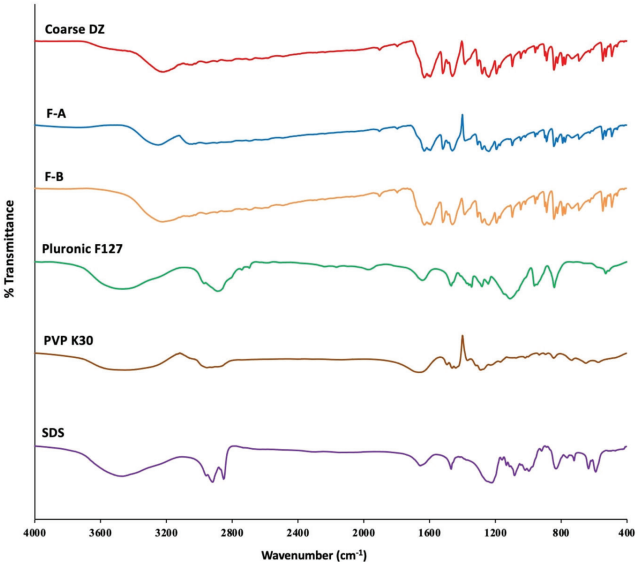

Figure 3. FTIR spectra of coarse DZ, F-A and F-B formulations, and the excipients in the formulation (pluronic F127, PVP K30, and SDS)

FTIR: Fourier transform infrared spectroscopy, DZ: Daidzein, PVP: Polyvinylpyrrolidone, SDS: Sodium dodecyl sulfate

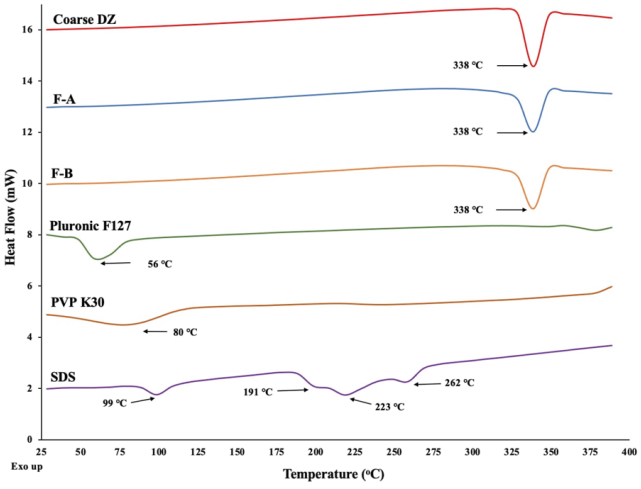

Figure 4. DSC thermograms of coarse DZ, F-A and F-B formulations, and the excipients in the formulation (pluronic F127, PVP K30, SDS)

DSC: Differential scanning calorimetry, DZ: Daidzein, PVP: Polyvinylpyrrolidone, SDS: Sodium dodecyl sulfate

formulation compared to that of F-A formulation (p<0.05). This reduction in F-B formulation can be attributed to the presence of SDS, which likely causes a slight increase in the solubility of DZ during the preparation of nanosuspension.

The saturation solubility of coarse DZ, F-A, and F-B formulations

DZ, which belonging to Biopharmaceutical Classification System class IV, has low solubility and poor bioavailability.[35] Saturation solubility studies for coarse DZ, F-A and F-B formulations were conducted in the buffer solutions with different pH (pH 1.2, 6.8, and 7.4) and with/without 5% Tween 80. The solubility results, which are given in Table 3, indicated that coarse DZ, F-A, and F-B formulations have a pH-dependent solubility. Panizzon et al.[35] reported that DZ has a higher solubility in alkaline pH compared to acidic and neutral pH; thus, its solubility is pH-dependent. In our study, the solubility of coarse DZ in the buffer solutions with different pH (HCl - pH 1.2; PB - pH 6.8; and PB - pH 7.4) were found to be just 0.99±0.15 μg/mL, 1.81±0.06 μg/mL, and, 3.21±0.24 μg/mL, respectively (Table 3). In F-A and F-B formulations, the solubility of DZ in the different buffer solutions (HCl - pH 1.2; PB - pH 6.8; and PB - pH 7.4) increased in the range of about 6-14-fold in compared to coarse DZ (p<0.05; Table 3). The saturation solubility of DZ increased in F-A and F-B formulations due to the large specific surface area because of the particle size decreasing to the nanosize range.

Moreover, it is significant to ensure a sink condition in the dissolution/release medium. In sink conditions, the saturation solubility of an/a active substance/compound is at least 3 times more than its concentration in the dissolution/release medium.[36] In the literature, to achieve sink condition in the study of dissolution/release, which was performed for the formulations genistein or DZ, the buffer solutions (PB or PBS pH 7.4) with ethanol (30%) or SDS (5%) or methanol (50%) or aqueous solutions with SDS (3%) or Tween 80 (0.5%) were used as release/dissolution medium.[10,37-40] Oliveira et al.[38] evaluated the solubilities of genistein and daidzein in several different mediums (sodium acetate buffer pH 4.5, water, water with 3% Tween 80, water with 3% Tween 20; water with 3% SDS) to properly design the dissolution test.

In our study, the solubility of DZ was also evaluated in the different buffer solutions with Tween 80 (5%) to properly

Table 3. The results of saturation solubility study

	Coarse-DZ (μg/mL)	F-A (μg/mL)	F-B (μg/mL)
pH 1.2 HCl	0.99±0.15	7.94±1.00	13.83±0.27
pH 6.8 PB	1.81±0.06	11.95±1.00	21.23±0.33
pH 7.4 PB	3.21±0.24	17.39±1.16	30.89±0.39
HCl + 5% Tween 80 - pH 1.2	80.68±6.80	102.16±6.36	118.99±7.65
PB + 5% Tween 80 - pH 6.8	107.06±5.54	143.80±5.34	159.53±7.02
PB + 5% Tween 80 - pH 7.4	128.77±3.66	150.04±2.01	188.69±4.36

(Mean ± SE; n=3). PB: Phosphate buffer, SE: Standard error, DZ: Daidzein

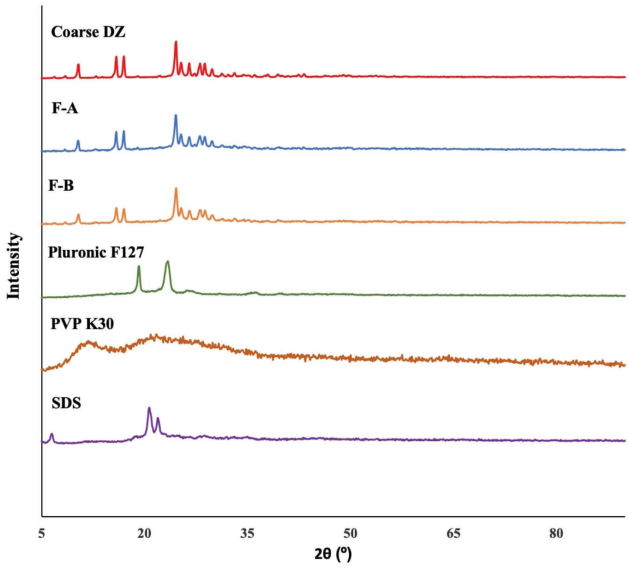

Figure 5. X-ray patterns of coarse DZ, F-A and F-B formulations, and the excipients in the formulation (pluronic F127, PVP K30, and SDS)
DZ: Daidzein, PVP: Polyvinylpyrrolidone, SDS: Sodium dodecyl sulfate

design the dissolution study. The solubility of coarse DZ in the buffer solutions (HCl - pH 1.2; PB - pH 6.8; and PB - pH 7.4) with Tween 80 (5%) was found to be 80.68±6.80 μg/mL, 107.06±5.54 μg/mL, and, 128.77±3.66 μg/mL, respectively (Table 3). Furthermore, the solubility of DZ in F-A and F-B formulations was higher than that of coarse DZ (p<0.05; Table 3).

Dissolution studies of coarse DZ, F-A, and F-B formulations

The dissolution studies of coarse DZ and nanosuspension formulations (F-A and F-B) were conducted in the different dissolution media (HCl + 5% Tween 80-pH 1.2; PB + 5% Tween 80 - pH 6.8, and 7.4), and the dissolution profiles for coarse DZ, F-A, and F-B formulations are shown in Figure 6. In HCl + 5% Tween 80 -pH 1.2, about 14% (for coarse DZ), 65% (for F-A), and 84% (for F-B) of DZ dissolved within 5 min. Besides, in PB + 5% Tween 80 - pH 6.8, and 7.4, 16%-17% (for coarse DZ), 66%-68% (for F-A) and, and 85%-86% (for F-B) of DZ dissolved within 5 min. At 60th min, about 60% (for coarse DZ) and 100% (for F-A and F-B) of DZ dissolved in all three dissolution media (Figure 6). As a result, it can be concluded that the dissolution of DZ can be improved and significantly increased by preparing a nanosuspension formulation of DZ. Wang et al.[41] prepared and evaluated the nanosuspension formulations of DZ using various stabilizers (soy lecithin, D-alpha-tocopherol polyethylene glycol 1000 succinate, hydroxypropyl-β-cyclodextrin, SDS, hydroxypropyl methylcellulose E5, sulfobutyl ether-β-cyclodextrin, or their combinations) to improve the solubility and oral bioavailability of DZ. They used the stabilizers to stabilize the small particles in a colloidal dispersion by electrostatic repulsion or steric hindrance to overcome the physical instability problem caused by small particle size and increased free energy in the colloidal dispersion. They reported that the DZ nanosuspension formulations with particle sizes of 360-600 nm and regular shapes. The authors also evaluated

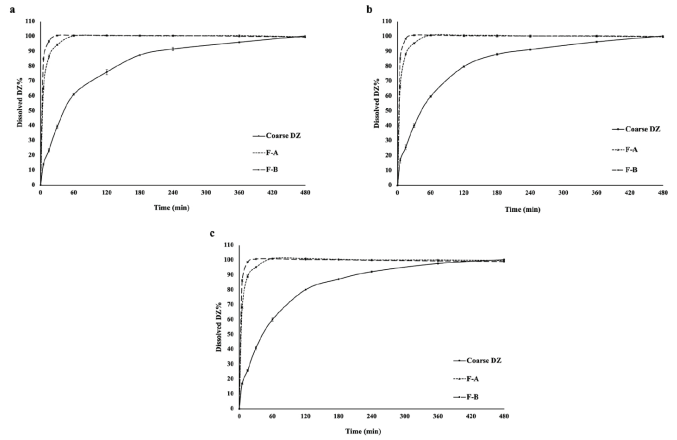

Figure 6. The dissolution profiles of coarse DZ, F-A and F-B formulations in the different dissolution media (a). HCl + 5% Tween 80 - pH-1.2; (b). PB + 5% Tween 80 - pH-6.8; (c). PB + 5% Tween 80 - pH-7.4 (mean ± SE; n=3)
DZ: Daidzein, PB: Phosphate buffer, SE: Standard error

the saturation solubility and the dissolution of coarse DZ and DZ nanosuspensions in distilled water and 900 mL of dissolution medium with 0.1% Tween-80, respectively. They found that the saturation solubility of crude DZ was very low (about 3 μg/mL), however, the saturation solubility (about 8-21 μg/mL) of DZ in nanosuspension formulations was higher than that of coarse DZ. Furthermore, they showed that less than 10% and 75% of coarse DZ dissolved in the dissolution medium with 0.1% Tween 80 within 5 min and 240 min, respectively; however, more than 80% and 90% of DZ in nanosuspension formulations dissolved within 5 min and 240 min, respectively. Because of the preparation of nanosuspension formulations of poorly soluble active substances/compounds, the particle surface area of these active substances/compounds increases significantly by reducing the particle size to the nanorange. The increased surface area provides a significant increase in the dissolution rate of the active substances/compounds according to Noyes-Whitney equation.[42] Additionally, the use of the appropriate amount of Tween-80 increases the dissolution rate of DZ.[43]

Moreover, Bhalla et al.[21] Prepared co-crystals of DZ with isonicotinamide, theobromine, and cytosine by solvent-assisted grinding. They evaluated the solubility and intrinsic dissolution of co-crystals of DZ in PB - pH 6.8. They stated that co-crystals of DZ showed an almost 2-fold improvement in the solubility and dissolution of DZ compared to pure DZ.

Cell culture study

The cytotoxic effect of DZ on cancer cells is dose-dependent.[17,44] In our study, the cytotoxic effects of DZ solution in the culture medium with 0.5% DMSO, and the suspensions of coarse DZ, and the nanosuspension formulations (F-A and F-B) in culture medium on RG2 cell lines were evaluated using MTT assay. Control cells were treated with only a culture medium (C1) or a culture medium with 0.5% DMSO (C2). The maximum DMSO concentration to be used for cell culture studies should be 0.5%.[17,45] There was no significant difference in the cell viability between C1 and C2 for 24 h and 48 h incubation (p>0.05; Figure 7). The cell viability was more than 93% after

incubation with exp F-A or exp F-B for 24 h and 48 h incubation (Figure 7). This suggests that Exp F-A and Exp F-B exhibited no significant cytotoxicity compared to C1 (p>0.05). After 24 h and 48 h incubation, high concentrations (200 and 400 µM) of DZ solutions had a significant cytotoxic effect on RG2 cells compared to C2 (p<0.05) and coarse DZ (p<0.05). Besides, coarse DZ showed a cytotoxic effect on cancer cells at high concentrations (100-400 µM; p<0.05 compared to C1; Figure 7) for 24 h and 48 h incubation.

After 24 h and 48 h incubation, the results of the cytotoxicity study indicated that F-A and F-B caused a significant decrease in cell viability of RG2 cells at all concentrations (p<0.05; except 400 µM for DZ solution) compared to C1, coarse DZ, and DZ solution. After 24 h incubation, F-A and F-B formulations reduced the viability of RG2 cells by about 28% and 20% (at 50 µM concentration) and by approximately 53% and 54% (at 400 µM concentration), respectively (Figure 7). After 48 h incubation, the decrease in the viability of RG2 cells was approximately 48% (at 50 µM concentration for both formulations F-A and F-B) and about 67% (at 400 µM concentration for both formulations F-A and F-B) (Figure 7). Coarse DZ, F-A and F-B formulations dose-dependently decreased RG2 cell viability.

CONCLUSION

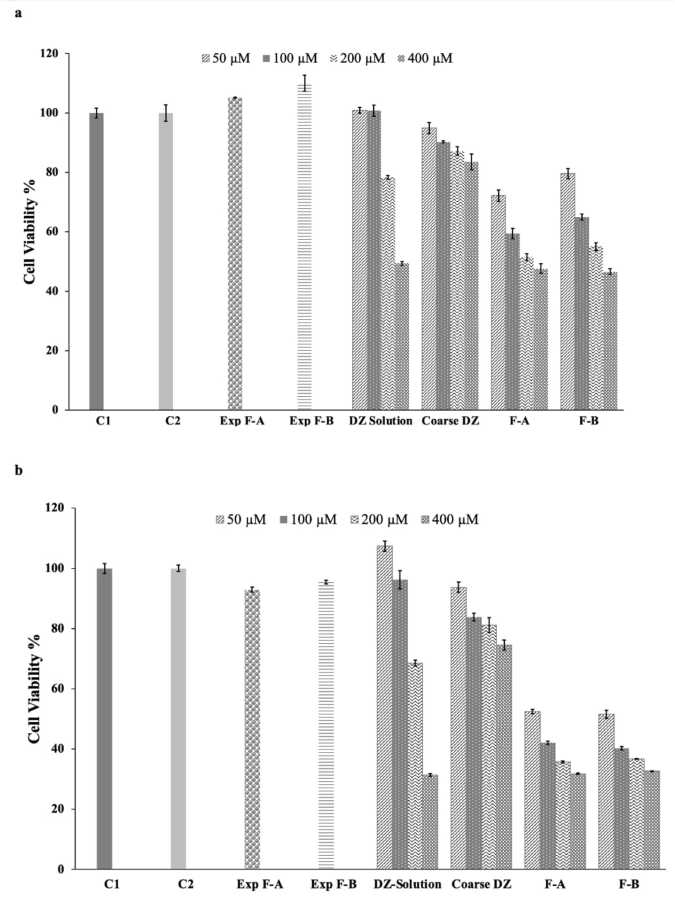

Figure 7. Cytotoxic effects of DZ solution, coarse DZ and the nanosuspension formulations (F-A and F-B) for 24 h (a) and 48 h (b) incubation.
DZ: Daidzein

In our study, DZ nanosuspension formulations were successfully prepared and characterized *in vitro*. The results of characterization studies showed that the prepared nanosuspension formulations significantly increased the saturation solubility and dissolution rate of DZ as well as its cytotoxic effect on RG2 GBM tumor cells.

ACKNOWLEDGMENTS

We would like to thank Kerim Göğebakan and "Kar Kimya San. ve Tic. Ltd. Şti." for their assistance in providing zirconium oxide beads.

Conflict of interest: No conflict of interest was declared by the authors. The authors are solely responsible for the content and writing of this paper.

REFERENCES

1. Thadkala K, Nanam PK, Rambabu B, Sailu C, Aukunuru J. Preparation and characterization of amorphous ezetimibe nanosuspensions intended for enhancement of oral bioavailability. Int J Pharm Investig. 2014;4:131-137.
2. Junyaprasert VB, Morakul B. Nanocrystals for enhancement of oral bioavailability of poorly water-soluble drugs. Asian J Pharm Sci. 2015;10:13-23.
3. Wang Y, Zheng Y, Zhang L, Wang Q, Zhang D. Stability of nanosuspensions in drug delivery. J Control Release. 2013;172:1126-1141.
4. Jethara SI, Patel MR, Patel AD. Nano suspension drug delivery system: an overview. Aperito J Drug Design Pharmacol. 2014;1:106.
5. Savjani KT, Gajjar AK, Savjani JK. Drug solubility: importance and enhancement techniques. ISRN Pharm. 2012;2012:195727.
6. Patel HM, Patel BB, Shah CN. Nanosuspension: a novel approach to enhance solubility of poorly water soluble drugs - a review. Int J Adv Pharm. 2016;5:21-29.
7. Bektaş AE, Uğur AB, Çetin M. Nanosuspensions: preparation methods and stability ıssue. Hacettepe Univ J Fac Pharm. 2018;38:85-101.
8. Verma S, Kumar S, Gokhale R, Burgess DJ. Physical stability of nanosuspensions: investigation of the role of stabilizers on Ostwald ripening. Int J Pharm. 2011;406:145-152.
9. Jacob S, Nair AB, Shah J. Emerging role of nanosuspensions in drug delivery systems. Biomater Res. 2020;24:3.
10. Ugur Kaplan AB, Cetin M, Orgul D, Taghizadehghalehjoughi A, Hacımuftuoglu A, Hekimoglu S. Formulation and *in vitro* evaluation of topical nanoemulsion and nanoemulsion-based gels containing daidzein. J Drug Deliv Sci Technol. 2019;52:189-203.
11. Ma Y, Zhao X, Li J, Shen Q. The comparison of different daidzein-PLGA nanoparticles in increasing its oral bioavailability. Int J Nanomedicine. 2012;7:559-570.
12. Gao Y, Gu W, Chen L, Xu Z, Li Y. The role of daidzein-loaded sterically stabilized solid lipid nanoparticles in therapy for cardio-cerebrovascular diseases. Biomaterials. 2008;29:4129-4136.
13. Zhang Z, Huang Y, Gao F, Bu H, Gu W, Li Y. Daidzein-phospholipid complex loaded lipid nanocarriers improved oral absorption: *in vitro* characteristics and *in vivo* behavior in rats. Nanoscale. 2011;3:1780-1787.

14. Lo FH, Mak NK, Leung KN. Studies on the anti-tumor activities of the soy isoflavone daidzein on murine neuroblastoma cells. Biomed Pharmacother. 2007;61:591-595.
15. Guo JM, Kang GZ, Xiao BX, Liu DH, Zhang S. Effect of daidzein on cell growth, cell cycle, and telomerase activity of human cervical cancer *in vitro*. Int J Gynecol Cancer. 2004;14:882-888.
16. Siegelin MD, Gaiser T, Habel A, Siegelin Y. Daidzein overcomes TRAIL-resistance in malignant glioma cells by modulating the expression of the intrinsic apoptotic inhibitor, bcl-2. Neurosci Lett. 2009;454:223-228.
17. Gundogdu G, Dodurga Y, Cetin M, Secme M, Cicek B. The cytotoxic and genotoxic effects of daidzein on MIA PaCa-2 human pancreatic carcinoma cells and HT-29 human colon cancer cells. Drug Chem Toxicol. 2020;43:581-587.
18. Qiu F, Chen XY, Song B, Zhong DF, Liu CX. Influence of dosage forms on pharmacokinetics of daidzein and its main metabolite daidzein-7-O-glucuronide in rats. Acta Pharmacol Sin. 2005;26:1145-1152.
19. Borghetti GS, Pinto AP, Lula IS, Sinisterra RD, Teixeira HF, Bassani VL. Daidzein/cyclodextrin/hydrophilic polymer ternary systems. Drug Dev Ind Pharm. 2011;37:886-893.
20. Ge YB, Chen DW, Xie LP, Zhang RQ. Optimized preparation of daidzein-loaded chitosan microspheres and *in vivo* evaluation after intramuscular injection in rats. Int J Pharm. 2007;338:142-151.
21. Bhalla Y, Chadha K, Chadha R, Karan M. Daidzein cocrystals: an opportunity to improve its biopharmaceutical parameters. Heliyon. 2019;5:e02669.
22. Romano-Feinholz S, Salazar-Ramiro A, Muñoz-Sandoval E, Magaña-Maldonado R, Hernández Pedro N, Rangel López E, González Aguilar A, Sánchez García A, Sotelo J, Pérez de la Cruz V, Pineda B. Cytotoxicity induced by carbon nanotubes in experimental malignant glioma. Int J Nanomed. 2017;12:6005-6026.
23. Danaei M, Dehghankhold M, Ataei S, Hasanzadeh Davarani F, Javanmard R, Dokhani A, Khorasani S, Mozafari MR. Impact of particle size and polydispersity index on the clinical applications of lipidic nanocarrier systems. Pharmaceutics. 2018;10:57.
24. Zhang X, Liu X, Zhang J, Zhou W, Lu J, Wang Q, Hu R. Daidzein derivative daid002 inhibits glioblastoma growth *via* disrupting the interaction between moesin and CD44. Oncotarget. 2018;5:1-12.
25. Patel VR, Agrawal YK. Nanosuspension: an approach to enhance solubility of drugs. J Adv Pharm Technol Res. 2011;2:81-87.
26. Attari Z, Kalvakuntla S, Reddy MS, Deshpande M, Rao CM, Koteshwara KB. Formulation and characterisation of nanosuspensions of BCS class II and IV drugs by combinative method. J Exp Nanosci. 2016;11:276-288.
27. Sharma M, Mehta I. Surface stabilized atorvastatin nanocrystals with improved bioavailability, safety and antihyperlipidemic potential. Sci Rep. 2019;9:16105.
28. Shah U, Joshi G, Sawant K. Improvement in antihypertensive and antianginal effects of felodipine by enhanced absorption from PLGA nanoparticles optimized by factorial design. Mater Sci Eng C Mater Biol Appl. 2014;35:153-163.
29. Kandilli B, Ugur Kaplan AB, Cetin M, Taspinar N, Ertugrul MS, Aydin IC, Hacimuftuoglu A. Carbamazepine and levetiracetam-loaded PLGA nanoparticles prepared by nanoprecipitation method: *in vitro* and *in vivo* studies. Drug Dev Ind Pharm. 2020;46:1063-1072.
30. Honary S, Zahir F. Effect of zeta potential on the properties of nano-drug delivery systems - a review (Part 2). Trop J Pharm Res. 2013;12:265-273.
31. Scheithauer EC, Li W, Ding Y, Harhaus L, Roether JA, Boccaccini AR. Preparation and characterization of electrosprayed daidzein-loaded PHBV microspheres. Mater Lett. 2015;158:66-69.
32. Daidzein, >99% | LC laboratories. Accessed date: 14, 2021. Available from: https://lclabs.com/products/d-2946-daidzein
33. Huang Z, Xia J, Li J, Gao X, Wang Y, Shen Q. Optimization and bioavailability evaluation of self-microemulsifying drug delivery system of the daidzein–nicotinamide complex. RSC Advances. 2016;6:112686-112694.
34. Kalvakuntla S, Deshpande M, Attari Z, Kunnatur B K. Preparation and characterization of nanosuspension of aprepitant by H96 process. Adv Pharm Bull. 2016;6:83-90
35. Panizzon GP, Giacomini Bueno F, Ueda-Nakamura T, Nakamura CV, Dias Filho BP. Manufacturing different types of solid dispersions of bcs class IV polyphenol (daidzein) by spray drying: formulation and bioavailability. Pharmaceutics. 2019;11:492.
36. The United States Convention. United States Pharmacopeia (USP 30-NF25).; 2007.
37. Silva AP, Nunes BR, De Oliveira MC, Koester LS, Mayorga P, Bassani VL, Teixeira HF. Development of topical nanoemulsions containing the isoflavone genistein. Pharmazie. 2009;64:32-35.
38. Oliveira SR, Taveira SF, Marreto RN, Valadares MC, Diniz DGA, Lima EM. Preparation and characterization of solid oral dosage forms containing soy isoflavones. Rev Bras Farmacogn. 2013;23:175-181.
39. Argenta DF, de Mattos CB, Misturini FD, Koester LS, Bassani VL, Simões CM, Teixeira HF. Factorial design applied to the optimization of lipid composition of topical antiherpetic nanoemulsions containing isoflavone genistein. Int J Nanomed. 2014;9:4737-4747.
40. Wang Q, Liu W, Wang J, Liu H, Chen Y. Preparation and pharmacokinetic study of daidzein long-circulating liposomes. Nanoscale Res Lett. 2019;14:321.
41. Wang H, Xiao Y, Wang H, Sang Z, Han X, Ren S, Du R, Shi X, Xie Y. Development of daidzein nanosuspensions: preparation, characterization, *in vitro* evaluation, and pharmacokinetic analysis. Int J Pharm. 2019;566:67-76.
42. Yao J, Cui B, Zhao X, Wang Y, Zeng Z, Sun C, Yang D, Liu G, Gao J, Cui H. Preparation, characterization, and evaluation of azoxystrobin nanosuspension produced by wet media milling. Appl Nanosci. 2018;8:297-307.
43. Hu L, Zhang N, Yang G, Zhang J. Effects of tween-80 on the dissolution properties of daidzein solid dispersion *in vitro*. Int J Chem Int. J. Quantum Chem.. 2011;3(1):68-73.
44. Farjadian S, Khaioei Neiad L, Fazeli M, Askari Firouziaei H, Zaeri S. Doxorubicin cytotoxicity in combination with soy isoflavone daidzein on MCF-7 breast cancer cells. Mal J Nutr. 2015;21:67-73.
45. Pal R, Mamidi MK, Das AK, Bhonde R. Diverse effects of dimethyl sulfoxide (DMSO) on the differentiation potential of human embryonic stem cells. Arch Toxicol. 2012;86:651-661.

Turk J Pharm Sci 2022;19(1):93-100
DOI: 10.4274/tjps.galenos.2021.56957

ORIGINAL ARTICLE

Molecular Docking Studies to Identify Promising Natural Inhibitors Targeting SARS-CoV-2 Nsp10-Nsp16 Protein Complex

SARS-CoV-2 Nsp10- Nsp16 Protein Kompleksini Hedefleyen Umut Veren Doğal İnhibitörleri Belirlemek için Moleküler Docking Çalışmaları

Anuradha BHARDWAJ[1], Swati SHARMA[2]*, Sandeep Kumar SINGH[3]

[1]Gautam Buddha University, Greater Noida, Uttar Pradesh, India
[2]Department of Pharmacology, All India Institute of Medical Sciences, New Delhi, India
[3]Indian Scientific Education and Technology (ISET) Foundation, Lucknow, India

ABSTRACT

Objectives: Unavailability of potential drugs/vaccines in the outbreak of the pandemic severe acute respiratory syndrome-coronavirus-2 (SARS-CoV-2) have devastated the human population globally. Several druggable targets have been analyzed against different viral proteins such as the spike protein. The study aims to explore the potential of natural compounds as an effective drug against a novel nsp10-nsp16 complex of SARS-CoV-2 using *in silico* approaches.

Materials and Methods: *In silico* screening (Docking analysis) was performed for 10 shortlisted natural compounds *viz*. allicin, ajoene, carvacrol, coumarin, curcumin, menthol, eugenol, theaflavin, ursolic acid, and catechin against a novel target of SARS-CoV-2, that has been anticipated to provide valuable lead molecules and potentially druggable compounds for the treatment of SARS-CoV-2.

Results: Theaflavin and catechin, the natural components of black tea and green tea, out of 10 shortlisted compounds have shown excellent performance in our docking studies with the minimum binding energy of -11.8 kcal/mol and -9.2 kcal/mol respectively, against a novel nsp10-nsp16 complex of SARS-CoV-2 that indicates their potential for inhibitory molecular interactions against the virus to assist rapid drug designing from natural products.

Conclusion: Either consumption of black tea and green tea or repurposing them as drug candidates may help individuals to fight against SARS-CoV-2, subject to their *in vivo* and *in vitro* further experimental validations.

Key words: SARS-CoV-2, nsp10-nsp16 protein complex, natural compounds, molecular docking, corona, antiviral natural compounds, drug design

ÖZ

Amaç: Şiddetli akut solunum sendromu-koronavirüs-2 (SARS-CoV-2) pandemi salgınında, potansiyel ilaçların/aşıların bulunamaması, küresel olarak insan popülasyonunu tahrip etmiştir. Spike proteini gibi farklı viral proteinler, ilaç uygulanabilecek bazı hedefler olarak analiz edilmiştir. Bu çalışma, SARS-CoV-2 nsp10-nsp-16 kompleksine karşı etkili bir ilaç olarak doğal bileşiklerin potansiyelini, *in siliko* yaklaşımlar kullanarak araştırmayı amaçlamaktadır.

Gereç ve Yöntemler: *İn siliko* taramalar (Docking analizi), yeni bir SARS-CoV-2 hedefinin tedavisi için değerli öncü moleküller ve ilaç olarak uygulanabilir potansiyelde bileşikler sağlaması beklenen, aday listeye alınmış 10 doğal bileşik olan allisin, ajoen, karvakrol, kumarin, kurkumin, mentol, öjenol, teaflavin, ursolik asit, kateşin üzerinde gerçekleştirilmiştir.

Bulgular: Aday listede yer alan 10 bileşikten, siyah çay ve yeşil çayın doğal bileşenleri olan, theaflavin ve kateşin, yeni bir SARS-CoV-2 nsp10-nsp16 kompleksine karşı sırasıyla -11,8 kcal/mol ve -9,2 kcal/mol minimum bağlanma enerjisi ile docking çalışmalarımızda mükemmel performans göstermiştir; bu da doğal ürünlerin, virüse karşı inhibitör moleküler etkileşimli, hızlı ilaç tasarımına yardımcı, potansiyellerini vurgulamaktadır.

Sonuç: Siyah çay ve yeşil çayın tüketilmesi veya ilaç adayları olarak yeniden kullanılması, *in vivo* ve *in vitro* ileri deneysel validasyonlarının tamamlanmasıyla, SARS-CoV-2'ye karşı savaşta yardımcı olabilir.

Anahtar kelimeler: SARS-CoV-2, nsp10-nsp16 protein kompleksi, doğal bileşikler, moleküler docking, korona, doğal anti-viral bileşikler, ilaç tasarımı

***Correspondence:** mail_swati84@yahoo.co.in, **Phone:** +9873730885, **ORCID-ID:** orcid.org/0000-0002-8732-335X

Received: 26.04.2021, **Accepted:** 30.06.2021

INTRODUCTION

A new coronavirus, officially named severe acute respiratory syndrome-coronavirus (SARS-CoV-2) by the International Committee on Taxonomy of Viruses outburst an alarming outbreak of a pneumonia-like illness, originating without a serious known origin from the seafood market of Wuhan City, Hubei, China in December 2019.[1] Sooner, its human-to-human transmission was also observed with a toll of 1,781,776 total deaths across the globe as per record till dated 28 December 2020. The World Health Organization realized the censoriousness of this infection and declared it as a global public health emergency on 30 January 2020 and a pandemic on 11 March 2020.[2] The lack of effective vaccines & approved drugs and the rapidly spreading of the virus through respiratory droplets or contact with infected droplets along with its long incubation period has worsened the situation with a toll of 81,680,270 total confirmed cases reported across the globe by December 28, 2020 compared with the previously known CoV epidemics like SARS-CoV in 2003 and middle east respiratory syndrome-CoV in 2012 with the total number of cases reported to be 8,439 and 2,519 respectively.[3]

SARS-CoV-2 mark onset with clinical symptoms like pneumonia, fever, dry cough, headache, and dyspnea leading to respiratory failure in case of severe infection and weaker immunity and even death in many cases. The members of the pathogenic corona family mainly have five protein regions namely replicase complex (ORF1ab), spike (S), envelope (E), membrane (M), and nucleocapsid (N) proteins that control the virus structure assembly and viral replications. The ORF1ab gene encodes the non-structural proteins (nsp) of the viral RNA synthesis complex through proteolytic processing. Sharing genetically similar to SARS-CoV,[4] the virus SARS-CoV-2 is a spherically enveloped pathogen bearing glycoprotein projections with single-stranded RNA (ssRNA) (+ve sense RNA) associated with a nucleoprotein within a capsid.

Recently, the research on various aspects of identifying novel antiviral compounds against the SARS-CoV-2 gained significant momentum. A wide spectrum of vaccines has now been proposed and approved for emergency use across the globe. Various pharmacological methods are currently under study, primarily focusing on repurposing drugs. Despite extensive experimental and computational studies, there is no proven discovery of SARS-CoV-2 drug treatment. However, many effective and potential drug targets are already being identified against SARS-CoV-2.

More than 20 proteins constitute the viral structure out of which 3-chymotrypsin-like protease ($3CL^{pro}$/M^{pro}) plays an important role in viral replication and is a promising drug target of SARS-CoV-2.[4] A recent study suggests that a complex of two critical non-structural proteins nsp10-nsp16 is also critical for virus survival and reproduction. This complex encodes 2′-O-MTase that helps the virus hide from the innate immune system of the host by modifying its genetic material in such a way that it resembles the host (human) cell RNA.[5] This gives the virus enough time to exponentially multiply in the human body. Thus, developing a drug targeting the nsp10-nsp16 complex of SARS-CoV-2 will empower the infected immune system to identify the pathogen and destroy it.

For ages, traditional plant products having various polyphenolic contents are popularly known for their medicinal properties. Effective treatments using plant-derived drugs have proved their immense potential by providing relief in many pathogenic diseases, including viral diseases. Realizing the potential of these natural drugs, need was felt to explore their interaction profiles with SARS-CoV-2 to identify novel drug compounds to inhibit this virus with least/no side effects. Several natural compounds such as allicin, ajoene, carvacrol, catechin, coumarin, curcumin, quercetin, baicalein, narasin, menthol, eugenol, theaflavin and ursolic acid, myricetin, raoulic acid, chebulagic acid, etc. are effective against human viral infections.[6] Therefore, to defeat corona, there is need realized to scan the active compounds from the plant extracts using computational approaches to accelerate the process of drug discovery.

SARS-CoV-2 has significant similarities with the influenza virus in terms of modes of transmission, clinical signs and symptoms, and immune responses. The potential of 10 plant-derived compounds viz. allicin, ajoene, carvacrol, coumarin, curcumin, menthol, eugenol, theaflavin, ursolic acid, and catechin has been confirmed active against human influenza[7] have been chosen for this study. Thus, we firstly computationally screened these 10 natural compounds against the SARS-CoV-2 nsp10-nsp16 protein complex to identify their potential to inhibit SARS-CoV-2. Later, we conducted molecular docking studies to understand their molecular interactions and mechanism of action against the pathogen growth in the human host. Our study comprises sequence and structural analysis of the potential target protein nsp10-nsp16 complex of SARS-CoV-2. Docking studies were conducted using the latest version of the AutoDock-Vina tool.[8] Our approach of computationally screening these plant-derived compounds (secondary metabolites) against the target of SARS-CoV-2 infection can provide valuable lead molecules and potentially druggable compounds for treating SARS-CoV-2.

MATERIALS AND METHODS

Hardware and software

This study was conducted on a Workstation (Dell) having a 6 GB RAM & 1 TB hard storage capacity, installed with AutoDock Vina 1.1.2 version. We also accessed web-based databases and tools online in this work.

Data collection

The viral nsp10-nsp16 complex was chosen as the potential drug target. The protein sequence and structure of the target protein complex was extracted from the protein data bank (PDB) (www.rcsb.org) with accession ID 6W4H.

Sequence analyses

Physicochemical parameters of the SARS-CoV-2 nsp10-nsp16 protein complex (both chains separately) including isoelectric point, instability index, hydropathicity, the atomic composition was computed using the ProtParam tool of ExPASy.[9]

Structural analyses

From the data repository of proteins, PDB (https://rcsb.org/), 1.80 angstrom resolution crystal Structure of nsp10-nsp16 complex from SARS-CoV-2 with PDB ID: 6W4H was retrieved in the.pdb format. Yet Another Scientific Artificial Reality Application (YASARA)[10] energy minimization server was employed for initial quality assessment, structural refinement and energy minimization of the target protein structure with its reliability evaluation through ProCheck,[11]] ProSA-web,[12] ProQ[13] and ERRAT server.[14]

Ligand preparation and molecular docking

From the PubChem database chemical structures of 10 potential phytochemicals having antiviral properties namely (A) allicin, (B) ajoene, (C) carvacrol, (D) coumarin, (E) curcumin, (F) menthol, (G) eugenol, (H) theaflavin, (I) ursolic acid, (J) catechin, was fetched (Table 1).[15] Both ligands and receptor molecules (nsp10-nsp16) were prepared in AutoDock Vina software, to predict our small molecule to the target receptors by performing blind docking. All analyses were performed using a standard protocol.[16]

A grid of 50 points each in x, y, and z directions was chosen for the docking to accommodate any possible ligand-receptor complex in our blind docking approach. The lower the value of ΔG indicates better the binding affinities between the target and the novel ligand molecule.

Visualization

The graphical user interface of the PyMOL tool was used to visualize structure files and the protein-ligand interactions were prepared in LigPlot.[17]

No statistical analysis was performed in this study.

RESULTS

SARS-CoV-2 viral genome structure

SARS-CoV-2 is a spherical, non-segmented enveloped virus with the largest known ssRNA as the genetic material of approximately 30 kb in length. SARS-CoV-2 Wuhan-Hu-1 isolate with 29,903 bp long RNA was the first full viral genome sequenced (GenBank ID: MN908947.3). The study of the genome sequence indicates that the 5' end is capped and the 3' end is polyadenylated comprising 2 non-coding untranslated regions, structural proteins (S, E, M, and N) (Figure 1). and accessory proteins (ORF1ab) replicase genes. Numerous reading frames encode several proteins. The largest ORF is ORF1a/b, located at the 5' end of the genome, and it encodes 15 nsps (nsp1-10 and nsp12-nsp16).[18]

Target protein sequence and structural analyses

We analysed the physicochemical parameters of the SARS-CoV-2 nsp10-nsp16 protein complex, both the chains separately. The instability index of a protein provides an estimate of the stability of the protein in the test tube. Based on the weight value of different dipeptides, a protein with an instability index smaller than 40 is considered stable. Our results revealed the good stability of this protein complex with an instability index of 25.95 and 34.04 for the two chains of the nsp10-nsp16 complex respectively (Table 2).

Structure evaluation of natural ligand molecules

The chemical structures of our 10 potential antiviral phytochemicals- (A) allicin, (B) ajoene, (C) carvacrol, (D) coumarin, (E) curcumin, (F) menthol, (G) eugenol, (H) theaflavin, (I) ursolic acid, (J) catechin, were obtained from the PubChem repository (Figure 2).

Structure evaluation and validation of nsp10-nsp16 complex receptor

The complex nsp10-nsp16 protein of coronavirus is a protein with two chains: nsp10 is of 142 amino acids long sequence and the other nsp16 is 301 amino acid residues. The experimentally determined structure (X-Ray Diffraction) of our target complex with 1.80 Angstrom resolution crystal structure of nsp16-nsp10 complex was obtained from the (PDB ID: 6W4H) (Figure 3).[19]

To validate the structure, the energy minimization and structural refinement of the above structure of the target was done using YASARA Energy Minimization Server. We could optimize the energy of the structure from 6632175.4 kJ/mol (score, -1.44)

Table 1. Antiviral compounds from plant-derived resources

S. no.	Compound	Source	PubChem CID	Molecular formula	Molecular weight
1	Coumarin	Lico rice	323	C9H6O2	146.14 g/mol
2	Carvacrol	Ajwain	10364	C10H14O	150.22 g/mol
3	Menthol	Mentha	1254	C10H20O	156.26 g/mol
4	Allicin	Garlic, ginger	65036	C6H10OS2	162.3 g/mol
5	Eugenol	Tulsi	3314	C10H12O2	164.2 g/mol
6	Ajoene	Garlic	5386591	C9H14OS3	234.4 g/mol
7	Catechin	Green tea	9064	C15H14O6	290.27 g/mol
8	Curcumin	Turmeric	969516	C21H20O6	368.4 g/mol
9	Ursolic acid	Tulsi	64945	C30H48O3	456.7 g/mol
10	Theaflavin	Green tea	135403798	C29H24O12	564.5 g/mol

to 330675.5 kJ/mol (score, 0.23) in the refined model. The stereochemistry of the refined model of target nsp10-nsp16 complex was then subjected to ProCheck for stereochemical analysis. The results have been shown on the Ramachandran plot, where most residues (98.8%) were occupying the most favorable region (red), allowed zones (yellow) and the remaining 0.8% of residues were in the generously allowed region (light yellow) followed by only 0.4% residues falling in the most unfavorable zone of the disallowed region (white) (Figure 4).

We also analyzed our protein in the ProSA-web server for protein structure analysis where a good Z score of -7.18 (Figure 5a) was obtained. The high accuracy of our structure was supported by Levitt-Gerstein's (LG) score of 6.388 and Maxus 0.370 extracted in the Protein Quality Predictor (ProQ) (Figure 5b) tool. A ProQ LG score >2.5 suggests the good quality of the model structure. The quality factor for A chain so obtained 98.966 and quality factor for B chain was 96.5035 (Figure 6a, b) in the ERRAT plot (which is used to evaluate and validate the crystal structure of a protein in which the error values are plotted as a function of the sliding 9-residue window location), further ensure the quality and reliability of structure as the higher quality score indicates higher quality. The regions of the structure that may be rejected at the 95% confidence level

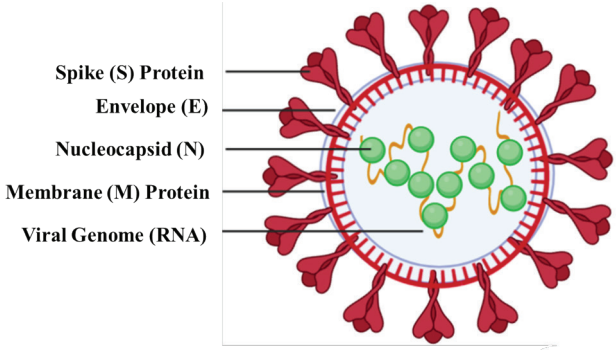

Figure 1. SARS-CoV-2 viral genome structure
SARS-CoV-2: Severe acute respiratory syndrome-coronavirus-2

are represented as yellow bars. The outcomes of our work recommend the stability, quality and reliability of the target protein structure.

Docking analysis of SARS-CoV-2 nsp10-nsp16 protein complex with plant-derived ligands

Earlier studies on the nsp10-nsp16 complex of coronavirus suggest that this complex is crucial for replicating the virus in hosts.[20] In this study, we selected the most recent structure of the nsp10-nsp16 complex of SARS-CoV-2 from PDB and performed the docking analysis of this target with 10 selected compounds obtained from the natural origin showing inhibitory effects for viral infections. Our study using *in silico* docking tools also confirmed the findings inhibitory properties of 10 selected natural compounds against target protein (nsp10-nsp16) in multiple conformations with the given range of binding energies (Table 3). The docking interactions profile of 10 selected natural antiviral compounds with nsp10-nsp16 protein complex of SARS-CoV-2 can be easily understood by the interaction of their ligands with the active site residues of receptors by forming hydrogen bonds drawn by LigPlot (Figure 7).

Our study shows that 7 out of 10 selected anti-viral natural compounds demonstrated remarkable results in our docking analysis with binding energies less than the upper threshold (-6kcal/mol), of generally accepted cut-off in ligand-binding/docking studies.[21] Our research reveals that theaflavin and catechin are the most promising candidates among all selected natural compounds we screened against the nsp10-nsp16 protein complex. The ligand theaflavin, a polyphenolic compound, docks with the target protein complex with the least binding energy of -11.8 kcal/mol. The theaflavin ligand interacts with the target molecule by forming a hydrogen bond with Ala285, Asp289, Gly283, Arg4, and Lys5 amino acid. The polyphenolic compound catechin ligand was found to interact with the target nsp10-nsp16 complex with binding energy of -9.2 kcal/mol. The major amino acid residues involved in the hydrogen bonds between the ligand and receptor are Arg4, Glu288, Lys5 and Gln127. Both these significant polyphenolic natural compounds

Table 2. Physicochemical parameters of SARS-CoV-2 nsp10-nsp16 complex

S. no.	Parameters	SARS-CoV-2 nsp16	SARS-CoV-2 nsp10
1	Molecular weight	33595.58	15062.19
2	Number of amino acids	301	142
3	Theoretical pI	7.59	6.23
4	Instability index (II)	25.95	34.04
5	Number of negatively charged residues (Asp + Glu)	26	11
6	Number of positively charged residues (Arg + Lys)	27	10
7	Aliphatic index	90.07	61.2
8	Grand average of gydropathicity	-0.093	-0.084
9	Atomic composition	C 1503, H 2347, N 397, O 442, S 17	C 646, H 1007, N 177, O 204, S 17

SARS-CoV-2: Severe acute respiratory syndrome-coronavirus-2

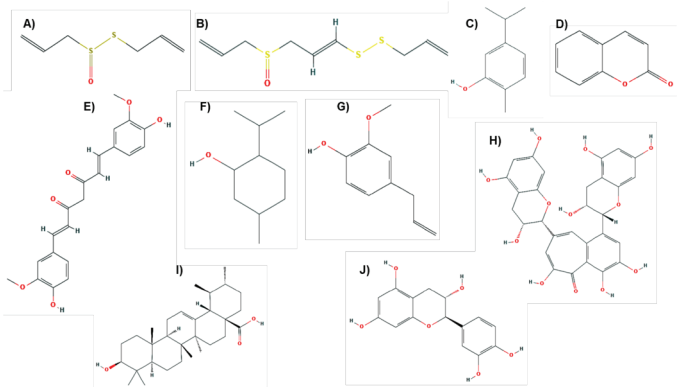

Figure 2. Chemical structures of 10 selected natural compounds with antiviral properties (A) allicin, (B) ajoene, (C) carvacrol, (D) coumarin, (E) curcumin, (F) menthol, (G) eugenol, (H) theaflavin, (I) ursolic acid, (J) catechin

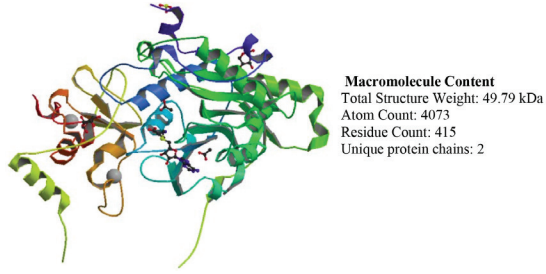

Figure 3. Target protein structure (3-D) of nsp10-nsp16 complex of SARS-CoV-2

SARS-CoV-2: Severe acute respiratory syndrome-coronavirus-2

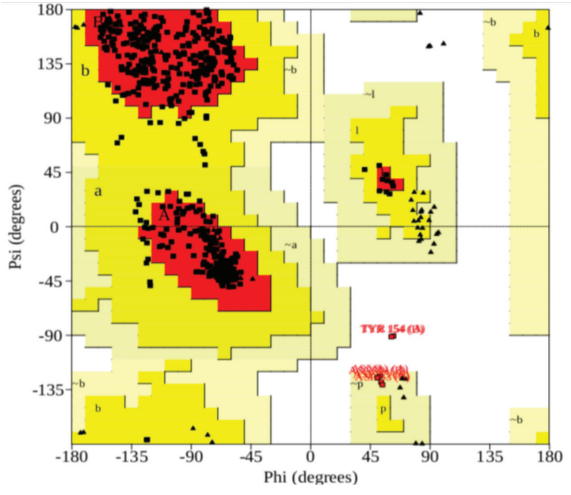

Figure 4. Ramachandran plot of target protein structure (the red, dark yellow, and light-yellow and white regions represent the most favoured, allowed, and generously allowed and disallowed regions respectively)

with anti-viral properties are present in green tea (catechin) and black tea (theaflavin) in a high amount.[6]

Our docking studies further revealed that ursolic acid, an active component of *O. sanctum* (tulsi) secures the third-lowest binding energy of -8.5 kcal/mol. It interacts with the receptor molecule by forming five hydrogen bonds with Glu288, Asp289, Lys137, Arg131, Thr199. Ursolic acid is used in Ayurveda for treating many diseases including swine flu, H1N1 flu, etc. and

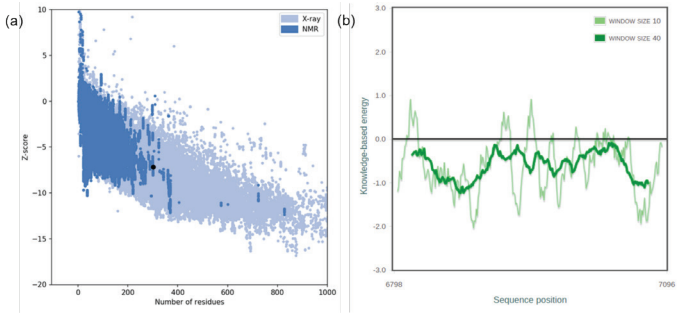

Figure 5. (a) ProSA-web Z-scores of target protein [all protein chains in protein data bank determined by X-ray crystallography (light blue) and nuclear magnetic resonance spectroscopy (dark blue) with respect to their length]. The black dot in the dark blue region represents the Z-score of our target; (b) energy plot for the nsp10-nsp16 complex of SARS-CoV-2

SARS-CoV-2: Severe acute respiratory syndrome-coronavirus-2

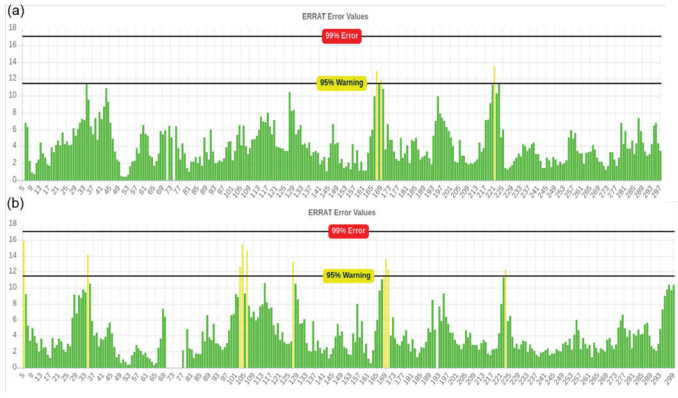

Figure 6. (a) ERRAT plot of nsp10 receptor protein chain, (b) ERRAT plot of nsp16 receptor protein chain

has tremendous antimicrobial properties.[22]

Curcumin is a strong antioxidant with anti-viral properties,[23] and was found to have a binding energy of -6.1 kcal/mol in our docking studies. Amino acids Lys137, Arg4, and Lys5 were involved in the hydrogen bond formation of curcumin with the target protein. Further, the interaction binding energy of menthol and nsp10-nsp16 complex was found to be -6 kcal/mol with only one hydrogen bond with Lys5 amino acid residues. Menthol, the principal component of the oil of *M. piperita* is known for its antimicrobial and antiviral activities. Its virucidal potential against certain viruses like herpes, influenza is already proved *in vitro*.[22] Carvacrol is a component of essential oils obtained from *Trachyspermum ammi* commonly known as 'ajwain and is commonly used to treat cold, cough, influenza, and asthma. With binding energy of -6.5 kcal/mol, carvacrol shows promising interaction with our target *via* amino acid Arg4. Coumarin is a colorless natural compound with a unique flavor and fragrance. It is majorly found in "Cassia cinnamon." Coumarin is found to interact with the nsp10-nsp16 target complex with the amino acids Arg4 and Lys5 having binding energy of -6.1 kcal/mol.

DISCUSSION

Medicinal plants have been widely used to treat many diseases ruled by viruses as pathogens. We evaluated 10 common

Table 3. Docking results revealing polar contact information and binding energy of different ligands with nsp10-nsp16 protein target of SARS-CoV-2

S. no.	Ligand	Binding eneregy	Residues	Atoms	Distance
1	Theaflavin	-11.8	Ala285 Asp289 Gly283 Arg4 Lys5	O3 - O O1 - O11 N - O6 O13 - O O5 - O	3.01 2.73 3.93 2.33 2.89
2	Cathechin	-9.2	Arg4 Glu288 Lys5 Gln127	O2 - NE O2 - NH2 O2 - O O5 - N OE2 - O3	3.00 2.80 2.88 3.07 3.09
3	Ursolic acid	-8.5	Glu288 Asp289 Lys137 Arg131 Thr199	OE2 - O1 OE1 - O1 O2 - OD2 O2 NH2 O3 - NZ	2.96 2.97 2.33 2.92 3.17
4	Carvacol	-6.5	Arg4	O1 - NE O1 -NH2	3.31 2.90
5	Curcumin	-6.1	Lys137 Ar 4 Lys5	O4 -NZ O3 - NE O3 - NH2 O1 - NE O3 - O	3.22 3.05 2.93 3.03 2.86
6	Coumarin	-6.1	Lys5 Ar 4	O2 - NZ O1 - NH2	3.20 2.83
7	Menthol	-6	Lys5	O1 - O	3
8	Eugnol	-5.9	Arg4	O1 - NE O1 - NH2 O2 - NH2	3.17 2.91 3.01
9	Ajoene	-4.7	Gln127	N - O4	2.99
10	Allicin	-4	Arg4 Lys5	O3 - N O3 - NE O3 - NH2	2.98 2.84 3.13

SARS-CoV-2: Severe acute respiratory syndrome-coronavirus-2

antiviral natural compounds namely allicin, ajoene, carvacrol, catechin, coumarin, curcumin, menthol, eugenol, theaflavin, and ursolic acid, out of which 7 natural compounds (Table 3) demonstrated significant results in computational analysis with binding energies less than the upper threshold (-6 kcal/mol), which is a generally accepted cut-off in ligand-binding /docking studies.[21] The binding affinity for the SARS-CoV-2 nsp10-nsp16 complex was observed lowest in the case of Theaflavin (-11.8 kcal/mol) to highest (-4 kcal/mol) for allicin. The seven natural compounds that fall in the acceptable range of binding energy are theaflavin (-11.8), catechin (-9.2), ursolic acid (-8.5), carvacrol (-6.5), curcumin (-6.1), coumarin (-6.1), and menthol (-6). Our molecular docking studies confirmed that the compounds present in tea (catechin in green tea and theaflavin in black tea) can inhibit infections from SARS-CoV-2.

Tea is one of the most commonly consumed beverages across the world and its health-promoting attributes are already validated by scientific interventions decades ago. These health benefits of tea are governed by the presence of polyphenols (flavonoids) and phytochemicals in them. Tea is prepared from the *Camellia sinensis* plant by harvesting and transforming the leaves into green tea or black tea by altering the flavonoid content in them.

Green tea is rich in catechin polyphenolic compounds. Catechin is already known for its health benefits including its antitumor, antioxidative, and antimicrobial activities.[24] The major components of catechin are epicatechin, epicatechin gallate, epigallocatechin and epigallocatechin gallate (EGCG). ECCG is considered the main active constituent of green tea. GTCs have shown significant inhibitory activities against various viruses, such as human viruses,[25] arboviruses, such as Zika virus, etc.[26] In our study, we found significant binding energy of -9.2 kcal/mol between this compound with our target molecule through its amino acids Arg4, Glu288, Lys5, and Gln12.

Oxidation and dimerization of the green tea catechins form an orange-red pigment called theaflavin (black tea), a flavanol, which is a mixture of theaflavin (TF1), theaflavin-3-gallate (TF2A), theaflavin-3'-gallate (TF2B) and theaflavin-3,3'-digallate (TF3). These derivatives have exhibited potent inhibitory effects on the influenza virus *in vitro*.[27] Theaflavins have been shown in our research to interact significantly with the receptors nsp10-nsp16 complex with amino acid residues Ala285, Asp289, Gly283, Arg4, and Lys5 with the highest binding energy of -11.8 kcal/mol. Its broad-spectrum biological properties include anti-tumor, anti-viral, anti-inflammatory, anti-oxidative, and anti-bacterial properties.[28,29]

Our body fight infections through its innate immunity to diminish disease progression. The impairment of our immune system results in disrupted signaling pathways upregulating the pro-inflammatory cytokines like interleukin-6, which may result in tissue injury and apoptosis. Theaflavin serves a dual purpose in fighting infection. Besides its function to act against the viral target protein, theaflavin also acts as a nutritional modulator and enhancer of human innate immunity response.

Hence, our *in silico* analysis advocates the usage of natural anti-viral compounds against SARS-CoV-2 to uncover their inhibitory potential to provide the first line of protection against this deadly virus. Our study also offers potential candidates (theaflavin & catechin) for repurposing them as successful therapeutic drugs in time, after comprehensive studies provided *in vitro* and *in vivo* validation studies are taken up.

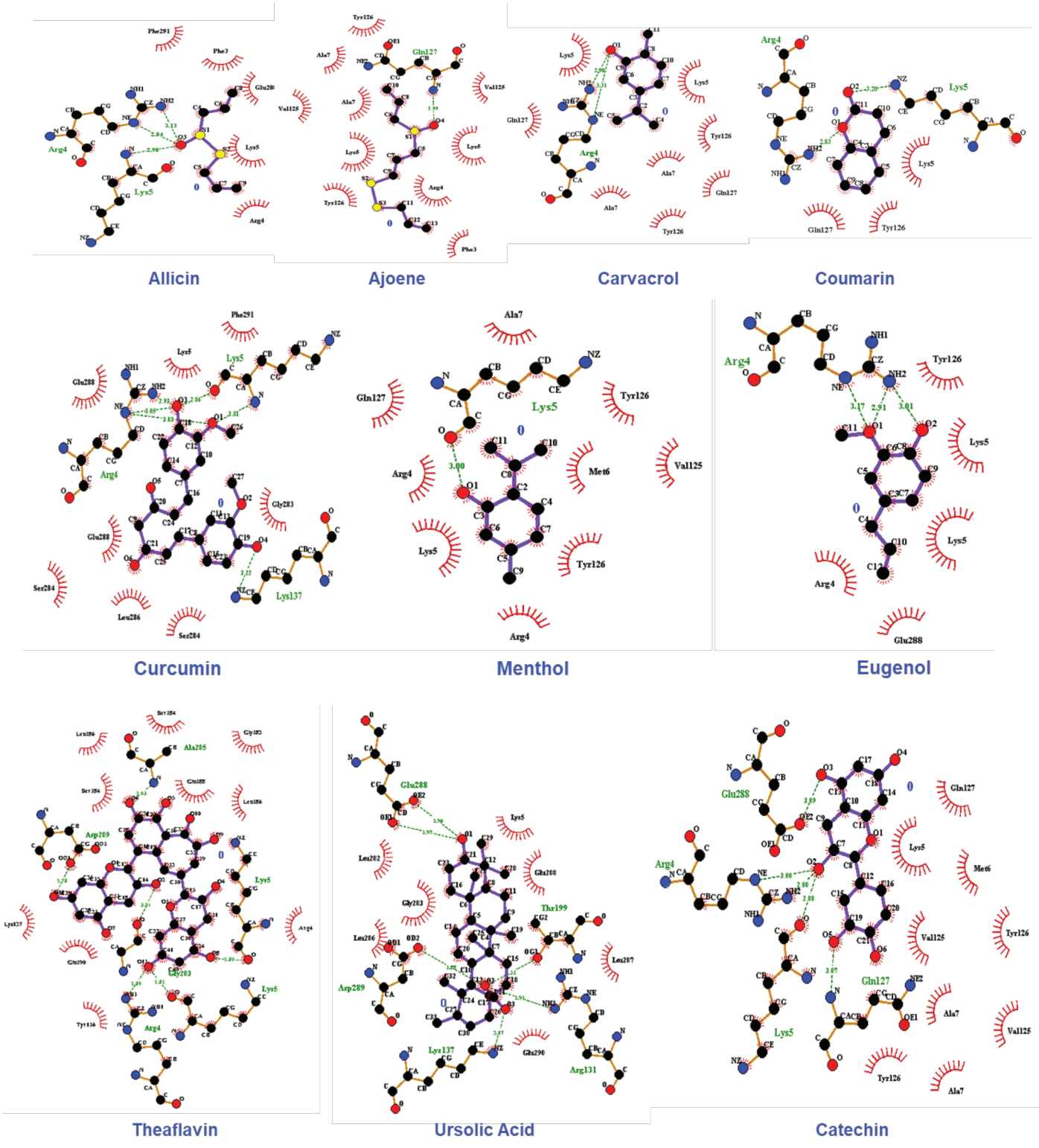

Figure 7. Interaction profile of 10 natural antiviral compounds with nsp10-16 protein complex of SARS-CoV-2 showing the interaction of ligands with the active site residues of receptors by forming hydrogen bonds drawn by LigPlot. In the above illuastration, Ligands are colored in purple, hydrogen bonds are represented as green dash lines, and hydrophobic contacts are represented as red arcs

SARS-CoV-2: Severe acute respiratory syndrome-coronavirus-2

CONCLUSION

The recent outbreak of the pandemic SARS-CoV-2 has devastated the human population due to the unavailability of potential drugs/vaccines to inhibit the virus. This serious issue has raised immediate need to promising drug candidates to combat this epidemic. It is quite evident to use plant-derived drugs against many viral infections. Many herbal molecules have significantly reduced the viral growth majorly targeting

3CL^{pro}, PL^{pro}, S, and angiotensin-converting enzyme 2 of SARS-CoV.We have performedi *in silico* docking methods against a novel target of the SARS-CoV-2, nsp10-nsp16 complex to identify their inhibitory molecular interaction against the virus to assist rapid drug designing from natural products. Theaflavin and catechin, the natural components of black tea and green tea have shown excellent performance in our docking studies with the minimum binding energy of -11.8 kcal/mol and -9.2 kcal/mol respectively. The lesser the value of the binding energy corresponds to a better binding affinity and thus it can be concluded that either consumption of black tea and green tea or repurposing them as drug candidates may help individuals fight against SARS-CoV-2, subject to their *in vivo* and *in vitro* further validatory steps.

Conflict of interest: No conflict of interest was declared by the authors. The authors are solely responsible for the content and writing of this paper.

REFERENCES

1. Zhou P, Yang XL, Wang XG, Hu B, Zhang L, Zhang W, Si HR, Zhu Y, Bei Li B, Huang CL, Chen HD, Chen J, Luo Y, Guo H, Jiang RD, Liu MQ, Chen Y, Shen XR, Wang X, Zheng XS, Zhao K, Chen QJ, Deng F, Liu LL, Yan B, Zhan FX, Wang YY, Xiao GF, Shi ZL. A pneumonia outbreak associated with a new coronavirus of probable bat origin. Nature. 2020;579:270-273.
2. Cucinotta D, Vanelli M. WHO Declares COVID-19 a Pandemic. Acta Biomed. 2020;91:157-160.
3. Yin Y, Wunderink RG. MERS, SARS and other coronaviruses as causes of pneumonia. Respirology. 2018;23:130-137.
4. Anand K, Ziebuhr J, Wadhwani P, Mesters JR, Hilgenfeld R. Coronavirus main proteinase (3CLpro) structure: basis for the design of anti-SARS drugs. Science. 2003;300:1763-1767.
5. Vithani N, Ward MD, Zimmerman MI, Novak B, Borowsky JH, Singh S, Bowman GR. SARS-CoV-2 Nsp16 activation mechanism and a cryptic pocket with pan-coronavirus antiviral potential. bioRxiv [Preprint]. 2020. doi: 10:2020.12.10.420109.
6. Yiannakopoulou ECh. Recent patents on antibacterial, antifungal and antiviral properties of tea. Recent Pat Antiinfect Drug Discov. 2012;7:60-65.
7. Sahoo M, Jena L, Rath SN, Kumar S. The identification of suitable natural inhibitor against influenza A (H1N1) neuraminidase protein by molecular docking. Genomics Inform. 2016;14:96-103.
8. Trott O, Olson AJ. AutoDock Vina: improving the speed and accuracy of docking with a new scoring function, efficient optimization, and multithreading. J Comput Chem. 2010;31:455-461.
9. Gasteiger E, Gattiker A, Hoogland C, Ivanyi I, Appel RD, Bairoch A. ExPASy: the proteomics server for in-depth protein knowledge and analysis. Nucleic Acids Res. 2003;31:3784-3788.
10. Krieger E, Joo K, Lee J, Lee J, Raman S, Thompson J, Tyka M, Baker D, Karplus K. Improving physical realism, stereochemistry, and side-chain accuracy in homology modeling: four approaches that performed well in CASP8. Proteins. 2009;(Suppl 9):114–122.
11. Laskowski RA, MacArthur MW, Moss DS, Thornton JM. PROCHECK: a program to check the stereochemical quality of protein structures. J Appl Crystallogr. 1993;26:283-291.
12. Wiederstein M, Sippl MJ. ProSA-web: interactive web service for the recognition of errors in three-dimensional structures of proteins. Nucleic Acids Res. 2007;(Web Server issue):W407-W410.
13. Wallner B, Elofsson A. Can correct protein models be identified? Protein Sci. 2003;12:1073-1086.
14. Colovos C, Yeates TO. Verification of protein structures: patterns of nonbonded atomic interactions. Protein Sci. 1993;2:1511-1519.
15. Torkamani A, Andersen KG, Steinhubl SR, Topol EJ. High-definition medicine. Cell. 2017;170:828-843.
16. Morris GM, Huey R, Lindstrom W, Sanner MF, Belew RK, Goodsell DS, Olson AJ. AutoDock4 and AutoDockTools4: Automated docking with selective receptor flexibility. J Comput Chem. 2009;30:2785-2791.
17. Wallace AC, Laskowski RA, Thornton JM. LIGPLOT: a program to generate schematic diagrams of protein-ligand interactions. Protein Eng. 1995;8:127-134.
18. Mittal A, Manjunath K, Ranjan RK, Kaushik S, Kumar S, Verma V. COVID-19 pandemic: insights into structure, function, and hACE2 receptor recognition by SARS-CoV-2. PLoS Pathog. 2020;16:e1008762.
19. Rosas-Lemus M, Minasov G, Shuvalova L, Inniss NL, Kiryukhina O, Brunzelle J, Satchell KJF. High-resolution structures of the SARS-CoV-2 2′-*O*-methyltransferase reveal strategies for structure-based inhibitor design. Sci Signal. 2020;13:eabe1202.
20. Wang Y, Sun Y, Wu A, Xu S, Pan R, Zeng C, Jin X, Ge X, Shi Z, Ahola T, Chen Y, Guo D. Coronavirus nsp10/nsp16 methyltransferase can be targeted by nsp10-derived peptide *in vitro* and *in vivo* to reduce replication and pathogenesis. J Virol. 2015;89:8416-8427.
21. Mukhtar M, Arshad M, Ahmad M, Pomerantz RJ, Wigdahl B, Parveen Z. Antiviral potentials of medicinal plants. Virus Res. 2008;131:111-120.
22. Naik GH, Priyadarsini KI, Naik DB, Gangabhagirathi R, Mohan H. Studies on the aqueous extract of *Terminalia chebula* as a potent antioxidant and a probable radioprotector. Phytomedicine. 2004;11:530-538.
23. Praditya D, Kirchhoff L, Brüning J, Rachmawati H, Steinmann J, Steinmann E. Anti-infective properties of the golden spice curcumin. Front Microbiol. 2019;10:912.
24. Chacko SM, Thambi PT, Kuttan R, Nishigaki I. Beneficial effects of green tea: a literature review. Chin Med. 2010;5:13.
25. Ide K, Kawasaki Y, Kawakami K, Yamada H. Anti-influenza virus effects of catechins: a molecular and clinical review. Curr Med Chem. 2016;23:4773-4783.
26. Carneiro BM, Batista MN, Braga ACS, Nogueira ML, Rahal P. The green tea molecule EGCG inhibits Zika virus entry. Virology. 2016;496:215-218.
27. Zu M, Yang F, Zhou W, Liu A, Du G, Zheng L. *In vitro* anti-influenza virus and anti-inflammatory activities of theaflavin derivatives. Antiviral Res. 2012;94:217-224.
28. Yang CS, Landau JM. Effects of tea consumption on nutrition and health. J Nutr. 2000;130:2409-2412.
29. Higdon JV, Frei B. Tea catechins and polyphenols: health effects, metabolism, and antioxidant functions. Crit Rev Food Sci Nutr. 2003;43:89-143.

Turk J Pharm Sci 2022;19(1):101-103
DOI: 10.4274/tjps.galenos.2021.63060

SHORT COMMUNICATION

Multi-drug Treatment for COVID-19-induced Acute Respiratory Distress Syndrome

COVID-19 Kaynaklı Akut Solunum Sıkıntısı Sendromu için Çoklu İlaç Tedavisi

Masashi OHE*

Jcho Hokkaido Hospital, Clinic of Internal Medicine, Sapporo, Japan

ABSTRACT

Coronavirus disease-2019 (COVID-19), caused by severe acute respiratory syndrome-coronavirus-2 (SARS-CoV-2), broke out in late 2019 to become a serious global threat to human health. In the absence of specific treatments for COVID-19, treatment options are being examined. Recently, the anti-SARS-CoV-2 activities of tetracyclines, macrolide antibiotics, and ivermectin (IVM), have attracted considerable attention for their potential as a single or multi-drug treatment regimen. Moreover, tetracyclines, macrolide antibiotics, and IVM possess anti-inflammatory and immunomodulatory effects to reduce the production of cytokines. COVID-19 is characterized by early exponential viral replication, cytokine storm-associated organ damage, including acute respiratory distress syndrome (ARDS) and thrombosis. Considering anti-inflammatory and immunomodulatory effects of the aforementioned drugs and corticosteroids, early treatment with doxycycline, azithromycin, IVM, and corticosteroids is thought to be the most promising option for combating COVID-19-induced ARDS.

Key words: COVID-19, doxycycline, azithromycin, ivermectin, corticosteroid

ÖZ

Şiddetli akut solunum yolu sendromu-koronavirüs-2'nin (SARS-CoV-2) neden olduğu Koronavirüs hastalığı-2019 (COVID-19), 2019'un sonlarında patlak vererek insan sağlığı için ciddi bir küresel tehdit haline gelmiştir. COVID-19 için spesifik tedavilerin yokluğunda tedavi seçenekleri inceleniyor. Son zamanlarda, tetrasiklinlerin, makrolid antibiyotiklerin ve ivermektinin (IVM) anti-SARS-CoV-2 aktiviteleri, tek veya çoklu ilaç tedavi rejimi olarak potansiyelleri nedeniyle büyük ilgi görmüştür. Dahası, tetrasiklinler, makrolid antibiyotikler ve IVM sitokin üretimini azaltmak için anti-inflamatuar ve immünomodülatör etkilere sahiptir. COVID-19, erken üstel viral replikasyon, akut solunum sıkıntısı sendromu (ARDS) ve tromboz dahil sitokin fırtınası ile ilişkili organ hasarı ile karakterizedir. Bahsi geçen ilaçların ve kortikosteroidlerin antiinflamatuar ve immünomodülatör etkileri göz önüne alındığında, doksisiklin, azitromisin, IVMve kortikosteroidlerle erken tedavinin, COVID-19 kaynaklı ARDS ile mücadelede en umut verici seçenek olduğu düşünülmektedir.

Anahtar kelimeler: COVID-19, doksisiklin, azitromisin, ivermektin, kortikosteroid

INTRODUCTION

Coronavirus disease-2019 (COVID-19), caused by severe acute respiratory syndrome-coronavirus-2 (SARS-CoV-2), broke out in late 2019 to become a serious global threat to human health. In the absence of specific treatments for COVID-19, treatment options are being examined. Recently, the anti-SARS-CoV-2 activities of tetracyclines [*e.g.*, doxycycline (DOX)], macrolide antibiotics [*e.g.*, azithromycin (AZM), and clarithromycin (CAM)], and macrolide antiparasitic [*e.g.*, ivermectin (IVM)], have attracted considerable attention for their potential as a single or multi-drug treatment regimen.

Apart from anti-SARS-CoV-2 activities, DOX, AZM, and IVM possess anti-inflammatory and immunomodulatory effects to reduce the production of interleukin-6 (IL-6), IL-8, and tumor necrosis factor-α (TNF-α); IL-1, IL-6, IL-8, and TNF-α; and IL-1, IL-6, and TNF-α, respectively.[1-3]

*Correspondence: oektsp1218@sweet.ocn.ne.jp, Phone: +07069574159, ORCID-ID: orcid.org/0000-0002-6684-6688

Received: 19.07.2021, Accepted: 06.09.2021

In single-drug treatment studies in COVID-19, DOX,[4] CAM,[5] and IVM[6] have proven effective against COVID-19.

In multi-drug treatment studies, Alam et al.[7] found that a combination of IVM and DOX was effective for viral clearance in patients with mild and moderate COVID-19. Prasad[8] reported on a patient where COVID-19 accompanied by pulmonary lesion was successfully treated with the early administration of IVM (6 mg twice daily for 3 days), AZM (500 mg daily for 5 days), DOX (100 mg twice daily for 5 days), and prednisolone (50 mg daily for 5 days) followed by dexamethasone (6 mg daily).

The primary purpose of the aforementioned drug treatments is to improve mild and moderate COVID-19 cases and prevent them from further deteriorating into the severe, life-threatening stage. Severe COVID-19 involves cytokine storm-associated organ damage, including acute respiratory distress syndrome (ARDS). Elevated blood levels of IL-6, IL-8, IL-10, and TNF-α were noted in COVID-19-induced ARDS,[9] which was effectively treated with cytokine storm suppression, either using IL-6 inhibitor tocilizumab (TCZ)[10] or a combination of TCZ and IVM.[11]

Corticosteroids known to reduce the production of IL-6, IL-8, IL-10, and TNF-α,[12] were also found to reduce mortality in the patients with COVID-19-induced-ARDS and non-COVID-19-induced ARDS.[13]

Tetracycline treatment within a year before ARDS diagnosis was associated with 75% reduced likelihood for mechanical ventilation during a hospital stay.[14] Furthermore, tetracycline treatment corresponded to significant reductions in the length of mechanical ventilation use and intensive care unit stay in patients with ARDS.[14] Although this study was conducted in patients with non-COVID-19, these results suggest that tetracycline is effective for COVID-19-induced ARDS. Additionally, treatment with macrolide antibiotics has also been associated with reduced mortality in ARDS.[15]

Multi-drug treatment is thought to be more effective than single-drug treatment because of the synergistic effect of the different mechanisms of action of the component drugs.[16]

Taken together, from a medical economic standpoint, early treatment with IVM, DOX, AZM, and corticosteroids may be the most promising option for combating COVID-19-induced ARDS.

However, clinical trials need to be conducted to better assess the optimal doses and durations for these medications as well as the efficacy and tolerability of this treatment before it can be implemented on a wider scale.

Conflict of interest: No conflict of interest was declared by the author. The author is solely responsible for the content and writing of this paper.

REFERENCES

1. Bernardino AL, Kaushal D, Philipp MT. The antibiotics doxycycline and minocycline inhibit the inflammatory responses to the Lyme disease spirochete Borrelia burgdorferi. J Infect Dis. 2009;199:1379-1388.
2. Zimmermann P, Ziesenitz VC, Curtis N, Ritz N. The Immunomodulatory effects of macrolides-a systematic review of the underlying mechanisms. Front Immunol. 2018;9:302.
3. Zhang X, Song Y, Ci X, An N, Ju Y, Li H, Wang X, Han C, Cui J, Deng X. Ivermectin inhibits LPS-induced production of inflammatory cytokines and improves LPS-induced survival in mice. Inflamm Res. 2008;57:524-529.
4. Gironi LC, Damiani G, Zavattaro E, Pacifico A, Santus P, Pigatto PDM, Cremona O, Savoia P. Tetracyclines in COVID-19 patients quarantined at home: literature evidence supporting real-world data from a multicenter observational study targeting inflammatory and infectious dermatoses. Dermatol Ther. 2021;34:e14694.
5. Tsiakos K, Tsakiris A, Tsibris G, Voutsinas P, Panagopoulos P, Kosmidou M, Petrakis V, Gravvani A, Gkavogianni T, Klouras E, Katrini K, Koufargyris P, Rapti I, Karageorgos A, Vrenzos E, Damoulari C, Zarkada V, Sidiropoulou C, Artemi S, Ioannidis A, Papapostolou A, Michelakis E, Georgiopoulou M, Myrodia DM, Tsiamalos P, Syrigos K, Chrysos G, Nitsotolis T, Milionis H, Poulakou G, Giamarellos-Bourboulis EJ. Oral clarithromycin in COVID-19 of moderate severity: the ACHIEVE open label trial using concurrent matched comparators medRxiv. doi: 10.1101/2020.12.22.20248753.
6. Ahmed S, Karim MM, Ross AG, Hossain MS, Clemens JD, Sumiya MK, Phru CS, Rahman M, Zaman K, Somani J, Yasmin R, Hasnat MA, Kabir A, Aziz AB, Khan WA. A five-day course of ivermectin for the treatment of COVID-19 may reduce the duration of illness. Int J Infect Dis. 2021;103:214-216.
7. Alam MT, Murshed R, Bhiuyan E, Saber S, Alam RF, Robin RC. A case series of 100 COVID-19 positive patients treated with combination of ivermectin and doxycycline. Bangladesh Coll Phys Surg. 2020;38(Supplement Issue):10-15.
8. Prasad A. Early administration of ivermectin, azithromycin & doxycycline along with *i.v.* prednisolone in a case of COVID -19 disease may lead to early recovery? Int J Pharm Chem Anal. 2020;7:149-150.
9. Wang J, Yang X, Li Y, Huang JA, Jiang J, Su N. Specific cytokines in the inflammatory cytokine storm of patients with COVID-19-associated acute respiratory distress syndrome and extrapulmonary multiple-organ dysfunction. Virol J. 2021;18:117.
10. Menzella F, Fontana M, Salvarani C, Massari M, Ruggiero P, Scelfo C, Barbieri C, Castagnetti C, Catellani C, Gibellini G, Falco F, Ghidoni G, Livrieri F, Montanari G, Casalini E, Piro R, Mancuso P, Ghidorsi L, Facciolongo N. Efficacy of tocilizumab in patients with COVID-19 ARDS undergoing noninvasive ventilation. Crit Care. 2020;24:589.
11. Chuang TY, Tsai MH, Wu LM, Ho SJ, Yeh PS, Liu YL, Fred Yang HJ. Successful treatment of tocilizumab and ivermectin for a patient with ARDS due to COVID-19. J Microbiol Immunol Infect. 2020;54:147-148.
12. Giamarellos-Bourboulis EJ, Dimopoulou I, Kotanidou A, Livaditi O, Pelekanou A, Tsagarakis S, Armaganidis A, Orfanos SE. *Ex-vivo* effect of dexamethasone on cytokine production from whole blood of septic patients: correlation with disease severity. Cytokine. 2010;49:89-94.
13. Chaudhuri D, Sasaki K, Karkar A, Sharif S, Lewis K, Mammen MJ, Alexander P, Ye Z, Lozano LEC, Munch MW, Perner A, Du B, Mbuagbaw L, Alhazzani W, Pastores SM, Marshall J, Lamontagne F, Annane D, Meduri GU, Rochwerg B. Corticosteroids in COVID-19 and non-COVID-19 ARDS: a systematic review and meta-analysis. Intensive Care Med. 2021;47:521-537.

14. Byrne JD, Shakur R, Collins JE, Becker S, Young CC, Boyce H, Traverso G. Prophylaxis with tetracyclines in ARDS: Potential therapy for COVID-19-induced ARDS? medRxiv. doi: 10.1101/2020.07.22.20154542.

15. Simonis FD, de Iudicibus G, Cremer OL, Ong DSY, van der Poll T, Bos LD, Schultz MJ; MARS consortium. Macrolide therapy is associated with reduced mortality in acute respiratory distress syndrome (ARDS) patients. Ann Transl Med. 2018;6:24.

16. Ohe M, Furuya K, Goudarzi H. Multidrug treatment for COVID-19. Drug Discov Ther. 2021;15:39-41.

Turk J Pharm Sci 2022;19(1):104-109
DOI: 10.4274/tjps.galenos.2020.89577

REVIEW

Resveratrol Delivery *via* Gene Therapy: Entering the Modern Era

Gen Terapisi Yoluyla Resveratrol İletimi: Modern Çağa Girme

Gurinder SINGH*

Micro Labs GmbH, Frankfurt, Germany

ABSTRACT

Resveratrol is a natural compound (an antioxidant) and exhibits numerous therapeutic activities. From a pharmacokinetic perspective, it is unclear whether resveratrol targets the site of action after oral administration because of quick metabolism and excretion that creates doubt on the biological application of the high doses characteristically used for clinical trials. However, these limitations act as a barrier and a challenge for the development of new delivery systems. Recently, gene delivery offers various advantages and has provided treatment options for diseases that are beyond the reach of traditional approaches. The objective of gene therapy for genetic diseases is to achieve durable expression of the therapeutic gene at a level sufficient to alleviate or cure disease symptoms with minimal adverse events. The perception of the molecular and cellular mechanisms steering to therapy and vector-related hindrances have caused in the progress of extremely complex gene delivery with enhanced protection and effectiveness. With the help of gene therapy, it could be possible to target the delivery of resveratrol directly into the host cells and bypass its pharmacokinetic limitations and enhancement of its therapeutic effect. This review is to provide a holistic view of the development of resveratrol gene treatment as a powerful option to treat various deadly diseases.

Key words: Gene therapy/delivery, lentivirus, resveratrol, viral vectors

ÖZ

Resveratrol, doğal bir bileşiktir (bir antioksidan) ve çok sayıda terapötik aktivite sergiler. Farmakokinetik bir perspektiften, resveratrolün, klinik deneyler için karakteristik olarak kullanılan yüksek dozlarının biyolojik uygulamasında şüphe yaratan hızlı metabolizma ve atılım nedeniyle oral uygulamadan sonra etki alanını hedefleyip hedeflemediği açık değildir. Bununla birlikte, bu sınırlamalar, yeni dağıtım sistemlerinin geliştirilmesi için bir engel ve zorluk teşkil etmektedir. Son zamanlarda, gen dağıtımının çeşitli avantajlar sağladığı ve geleneksel yaklaşımların ulaşamayacağı hastalıklar için tedavi seçenekleri sağladığı görülmüştür. Genetik hastalıklar için gen terapisinin amacı, minimum yan etki ile hastalık semptomlarını iyileştirmek veya iyileştirmek için yeterli bir seviyede terapötik genin kalıcı ifadesini elde etmektir. Tedaviye yönlendiren moleküler ve hücresel mekanizmaların algılanması ve vektöre bağlı engeller, gelişmiş koruma ve etkililik ile aşırı derecede karmaşık gen dağıtımının ilerlemesine neden olmuştur. Gen terapisinin yardımıyla, resveratrolün doğrudan konakçı hücrelere verilmesini hedeflemek ve farmakokinetik sınırlamalarını ve terapötik etkisinin arttırılmasını atlamak mümkün olabilir. Bu derleme, çeşitli ölümcül hastalıkları tedavi etmek için güçlü bir seçenek olarak resveratrol gen tedavisinin gelişiminin bütünsel bir görünümünü sağlamaktır.

Anahtar kelimeler: Gen tedavisi/doğum, lentivirüs, resveratrol, viral vektörler

INTRODUCTION

Resveratrol is a natural compound separated from *Veratrum grandiflorum* plant, in the 1940s.[1] It is originated in various plants, particularly peanuts, grapes, and berries. Recently, resveratrol enticed several research considerations because of its stimulating pharmacological ability.[2,3] Some clinical studies state that resveratrol can avert and slow down the evolution of an extensive variety of illnesses including cardiovascular disease[4] and HIV/AIDS.[5,6] Nevertheless, beneficial applications of resveratrol are inadequate by virtue of its low biological half-life and rapid metabolism.[7] *In vivo* data designate that the resveratrol bioavailability is practically zero, which mold distrust on the high doses usually used *in vitro*.[8] It is expressed that after an oral administration, the resveratrol bioavailability in systemic circulation and in tissues is very less due to raid

*Correspondence: gurindersinghgermany@gmail.com, ORCID-ID: orcid.org/0000-0003-1525-3898

Received: 20.07.2020, Accepted: 18.10.2020

metabolism.[9] Correspondingly, in the case of nanocarriers, it is a promising approach to be a potential bio-nanocarrier for the drug delivery system. Some recent reports depicted that nanocarriers (to some extent) might be an appropriate transporter for oral administration and released the drug in a controlled manner.[10] Thus, there is an urgent need to develop suitable systems of delivering resveratrol at a site of action, which can protect from diseases and give new hope in the treatment options. Such a system called "gene therapy" is widely available and is under clinical trial consideration.[11]

Gene therapy is the delivery of a genetic substances to a patient to target tissues or cells to treat a disease.[12] Gene therapy is specifically designed to alter the expression of a gene or to modify the biological attributes of cells for beneficial use.[13,14] In the future, this practice might permit specialists to address a syndrome by implanting a gene into a patient's cells in lieu of other drug delivery approaches.[15] It includes the use of nucleic acids for the therapy, heals or preclusion of patient illness.[16] Genetic material is intended to introduce into cells to redress for irregular genes and to produce a beneficial protein. This treatment is capable of presenting a usual copy of the gene to restore the function of the protein if a metamorphosed gene produces a required defective or lost protein.[15] Gene therapy can operate by numerous mechanisms viz. a virus-infected gene can be exchanged with a healthy gene, inactivate the gene caused by disease which is not working appropriately, and to treat a disease, inserting a modified gene into the body.[14,15]

Several approaches for current gene delivery have been developed and classified as viral vectors, non-viral vectors (chemical and physical), and vaccination.[17] Viral vector-based gene delivery systems can deliver genetic material, the most widely used ones are depicted in Table 1. A gene that is introduced directly into a cell typically does not work. Therefore, a transporter named as a vector is hereditarily/genetically engineered to transport the gene.[18] Specific viruses are frequently used as vectors in view of the fact that they may transport the new gene by infecting the cell. The viruses are altered so they cannot induce disease when used in patients.[15,19] Retroviruses consolidate their genetic material (including the new gene) into the cell without altering the cell's own genetic material.[20]

The vector can be injected intravenously, in the body it is then occupied by specific cells. Consecutively, in the laboratory a sample of the patient's cells can be withdrawn and revealed. The cells comprising the vector are then returned to the patient. If the therapy is successful, the novel gene transported by the vector will lead to the production of a functioning protein.[15,21,22] There is a possibility where vector-resveratrol can be delivered to the cells or particular tissues to treat various diseases and enhance the therapeutic potential of resveratrol. Recent reports on resveratrol gene therapy have fascinated attention with 872 articles/manuscripts available on the PubMed portal between 1993 and 2020 are illustrated in Figure 1.[23]

SCOPE OF THE REVIEW

This review attempted on the present inventions of resveratrol gene therapy to augment its therapeutic effect. As per literature survey, this is the first review analysis on resveratrol gene therapy as literature lacks such review data.

DELIVERY OF LENTIVIRAL VECTORS IN GENE THERAPY

Gene therapy carries an excessive possibility for addressing an abundant various diseases, some of which are not curable.[22] A virus called a vector to transport/deliver therapeutic genes into cells is a approach. Viral vectors are expressly altered so they cannot replicate/multiply within the target cells.[24,25] Viruses are compact parasites with either an RNA or DNA genome that are enclosed by a defensive protein coat and transmission their genetic material to infected cells. Lentivirus is a class of retroviruses that causes deadly diseases categorized by long incubation periods. Lentiviral vectors (LVs), derived from HIV, have been broadly examined and considered.[26,27] To accurate main immunodeficiencies and hemoglobinopathies, self-inactivating (third generation) LV has been used in several medical studies to insert genes into hematopoietic stem cells.[28] Because of LV capability to further proficiently transform non-proliferating cells, it has become predominantly attractive for clinical demands.[29] LV present exceptional benefits over diverse gene delivery systems, specifically the capability to incorporate transgenes into the genome of dividing and non-dividing cells.[27]

Table 1. Viral vector for gene delivery

Gene delivery method (viral vectors)	Functional components	Features	Features
Retrovirus	RNA	High efficiency	Random integration
Lentivirus	RNA	High efficiency sustained gene expression	Random integration
Adenovirus	Double stranded DNA	High efficiency, sustained gene expression,	Host inmate immune response
Adenovirus associated virus	Single stranded DNA	Non-pathogenic, sustained gene expression	Integration may happen small volume of transgene
Herps simplex virus	Double stranded DNA	No integration sustained gene expression	Small transduction efficacy

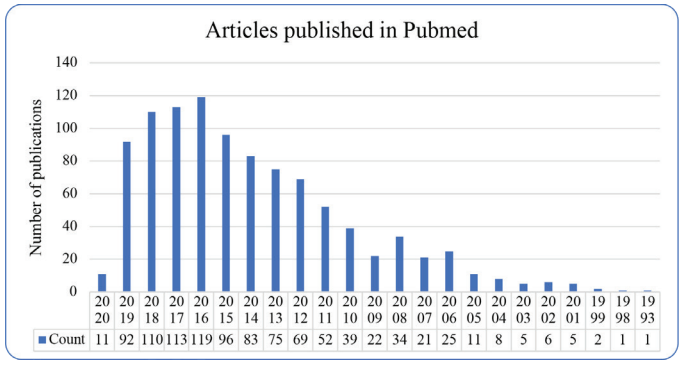

Figure 1. Graphical illustration of publications year wise on resveratrol gene therapy/expression over the last 28 years

Non-integrating vectors, such as adeno-associated viruses (AAV) transduce inactive or slowly dividing cells, as they can be rapidly vanished from dividing cells.[30] The cumulative number of fruitful clinical studies has pushed the progress of gene transfer techniques in various diseases, such as cancer,[31] neurodegenerative,[32] diabetes,[33] HIV/AIDS,[34] and metabolic liver diseases.[35]

EX VIVO GENE TREATMENT

Ex vivo gene treatment includes the collecting of the patient cells accompanied by following viral transduction *ex vivo* in a lab by a virus transporting the therapeutic gene. The cells have been transformed and got back to the patient. Contrary, *in vivo* treatment comprises the inoculation of a virus transporting the healing gene straight into a body.[36] Lentivirus, adenovirus, retrovirus and AAV are the utmost usual viral vectors exploit for *ex vivo* and *in vivo* gene therapy. AAV has numerous exceptional characteristics that turn it a superlative vector for gene delivery. Gene expression for a long period, AAV vectors may dwell for the complete lifecycle of a given cell is highly recommended and used, which reduces the amount of therapy. Contrarily, to carry on a small period (days to weeks) gene expression, adenovirus is classically used in circumstances where the essential level of expression is required.[37,38]

RESVERATROL GENE DELIVERY

Resveratrol performs a valuable character in the inhibition and in the progress of long-lasting diseases such as cardiovascular, cancers, liver disorders, diabetes, neurodegeneration, and many more. The idea of gene treatment is an investigational system that uses genes to cure or stop disease and viruses. The non-existence of appropriate therapy has converted a rational basis for encompassing the possibility of gene therapy.[38,39] Resveratrol gene therapy presents numerous advantages such as, the impact of a treatment is long-lasting and less time consuming and can eliminate diseases and strengthen the quality of life.[39,40] The strategy of new resveratrol gene therapy is to target oxidative stress and redox imbalance could signify imperative beneficial methods towards neurological diseases.[41] Further, resveratrol gene therapy could bring the solution of resveratrol pharmacokinetics limitations which enhances its therapeutic effect.

RESVERATROL GENE THERAPY IN CANCER

Cancer is one of the utmost frequently identified diseases and establishes a substantial illness globally. However, countless efforts have been made to find a therapy but remains an eminent source of mortality in individuals, and effectual therapy/cure remains a terrific challenge.[42,43] Notwithstanding numerous new developments in diagnosis and investigation, the cancer endurance amount has not enhanced. Recently, novel/targeted treatments have developed, providing better results for cancer patients. Existing cancer treatments include chemotherapy, nano-carriers, radiation, and surgery, have boundaries subsequent from the progress of resistance to the therapy.[44] Recently, a substantial volume of investigation has designated that consumption of resveratrol may prevent the development of cancer.[43] Since then researchers have started a resveratrol gene therapy against cancer. Izquierdo-Torres et al.[45] investigated the epigenetic mechanisms of resveratrol-induced ATP2A3 up-regulation. The outcomes designated that approximately 50% decreased in HDAC activity and nuclear HDAC2 expression was observed. Further finding suggests that HAT activity can be increased with resveratrol therapy; nevertheless, pharmacological hindrance of p300, one of the main HATs, have not shown important impacts in resveratrol gene expression.[45] In another study, authors reported the exceptional properties of resveratrol, if they could empower viral vectors, used in gene therapy to deliver genes, to enter blood stem cells more easily. The provisional co-application of resveratrol trimer caraphenol A augments *LV* gene delivery productivity to primate hematopoietic stem. Results showed that the alteration of important immune constraint factors is a capable and non-toxic method to enhance resveratrol LV-mediated gene therapy.[42] Shi et al.[46] reproduced natural or synthetic Egr-1 promoter upstream of GADD45α cDNA to produce a suicide gene therapy vector. Authors analysed that synthetic promoter that comprises of CArG elements important in the Egr-1 promoter to initiative the expression of GADD45α following resveratrol therapy. Results affirmed that both promoters were capable of activating the expression of GADD45α with resveratrol, and consequently directed to the abolition of cell multiplication and apoptosis.[46] Novel peptide-cationic lipid (CDO14) liposome was developed to combine the delivery of resveratrol and *p53* gene for gene transfer capability of resveratrol liposomes and antitumor effect on breast cancer cells was examined. MTT assay demonstrated that combination therapy of resveratrol and p53 had greater progress restraint on breast cancer cells.[47]

Xiao et al.[48] investigated that resveratrol might augment intercellular transmission at the opening intersections in CBRH7919 hepatoma cells and thus boost the spectator killing impact of GCV on CBRH7919TK cells. The outcomes determine that co-treatment of resveratrol and GCV in tumor-bearing mice with CBRH7919TK and CBRH7919WT cells resulted in a momentous reduction in the size and mass of the tumor.[48] DNA methylation on human multidrug resistance gene 1 (MDR1) was scrutinized and the effect of resveratrol and prednisolone on *MDR1* gene agent in the CCRF-CEM cell line was appraised.

Results suggested that in spite of a substantial influence to decrease the MDR1 expression, methylation form was not later by resveratrol and prednisolone, which needs additional studies to understand the mechanisms.[49] Bickenbach et al.[50] stated that resveratrol stimulates the cancer gene therapy vector Ad.Egr. TNF and *in vitro* prevention of SIRT1 activity did not revoke the resveratrol mechanism of Egr-1 expression. The authors concluded that control of transgene expression *via* resveratrol stimulation of Egr-1 might spread the use of Ad. Egr. TNF to candidate indignant of cytotoxic treatment and provide a new means for the progress of further gene therapies.[50]

RESVERATROL GENE THERAPY IN OSTEOGENESIS IMPERFECTA

Osteogenesis imperfecta is an intermittent genetic disorder of bone and connective tissue defined by bone brittleness which results in bones that breakdown effortlessly.[51] It has been reported that *SIRT1* gene as an applicant for therapy of osteogenesis and augments adipogenesis.[52] Some studies speculated that resveratrol may boost osteogenesis through SIRT1, but the mechanism stays uncertain. Tseng et al.[53] investigated and found that resveratrol can modify and promote natural osteogenesis in human mesenchymal stem cells and upregulated the expression of osteo-lineage genes RUNX2. Further, resveratrol triggered SIRT1 action and boosted FOXO3A protein expression, recognised goal of SIRT1. Ectopic overexpression plays a vital character for SIRT1-FOXO3A complex in governing resveratrol-induced *RUNX2* gene transcription. In the end, these results designated that the resveratrol upregulating *RUNX2* gene expression *via* the SIRT1/FOXO3A.[53] The impacts of resveratrol on trauma from occlusion-induced bone loss in mice was investigated. Resveratrol was administered for around 15 days and the impact on bone resorption was evaluated. *In vitro* outcome of resveratrol was assessed on RAW 264.7 cells and macrophages into osteoclastic cells. The authors concluded that resveratrol expressively declined the bone loss and blocked the raised expression of osteoclastogenesis-related gene in periodontal ligament tissue by trauma from occlusion.[54] Zhou et al.[55] studied the resveratrol osteogenic effect on mesenchymal stem cells, AMP-activated protein kinase and reactive oxygen species signaling pathway. Results demonstrated that resveratrol therapy undoubtedly boosted the osteogenic-related genes expression prevented the reactive oxygen species, whereas AMP-activated protein kinase expression was improved by resveratrol.[55] The impact of resveratrol on the gene expression of osteogenic markers was investigated. Two calvarial defects were created and rats were administered resveratrol 10 mg/kg (n=15) for 1 month and placebo (control group, n=15) and sacrificed. Histomorphometric analysis was performed on one calvarial defects and the tissue was collected for mRNA quantification of bone morphogenetic protein. Results confirmed resveratrol augmented the repair of bone defects and may boost the gene expression of significant osteogenic markers.[56]

RESVERATROL GENE THERAPY IN DIABETES

Diabetes mellitus is a permanent metabolic syndrome and has been growing gradually worldwide. It is a collection of metabolic diseases categorized by hyperglycemia resulting from shortcomings in insulin secretion. Long-lasting hyperglycemia is related to injury and failure of organs.[57] Published data demonstrated that inhibition of beta-cell autoimmunity is a precise gene therapy for stoppage of type 1 diabetes, while enhancement in insulin sensitivity of peripheral tissues is an exact gene therapy for type 2 diabetes.[58] Welsh, suggested that progress in gene transfer methods are checked on the pancreatic insulin manufacturing beta-cell. If effective and harmless vectors are existing that transduce beta-cells *in vivo*/*ex vivo*, autoimmune beta-cell devastation in type 1 diabetes might be prohibited and gene delivery will defend the rest beta-cell mass in a pre-diabetic patient at a serious threat of becoming diabetic from autoimmune obliteration.[59] Sarkar et al.[60] investigated the impacts of resveratrol and mangiferin on biochemical parameters of *PPARγ* and *FALDH* gene expression in adipose tissue of streptozotocin nicotinamide diabetic rats. Rats were analysed after giving an oral dose of resveratrol (40 mg/kg), mangiferin (40 mg/kg) and glibenclamide (0.6 mg/kg). Results portrayed that resveratrol and mangiferin to streptozotocin nicotinamide induced diabetic rats exhibited the noteworthy defensive outcome on all the biochemical parameters. Additionally, both resveratrol and mangiferin presented substantial augmentation of *PPARγ* and *FALDH* gene expression in rat adipose tissue related to non-treated rats.[60]

RESVERATROL GENE THERAPY IN LIVER DISORDERS

Studies verified that resveratrol has numerous therapeutic effects on liver disorders. Resveratrol considerably decreased fat deposition and protect the liver from chemical and alcohol injury. It may augment glucose metabolism and lipid profile and reduce liver fibrosis and steatosis.[61] Azirak et al.[62] studied the impact of resveratrol on the fatty acid synthase gene expression towards the adverse effects of risperidone in rat liver. The resveratrol therapy expressively diminished weight gain and the fatty acid synthase gene expression level improved pointedly in the RSV1 group. Findings concluded that treatment with resveratrol could guard liver tissue towards the undesirable effects of risperidone over fatty acid synthase gene expression.[62]

CONCLUSION

Conventional resveratrol delivery systems display poor absorption and pose a daunting challenge for the existing methods for bioavailability limitations. Considering these obstacles, the nanocarriers are being measured as extraordinary inventions to conquer these glitches of deprived and inconsistent bioavailability, but it is unclear whether this entity targets the site of action after oral administration. Recently, resveratrol gene therapy is an auspicious option for numerous diseases (HIV/AIDS, cancer, cardiovascular,

liver disorders, and infections). For example, resveratrol may act as an anticancer agent for breast cancer by influencing the epigenetics of breast cancer-associated genes. Similarly, resveratrol influences other disease-associated genes. There is a possibility where vector-resveratrol can be delivered to the cells or particular tissues to treat various diseases and enhance the therapeutic potential of resveratrol which both directly and indirectly overcome the pharmacokinetic limitations. The huge volume of preclinical findings in support of resveratrol's use as chemotherapeutic agents warrants further clinical studies. With gene therapy, resveratrol and its by-products may lead to treatments in diseases as an attempt to decline or eradicate the reservoir of disease-ridden cells with the anticipation of finally healing a patient. This method remains dangerous and is under testing to ensure that it will be safe and efficient. The cost of these therapies has been highlighted as a subject that may hamper the growth of gene therapies as commercially feasible treatments. The anticipation is that the sustained benefits of these one-time treatments will validate the excessive costs. Beyond that, the administration bodies of the developed nations and authorities like Food and Drug Administration/World Health Organization/ European Medicines Agency should take a step to initiate these therapies with courage and expectation otherwise these treatments might no longer be acceptable solitary as a substitute therapy for incurably sick individuals who failed conventional therapies. Further studies are obligatory to elucidate whether resveratrol gene therapy has any effect on the normal function and shows any therapeutic potential to the number of incurable diseases.

ACKNOWLEDGMENTS

I am grateful to Prof. Param Sharma for their valuable advice and support in the preparation and editing of this review.

Conflict of interest: The author declares no conflicts of interest and there is no association between the contents of this review and Micro Labs GmbH and no confidential information of the latter is disclosed.

REFERENCES

1. Takaoka MJ. Of the phenolic substances of white hellebore (Veratrumgrandiflorum Loes. fil). J Faculty Sci Hokkaido Im Univ. 1940;3:1-16.
2. Singh G, Pai RS. Recent advances of resveratrol in nanostructured based delivery systems and in the management of HIV/AIDS. J Control Release. 2014;194:178-188.
3. Rauf A, Imran M, Butt MS, Nadeem M, Peters DG, Mubarak MS. Resveratrol as an anti-cancer agent: a review. Crit Rev Food Sci Nutr. 2018;58:1428-1447.
4. Dyck GJB, Raj P, Zieroth S, Dyck JRB, Ezekowitz JA. The effects of resveratrol in patients with cardiovascular disease and heart failure: a narrative review. Int J Mol Sci. 2019;20:904.
5. Heredia A, Davis C, Amin MN, Le NM, Wainberg MA, Oliveira M, Deeks SG, Wang LX, Redfield RR. Targeting host nucleotide biosynthesis with resveratrol inhibits emtricitabine-resistant HIV-1. AIDS. 2014;28:317-323.
6. James JS. Resveratrol: why it matters in HIV. AIDS Treat News. 2006:3-5.
7. Chimento A, De Amicis F, Sirianni R, Sinicropi MS, Puoci F, Casaburi I, Saturnino C, Pezzi V. Progress to improve oral bioavailability and beneficial effects of resveratrol. Int J Mol Sci. 2019;20:1381.
8. Walle T. Bioavailability of resveratrol. Ann N Y Acad Sci. 2011;1215:9-15.
9. Gambini J, López-Grueso R, Olaso-González G, Inglés M, Abdelazid K, Alami MEL, Bonet-Costa V, Borrás C, Viña J. Resveratrol: distribution, properties and perspectives. Rev Esp Geriatr Gerontol. 2013;48:79-88.
10. Neves AR, Lúcio M, Martins S, Lima JL, Reis S. Novel resveratrol nanodelivery systems based on lipid nanoparticles to enhance its oral bioavailability. Int J Nanomedicine. 2013;8:177-187.
11. https://www.fda.gov/regulatory-information/search-fda-guidance-documents/considerations-design-early-phase-clinical-trials-cellular-and-gene-therapy-products (Accessed date: 24/05/2020).
12. Anguela XM, High KA. Entering the modern era of gene therapy. Annu Rev Med. 2019;70:273-288.
13. Long Term Follow-Up After Administration of Human Gene Therapy Products; Draft Guidance for Industry, July 2018. (Accessed date: 24/05/2020).
14. https://www.fda.gov/vaccines-blood-biologics/cellular-gene-therapy-products/what-gene-therapy#footnote1 (Accessed date: 24/05/2020).
15. https://ghr.nlm.nih.gov/primer/therapy/genetherapy (Accessed date: 24/05/2020).
16. Kaufmann KB, Büning H, Galy A, Schambach A, Grez M. Gene therapy on the move. EMBO Mol Med. 2013;5:1642-1661.
17. Wirth T, Parker N, Ylä-Herttuala S. History of gene therapy. Gene 2013;525:162-169.
18. Brody H. Gene Therapy. Nature 2018;564:565.
19. High KA, Roncarolo MG. Gene Therapy. N Engl J Med. 2019;381:455-464.
20. Pederson T. Gene Therapy Now? FASEB J. 2018;32:1731-1732.
21. Smith CIE, Blomberg P. Gene therapy – from idea to reality. Lakartidningen. 2017;114:EWYL.
22. Athanasopoulos T, Munye MM, Yáñez-Muñoz RJ. Nonintegrating gene therapy vectors. Hematol Oncol Clin North Am. 2017;31:753-770.
23. https://pubmed.ncbi.nlm.nih.gov/?term=resveratrol+gene+therapy (Accessed date: 24/05/2020).
24. https://www.fda.gov/vaccines-blood-biologics/biologics-research-projects/cell-specific-and-gene-specific-targeting-gene-therapy-vectors (Accessed date: 24/05/2020).
25. Milone MC, O'Doherty U. Clinical use of lentiviral vectors. Leukemia. 2018;32:1529-1541.
26. Benskey MJ, Manfredsson FP. Lentivirus production and purification. Methods Mol Biol. 2016;1382:107-114.
27. McCarron A, Donnelley M, McIntyre C, Parsons D. Challenges of up-scaling lentivirus production and processing. J Biotechnol. 2016;240:23-30.
28. Hauber I, Beschorner N, Schrödel S, Chemnitz J, Kröger N, Hauber J, Thirion C. Improving lentiviral transduction of $CD34^+$ hematopoietic stem and progenitor cells. Hum Gene Ther Methods. 2018;29:104-113.

29. McGarrity GJ, Hoyah G, Winemiller A, Andre K, Stein D, Blick G, Greenberg RN, Kinder C, Zolopa A, Binder-Scholl G, Tebas P, June CH, Humeau LM, Rebello T. Patient monitoring and follow-up in lentiviral clinical trials. J Gene Med. 2013;15:78-82.

30. Chen YH, Keiser MS, Davidson BL. Viral vectors for gene transfer. Curr Protoc Mouse Biol. 2018;8:e58.

31. Libutti SK. Recording 25 years of progress in cancer gene therapy. Cancer Gene Ther. 2019;26:345-346.

32. Sudhakar V, Richardson RM. Gene therapy for neurodegenerative diseases. Neurotherapeutics. 2019;16:166-175.

33. Stafeev YS, Menshikov MY, Parfyonova YV. Gene therapy of type 2 diabetes mellitus: state of art. Ter Arkh. 2019;91:149-152.

34. Xiao Q, Guo D, Chen S. Application of CRISPR/Cas9-based gene editing in HIV-1/AIDS therapy. Front Cell Infect Microbiol. 2019;9:69.

35. Zabaleta N, Hommel M, Salas D, Gonzalez-Aseguinolaza G. Genetic-Based approaches to inherited metabolic liver diseases. Hum Gene Ther. 2019;30:1190-1203.

36. https://www.jyi.org/2009-january/2017/10/2/evaluation-of-the-clinical-success-of-ex-vivo-and-in-vivo-gene-therapy#(Accessed date: 24/05/2020).

37. Templeton NS. Gene and Cell Therapy: Therapeutic Mechanisms and Strategies. 4th ed. New York: CRC Press; 2008.

38. Jafarlou M, Baradaran B, Saedi TA, Jafarlou V, Shanehbandi D, Maralani M, Othman F. An overview of the history, applications, advantages, disadvantages and prospects of gene therapy. J Biol Regul Homeost Agents. 2016;30:315-321.

39. http://www.biolyse.ca/gene-therapy-pros-and-cons/ (Accessed date: 25/05/2020).

40. https://futureofworking.com/6-advantages-and-disadvantages-of-gene-therapy/ (Accessed date: 25/05/2020).

41. Navarro-Yepes J, Zavala-Flores L, Anandhan A, Wang F, Skotak M, Chandra N, Li M, Pappa A, Martinez-Fong D, Del Razo LM, Quintanilla-Vega B, Franco R. Antioxidant gene therapy against neuronal cell death. Pharmacol Ther. 2014;142:206-230.

42. Ozog S, Timberlake ND, Hermann K, Garijo O, Haworth KG, Shi G, Glinkerman CM, Schefter LE, D'Souza S, Simpson E, Sghia-Hughes G, Carillo RR, Boger DL, Kiem HP, Slukvin I, Ryu BY, Sorrentino BP, Adair JE, Snyder SA, Compton AA, Torbett BE. Resveratrol trimer enhances gene delivery to hematopoietic stem cells by reducing antiviral restriction at endosomes. Blood. 2019;134:1298-1311.

43. Ko JH, Sethi G, Um JY, Shanmugam MK, Arfuso F, Kumar AP, Bishayee A, Ahn KS. The role of resveratrol in cancer therapy. Int J Mol Sci. 2017;18:2589.

44. Granier C, Karaki S, Roussel H, Badoual C, Tran T, Anson M, Fabre E, Oudard S, Tartour E. Cancer immunotherapy: rational and recent breakthroughs. Rev Med Interne 2016;37:694-700.

45. Izquierdo-Torres E, Hernández-Oliveras A, Meneses-Morales I, Rodríguez G, Fuentes-García G, Zarain-Herzberg Á. Resveratrol up-regulates ATP2A3 gene expression in breast cancer cell lines through epigenetic mechanisms. Int J Biochem Cell Biol. 2019;113:37-47.

46. Shi Q, Geldenhuys W, Sutariya V, Bishayee A, Patel I, Bhatia D. CArG-driven GADD45α activated by resveratrol inhibits lung cancer cells. Genes Cancer. 2015;6:220-230.

47. Xu X, Liu A, Bai Y, Li Y, Zhang C, Cui S, Piao Y, Zhang S. Co-delivery of resveratrol and p53 gene *via* peptide cationic liposomal nanocarrier for the synergistic treatment of cervical cancer and breast cancer cells. J Drug Deliv Sci Technol. 2018;51:746-753.

48. Xiao J, Wang X, Wu Y, Zhao Q, Liu X, Zhang G, Zhao Z, Ning Y, Wang K, Tan Y, Du B. Synergistic effect of resveratrol and HSV-TK/GCV therapy on murine hepatoma cells. Cancer Biol Ther. 2019;20:183-191.

49. Zadi Heydarabad M, Nikasa M, Vatanmakanian M, Azimi A, Farshdousti Hagh M. Regulatory effect of resveratrol and prednisolone on *MDR1* gene expression in acute lymphoblastic leukemia cell line (CCRF-CEM): an epigenetic perspective. J Cell Biochem. 2018;119:4890-4896.

50. Bickenbach KA, Veerapong J, Shao MY, Mauceri HJ, Posner MC, Kron SJ, Weichselbaum RR. Resveratrol is an effective inducer of CArG-driven TNF-alpha gene therapy. Cancer Gene Ther. 2008;15:133-139.

51. Brizola E, Felix T, Shapiro J. Pathophysiology and therapeutic options in osteogenesis imperfecta: an update. Res Rep Endocr Disord. 2016;6:17-30.

52. Li M, Yan J, Chen X, Tam W, Zhou L, Liu T, Pan G, Lin J, Yang H, Pei M, He F. Spontaneous up-regulation of SIRT1 during osteogenesis contributes to stem cells' resistance to oxidative stress. J Cell Biochem. 2018;119:4928-4944.

53. Tseng PC, Hou SM, Chen RJ, Peng HW, Hsieh CF, Kuo ML, Yen ML. Resveratrol promotes osteogenesis of human mesenchymal stem cells by upregulating *RUNX2* gene expression *via* the SIRT1/FOXO3A axis. J Bone Miner Res. 2011;26:2552-2563.

54. Matsuda Y, Minagawa T, Okui T, Yamazaki K. Resveratrol suppresses the alveolar bone resorption induced by artificial trauma from occlusion in mice. Oral Dis. 2018;24:412-421.

55. Zhou T, Yan Y, Zhao C, Xu Y, Wang Q, Xu N. Resveratrol improves osteogenic differentiation of senescent bone mesenchymal stem cells through inhibiting endogenous reactive oxygen species production *via* AMPK activation. Redox Rep. 2019;24:62-69.

56. Casarin RC, Casati MZ, Pimentel SP, Cirano FR, Algayer M, Pires PR, Ghiraldini B, Duarte PM, Ribeiro FV. Resveratrol improves bone repair by modulation of bone morphogenetic proteins and osteopontin gene expression in rats. Int J Oral Maxillofac Surg. 2014;43:900-906.

57. American Diabetes Association. Diagnosis and classification of diabetes mellitus. Diabetes Care. 2014;37(Suppl 1):S81-S90.

58. Yamaoka T. Gene therapy for diabetes mellitus. Curr Mol Med. 2001;1:325-337.

59. Welsh N. Gene therapy in diabetes mellitus: promises and piffalls. Curr Opin Mol Ther. 1999;1:464-470.

60. Sarkar P, Bhowmick A, Kalita MC, Banu S. Effects of resveratrol and mangiferin on *PPARγ* and *FALDH* gene expressions in adipose tissue of streptozotocin-nicotinamide-induced diabetes in rats. J Diet Suppl. 2019;16:659-675.

61. Faghihzadeh F, Hekmatdoost A, Adibi P. Resveratrol and liver: a systematic review. J Res Med Sci. 2015;20:797-810.

62. Azirak S, Bilgic S, Tastemir Korkmaz D, Guvenc AN, Kocaman N, Ozer MK. The protective effect of resveratrol against risperidone-induced liver damage through an action on *FAS* gene expression. Gen Physiol Biophys. 2019;38:215-225.

Turk J Pharm Sci 2022;19(1):110-115
DOI: 10.4274/tjps.galenos.2020.43078

REVIEW

WLBU2 Antimicrobial Peptide as a Potential Therapeutic for Treatment of Resistant Bacterial Infections

Dirençli Bakteriyel Enfeksiyonların Tedavisinde Potansiyel Bir Terapötik Olarak WLBU2 Antimikrobiyal Peptit

Lina ELSALEM[1]*, Ayat KHASAWNEH[1,2], Suhaila AL SHEBOUL[3]

[1]Jordan University of Science and Technology Faculty of Medicine, Department of Pharmacology, Irbid, Jordan
[2]Royal Medical Services, Department of Clinical Pathology and Microbiology, Amman, Jordan
[3]Jordan University of Science and Technology Faculty of Applied Medical Sciences, Department of Medical Laboratory Sciences, Irbid, Jordan

ABSTRACT

Antimicrobial resistance is considered a major health problem, worldwide. It is significantly associated with high morbidity and mortality rates. The current antibiotics have limited therapeutic efficacy in providing treatment for multidrug resistant bacteria. Accordingly, research in the antimicrobial field has been directed toward the discovery of new agents to overcome bacterial resistance. Antimicrobial peptides (AMP) have been extensively studied as potential antimicrobial agents with lower incidence of drug resistance compared to conventional antibiotics. WLBU2 is an engineered cationic AMP with promising antibacterial activity. It is composed of 24 amino acids including; 13 arginine, 8 valine and 3 tryptophan residues. Findings from *in vitro* and *in vivo* studies showed that WLBU2 is a potent peptide with a broad spectrum activity against Gram-positive, Gram-negative, multidrug resistant, and biofilm forming bacteria. Additionally, WLBU2 appears as a salt-resistant peptide with potential application for treatment of infections at conditions with disturbed normal salt homeostasis. Furthermore, WLBU2 was found as AMP with limited host toxicity. Recent investigations have shown that combination of WLBU2 with conventional antibiotics can result in synergism against resistant bacteria. In this review we highlight the evidence supporting the promising properties of WLBU2 as an antibacterial agent with potential applications for the treatment of infections caused by resistant bacteria.

Key words: Antimicrobial peptide, WLBU2, resistant bacteria, salt resistant, synergism, combination, non-cytotoxic

ÖZ

Antimikrobiyal direnç, dünya çapında önemli bir sağlık sorunu olarak kabul edilmektedir. Yüksek morbidite ve mortalite oranları ile önemli oranda ilişkilidir. Mevcut antibiyotikler, çoklu ilaca dirençli bakterilerin tedavisini sağlamada sınırlı terapötik etkinliğe sahiptir. Bu nedenle, antimikrobiyal alanda yapılan araştırmalar, bakteriyel direncin ortadan kaldırmak için yeni ajanların keşfedilmesine yöneliktir. Antimikrobiyal peptitler (AMP), geleneksel antibiyotiklere kıyasla daha düşük ilaç direnci insidansına sahip potansiyel antimikrobiyal ajanlar olarak kapsamlı bir şekilde incelenmiştir. WLBU2, umut verici antibakteriyel aktiviteye sahip, tasarlanmış bir katyonik AMP'dir. On üç arjinin, 8 valin ve 3 triptofan rezidülerini içeren 24 amino asitten meydana gelmektedir. *İn vitro* ve *in vivo* çalışmalardan elde edilen bulgular, WLBU2'nin Gram-pozitif, Gram-negatif, çoklu ilaç direnci ve biyofilm oluşturan bakterilere karşı geniş spektrumlu aktiviteye sahip güçlü bir peptit olduğunu göstermektedir. Ayrıca, WLBU2, normal tuz homeostazı bozulmuş koşullarda enfeksiyonların tedavisi için potansiyel uygulamayla tuza dirençli bir peptit olarak görünmektedir. Dahası, WLBU2 sınırlı konakçı toksisitesine sahip AMP olarak bulunmuştur. Son araştırmalar, WLBU2'nin geleneksel antibiyotiklerle kombinasyonunun dirençli bakterilere karşı sinerjizm ile sonuçlanabileceğini göstermiştir. Bu derlemede, dirençli bakterilerin neden olduğu enfeksiyonların tedavisi için potansiyel uygulamaları olan bir antibakteriyel ajan olarak WLBU2'nin umut verici özelliklerini destekleyen kanıtları vurguluyoruz.

Anahtar kelimeler: Antimikrobiyal peptit, WLBU2, dirençli bakteri, tuza dirençli, sinerjizm, kombinasyon, non-sitotoksik

***Correspondence:** lmelsalem@just.edu.jo, **Phone:** +0096227201000, **ORCID-ID:** orcid.org/0000-0002-3814-4865
Received: 15.10.2020, **Accepted:** 20.11.2020

INTRODUCTION

Antimicrobial resistance (AMR) is recognized as a major global threat of negative impact on the public health systems around the world.[1] AMR has reached an alarming level since it is significantly associated with high morbidity and mortality rates.[2] According to the 2019 Antibiotic Resistance Threats report published by the United States Centers for Disease Control and Prevention, more than 2.8 million antibiotic-resistant infections occur in the U.S. each year, and more than 35,000 people die.[3] Indeed, the World Health Organization and the United Nations, Interagency Coordination Group on AMR have described the global impact of AMR as being very critical causing more than 700,000 deaths around the world, with expectations to reach 10 million at the end of 2050.[4] AMR is also well recognized to be associated with increasing healthcare cost.[5] This is mainly due to the need for expensive antibiotics and prolonged hospitalization and isolation of affected patients.[2,6]

Among Gram-positive pathogens, resistant *Staphylococcus aureus* has been described as the biggest threat.[7] Methicillin-resistant *S. aureus* (MRSA), known as being resistant to penicillin-like beta-lactam antibiotics, first emerged 6 decades ago.[8] After that, MRSA infections have rapidly spread around the world, with high incidence were reported in many countries in Europe, USA, UK and the Asia-Pacific region.[9] Previous studies reported that most MRSA strains were inhibited by vancomycin at minimum inhibitory concentration (MIC) values of 0.125 to 1 µg/mL.[10] However, increased resistance of certain strains of *S. aureus* toward vancomycin have been observed.[11] This was first reported in Japan in 1996, with the discovery of clinical isolate with reduced susceptibility to vanocmycin (MIC: 8 µg/mL), and was called vancomycin intermediate *S. aureus*.[12] In 2002, the U.S. reported the first *S. aureus* isolate with complete resistance to vancomycin (MIC ≥32 µg/mL) and was called vancomycin-resistant *S. aureus*.[13]

Currently, substantial evidence points to the negative impact of Gram-negative pathogens, which are considered very common in the community.[3,14] Indeed, many of these were reported as being multidrug-resistant (MDR) including extended spectrum beta-lactamase-producing *Escherichia coli, Neisseria gonorrhoeae* and *Enterobacter cloacae,*[3,14-16] which are resistant to third generation cephalosporins (ceftriaxone and ceftazidime) and monobactams.[17]

Recognizing the fact that the current antibiotics have limited therapeutic efficacy in providing treatment for MDR Gram-positive and negative bacteria, new strategies have been developed to overcome antibiotic bacterial resistance.[6] Antimicrobial peptides (AMPs) have been extensively studied as potential antimicrobial agents with lower incidence of drug resistance compared to conventional antibiotics.[18-20] In this review we highlight the evidence of antibacterial activity of WLBU2 peptide as a novel engineered cationic antimicrobial agent with potential applications for treatment of infections caused by resistant bacteria.

Antimicrobial peptides

AMPs are a large family of low molecular weight peptides that play a key role in innate immunity. Most AMPs are cationic peptides and can kill and/or inhibit bacterial growth.[21] The exact mechanism of AMP antibacterial effect is not understood. However, AMPs have been suggested to bind the bacterial cell membrane and cause disruption of the lipid components.[22] This is usually induced by electrostatic interactions between positively charged amino acids within the peptide and negatively charged lipids in bacterial cell membrane.[23,24] As a consequence, increasing the plasma membrane permeability and disruption of the plasma membrane will cause leakage of ions and metabolites as well as cessation of membrane-coupled respiration and biosynthesis that can contribute to bacterial cell death.[23,24]

WLBU2 antibacterial activity

WLBU2 is an engineered cationic peptide that contains 24 amino acids including; 13 arginine. Eight valine and 3 tryptophan residues in the hydrophobic face separated from each other by at least 7 amino acids (Figure 1).[25] Results from *in vitro* and *in vivo* investigations revealed the potency of WLBU2 with broad spectrum activity against different types of microorganisms including bacteria and diverse *Candida* species.[26-32] Preclinical studies on *Pseudomonas aeruginosa* described WLBU2 as salt resistant peptide with potent inhibitory effects against bacterial growth and biofilm formation.[26,33,34] Further investigations on lung infections caused by *P. aeruginosa* supported the antibacterial effects of WLBU2 as well as induction of protective proinflammatory responses upon treatment.[33,35] The antibacterial potency of WLBU2 was also reported against three oral microorganisms (*Streptococcus gordonii, Fusobacterium nucleatum*, and *Porphyromonas gingivalis*).[27] Additionally, WLBU2 was found to have bactericidal activity against three highly pathogenic bacteria: *Francisella tularensis, Yersinia pestis* and *Burkholderia pseudomallei.*[28] Recently, WLBU2 eliminates pneumonia and MRSA superinfection during influenza and

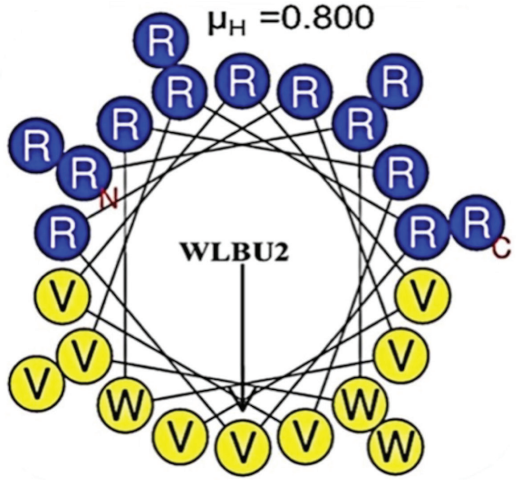

Figure 1. WLBU2 peptide structure. WLBU2 contains 24 amino acids including; 13 arginine (R). Eight valine (V) and 3 tryptophan (W) residues in the hydrophobic face separated from each other by at least 7 amino acids Adopted from Deslouches et al.[36] license number 4927790008448.

antibiotic resistant surgical implant biofilms caused by *Staphylococcus aureus* and MRSA.[29,37] Additionally, it has been found to be very effective in preventing *Enterococcus faecium, Staphylococcus aureus, Klebsiella pneumoniae, Acinetobacter baumannii*, *P. aeruginosa, E. cloacae* (ESKAPE) pathogens' biofilm formation and attachment.[30] Recent results have revealed potent antibacterial effects against biofilms of MDR *A. baumannii* and *K. pneumoniae*.[31]

The values of MIC and minimum bactericidal concentrations (MBC) of WLBU2 from previous investigations showed that WLBU2 has fast killing effects on bacterial cells with MIC values ≤l0 μM.[19,31,36] The MIC values of WLBU2 from previous reports were as 1.5-3.2 μM for extensively drug-resistant (XDR) *A. baumannii*, 2.9-4.7 μM for XDR *K. pneumoniae*, and 9.3 μM for *K. pneumoniae* KP2 strain.[19] Additionally, Deslouches et al.[36] have shown that the MIC values of WLBU2 were ≤l0 μM against both Gram-negative and Gram-positive bacteria including MRSA, vancomycin-resistant *enterococci*, *K. pneumoniae, E. aerogenes, E. cloacae, Escherichia coli, P. aeruginosa,* and *A. baumannii*. Recent investigations found that the MIC was 7.943 μM for *K. pneumoniae* and 7.484 μM for *A. baumannii* clinical isolates.[31] Of note, the MBC values for WLBU2 against previous bacterial isolates were found to be identical to the MIC values of respective bacteria, indicating that WLBU2 is bactericidal.[38]

The exact mechanisms for the antimicrobial effect of WLBU2 are yet to be elucidated. However, it was suggested to be mediated by electrostatic interactions between peptide' cationic amino acid residues and the negatively charged lipid molecules on the surface of bacterial targets.[26] The potent activity of WLBU2 may be attributed to the high cationic charge and the increased length of amino acids of WLBU2 (24 residues).[26] Previous studies reported that the antibacterial activity of cationic AMP might also be mediated by binding to bacterial DNA.[39] However, limited investigations have been conducted in this regard for WLBU2. Only recent findings have revealed that WLBU2 at up to the tested 200 μM could not delay DNA mobility.[31]

WLBU2 and host cell toxicity

WLBU2 has been considered potent AMP without significant host cell toxicity.[31] A previous study showed that WLBU2 had no cytotoxic effect at concentration of ≤20 μM against peripheral blood mononuclear cells, upon testing with the hemolytic assay and MTT assay.[19] A recent study has also revealed that WLBU2 is not cytotoxic when evaluated against human skin fibroblasts.[31] The selective toxicity of WLBU2 against bacteria and low toxicity against host cells suggest that WLBU2 form weak interactions with eukaryotic membranes which are highly rich with cholesterol. In comparison, WLBU2 might form robust electrostatic interactions with the negatively charged bacterial membranes.[40]

WLBU2 as salt-resistant peptide

One of the major drawbacks with the use of AMPs, mainly the natural AMPs, is their limited antibacterial activity due to inactivation by physiological concentrations of salts including sodium chloride and divalent cations.[39] It has been shown that the antibacterial activity of well-studied natural AMPs (such as LL-37, human β-defensin-1, gramicidins, bactenecins, and magainins) was substantially reduced under salt conditions.[41] Turner et al.[42] showed that MIC values of LL-37 and human neutrophil peptide-1 were significantly increased when NaCl was added. In comparison, Mohamed et al.[39] described engineered AMP, RRIKA and RR, as salt-resistant since their antibacterial activity against MRSA was retained in the presence of physiological concentrations of NaCl and $MgCl_2$. Recent studies also have shown that the synthetic AMPs such as D-RR4 and Hp1404 are salt resistant with retained activity against Gram-negative bacteria including *P. aeruginosa* and *A. baumannii*.[43,44] WLBU2 appeared as salt resistant since it retained the antibacterial activity when tested in different concentrations of NaCl, $CaCl_2$ and $MgCl_2$ against Gram-negative *P. aeruginosa* or Gram-positive MRSA strains.[26] This is considered highly important for the treatment of infections in conditions with disturbed normal salt homeostasis.[26] The ability of WLBU2 to resist the effects of salts suggests that the chemical structure of WLBU2 has been well designed to relatively retain antimicrobial activity in the presence of NaCl and divalent cations concentrations that is considered a major challenge for natural peptides. Additionally, it provides a selective advantage as potential therapeutics in physiological solutions. However, further studies are needed to provide more evidence for WLBU2 as a salt-resistant peptide since salt sensitivity might be sometimes dependent on the test organism.[26]

WLBU2 and synergism effects with conventional antibiotics

Recently, the effects of synthetic AMPs in combination with conventional antibiotics have been investigated against many Gram-negative and Gram-positive bacteria including MDR strains with biofilm formation ability.[45-48] Studies showed the efficacy of using synthetic peptides in combination with conventional antibiotics to augment the treatment of murine cutaneous abscesses caused by difficult to treat pathogens including all ESKAPE and *E. coli.* [49] Gopal et al.[50] also reported that synergism was obtained upon combination of conventional antibiotics (cefotaxime, ciprofloxacin, or erythromycin) with four cationic AMP (HPME, HPMA, CAME and CA) against 19 MDR *A. baumannii* isolates.[50] In addition, synergistic effects were observed upon combination of the AMP DP7 and antibiotics (gentamicin, vancomycin, azithromycin, and amoxicillin) against several MDR bacterial strains including *S. aureus, P. aeruginosa, A. baumannii*, and *E. coli*.[51] SPR741 peptide also potentiated the effect of conventional antibiotics against *E. coli, K. pneumoniae,* and *A. baumannii*.[52] Recent findings from combination treatment have shown that T3 and T4 AMP resulted in potentiation of ampicillin and oxacillin against MRSA clinical isolates.[48] A synthetic cationic peptide, pexiganan, is currently in phase 3 clinical trials as a contemporary antimicrobial agent for the treatment of *E. coli, K. pneumoniae, Citrobacter koseri, E. cloacae, A. species*, and *P. aeruginosa* infections associated with diabetic foot ulcers.[53]

Upon reviewing the literature, limited evidence is available regarding the combination of WLBU2 and other conventional

antibiotics. Only a recent study has revealed that combination of sub-inhibitory concentrations of WLBU2 with amoxicillin-clavulanate or ciprofloxacin for *K. pneumoniae*, and with tobramycin or imipenem for *A. baumannii,* resulted in synergism with significant reduction in MIC values for some investigated isolates and ATCC strains.[31] Synergism and potentiation upon a combination of WLBU2 and conventional antibiotics might result from increased membrane permeability caused by the action of WLBU2 cationic peptide, which enhanced the penetration of antibiotics toward bacterial cells and thus, improved the drug efficacy and killing effects.[45,54] Further, it might result in obtaining synergistic effects and thus enhances efficacy.[54] Advantages of combination treatment may also include broadening the spectrum of antimicrobial coverage and reducing the needed doses of each antimicrobial agent and thus, drug toxicity.[54] However, future studies are needed to explore the potential of using WLBU2 along with conventional antibiotics against other MDR and biofilm forming bacteria.

Cationic AMP are emerging as potential antimicrobial agents that can be used as alternative or complement to conventional antibiotics to overcome drug-resistant infections. WLBU2 appears as a novel peptide with promising properties summarized in (Figure 2).

CONCLUSION

In vitro and *in vivo* studies showed that WLBU2 is potent antimicrobial agent with bactericidal effects and broad spectrum activity against many Gram-positive, Gram-negative, multidrug resistant, and biofilm forming bacteria. The therapeutic potential of AMPs can be affected by physiological conditions including

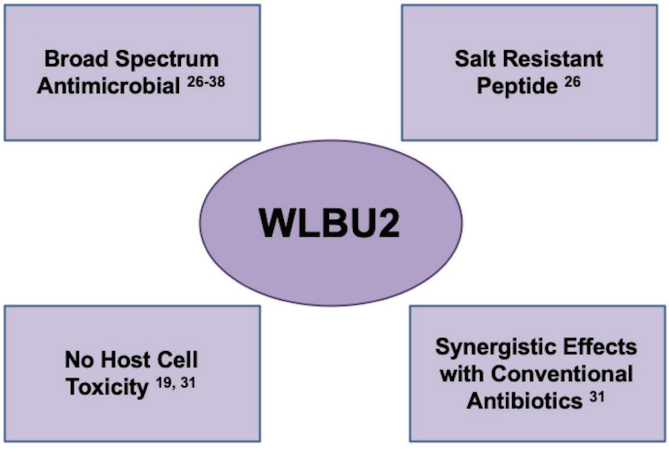

Figure 2. Properties of WLBU2 antimicrobial peptide

the presence of salts and divalent cations at infection site or body fluids. WLBU2 showed the ability to resist the effects of salts which provides a selective advantage as potential therapeutics in physiological solutions and suggests that WLBU2 has been successfully synthetized to resist different salts types and concentrations, that is considered a major drawback of natural AMPs. WLBU2 also appears as AMP with minimal cytotoxic effects against host cells Recent studies have provided proof of concept that WLBU2 as a cationic AMP can be used in combination with conventional antibiotics to reduce antimicrobial drug resistance which is considered a major issue to any health care system.

Future studies on the ability of WLBU2, either alone or along with conventional antibiotics, to eradicate or prevent biofilm formation will increase our knowledge regarding WLBU2 antibacterial activity. This might be considered under normal conditions and in the presence of salts, serum and proteases. Limited evidence is available regarding the potential synergism between WLBU2 and other cationic AMPs and therefore, it might be considered for future studies. Additionally, *in vivo* animal studies evaluating WLBU2 antibacterial activity as potential peptide for treatment of bacterial infections might be highly valuable to be carried in the future. Similar investigations could be conducted for many MDR Gram-positive and Gram-negative bacteria to characterize the spectrum of WLBU2 activity which is expected to be broad spectrum.

Investigations regarding the exact underlying mechanisms of the antibacterial activity of WLBU2 alone and combined with conventional antibiotics might be considered future experiments, since the underlying mechanisms are still to be elucidated. These investigations might involve studies on morphological changes or effects at the molecular level including genes playing role in bacterial resistance or bacterial metabolism as well as other energetics aspects.

Conflict of interest: No conflict of interest was declared by the authors. The authors alone are responsible for the content and writing of this article.

REFERENCES

1. Ferri M, Ranucci E, Romagnoli P, Giaccone V. Antimicrobial resistance: A global emerging threat to public health systems. Crit Rev Food Sci Nutr. 2017;57:2857-2876.
2. Prestinaci F, Pezzotti P, Pantosti A. Antimicrobial resistance: a global multifaceted phenomenon. Pathog Glob Health. 2015;109:309-318.
3. https://www.cdc.gov/drugresistance/pdf/threats-report/2019-ar-threats-report-508.pdf
4. No Time to Wait: Securing the future from drug-resistant infections. UN Interagency Coordination Group (IACG) on Antimicrobial Resistance, 2019.
5. Dadgostar P. Antimicrobial resistance: implications and costs. Infect Drug Resist. 2019;12:3903-3910.
6. Thabit AK, Crandon JL, Nicolau DP. Antimicrobial resistance: impact on clinical and economic outcomes and the need for new antimicrobials. Expert Opin Pharmacother. 2015;16:159-177.
7. Gajdács M. The continuing threat of methicillin-resistant *Staphylococcus aureus*. Antibiotics (Basel). 2019;8:52.
8. Harkins CP, Pichon B, Doumith M, Parkhill J, Westh H, Tomasz A, de Lencastre H, Bentley SD, Kearns AM, Holden MTG. Methicillin-resistant *Staphylococcus aureus* emerged long before the introduction of methicillin into clinical practice. Genome Biol. 2017;18:130.
9. Mutters NT, Günther F, Sander A, Mischnik A, Frank U. Influx of multidrug-resistant organisms by country-to-country transfer of patients. BMC Infect Dis. 2015;15:466.

10. Kshetry AO, Pant ND, Bhandari R, Khatri S, Shrestha KL, Upadhaya SK, Poudel A, Lekhak B, Raghubanshi BR. Minimum inhibitory concentration of vancomycin to methicillin resistant *Staphylococcus aureus* isolated from different clinical samples at a tertiary care hospital in Nepal. Antimicrob Resist Infect Control. 2016;5:27.
11. McGuinness WA, Malachowa N, DeLeo FR. Vancomycin resistance in *Staphylococcus aureus* . Yale J Biol Med. 2017;90:269-281.
12. Perl TM. The threat of vancomycin resistance. Am J Med. 1999;106:26S-37S; discussion 48S-52S.
13. Centers for Disease Control and Prevention (CDC). *Staphylococcus aureus* resistant to vancomycin--United States, 2002. MMWR Morb Mortal Wkly Rep. 2002;51:565-567.
14. Exner M, Bhattacharya S, Christiansen B, Gebel J, Goroncy-Bermes P, Hartemann P, Heeg P, Ilschner C, Kramer A, Larson E, Merkens W, Mielke M, Oltmanns P, Ross B, Rotter M, Schmithausen RM, Sonntag HG, Trautmann M. Antibiotic resistance: what is so special about multidrug-resistant Gram-negative bacteria? GMS Hyg Infect Control. 2017;12:Doc05.
15. Kaye KS, Pogue JM. Infections caused by resistant Gram-negative bacteria: epidemiology and management. Pharmacotherapy. 2015;35:949-962.
16. Ventola CL. The antibiotic resistance crisis: part 1: causes and threats. P T. 2015;40:277-283.
17. Coque TM, Baquero F, Canton R. Increasing prevalence of ESBL-producing Enterobacteriaceae in Europe. Euro Surveill. 2008;13:19044. Erratum in: Euro Surveill. 2008;13.
18. Peschel A, Sahl HG. The co-evolution of host cationic antimicrobial peptides and microbial resistance. Nat Rev Microbiol. 2006;4:529-536.
19. Deslouches B, Steckbeck JD, Craigo JK, Doi Y, Mietzner TA, Montelaro RC. Rational design of engineered cationic antimicrobial peptides consisting exclusively of arginine and tryptophan, and their activity against multidrug-resistant pathogens. Antimicrob Agents Chemother. 2013;57:2511-2521.
20. Sinha R, Shukla P. Antimicrobial peptides: recent insights on biotechnological interventions and future perspectives. Protein Pept Lett. 2019;26:79-87.
21. Zhu X, Dong N, Wang Z, Ma Z, Zhang L, Ma Q, Shan A. Design of imperfectly amphipathic α-helical antimicrobial peptides with enhanced cell selectivity. Acta Biomater. 2014;10:244-257.
22. Sani MA, Separovic F. How membrane-active peptides get into lipid membranes. Acc Chem Res. 2016;49:1130-1138.
23. Schmidt NW, Wong GC. Antimicrobial peptides and induced membrane curvature: geometry, coordination chemistry, and molecular engineering. Curr Opin Solid State Mater Sci. 2013;17:151-163.
24. Li J, Koh JJ, Liu S, Lakshminarayanan R, Verma CS, Beuerman RW. Membrane active antimicrobial peptides: translating mechanistic insights to design. Front Neurosci. 2017;11:73.
25. Deslouches B, Phadke SM, Lazarevic V, Cascio M, Islam K, Montelaro RC, Mietzner TA. De novo generation of cationic antimicrobial peptides: influence of length and tryptophan substitution on antimicrobial activity. Antimicrob Agents Chemother. 2005;49:316-322.
26. Deslouches B, Islam K, Craigo JK, Paranjape SM, Montelaro RC, Mietzner TA. Activity of the de novo engineered antimicrobial peptide WLBU2 against *Pseudomonas aeruginosa* in human serum and whole blood: implications for systemic applications. Antimicrob Agents Chemother. 2005;49:3208-3216.
27. Novak KF, Diamond WJ, Kirakodu S, Peyyala R, Anderson KW, Montelaro RC, Mietzner TA. Efficacy of the de novo-derived antimicrobial peptide WLBU2 against oral bacteria. Antimicrob Agents Chemother. 2007;51:1837-1839.
28. Abdelbaqi S, Deslouches B, Steckbeck J, Montelaro R, Reed DS. Novel engineered cationic antimicrobial peptides display broad-spectrum activity against *Francisella tularensis*, *Yersinia pestis* and *Burkholderia pseudomallei*. J Med Microbiol. 2016;65:188-194.
29. Rich H, Deslouches B, McHugh KJ, Montelaro R, Robinson KM, Alcorn JF. The synthetic antimicrobial peptide WLBU2 promotes *Staphylococcus aureus* clearance in the mouse lung. Am J Respir Crit Care Med 2016;A6727.
30. Lin Q, Deslouches B, Montelaro RC, Di YP. Prevention of ESKAPE pathogen biofilm formation by antimicrobial peptides WLBU2 and LL37. Int J Antimicrob Agents. 2018;52:667-672.
31. Swedan S, Shubair Z, Almaaytah A. Synergism of cationic antimicrobial peptide WLBU2 with antibacterial agents against biofilms of multi-drug resistant *Acinetobacter baumannii* and *Klebsiella pneumoniae*. Infect Drug Resist. 2019;12:2019-2030.
32. Deslouches B, Clancy C, Nguyen M, Cheng S, Mietzner T. The antimicrobial peptide Wlbu2 is active against *candida* spp., *Cryptococcus neoformans* and Leading Causes of Bacterial Sepsis. 2008.
33. Chen C, Deslouches B, Montelaro RC, Di YP. Enhanced efficacy of the engineered antimicrobial peptide WLBU2 *via* direct airway delivery in a murine model of *Pseudomonas aeruginosa* pneumonia. Clin Microbiol Infect. 2018;24:547.e1-547.e8.
34. Lashua LP, Melvin JA, Deslouches B, Pilewski JM, Montelaro RC, Bomberger JM. Engineered cationic antimicrobial peptide (eCAP) prevents *Pseudomonas aeruginosa* biofilm growth on airway epithelial cells. J Antimicrob Chemother. 2016;71:2200-2207.
35. Paranjape SM, Lauer TW, Montelaro RC, Mietzner TA, Vij N. Modulation of proinflammatory activity by the engineered cationic antimicrobial peptide WLBU-2. F1000Res. 2013;2:36.
36. *Deslouches B, Steckbeck JD, Craigo JK, Doi Y, Burns JL, Montelaro RC. Engineered cationic antimicrobial peptides to overcome multidrug resistance by ESKAPE pathogens. Antimicrob Agents Chemother. 2015;59:1329-1333.*
37. *Mandell JB, Deslouches B, Montelaro RC, Shanks RMQ, Doi Y, Urish KL. Elimination of antibiotic resistant surgical implant biofilms using an engineered cationic amphipathic peptide WLBU2. Scientific Reports. 2017;7:18098.*
38. Tripathi K. Essentials of Medical Pharmacology. 7th ed. New Delhi, India: Jaypee Brothers Medical Publishers; 2013.
39. Mohamed MF, Hamed MI, Panitch A, Seleem MN. Targeting methicillin-resistant *Staphylococcus aureus* with short salt-resistant synthetic peptides. Antimicrob Agents Chemother. 2014;58:4113-4122.
40. Biggin PC, Sansom MS. Interactions of alpha-helices with lipid bilayers: a review of simulation studies. Biophys Chem. 1999;76:161-183.
41. Chu HL, Yu HY, Yip BS, Chih YH, Liang CW, Cheng HT, Cheng JW. Boosting salt resistance of short antimicrobial peptides. Antimicrob Agents Chemother. 2013;57:4050-4052.
42. Turner J, Cho Y, Dinh NN, Waring AJ, Lehrer RI. Activities of LL-37, a cathelin-associated antimicrobial peptide of human neutrophils. Antimicrob Agents Chemother. 1998;42:2206-2214.

43. Mohamed MF, Brezden A, Mohammad H, Chmielewski J, Seleem MN. A short D-enantiomeric antimicrobial peptide with potent immunomodulatory and antibiofilm activity against multidrug-resistant *Pseudomonas aeruginosa* and *Acinetobacter baumannii*. Sci Rep. 2017;7:6953.

44. Kim MK, Kang HK, Ko SJ, Hong MJ, Bang JK, Seo CH, Park Y. Mechanisms driving the antibacterial and antibiofilm properties of Hp1404 and its analogue peptides against multidrug-resistant *Pseudomonas aeruginosa*. Sci Rep. 2018;8:1763.

45. Mohamed MF, Abdelkhalek A, Seleem MN. Evaluation of short synthetic antimicrobial peptides for treatment of drug-resistant and intracellular *Staphylococcus aureus*. Sci Rep. 2016;6:29707.

46. Galdiero E, Lombardi L, Falanga A, Libralato G, Guida M, Carotenuto R. Biofilms: novel strategies based on antimicrobial peptides. Pharmaceutics. 2019;11:322.

47. Ciandrini E, Morroni G, Arzeni D, Kamysz W, Neubauer D, Kamysz E, Cirioni O, Brescini L, Baffone W, Campana R. Antimicrobial activity of different antimicrobial peptides (AMPs) against clinical methicillin-resistant *Staphylococcus aureus* (MRSA). Curr Top Med Chem. 2018;18:2116-2126.

48. Rishi P, Vij S, Maurya IK, Kaur UJ, Bharati S, Tewari R. Peptides as adjuvants for ampicillin and oxacillin against methicillin-resistant *Staphylococcus aureus* (MRSA). Microb Pathog. 2018;124:11-20.

49. Pletzer D, Mansour SC, Hancock REW. Synergy between conventional antibiotics and anti-biofilm peptides in a murine, sub-cutaneous abscess model caused by recalcitrant ESKAPE pathogens. PLoS Pathog. 2018;14:e1007084.

50. Gopal R, Kim YG, Lee JH, Lee SK, Chae JD, Son BK, Seo CH, Park Y. Synergistic effects and antibiofilm properties of chimeric peptides against multidrug-resistant *Acinetobacter baumannii* strains. Antimicrob Agents Chemother. 2014;58:1622-1629.

51. Wu X, Li Z, Li X, Tian Y, Fan Y, Yu C, Zhou B, Liu Y, Xiang R, Yang L. Synergistic effects of antimicrobial peptide DP7 combined with antibiotics against multidrug-resistant bacteria. Drug Des Devel Ther. 2017;11:939-946.

52. Corbett D, Wise A, Langley T, Skinner K, Trimby E, Birchall S, Dorali A, Sandiford S, Williams J, Warn P, Vaara M, Lister T. Potentiation of antibiotic activity by a novel cationic peptide: potency and spectrum of activity of SPR741. Antimicrob Agents Chemother. 2017;61:e00200-e00217.

53. Flamm RK, Rhomberg PR, Simpson KM, Farrell DJ, Sader HS, Jones RN. *In vitro* spectrum of pexiganan activity when tested against pathogens from diabetic foot infections and with selected resistance mechanisms. Antimicrob Agents Chemother. 2015;59:1751-1754.

54. Tyers M, Wright GD. Drug combinations: a strategy to extend the life of antibiotics in the 21st century. Nature Rev Microbiol. 2019;17:141-155.